



Faculteit Farmaceutische, Biomedische en Diergeneeskundige Wetenschappen

Departement Farmaceutische Wetenschappen

Cyclopeptide Alkaloids: Isolation, Structure Elucidation,
Antiplasmodial Activity and AGEs Inhibiting Properties

Cyclopeptide Alkaloiden: Isolatie, Structuuropheldering,
Antiplasmodiale Activiteit en AGEs Inhiberende Eigenschappen

Proefschrift voorgelegd tot het behalen van de graad van Doctor in de Farmaceutische
Wetenschappen aan de Universiteit Antwerpen te verdedigen door

Emmy TUENTER

Promotoren

Prof. Dr. L. Pieters

Prof. Dr. N. Hermans

Antwerpen, 2017

"I was taught that the way of progress was neither swift nor easy."

Marie Curie

TABLE OF CONTENTS

LIST OF ABBREVIATIONS	XI
CHAPTER 1 Introduction	1
1.1 Medicinal Plants and Natural Product Research	3
1.2 Alkaloids	4
1.3 Malaria	4
1.3.1 Epidemiology	5
1.3.2 Lifecycle of <i>Plasmodium</i>	6
1.3.3 Clinical manifestations	8
1.3.4 Pathogenesis	9
1.3.5 Diagnosis	10
1.3.6 Profylaxis and treatment	10
1.4 Advanced Glycation End Products (AGEs)	13
1.4.1 Formation of advanced glycation end products	13
1.4.2 AGEs and pathogenesis of diabetic complications	17
1.4.3 AGEs inhibitors	21
1.5 Aim of this Work	28
References	31
CHAPTER 2 General experimental procedures	37
2.1 Chromatographic Methods	39
2.1.1 Solvents and reagents	39
2.1.2 Thin layer chromatography	39
2.1.3 Flash chromatography	39

2.1.4	High-performance liquid chromatography	40
2.1.5	High-performance liquid chromatography – solid-phase extraction – nuclear magnetic resonance spectroscopy	40
2.1.6	Semi-preparative high-performance liquid chromatography	41
2.2	Spectroscopic Methods	41
2.2.1	Nuclear magnetic resonance spectroscopy	41
2.2.2	Mass spectrometry	42
2.2.3	Optical rotation	43
2.3	Biological Methods	44
2.3.1	Antiplasmodial activity	44
2.3.2	Cytotoxicity	44
	References	46
CHAPTER 3	Cyclopeptide Alkaloids - Review	47
3.1	Introduction	49
3.2	Classification	49
3.3	Structures of New Compounds	51
3.3.1	Cyclopeptide alkaloids of the 4(13) type (nummularine-C type)	51
3.3.2	Cyclopeptide alkaloids of the 5(13) type (ziziphine-A type)	53
3.3.3	Cyclopeptide alkaloids of the 4(14) type (integerrine and frangulanine type)	54
3.3.4	Cyclopeptide alkaloids of the 5(14) type	55
3.3.5	Neutral cyclopeptide alkaloids	58
3.4	Distribution of Cyclopeptide Alkaloids	61
3.5	Configurational Studies and Total Synthesis	61
3.6	Biological Activity	63
3.6.1	Activity on the central nervous system (CNS), analgesic and anti-inflammatory activity	63

3.6.2	Antimicrobial activity	65
3.6.3	Other activities	66
3.7	Conclusions	67
	References	68
CHAPTER 4	<i>Hymenocardia acida</i>	73
4.1	Introduction	75
4.2	Results and Discussion	76
4.3	Materials and Methods	95
4.3.1	General experimental procedures	95
4.3.2	Plant material	95
4.3.3	Extraction and isolation	95
4.3.4	Antiplasmodial and cytotoxic activities	97
	References	98
CHAPTER 5	<i>Ziziphus oxyphylla</i>	101
5.1	Introduction	103
5.2	Results and Discussion	104
5.3	Materials and Methods	140
5.3.1	General experimental procedures	140
5.3.2	Plant material	140
5.3.3	Extraction and isolation	140
5.3.4	Antiplasmodial and cytotoxic activities	145
	References	146

CHAPTER 6	<i>Ziziphus nummularia & Ziziphus spina-christi</i>	149
6.1	Introduction	151
6.2	Results and Discussion	152
6.3	Experimental	185
6.3.1	General experimental procedures	185
6.3.2	Plant materials	185
6.3.3	Extraction and isolation	185
	References	190
 CHAPTER 7	 Gastrointestinal Absorption and Metabolic Conversion of Hymenocardine	 193
7.1	Introduction	195
7.2	Results and Discussion	197
7.3	Materials and Methods	212
7.3.1	Chemicals and reagents	212
7.3.2	<i>In vitro</i> gastrointestinal dialysis model (GIDM)	212
7.3.4	Incubation with liver S9 fraction	213
7.3.5	Animal study	215
	References	218
 CHAPTER 8	 SAR study	 221
8.1	Introduction	223
8.2	Results and Discussion	224
8.2.1	Antiplasmodial and cytotoxic activities	224
8.2.2	Qualitative structure-activity relationship study	226
8.2.3	Quantitative structure-activity relationship study	229

8.3	Materials and Methods	231
8.3.1	General experimental procedures	231
8.3.2	Plant material, extraction and isolation	231
8.3.3	Antiplasmodial and cytotoxic activities	233
8.3.4	QSAR	233
8.4	Conclusions	234
	References	235
CHAPTER 9	Advanced Glycation End Products (AGEs)	237
9.1	Introduction	239
9.2	Experimental Procedures	239
9.2.1	BSA-Glc assay	239
9.2.2	BSA-Glc assay, with protein precipitation	240
9.2.3	BSA-MGO assay	240
9.2.4	Fructosamine determination	240
9.2.5	Dicarbonyl entrapment	241
9.2.6	ELISA (enzyme linked immunosorbent assay)	242
9.3	Results and Discussion	243
9.3.1	BSA-Glc assay	243
9.3.2	BSA-Glc assay, with protein precipitation	247
9.3.3	BSA-MGO assay	249
9.3.4	Fructosamine determination	251
9.3.5	Dicarbonyl entrapment	252
9.3.6	ELISA experiment	253
9.4	Conclusions	256
	References	257

General Conclusions and Future Perspectives	259
Summary	265
Samenvatting	271
Acknowledgement – Dankwoord	277
Scientific Curriculum Vitae	283

LIST OF ABBREVIATIONS

3-DG	3-deoxyglucosone
ACT	artemisinin-based combination therapy
ADH	alcohol dehydrogenase
AFGP	1-alkyl-2-formyl-3,4-glycosyl-pyrrole
AGE-R1	advanced glycation end products receptor 1
AGEs	advanced glycation end products
APAD	3-acetyl pyridine adenine dinucleotide
BBI	broadband inverse
BSA	bovine serum albumine
COSY	correlation spectroscopy
CEL	carboxyethyllysine
CML	carboxymethyllysine
CNS	central nervous system
CYP450	cytochrome P450
DAD	diode array detector
DEET	<i>N,N</i> -diethyl-3-methylbenzamide
DEPT	distortionless enhancement by polarization transfer
DMSO	dimethylsulfoxide
DOLD	deoxyglucosone-derived lysine dimer
DOSC	direct orthogonal signal correction
ELISA	enzyme linked immunosorbent assay
ELSD	evaporative light scattering detector
EMA	European Medicines Agency
ESI	electrospray ionization
FA	formic acid
FFI	2-(2-furoyl)-4(5)-furanyl-1 <i>H</i> -imidazole
FTIR	fourier transform infrared
FWHM	full width at half maximum
GC	gas chromatography

GIDM	gastrointestinal dialysis model
GLA	glycolaldehyde
Glc	glucose
GO	glyoxal
GOLD	glyoxal-derived lysine dimer
GP	general phase
HbA _{1c}	glycosylated hemoglobin A _{1c}
HCD	higher-energy collisional dissociation
HEPES	4-(2-hydroxyethyl)-1-piperazineethanesulfonic acid
HESI	heated electrospray ionization
HPLC	high-performance liquid chromatography
HMBC	heteronuclear multiple bond correlation
HR(ESI)MS	high-resolution (electrospray ionization) mass spectrometry
HRP	horseradish peroxidase
HSQC	heteronuclear single quantum coherence
ICAM-1	intercellular adhesion molecule 1
IgG	immunoglobuline G
IgM	immunoglobuline M
IV	intravenous
LC	liquid chromatography
LDH	lactate dehydrogenase
LDL	low-density lipoproteins
MEM	minimum essential medium
MGO	methylglyoxal
MIC	minimal inhibitory concentration
MLR	multiple linear regression
MOLD	methylglyoxal-derived lysine dimer
MRM	multiple reaction monitoring
MS	mass spectrometry
NAD(P)	nicotinamide adenine dinucleotide (phosphate)
NADPH	reduced nicotinamide adenine dinucleotide phosphate

NADPH RS	reduced nicotinamide adenine dinucleotide phosphate regenerating system
NF-κB	nuclear factor kappa light chain enhancer of activated B cells
NBT	nitro blue tetrazolium chloride
NMR	nuclear magnetic resonance
NO	nitric oxide
NOS	nitric oxide synthase
NP	normal phase
PBS	phosphate buffered saline
PCR	polymerase chain reaction
PDA	photo diode array
PES	phenazine ethosulphate
PfEMP1	<i>Plasmodium falciparum</i> erythrocyt membrane protein 1
PLS	partial least squares
PO	per os
PPAR-γ	peroxisome proliferator activated receptor gamma
PTB	<i>N</i> -phenacylthiazolium bromide
QSAR	quantitative structure-activity relationship
QTOF	quadrupole time-of-flight
QqQMS	triple quadrupole mass spectrometry
RAGE	receptor for advanced glycation end products
RDTs	rapid diagnostic tests
RFU	relative fluorescence units
RMSEC	root mean squared error of calibration
RMSECV	root mean squared error of cross validation
ROS	reactive oxygen species
SAR	structure-activity relationship
S _N Ar	aromatic nucleophilic substitution
SPE	solid-phase extraction
SR-A	scavenger receptor class A
sRAGE	soluble receptor for advanced glycation end products
SR-B1	scavenger receptor class B, type 1

STZ	streptozotocine
TCM	traditional Chinese medicine
TLC	thin-layer chromatography
TOF	time-of-flight
TQD	triple quadrupole detector
UPLC	ultra-performance liquid chromatography
UV	ultraviolet
WHO	World Health Organization
ZN	<i>Ziziphus nummularia</i>
ZSC	<i>Ziziphus spina-christi</i>

CHAPTER 1

Introduction

1.1 Medicinal Plants and Natural Product Research

Medicinal plants have been applied in Traditional Medicine for about 5000 years, for example, in Traditional Chinese Medicine (TCM) and Indian Ayurveda. These days, about 80% of the world population still uses plant-based medicine for some aspects of their primary health care and an estimated two thirds of the world population resorts to medicinal plants derived from folk medicines for their primary health care needs. In general, in many parts of the world, herbal medicines are easily available and affordable compared to synthetic drugs, which are important factors in third world countries. Moreover, herbal medicines gained interest in the Western world in the last decade, and a growing number of people favor natural products over (semi)-synthetic drugs (Efferth, 2010; WHO, 2014).

Apart from the use of herbal medicines as such, natural products, and more specifically medicinal plants, are interesting resources for pharmaceutical research. The development of new drugs is booming business and one approach which can lead to the identification of new lead compounds is the characterization of extracts from medicinal plants. This approach has proven to be successful in the past, for example, in the discovery of artemisinin derivatives as antimalarial agents (Harvey, 2007; Butler *et al.*, 2008; Gamo *et al.*, 2010).

In the classic approach, high-throughput screening of large numbers of extracts and fractions is performed, followed by bioassay-guided isolation of active principles. However, there are some downsides to this approach: a lot of resources are needed, the work is slow and laborious, and the result is often disappointing. The isolation of known compounds, or constituents with a poor activity, is as difficult and time-consuming as for promising new leads, but useless when looking backwards. Alternatively, a more targeted purification and isolation procedure can be performed, with the purpose of identifying low-abundant, but promising compounds, which might have been overlooked in the classic approach. In this PhD project the latter strategy was followed and the focus was put on a specific type of natural products: the cyclopeptide alkaloids.

1.2 Alkaloids

In phytochemistry, plant-derived natural products are divided into different classes. The classification is based on the chemical structure of the compound and the type of building block from which it originates. The alkaloids are one of those classes; they are defined as low molecular weight nitrogen-containing compounds. The presence of one or more nitrogen atoms often confers basic properties, which can facilitate isolation and purification. The name alkaloid is in fact derived from alkali. However, the degree of basicity varies greatly and alkaloids bearing a nitrogen atom as part of an amide function, for example, are essentially neutral (Dewick, 2009).

This PhD project was focused on a specific subclass of alkaloids: the cyclopeptide alkaloids. Cyclopeptide alkaloids form a relatively small class, with around 250 representatives, among the 21,000 alkaloids that were identified in plants. More information about this type of alkaloids is given in Chapter 3, where their structural characteristics, distribution among plant species and biological activities are described and where an overview of newly discovered cyclopeptide alkaloids of the last decade is given. In the context of this project, the bioactivity of the isolated cyclopeptide alkaloids was assessed in relation to two different pathological conditions, selected on the basis of recently reported pharmacological properties for this class of compounds (see below), i.e. malaria and hyperglycemia; the latter condition is associated with an increased formation of advanced glycation end products (AGEs).

1.3 Malaria

Malaria is an infectious, vector-borne disease, caused by protozoan parasites from the genus *Plasmodium*. It is transmitted by the sting of an infected female Anopheles mosquito. Four different species of *Plasmodium* can cause human malaria: *P. falciparum*, *P. vivax*, *P. malariae*, and *P. ovale*. In recent years, also human cases of malaria due to *P. knowlesi* have been reported, but this species primarily causes malaria among macaques in certain areas of South-East Asia. Current information suggests that *P. knowlesi* malaria can occur in people when

they are bitten by an *Anopheles* mosquito that was previously infected by a monkey (zoonotic transmission) (Acheson *et al.*, 2007; Vinay *et al.*, 2007; Finch *et al.*, 2009).

According to the WHO (World Health Organization), there were 214 million new cases of malaria worldwide in 2015. The African region accounts for most global cases of malaria (90%), followed by the South-East Asian region (7%) and the Eastern Mediterranean region (2%). For the last decades, serious efforts have been made in order to reduce the disease burden of malaria and not without success; the incidence rate fell by 37% in the last 15 years. Moreover, malaria mortality rates fell by 60%. However, in 2015 the amount of malaria deaths was still estimated to be 438,000 worldwide, with a majority of the lethal cases concerning children under the age of five (306,000). Given the fact of increasing resistance against the currently available medicines, and over 3 billion people living in areas at risk of malaria transmission, research for new antiparasmodial treatments is still needed (WHO, 2016a; CDC, 2016).

1.3.1 Epidemiology

The occurrence of malaria is dependent on factors that influence the three components of the malaria life cycle: *Anopheles* mosquitoes, malaria parasites, and humans. Only in rare cases, malaria parasites can be transmitted from one person to another, without requiring passage through a mosquito, for example in 'congenital malaria' (transmission from mother to child), through blood transfusion, or shared needles.

An important factor in the geographic distribution and the seasonality of malaria is the climate. At temperatures below 15 or 20 °C, the *Plasmodium* parasites cannot complete the part of the life cycle which takes place inside the *Anopheles* mosquito. Moreover, rainfall is important. Due to rainfall, puddles of stagnant water can arise, which form an important breeding site for mosquitoes. The eggs are deposited in the water and larvae and pupae will develop into adulthood here. Another factor of importance is the type of *Anopheles* mosquito that occurs in a certain region, since not all *Anopheles* species are equally good vectors for transmitting malaria from one person to another. *Anopheles gambiae*, for example, is an extremely effective vector and is one of the reasons why malaria is so prevalent in Africa.

As for susceptibility of humans towards an infection with *Plasmodium*, two genetic factors, both associated with human red blood cells, have been shown to be epidemiologically important. Persons who are negative for the Duffy blood group are resistant to infection by *P.*

vivax and persons who have the sickle cell trait are relatively protected against *P. falciparum*. (Sickle cell trait is a condition caused by a heterozygous hemoglobine beta-globin gene. One of the alleles is normal, the other one is abnormal, and since these alleles are co-dominant, both normal and sickle-shaped red blood cells will coexist in the patient's circulation.)

In areas with high transmission (most of the African continent, south of the Sahara), a person may develop a partially protective immunity after repeated attacks of malaria. They can still be infected, but may not display any symptoms. Also newborns are protected by this 'immunity' during the first few months of their life, presumably by the transfer of maternal antibodies. After this period, the young children are vulnerable to disease and death by malaria, and they are considered as a major risk group. Pregnant women are another risk group, since a malaria infection is both harmful to the mother and to the unborn child. It may lead to premature delivery, and/or low birth weight, with decreased chances of survival during the early months of life (CDC, 2015).

1.3.2 Lifecycle of *Plasmodium*

The lifecycle of *Plasmodium* parasites (Figure 1.1) involves two hosts: sexual reproduction of the parasites mainly takes place in the female *Anopheles* mosquito, while asexual reproduction occurs in the human host. Furthermore, the part of the *Plasmodium* life cycle which takes place in humans can be divided into a liver stage and a red blood cell stage.

When an infected *Anopheles* mosquito takes a blood meal, sporozoites are injected into the human blood stream. These sporozoites are rapidly taken up by the liver and develop to form schizonts. Schizonts are multinucleate cells and when they rupture, thousands of merozoites are released into the bloodstream (liver phase, exo-erythrocytic schizogony). Next, these merozoites enter erythrocytes, where they will develop into new schizonts, which will rupture and release more merozoites, destroying the respective erythrocyte. The merozoites can infect new red blood cells, transform into a ring form, trophozoites and schizonts consecutively, release new merozoites etc. (red blood cell stage, erythrocytic schizogony). In this way, the parasite burden will increase quickly and at this point, the clinical symptoms of malaria will appear. The schizonts will burst in near synchrony with other parasites, which causes the characteristic fever cycle, typical for malaria.

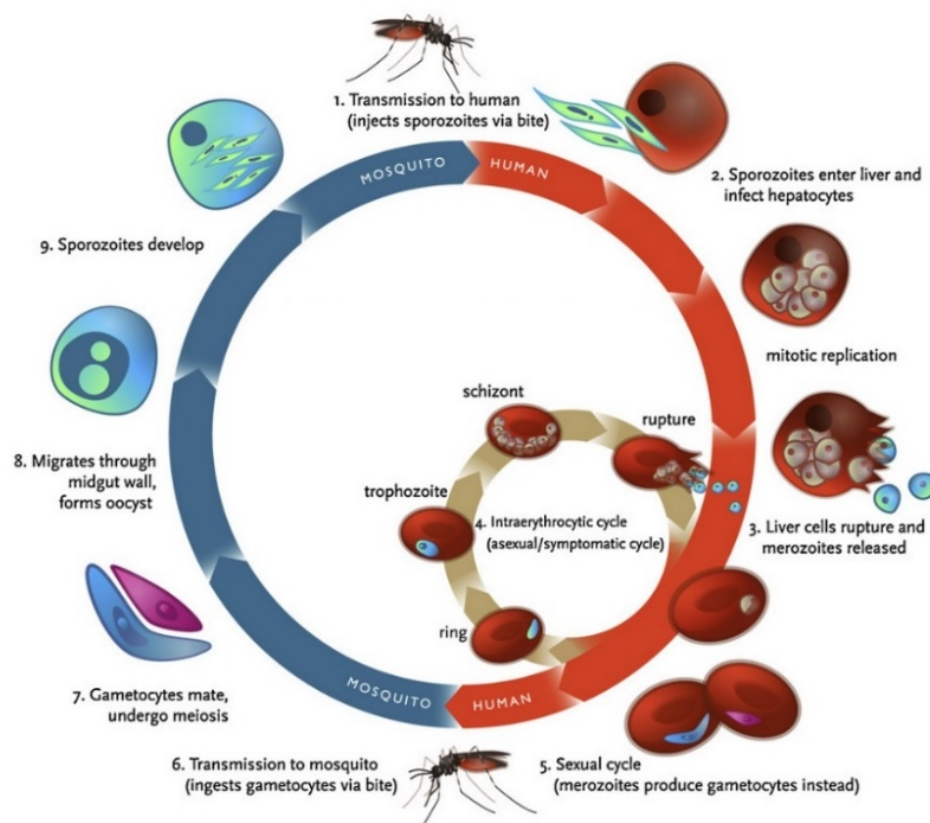


Fig. 1.1 Life cycle of the *Plasmodium* parasite. Adopted from Klein *et al.*, 2013.

So far, the asexual stage of the lifecycle is described. At some point however the sexual stage will be initiated, as a small percentage of merozoites differentiates into male and female gametocytes (microgametocytes and macrogametocytes, respectively).

If another female *Anopheles* mosquito takes a blood meal now, it will take up these gametocytes and once they reach the stomach of the mosquito, a microgametocyte can penetrate a macrogametocyte, generating a diploid zygote. The zygotes undergo meiosis and transform into an ookinete, which will invade the midgut wall of the parasite. Here, they develop into oocysts. The oocysts on their turn will grow, rupture and release thousands of sporozoites. The sporozoites will migrate to the salivary gland of the mosquito, ready to infect another human host. This cycle takes about 10 to 18 days.

In *P. vivax* and *P. ovale*, so-called hypnozoites can remain dormant in the hepatocytes and can cause relapses, by invading the bloodstream, weeks, months or even years later (Acheson *et al.*, 2007; Vinay *et al.*, 2007; Finch *et al.*, 2009; Klein *et al.*, 2013; CDC, 2015; MMV, 2016).

1.3.3 Clinical manifestations

Typically, malaria is categorized in two types, namely, uncomplicated and severe (or complicated) malaria. The clinical manifestations of malaria are dependent on the type of *Plasmodium* species which causes the infection.

P. vivax and *P. ovale* can only provoke uncomplicated malaria and cause rather similar clinical symptoms. These symptoms include fever and flu-like symptoms, such as chills, perspiration, headache, muscle aches, tiredness, and gastro-enteritis (nausea, vomiting, and diarrhea). The recurrence pattern of the fever is an indication of the type of *Plasmodium* species and in case of *P. vivax* or *P. ovale*, the fever typically flares up with 48 hour intervals, or in other words, every other day (day 1, day 3, etc.). Thus, this type of malaria is also referred to as 'malaria tertiana'. In general, the infection is rather mild and patients will only show acute symptoms. However, as mentioned before, reactivation of hypnozoites can cause relapses.

P. malariae leads to uncomplicated malaria as well and the clinical symptoms are similar to those described for *P. vivax* and *P. ovale*. However, in contrast to the latter two, the fever attacks occur every 72 hours, and thus, this type of malaria is called 'malaria quartana'. Often, an infection with *P. malariae* has a more chronic character.

Since the symptoms of uncomplicated malaria are quite non-specific, the disease is not always diagnosed (in an early stage) and the symptoms may be attributed to influenza, a cold, or other common infections, especially in countries where cases of malaria are infrequent.

P. falciparum is the only species which can cause severe (complicated) malaria, involving organ failure and/or abnormalities in the patient's blood or metabolism. In a majority of *P. falciparum* infections, the fevers don't appear on a regular basis, although it is possible that they return each 48 hours. Apart from the symptoms that were described for uncomplicated malaria, patients can appear confused or show abnormal behavior and can suffer from a decreased level of consciousness and seizures, since an infection with this species can affect the brain (cerebral malaria). If proper treatment is given, neurological defects may occasionally persist following cerebral malaria, including ataxia, speech difficulties, deafness or blindness.

When left untreated, the disease will progress, and this could lead to thrombocytopenia, hypoglycemia, metabolic acidosis, hypotension, tachypneu, shock and/or coma. Another

complication is the so-called 'blackwater fever'. In this case, severe intravascular hemolysis will lead to anemia, jaundice, hemoglobinemia, hemoglobinuria and acute kidney failure, which can lead to death in a period of days to weeks.

The incubation period of malaria varies from 7 to 30 days. Shorter periods are observed most frequently with *P. falciparum* and longer ones with *P. malariae*. Travelers who visited a country where malaria is endemic should take into account that, in case they were infected, malaria symptoms could appear months after their return, even if they took antimalaria drugs for prophylaxis (Acheson *et al.*, 2007; Vinay *et al.*, 2007; Finch *et al.*, 2009; CDC, 2015).

1.3.4 Pathogenesis

A malaria infection can affect several organ systems. Mainly the cardiovascular system is affected via different mechanisms. First of all, when the erythrocytes are invaded, their ability to deform decreases. They will be recognized as 'defective erythrocytes' by the spleen and they will be eliminated from the blood circulation. This can result in anemia and splenomegalia.

When the red blood cells lyse and release the merozoites, also numerous substances, such as hemozoin and other toxic factors are released at the same time. This will trigger the patient's immune system to fight the infection. Furthermore, the aggregation of both infected and non-infected erythrocytes is increased, which can cause formation of thrombi, and subsequently occlusion of a blood vessel.

In case the malaria infection is caused by *P. falciparum*, the red blood cells will produce the so-called '*Plasmodium falciparum* erythrocyte membrane protein 1' (PfEMP1). The presence of this protein will cause for the charge of the cell membrane of the erythrocyte to be changed from negative to positive. As a consequence, the erythrocyte will adhere to certain receptors on the endothelium of venules and capillaries, for example, ICAM-1 (intercellular adhesion molecule 1). In case a large number of red blood cells binds to endothelial receptors in this way, the perfusion of small blood vessels can be compromised and oxygen supply may become insufficient. On short term this can result in lactate acidosis, and on long term, this can cause organ dysfunction and even death. When this sequestration of infected erythrocytes occurs in the vessels of the brain, it is believed to be a factor in causing cerebral malaria (Acheson *et al.*, 2007; Vinay *et al.*, 2007; Finch *et al.*, 2009).

1.3.5 Diagnosis

Up to three months after visiting an area where *Plasmodium* parasites are endemic, the possibility of a malaria infection should be considered. Usually the diagnosis is made after an examination of a Giemsa-stained blood sample under a light microscope. An experienced eye is even capable of distinguishing the different *Plasmodium* species by the appearance of the trophozoites in the blood sample. In addition, several other diagnostic methods exist, for example, RDTs (Rapid diagnostic tests, based on plasmodial antigen detection), microscopy with fluorescent stain techniques or PCR (polymerase chain reaction) assays, but these are much less common.

When the required resources are not available, the diagnosis is solely based on clinical symptoms. However, this is not favorable, since it can lead to overutilization of antiparasmodial drugs, and the WHO recommends that diagnostic testing (either by microscopy or by RDTs) is applied in all cases of suspected malaria, prior to the start of an antiparasmodial treatment (Acheson *et al.*, 2007; Vinay *et al.*, 2007; Finch *et al.*, 2009; CDC, 2015).

1.3.6 Prophylaxis and treatment

An important factor in preventing and reducing malaria transmission is vector control.

People traveling to areas where malaria is endemic, should protect themselves against mosquito bites by the use of lotions or sprays with 20% to 50% DEET (*N,N*-diethyl-3-methylbenzamide). Moreover, it is recommended to sleep under a mosquito net treated with an insecticidal agent. Another approach is the indoor spraying with insecticides, which can remain effective for a period of 3 to 6 months. Pyrethroids, like permethrin, are mainly used for this purpose. Unfortunately, increasing resistance of mosquitoes is observed, making it increasingly important to check for susceptibility of mosquitoes in the different areas and for a combination of insecticides to be used (Acheson *et al.*, 2007; Finch *et al.*, 2009)

Both for chemoprophylaxis and treatment of malaria, different medicines are available (Figure 1.2). Interestingly, two of the antiparasmodial drugs are derived from plants whose medicinal values had been noted for centuries: the alkaloids quinine from *Cinchona* (South America, 17th century), and artemisinin from the Qinghao plant (*Artemisia annua* L., China, 4th century).

Quinine was isolated from the bark of *Cinchona* (or quina) by two French chemists in 1820. It became widely used in the treatment of intermittent fever throughout the world and is still

an important and effective treatment for malaria nowadays. Medicinal chemists tried to modify quinine in order to find new compounds with antiparasmodial activity and during World War II, **chloroquine** was developed. Chloroquine belongs to the class of aminoquinolines. Later in the 20th century, also **mefloquine** and **amodiaquine** were developed, belonging to the same class of drugs. The antiparasmodial activity of the aminoquinolines is based on the inhibition of parasite mediated heme detoxification. Nowadays, they are still used for the treatment of malaria, but mainly against chloroquine and mefloquine resistance is increasing.

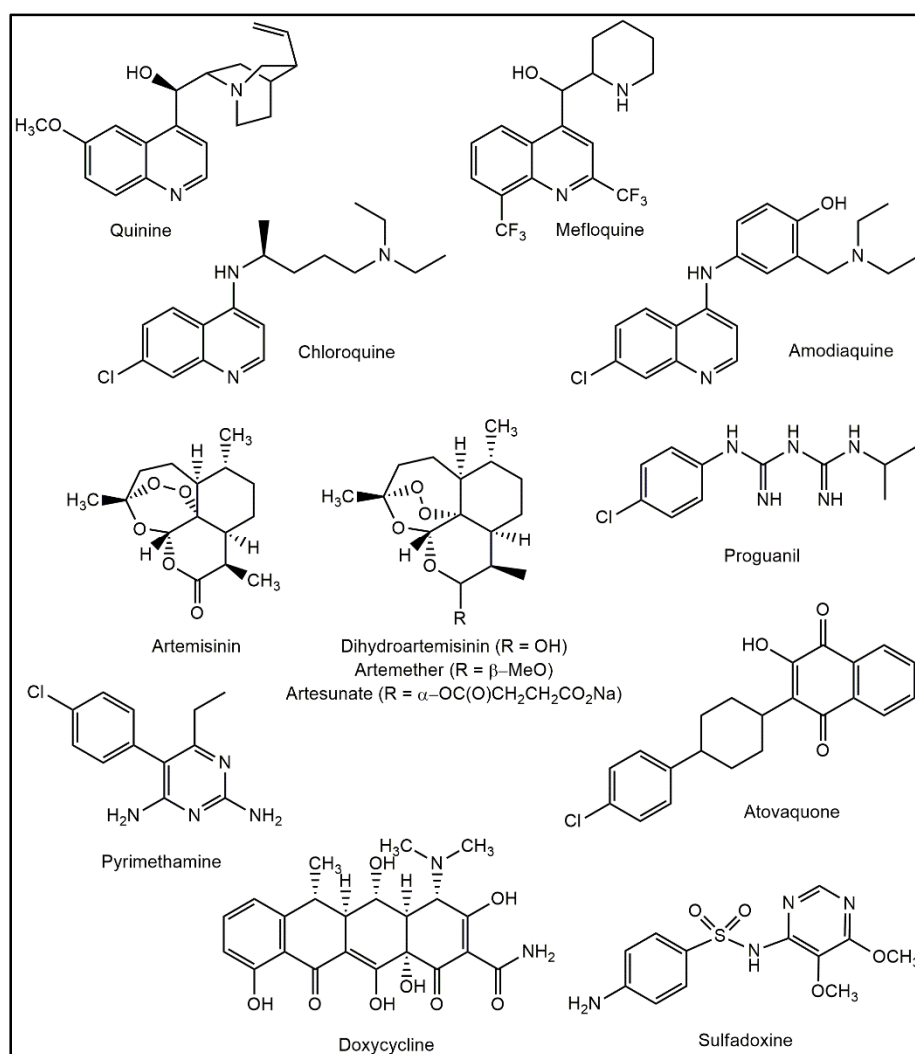


Fig. 1.2 Chemical structures of some commonly used antiparasmodial drugs.

Artemisinin was isolated from *Artemisia annua* L. (sweet wormwood) by the Chinese scientist Tu Youyou in 1972. Later on, derivatives like **dihydroartemisinin**, **artemether** and **artesunate** were developed, bearing a typical endoperoxide bridge like artemisinin. This class of drugs became the main line of defense against drug-resistant malaria in many parts of South-East

Asia. They are used for treatment of malaria and are specifically active against blood-stage parasites. A combination therapy based on artemisinin plus another antiplasmodial drug was often used and could improve treatment efficacy, while the likelihood of development of resistance was thought to be reduced. However, in 2009 evidence of resistance to artemisinin-based combination therapy was reported and its efficacy seems to decrease gradually. The best available treatment, particularly for *P. falciparum* malaria, is still an artemisinin-based combination therapy (ACT) and in 2015, Tu Youyou shared the Nobel Prize in Physiology or Medicine for her discovery.

During World War II the pyrimidine derivative **proguanil** was discovered. Later on, another pyrimidine derivative, namely **pyrimethamine** was developed. Unfortunately, resistance to the two monotherapies appeared quickly. A combination therapy with sulfones or sulfonamide antibiotics (for example, **sulfadoxine** with pyrimethamine) was then given, based on two different mechanisms of antifolate activity. However, the emerging resistance in South-East Asia could not be stopped and since the late 1990s resistance against these drugs also has been spreading rapidly. Nowadays, a combination of **atovaquone** with proguanil is still prescribed, mainly for prophylaxis, but also as treatment in certain cases. Atovaquone is a hydroxynaphthoquinone with antimalarial activity against all stages of all *Plasmodium* species. It interferes with the cytochrome electron transport system, resulting in the collapse of the mitochondrial membrane potential.

Another drug that is used to treat malaria is the broad-spectrum tetracyclic antibiotic drug **doxycycline**. It is indicated for prophylaxis of malaria, but it is also applied in a combination therapy and it acts by inhibiting protein synthesis of the parasite (Acheson *et al.*, 2007; Finch *et al.*, 2009; WHO, 2015; MMV, 2016).

The choice of treatment in case of malaria depends on the causative *Plasmodium* species, as well as on the severity of the disease and the area in which the infection took place, since resistance against the available drugs is strongly subjected to regional differences. People in developing countries do not always have access to these drugs. Instead, they seek refuge in traditional medicine, derived from various plants, to treat malaria.

For the past decades, pharmaceutical companies also made efforts to develop a vaccine against malaria. One of those, known as RTS,S/AS01, is the most advanced and phase I, II and III clinical trials have been conducted already. It acts against *P. falciparum* and it could serve as a complementary tool to control malaria. In July 2015, the European Medicines Agency (EMA) announced a positive 'European scientific opinion', taking into account both the quality and the risk/benefit profile of the vaccine. However, registration of the vaccine should be done by the national regulatory authorities of the African countries and at present, no regulatory authority has licensed RTS,S for use as a malaria vaccine. WHO is strongly supportive of pilot implementation of RTS,S. The pilot implementation program will generate more data to enable decision-making about the potential wider scale use of this vaccine in three to five years. In November 2016, the WHO announced that funding for the first phase of the vaccine pilots (2017-2021) had been secured and that vaccinations would begin in 2018 (WHO, 2016b).

1.4 Advanced Glycation End Products (AGEs)

Advanced glycation end products (AGEs) are a group of products, formed by a complex cascade of reactions, involving sugars and/or dicarbonyl compounds and proteins. In hyperglycemic conditions, their rate of formation is accelerated, and they are considered as an important factor in the development and progression of diabetic complications. Moreover, they are thought to play a role in neurodegenerative diseases, like Alzheimer's disease, in chronic inflammatory conditions, like rheumatoid arthritis, and in the normal aging process.

1.4.1 Formation of advanced glycation end products

The reactions that lead to the formation of AGEs can roughly be divided into early, intermediate, and advanced glycation reactions. The first step in the AGEs formation is a Maillard reaction or browning reaction, which is a spontaneous, non-enzymatic, reversible amino-carbonyl reaction between a reducing sugar (glucose, fructose, pentoses) and the free amino group of a protein (amino acids: lysine, arginine) (Figure 1.3). This reaction results in a Schiff base, which can undergo an Amadori rearrangement, with the formation of an Amadori

product (ketosamine) as result. One example of an Amadori product is HbA_{1c} (glycated hemoglobin), which is widely used as a diabetes control marker. These steps are considered as the early and intermediate stages (Peyroux *et al.*, 2006; Peng *et al.*, 2011; Sero *et al.*, 2013; Sadowska-Bartosz *et al.*, 2015).

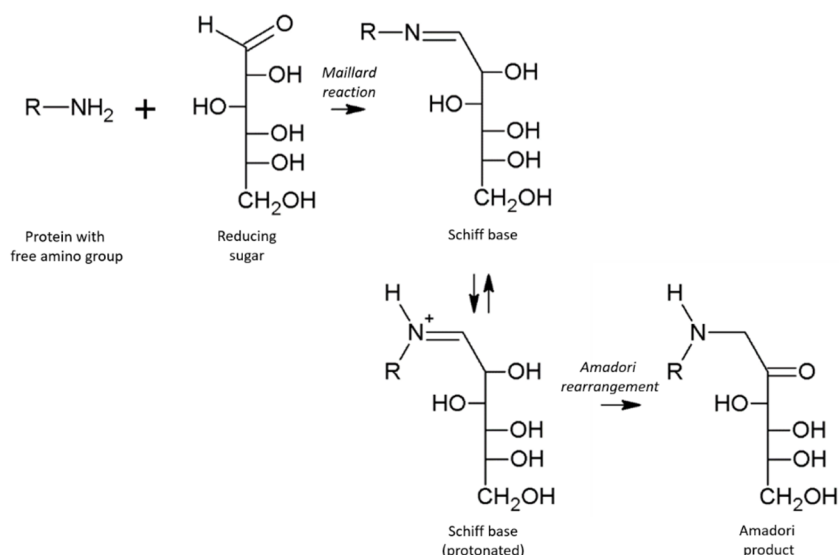


Fig. 1.3 Early and intermediate glycation reactions.

Dicarbonyl compounds like glyoxal (GO), methylglyoxal (MGO) and 3-deoxyglucosone (3-DG) (Figure 1.4) are important intermediates in the process of AGEs formation. A number of different reactions can lead to their formation, for example the autooxidation of carbohydrates, but also lipid peroxidation, or spontaneous decomposition of triose phosphates. Some of these reactions also produce free radicals, causing oxidative stress, which in turn will lead to an increased formation of AGEs. Dicarbonyl compounds are highly reactive and will thus form AGEs more rapidly, compared to AGEs derived from Amadori products (Rahbar *et al.*, 2003; Voziyan *et al.*, 2003; Borg *et al.*, 2016; Khangoli *et al.*, 2016).

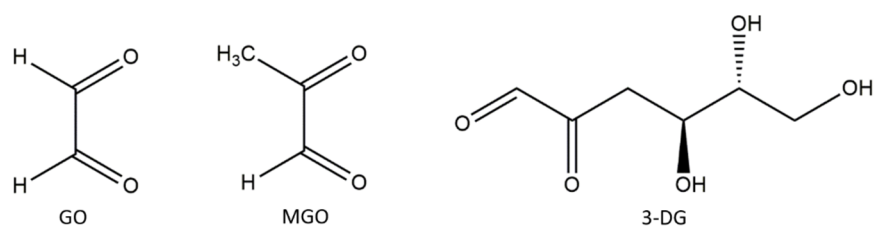


Fig. 1.4 Chemical structures of glyoxal (GO), methylglyoxal (MGO) and 3-deoxyglucosone (3-DG)

In the advanced steps of the AGEs formation, a combination of oxidation, dehydrogenation, condensation and/or cross-linking reactions will take place. AGEs formation starting from an Amadori product can occur by a combination of both oxidative and non-oxidative reactions, while AGEs formed by reaction of dicarbonyl compounds with proteins typically takes place by non-oxidative reactions. Proteins which have undergone such reactions are referred to as 'glycated proteins', 'Maillard reaction products' or advanced glycation end products. The AGEs can be divided into fluorescent and non-fluorescent AGEs and cross-linked or non-crosslinked AGEs (Rahbar *et al.*, 2003; Peng *et al.*, 2011). A general scheme of the AGEs formation is given in Figure 1.5 and an overview of the most common AGEs is given in Table 1.1.

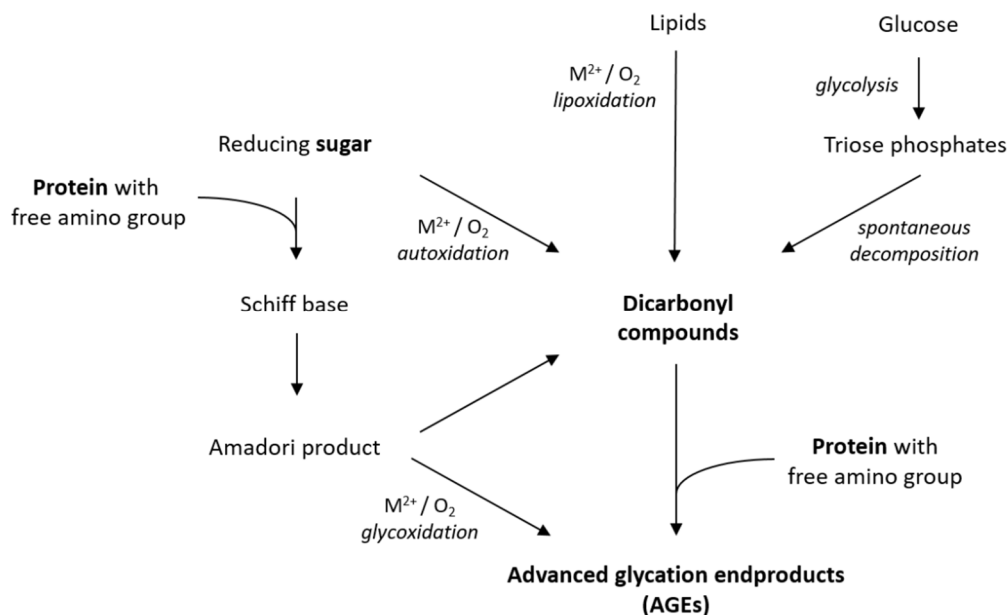
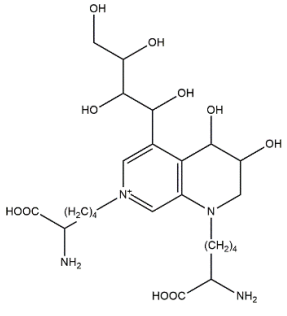
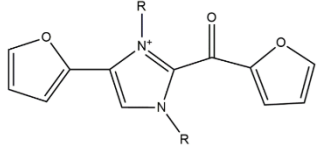
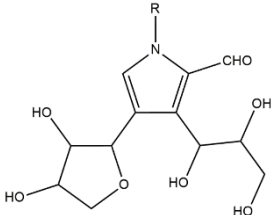
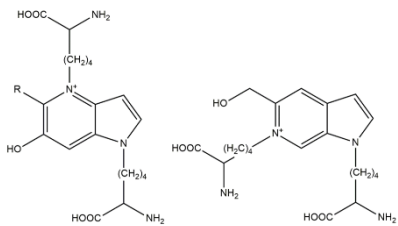


Fig. 1.5 Basic scheme, displaying the AGEs formation process.

Table 1.1. Overview of some common AGEs, their abbreviations, fluorescence maxima and chemical structures.

Full name	Abbreviation	Fluorescence maxima ($\lambda_{em}/\lambda_{el}$)	Chemical structure
carboxymethyllysine	CML	-	
carboxyethyllysine	CEL	-	
glyoxal-derived lysine dimer	GOLD	-	<p> $R = H$ GOLD $R = CH_3$ MOLD $R =$ (deoxyglucosone derivative) DOLD </p>
methylglyoxal-derived lysine dimer	MOLD		
deoxyglucosone-derived lysine dimer	DOLD		
argpyrimidine	-	320 nm / 385 nm	
pentosidine	-	335 nm / 385 nm	
hydroimidazolone (MGO-derived, 3 isomers)	-	-	<p>MG-H1 MG-H2 MG-H3</p>

Full name	Abbreviation	Fluorescence maxima ($\lambda_{em}/\lambda_{el}$)	Chemical structure
crossline	-	380 nm / 460 nm	
2-(2-furoyl)-4(5)-furan-1 <i>H</i> -imidazole	FFI	-	 <p>R = Lys or Arg</p>
1-alkyl-2-formyl-3,4-glycosyl-pyrrole	AFGP	-	 <p>R = Lys or Arg</p>
vesperlysine-A	-	370 nm / 440 nm	 <p>R = H Vesperlysine-A R = CH₃ Vesperlysine-B</p> <p>Vesperlysine-C</p>
vesperlysine-B	-	370 nm / 440 nm	
vesperlysine-C	-	370 nm / 440 nm	

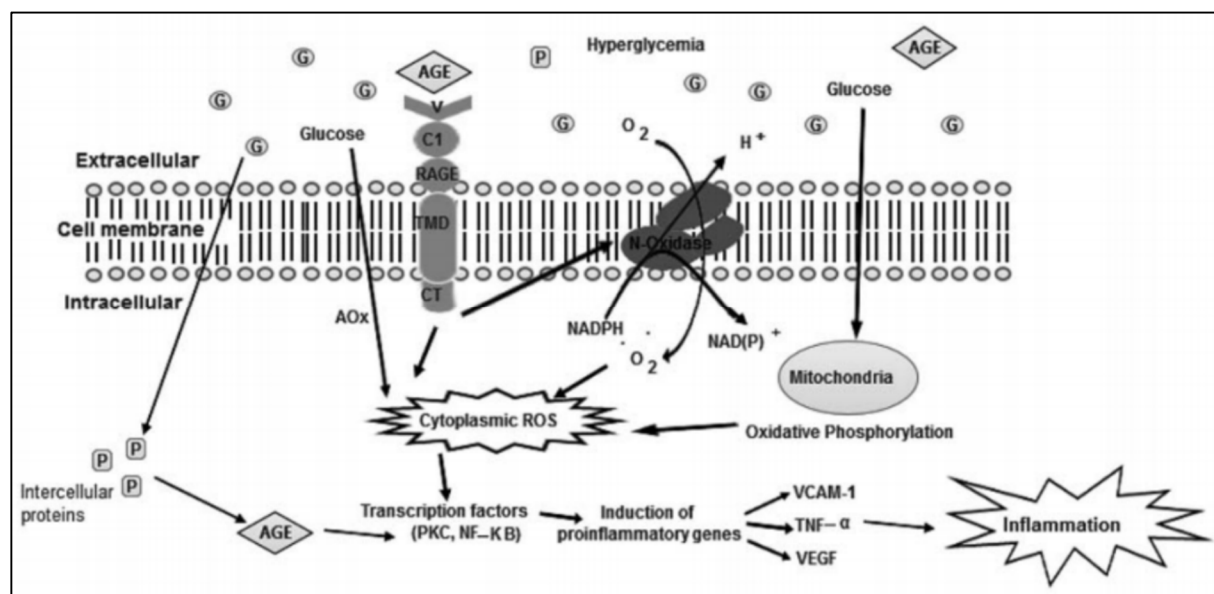
Lys: lysine; Arg: arginine

1.4.2 AGEs and pathogenesis of diabetic complications

Glycation of proteins causes structural and functional changes of the respective proteins, both intracellularly and extracellularly. The direct consequences of the structural changes can vary from immobilization by crosslinkage, to addition of resistance to proteases. Several functional changes can be caused by glycation: extracellular matrix proteins can show aberrant interactions with other matrix compounds and with receptors for matrix proteins. Also

changes in cell receptor activity and/or altered enzyme activity are possible. Furthermore, the formation of high amounts of AGEs is associated with increased production of free radicals and a rise in carbonyl stress, both leading to increased oxidative stress. This is the start of a positive feedback loop, since increased oxidative stress in turn will stimulate more AGEs formation, and thus, more and more AGEs will be formed.

Moreover, the binding of AGEs to the receptor for AGEs (RAGE) on endothelial cells, mesangial cells and macrophages, will induce the production of reactive oxygen species (ROS), either directly, or through activation of NADPH-oxidases (reduced nicotinamide adenine dinucleotide phosphate-oxidases). Increased levels of cytoplasmic ROS will lead to nuclear translocation of transcription factors such as NF- κ B (nuclear factor kappa light chain enhancer of activated B cells), and these transcription factors will cause an upregulation of several pro-inflammatory genes, resulting in a rise of pro-inflammatory cytokines, growth factors and adhesion molecules, eventually leading to inflammation (Figure 1.6) (Brownlee, 2001; Rahbar *et al.*, 2003; Peyroux, 2006 *et al.*; Khangoli *et al.*, 2016).



G: glucose; P: phosphate, RAGE: receptor for AGEs, composed of V, C1, C2 (extracellular domains) RAGE, TMD: transmembrane domain, and CT: cytoplasmic tail. AOx: autooxidation; ROS: reactive oxygen species; NADPH: reduced nicotinamide adenine dinucleotide phosphate; NAD(P): nicotinamide adenine dinucleotide (phosphate); PKC: protein kinase C; NF- κ B: nuclear factor kappa light chain enhancer of activated B cells; VCAM: vascular cell adhesion protein 1; TNF- α : tumor necrosis factor α ; VEGT: vascular endothelial growth factor.

Fig. 1.6 Simplified mechanisms of the pathogenesis of AGEs in hyperglycemic conditions.
(Adopted from Khangoli *et al.*, 2016)

AGEs contribute to the development and progression of several diabetic complications, both micro- and macroangiopathies (Peng *et al.*, 2011; Khangoli *et al.*, 2016).

One common complication of diabetes is **retinopathy**. Accumulation of AGEs will affect capillaries of the eye, for example, by thickening of the basement membrane, leading to retinal ischemia, neovascularization, and increase of the capillary permeability (dysfunction of the blood-retinal barrier). Moreover, the loss of endothelial cells and pericytes (perivascular cells located within the basal lamina of the microvessel, which are believed to have a contractile role, similar to that of smooth muscle cells in larger vessels) will be increased. The clinical expression of retinopathy is associated with this vascular damage and eventually these changes can lead to visual impairment or even blindness. Also a reduced transparency of the lens may occur, as a consequence of the alteration of the surface charge of proteins due to AGEs formation, leading to **cataract**. Since many of the cells of the eye have little or no regenerative capacity, these cells are particularly susceptible to the effects of AGEs (Zong *et al.*, 2011; Milne *et al.*, 2013; Sadowska-Bartosch *et al.*, 2015).

Thickening of the basal membrane and expansion of the mesangial layer in the glomeruli of the kidney can cause a decrease in the filtration capacity of the glomeruli. The promotion of certain growth factors on the other hand, will increase vascular permeability. These changes can lead to diabetic **nephropathy** (Khangoli *et al.*, 2016).

Diabetic **neuropathy** is promoted by AGEs via two mechanisms that are specific for the nerve system. The first one is a demyelination of the nerves, which is related to the interaction of glycated myelin with IgM and IgG (immunoglobulins M and G) and to the uptake of glycated myelin by macrophages. The second is nerve dysfunction, caused by glycation of neurofilaments and tubulin proteins, which interferes with the axonal transport, and which can lead to atrophy and degeneration of the affected nerve fibers (Wada *et al.*, 2005).

High levels of AGEs in the blood vessels will lead to an increased risk of **atherosclerosis** and **cardiovascular diseases**. AGEs induce the proliferation of vascular smooth muscle cells, leading to thickening of the intima and rigidity and stiffness of the vessels, while collagen-linked AGEs may quench nitric oxide (NO), both augmenting vascular dysfunction. Moreover,

the permeability of endothelial cells increases under influence of AGEs. AGEs initiate oxidative reactions on plasma low-density lipoproteins (LDL), which promotes the formation of oxidized LDL. Through several mechanisms, AGEs also induce the transition of macrophages into foam cells, thus leading to accelerated plaque formation, and eventually atherosclerosis. Moreover, AGEs will increase the procoagulant activity, which causes an increased risk of thrombosis (Aronson *et al.*, 2002; Basta *et al.*, 2004).

Apart from pathological conditions related to diabetes, AGEs are also thought to play a role in **neurodegenerative diseases**, in **chronic inflammatory diseases**, like **rheumatoid arthritis**, and in the **normal aging process**.

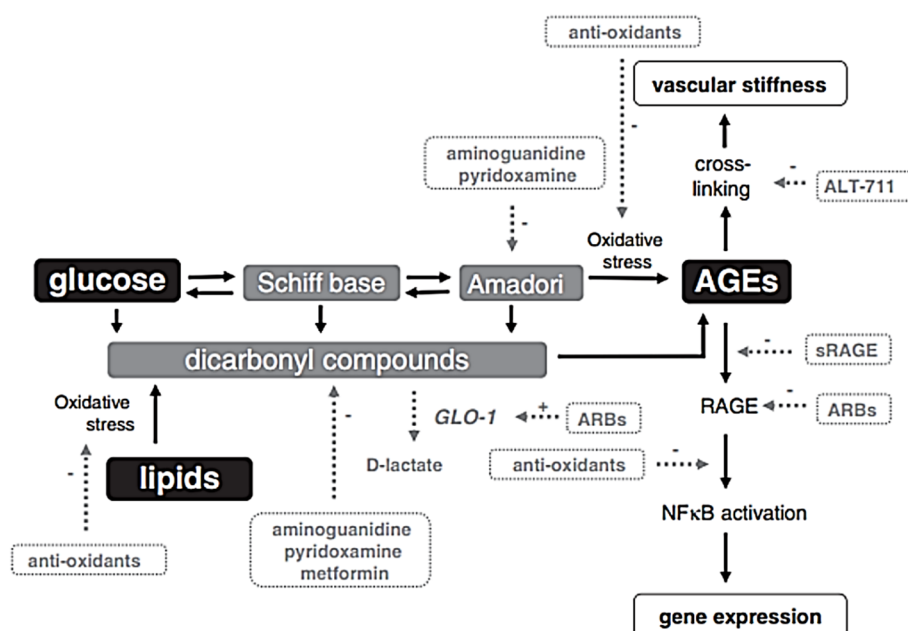
Increased levels of AGEs may explain many of the neuropathological and biochemical features of **Alzheimer's disease**, such as oxidative stress and neuronal cell death. Moreover, AGEs related crosslinking of β -amyloid peptides accelerates the β -amyloid polymerization, and plaque formation, which is one of the most typical markers of Alzheimer's disease (Munch *et al.*, 1997; Rahbar *et al.*, 2003). However, a more recent study revealed a lower level of circulating serum AGEs in patients with Alzheimer's disease in relation to healthy controls, and a controversy remains regarding the content of AGEs as a biochemical marker of Alzheimer's disease (Sadowska-Bartosz *et al.*, 2015).

Various natural defense mechanisms are capable of inhibiting the accumulation of AGEs in the body. The enzymes oxoaldehyde reductase and aldose reductase are able to detoxify reactive dicarbonyl intermediates and the glyoxalase system (I and II) catalyzes the deglycation of reactive dicarbonyls, like MGO. Additionally, the enzyme fructosamine-3-kinase phosphorylates fructoselysine residues on glycated proteins, which leads to its spontaneous decomposition, thereby reversing the non-enzymatic glycation process at an early stage (Jack *et al.*, 2012; Rahbar *et al.*, 2003). It is hypothesized that the human body can regulate the flux of circulating and extracellular AGEs through binding and internalization via receptor-mediated endocytosis. This can occur via scavenger receptors such as SR-A, SR-B1, or AGE receptor 1 (AGE-R1) and galectin-3 (or AGE-R3) (Borg *et al.*, 2016).

1.4.3 AGEs inhibitors

Products with the capability to reduce AGEs formation could contribute to the health of diabetic patients, by delaying the onset of complications, and could be beneficial to Alzheimer's patients or patients with chronic inflammatory diseases. Their mechanism of action can be based on different principles: entrapment or indirect inhibition of formation of reactive dicarbonyl compounds, metal chelation, antioxidant (radical scavenging) activity or inhibition of the conversion of Amadori products into AGEs. Other modes of action involve blockage of the receptor for advanced glycation end products (RAGE), or the breakage of already formed AGEs (so called 'crosslink breakers') (Rahbar *et al.*, 2003; Peyroux *et al.*, 2006; Peng *et al.*, 2011; Wu *et al.*, 2011; Borg *et al.*, 2016).

Several products are known to act as AGEs inhibitors (Figures 1.7 and 1.8), and an overview is given in the next paragraphs. Compounds for which their mode of action can solely be attributed to their antioxidant activity are not taken into account here, since this activity is not specific for the inhibition of AGEs formation.



ARBs: angiotensin receptor blockers; GLO1: glyoxalase, NF-κB: nuclear factor kappa light chain enhancer of activated B cells; NO: nitric oxide; (s)RAGE: (soluble) receptor for advanced glycation end products.

Fig. 1.7 Potential sites of intervention in the glycation pathway, adopted from Engelen *et al.*, (2013). The various pathways of AGEs formation and the deleterious consequences of AGEs are shown in grey and black, respectively. A detoxification pathway and potential sites of intervention are indicated with dotted arrows and lines.

- Hydrazine-containing compounds

Aminoguanidine is the most studied AGEs inhibitor, both *in vitro* and *in vivo*. It acts by the entrapment of reactive dicarbonyl compounds and by inhibition of NOS (nitric oxide synthase). Clinical trials have been performed with this compound, but side effects, such as elevated liver enzyme levels and the development of autoantibodies, were reported. The respective study was then terminated due to an unfavorable perceived risk-to-benefit ratio (Rahbar *et al.*, 2003; Peyroux *et al.*, 2006; Engelen *et al.*, 2013; Nenna *et al.*, 2015; Borg *et al.*, 2016). These days, aminoguanidine is still the most used positive control in many *in vitro* tests.

Metformin, the first choice medicine for treatment of type II diabetes, also acts as an AGEs inhibitor. It is thought to cause a reduction of circulatory MGO in type II diabetic patients, which is attributed to the entrapment of MGO and other dicarbonyls. However, in two randomized trials no additional effects of metformin were observed in comparison to other anti-hyperglycemic treatments, which suggests that these AGEs inhibiting effects result from an improvement in glycemic control rather than from a specific dicarbonyl detoxification (Rahbar *et al.*, 2003).

ALT-946, or *N*-(2-acetamidoethyl) hydrazinecarboximidamide hydrochloride, also entraps dicarbonyl compounds, but inhibits NOS only minimally. No clinical studies have been performed with ALT-946 (Rahbar *et al.*, 2003; Nenna *et al.*, 2015).

- Vitamins and vitamin derivatives

Pyridoxamine, a vitamin B6 derivative, inhibits the conversion of Amadori products to AGEs (post-Amadori inhibitor), and can react with GO or GLA (glycolaldehyde). The reaction with GO or GLA results in the formation of relatively stable cyclic aminor derivatives, and makes the reactive carbonyl species unavailable for reaction with proteins, thus inhibiting the formation of AGEs. Moreover, chelation of dicationic metal ions was shown *in vitro*. A phase II clinical study has shown a reduction in CML and CEL in diabetic individuals with nephropathy after treatment with pyridoxamine for up to 24 weeks (Voziyan *et al.*, 2002; Peyroux *et al.*, 2006; Engelen *et al.*, 2013; Borg *et al.*, 2016).

Thiamine (pyrophosphate) and **benfotiamine**, the water- and lipid-soluble forms of vitamin B1, are also reported as AGEs inhibitors. Benfotiamine is an activator of transketolase, which converts glyceraldehyde-3-phosphate into pentose-5-phosphate. This conversion causes

shunting from the glycolytic pathway towards the reductive, anaerobic glycolytic pentose phosphate pathway. Thus, less spontaneous decomposition of triose phosphates into reactive dicarbonyl compounds will occur. AGEs inhibiting activity was found *in vitro* and decreased levels of different AGEs were found in STZ (streptozotocine) diabetic rats. However, results of clinical trials with benfotiamine were disappointing (Rahbar *et al.*, 2003; Peyroux *et al.*, 2006; Nenna *et al.*, 2015; Borg *et al.*, 2016).

(It is important to stress that in all clinical trials related to AGEs, mostly the levels of circulating AGEs are assessed. It is uncertain whether elevated circulating AGE levels adequately reflect the burden of the glycation pathway in the organs/tissues. Therefore, there might be a possibility that the discrepancy between the results obtained with clinical studies and the beneficial effects that were found previously in *in vitro* experiments and animal experiments lies in the type of tissue examined. Moreover, different clinical trials display a large heterogeneity, both in the outcome measures evaluated as in the techniques used, which makes it difficult to compare results and to evaluate the potential of different therapies to inhibit the glycation pathway (Engelen *et al.*, 2013).)

- Others

The anti-diabetic **thiazolidinediones** are so-called 'insuline sensitizers', by acting as agonists of PPAR-γ (peroxisome proliferator activated receptor gamma). In addition, **pioglitazone**, has been reported as an AGEs inhibitor. Also **OPB-9195**, another thiazolidinedione compound, showed AGEs inhibiting activity. They possess metal-chelating properties, and their activity as PPAR-γ agonists will induce an increase in sRAGE (soluble receptor for advanced glycation end products). sRAGE is the truncated form of RAGE, constituted by the extracellular ligand-binding domain of the receptor. AGEs can bind to sRAGE in the same way as they bind to other receptors for AGEs. However, binding to sRAGE makes the respective AGEs harmless, since they will not elicit any activity. The increase in sRAGE could be confirmed *in vivo*, but unfortunately clinical trials were hampered by side effects, related to the trapping of pyridoxal, resulting in a vitamin B6 deficiency syndrome (Rahbar *et al.*, 2000; Rahbar *et al.*, 2003; Peyroux *et al.*, 2006; Nenna *et al.*, 2015).

Certain **ACE-inhibitors** (angiotensin converting enzyme inhibitors) and **ARBs** (angiotensin receptor blockers) have been proven to cause a reduction in AGEs levels *in vitro* and *in vivo*, as well as during clinical trials. This may be attributed to anti-oxidant and metal-chelating properties. Possibly, the treatment with ACE-inhibitors leads to an increase in sRAGE too (Peyroux *et al.*, 2006; Engelen *et al.*, 2013; Nenna *et al.*, 2015).

The group of LR-compounds (named after the developers, Lalezari-Rahbar) were produced as derivatives of aryl (and heterocyclic) ureido and aryl (and heterocyclic) carboxaminidophenoxyisobutyric acids. They are potent chelators of Cu²⁺ ions, and they can interact directly with α -dicarbonyl species. **LR-90** is one of the most promising compounds of this type. *In vivo* studies in rats led to promising results, however, none of the LR compounds have been tested in clinical trials yet (Peyroux *et al.*, 2006; Borg *et al.*, 2016).

PTB (*N*-phenacylthiazolium bromide) is a thiazolium-containing compound, which acts as an AGE crosslink breaker. The activity was seen *in vitro*, but did not occur *in vivo*. Since PTB was not stable under physiological conditions, further analogs were developed. The most studied analog is **alagebrium** (ALT-711®). Apart from acting as AGE crosslink breaker, alagebrium is also capable of scavenging MGO, and it has metal-chelating properties. However, its exact mechanism of action remains controversial. Phase I clinical trials reported that no detrimental effects on liver function were observed and no serious adverse events or deaths resulted from alagebrium therapy. A number of phase II clinical trials were performed, mainly focused on the effect of alagebrium on different parameters related to the cardiovascular system in patients with or without diabetes. Due to financial constraints, several of these trials were prematurely discontinued and at this moment, the effects that were observed in diabetic rodent models can not be confirmed in humans (Peyroux *et al.*, 2006; Engelen *et al.*, 2013; Borg *et al.*, 2016).

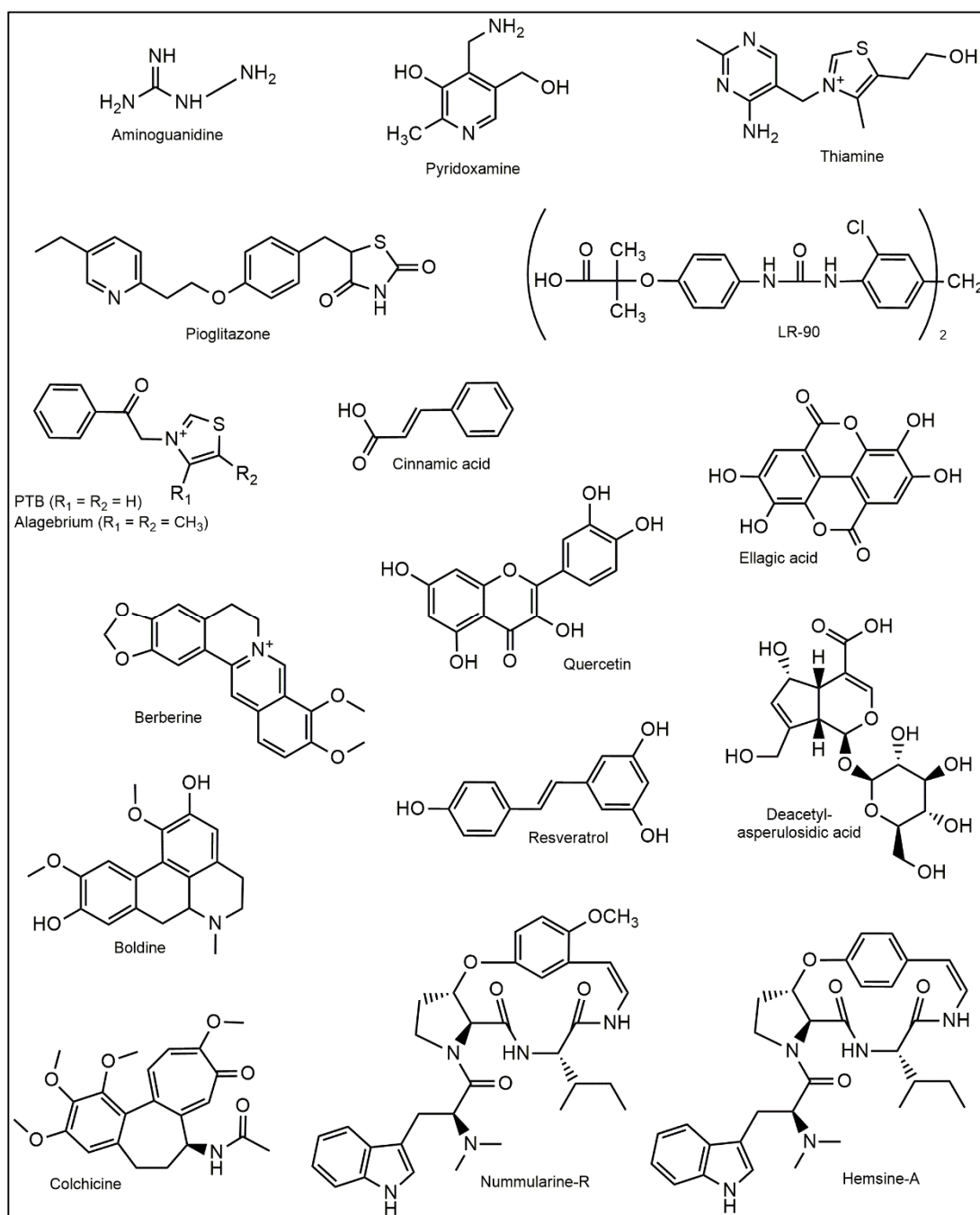


Fig. 1.8 Chemical structures of some AGEs inhibitors of synthetic or natural origin.

■ Plant-derived natural products

It is noted that the inhibitory effects on the formation of AGEs of extracts from plants are mainly due to the abundant amount of **polyphenols**. *In vitro* glycation assays showed that a number of polyphenolic compounds exerted inhibitory effects on the glycation reaction. Polyphenols are known for their antioxidant activity, but this is not always the only reason for their AGEs inhibitory properties.

Examples of **phenolic acids** with *in vitro* AGEs inhibitory activity are cinnamic acid, ferulic acid, isoferulic acid and ellagic acid. The latter acid, a benzoic acid derivative, predominantly inhibits the formation of CEL through scavenging of dicarbonyl compounds, while isoferulic acid, a phenylpropene compound, has been found to be a metal ion chelating agent, which could support its AGEs inhibiting activity. Also chlorogenic acid, formed by the esterification of caffeic and quinic acid, acts as an AGEs inhibitor. Its inhibitory effects on AGEs formation and collagen cross-linking may be caused by its interaction with reactive dicarbonyl compounds, such as MGO. Furthermore, certain **tannins** and **anthocyanins** were reported as AGEs inhibitors (Kim *et al.*, 2011; Silván *et al.*, 2011; Peng *et al.*, 2011; Adisakwattana *et al.*, 2012; Meeprom *et al.*, 2013; Sadowska-Bartosz *et al.*, 2015).

A range of **flavonoids**, including quercetin, rutin, naringin and kaempferol, **isoflavonoids** (like genistein) and **stilbenes** (resveratrol), also have been demonstrated to be effective inhibitors of AGEs formation. In general, the flavonoids with evident AGEs inhibitory activities also possess strong radical scavenging activities. However, apart from their antioxidant activity, some were found to inhibit the increase in 3-DG, but the mechanism behind this is not known (Matsuda *et al.*, 2003; Sasaki *et al.*, 2014; Sadowska-Bartosz, 2015).

Matsuda *et al.* (2003) investigated the structural requirements of flavonoids for inhibition of protein glycation and radical scavenging activities. Ten years later, Xie and Chen published an article concerning the influence of hydroxylation, methylation, glycosylation and other structural changes on flavonoids, stilbenes and phenolic acids, and summarized which structural features are relevant for their anti-glycation activity (Matsuda *et al.*, 2003; Xie *et al.*, 2013). These are the only reports so far involving a structure-activity relationship study of natural products and their AGEs inhibiting activity.

The **iridoids** deacetylasperulosidic acid and loganic acid, major iridoids from *Morinda citrifolia*, were shown to inhibit *in vitro* AGEs inhibition in a concentration-dependent manner. Further positive results for other iridoids in *in vitro* experiments are limited. *In vivo* tests on the contrary, revealed positive effects on the level of AGEs for various extracts rich in iridoid (glycosides) and for purified iridoids. A likely explanation for this is the *in vivo* metabolism of iridoids, resulting in more biologically active compounds. An example of this is hydroxytyrosol, a major metabolite of oleuropein. Oleuropein displayed little activity in an *in vitro*

antiglycation activity assay, while hydroxytyrosol was active by binding to MGO, thereby limiting the formation of AGEs via carbonyl scavenging. Although this mode of action was found for hydroxytyrosol, also antioxidant activity, and effects on NF- κ B and aldose reductase seem to be involved in the AGEs inhibiting properties of iridoids (West *et al.*, 2014; West *et al.*, 2016).

Various **alkaloids** were also reported as inhibitors of AGEs formation. Derbré *et al.*, (2010) screened a library of 81 natural products for their *in vitro* AGEs inhibiting activity. Several of the tested compounds were found to be more active than the reference compound aminoguanidine, including the alkaloids berberine, boldine and colchicine. (It is interesting to note that two other tested alkaloids, harmine and emetine, caused a significant increase in the amount of AGEs.) Moreover, the **cyclopeptide alkaloids** nummularine-R and hemsine-A, isolated from *Ziziphus oxyphylla*, showed moderate antiglycating activities *in vitro* (Choudhary *et al.*, 2011).

1.5 Aim of this Work

The aim of this thesis was to create a small library of cyclopeptide alkaloids, including data related to their structural characteristics (spectroscopic data) and data obtained from biological activity tests (antiplasmodial activity, cytotoxicity, AGEs inhibition). These data are then used to establish structure-activity relationships for the class of cyclopeptide alkaloids in these different fields.

Four different plant species were selected for this project, based on a literature search for the presence of cyclopeptide alkaloids, the traditional use of plant extracts in the treatment of malaria, and/or reported biological activities (antiplasmodial and/or AGEs inhibiting properties) of plant extracts or isolated compounds. The following plant species were selected: *Hymenocardia acida*, *Ziziphus oxyphylla*, *Ziziphus nummularia* and *Ziziphus spinachristi*.

***Hymenocardia acida* Tul.** (Phyllanthaceae) (**Chapter 4**) is a shrub or small tree of about 6 m high that grows in the African Savannah. Extracts of this plant have been used in traditional African medicine for treatment of different medical conditions. For example, the leaves and roots are used to treat malaria, the roots are used against hypertension, and the plant may be employed as an antiseptic and to treat skin diseases. Another application is the use of decoctions of the leaves or roots to relieve pain. Previous phytochemical studies have shown the presence of alkaloids, anthocyanins, anthraquinones, cardiac glycosides, flavonoids, phenols, saponins, steroids, stilbenoids, tannins and triterpenoids. Pais *et al.* (1968) were the first to isolate and identify the cyclopeptide alkaloid hymenocardine from the stem bark of *H. acida*.

The *in vitro* antiplasmodial activity and cytotoxicity of extracts from the leaves of *H. acida* has been shown by Vonthron-Senecheau *et al.* (2003). Mahmout *et al.* (2005) reported lupeol, lupeyl docosanoate and β -sitosterol to be present in *H. acida*, which showed antiplasmodial activity, related to their amphiphilic nature. Apart from this, little is known about its antiplasmodial constituents.

***Ziziphus oxyphylla* Edgew.** (Rhamnaceae) (**Chapter 5**) is a small- to medium-sized tree that grows in the northern regions of Pakistan. The fruits are used as common food and in traditional medicine different parts of the plant are applied in a wide range of pathological conditions, for example, to treat inflammation, microbial infections, fever or pain, allergy and diabetes. Previous investigations have already shown *in vivo* antipyretic effect of a methanolic extract of *Z. oxyphylla* leaves and the antinociceptive activity of methanolic extracts of the leaves and roots of this plant (Nisar *et al.*, 2007; Kaleem *et al.*, 2013), but the active compounds are not known. Phytochemical tests revealed the presence of alkaloids, anthraquinones, flavonoids, glycosides, phenols, saponins and tannins and so far seven cyclopeptide alkaloids were isolated and identified from roots and stem (bark) of this species, *i.e.* hemsine-A, nummularine-C and -R, and oxyphylline-A, -B, -C and -D (Inayat-ur-Rahman *et al.*, 2007; Choudhary *et al.*, 2011; Kaleem *et al.*, 2012). Nummularine-C, nummularine-R and hemsine-A were found to inhibit α -glucosidase, the latter two also could inhibit the formation of AGEs (Choudhary *et al.*, 2011). Moreover, hemsine-A was shown to possess antiplasmodial activity *in vitro* (Panseeta *et al.*, 2011).

***Ziziphus nummularia* (Burm.f.) Wight & Arn.** (Rhamnaceae) (**Chapter 6**) is a thorny shrub that grows in India and Pakistan. It is widely used in ethnomedicine, for example, the fruit and root are used to treat diarrhea, and the leaves as an antipyretic and against pain and inflammation. Phytochemical analysis has revealed the presence of flavanoids, phenolic acids, tannins, sterols, saponins, pectin, glycosides and triterpenoic acids (Goyal *et al.*, 2013; Ray *et al.*, 2015; Rauf *et al.*, 2016;). In addition, it is a rich source of cyclopeptide alkaloids, with almost 30 different compounds reported until now (Tschesche *et al.*, 1975; Dwivedi *et al.*, 1987; Singh *et al.*, 1995).

***Ziziphus spina-christi* (L.) Desf.** (Rhamnaceae) (**Chapter 6**) is a shrub or tree, growing in areas with a sub-tropical climate, for example, Egypt, Saudi Arabia, Iraq, Iran and Pakistan. It is used for various medicinal purposes: fruits of this species are used in cases of dysentery and to treat bronchitis and cough, and a decoction of the bark and fresh fruit is used to promote the healing of fresh wounds. It is also used in some inflammatory conditions and against pain. Previous studies indicated that *Z. spina-christi* contained flavonoids, tannins, sterols, saponins, and triterpenoids (Shahat *et al.*, 2001; Farmani *et al.*, 2016). In addition, eleven different

cyclopeptide alkaloids were reported from its stem bark and/or root bark (Tschesche *et al.*, 1974; Shah *et al.*, 1986; Abdel-galil *et al.*, 1991).

Chapter 7 is dedicated to the investigation of the *in vitro* and *in vivo* gastrointestinal absorption and biotransformation of hymenocardine. In view of the peptide-like nature of cyclopeptide alkaloids, the potential metabolism after oral ingestion has to be taken into account. Absorption and metabolic conversion are important factors when performing *in vivo* experiments and can be the reason for sometimes strikingly different results of *in vitro* and *in vivo* experiments.

In order to establish the influence of particular structural characteristics of the cyclopeptide alkaloids on their biological activity, a quantitative structure-activity relationship study (QSAR) was performed (**Chapter 8**).

Finally, **Chapter 9** gives an overview of the *in vitro* experiments that were carried out for the determination of the inhibition of AGEs formation. Apart from the methodology and the results obtained, also the advantages and disadvantages of each technique will be described.

Thus, the research envisaged in this project comprised three stages:

1. Isolation and identification of cyclopeptide alkaloids using chromatographic and spectroscopic techniques;
2. Assessment of *in vitro* antiplasmodial activity, cytotoxicity, and AGEs inhibitory activity;
3. Establishment of structure-activity relationships of cyclopeptide alkaloids, with respect to the investigated targets.

References

- Abdel-galil, F. M. and El-Jissry, M. A., 1991. Cyclopeptide alkaloids from *Zizyphus spina-christi*. *Phytochemistry* **30**(4): 1348-1349.
- Acheson, D., Anderson, A. C., Androphy, E. J., Atmar, R. L., Barbieri, J. T., *et al.*, 2007. Parasites of red blood cells - Plasmodium species. In: Schaechter's mechanisms of microbial diseases. 4th edition. Lippincott Williams & Wilkins (Wolters Kluwer health), Philadelphia, pp. 490-495.
- Adisakwattana, S., Sompong, W., Meeprom, A., Ngamukote, S. and Yibchok-anun, S., 2012. Cinnamic acid and its derivatives inhibit fructose-mediated protein glycation. *Int J Mol Sci* **13**(2): 1778-1789.
- Aronson, D. and Rayfield, E. J., 2002. How hyperglycemia promotes atherosclerosis: molecular mechanisms. *Cardiovasc Diabetol* **1**.
- Basta, G., Schmidt, A. M. and De Caterina, R., 2004. Advanced glycation end products and vascular inflammation: implications for accelerated atherosclerosis in diabetes. *Cardiovasc Res* **63**(4): 582-592.
- Borg, D. J. and Forbes, J. M., 2016. Targeting advanced glycation with pharmaceutical agents: where are we now? *Glycoconjugate J* **33**(4): 653-670.
- Brownlee, M., 2001. Biochemistry and molecular cell biology of diabetic complications. *Nature* **414**(6865): 813-820.
- Butler, M. S., 2008. Natural products to drugs: natural product-derived compounds in clinical trials. *Nat Prod Rep* **25**(3): 475-516.
- Center-for-Disease-Control-and-Prevention, 2015. About Malaria. Retrieved 13 December, 2016, from <https://www.cdc.gov/malaria/about/index.html>.
- Choudhary, M. I., Adhikari, A., Rasheed, S., Marasini, B. P., Hussain, N., Kaleem, W. A. and Attaur-Rahman, 2011. Cyclopeptide alkaloids of *Ziziphus oxyphylla* Edgw as novel inhibitors of alpha-glucosidase enzyme and protein glycation. *Phytochem Lett* **4**(4): 404-406.
- Derbre, S., Gatto, J., Pelleray, A., Coulon, L., Seraphin, D. and Richomme, P., 2010. Automating a 96-well microtiter plate assay for identification of AGEs inhibitors or inducers: application to the screening of a small natural compounds library. *Anal Bioanal Chem* **398**(4): 1747-1758.

- Dewick, P. M., 2009. Alkaloids. In: Medicinal natural products: a biosynthetic approach. 3rd ed. John Wiley & Sons Ltd, Chichester, West Sussex, United Kingdom, pp. 311-420.
- Dwivedi, S. P. D., Pandey, V. B., Shah, A. H. and Eckhardt, G., 1987. Cyclopeptide Alkaloids from *Zizyphus nummularia*. *J Nat Prod* **50**(2): 235-237.
- Efferth, T., 2010. Personalized cancer medicine: from molecular diagnostics to targeted therapy with natural products. *Planta Med* **76**(11): 1143-1154.
- Engelen, L., Stehouwer, C. D. A. and Schalkwijk, C. G., 2013. Current therapeutic interventions in the glycation pathway: evidence from clinical studies. *Diabetes Obes Metab* **15**(8): 677-689.
- Farmani, F., Moein, M., Amanzadeh, A., Kandelous, H. M., Ehsanour, Z. and Salimi, M., 2016. Antiproliferative evaluation and apoptosis induction in MCF-7 cells by *Zizyphus spina christi* leaf extracts. *Asian Pacific Journal of Cancer Prevention* **17**(1): 315-321.
- Finch, R., Irving, W., Moss, P. and Anderson, J., 2009. Malaria. In: Clinical medicine. 7th edition. Saunders Elsevier, Edinburgh, pp. 153-157.
- Gamo, F. J., Sanz, L. M., Vidal, J., de Cozar, C., Alvarez, E., Lavandera, J. L., Vanderwall, D. E., Green, D. V. S., Kumar, V., Hasan, S., Brown, J. R., Peishoff, C. E., Cardon, L. R. and Garcia-Bustos, J. F., 2010. Thousands of chemical starting points for antimalarial lead identification. *Nature* **465**(7296): 305-310.
- Goyal, M., Ghosh, M., Nagori, B. P. and Sasmal, D., 2013. Analgesic and anti-inflammatory studies of cyclopeptide alkaloid fraction of leaves of *Zizyphus nummularia*. *Saudi J Biol Sci* **20**(4): 365-371.
- Harvey, A. L., 2008. Natural products in drug discovery. *Drug Discov Today* **13**(19-20): 894-901.
- Inayat-Ur-Rahman, Khan, M. A., Arfan, M., Akhtar, G., Khan, L. and Ahmad, V. U., 2007. A new 14-membered cyclopeptide alkaloid from *Zizyphus oxyphylla*. *Nat Prod Res* **21**(3): 243-253.
- Jack, M. and Wright, D., 2012. Role of advanced glycation end products and glyoxalase I in diabetic peripheral sensory neuropathy. *Transl Res* **159**(5): 355-365.
- Kaleem, W. A., Muhammad, N., Qayum, M., Khan, H., Khan, A., Aliberti, L. and De Feo, V., 2013. Antinociceptive activity of cyclopeptide alkaloids isolated from *Zizyphus oxyphylla* Edgew (Rhamnaceae). *Fitoterapia* **91**: 154-158.

- Kaleem, W. A., Nisar, M., Qayum, M., Zia-Ul-Haq, M., Adhikari, A. and De Feo, V., 2012. New 14-membered cyclopeptide alkaloids from *Zizyphus oxyphylla* Edgew. *Int J Mol Sci* **13**(9): 11520-11529.
- Khangoli, S., Majid, F. A. A., Berwary, N. J. A., Ahmad, F. and Aziz, R. B. A., 2016. The mechanisms of inhibition of advanced glycation end products formation through polyphenols in hyperglycemic condition. *Planta Medica* **82**: 32-45.
- Kim, J., Jeong, I. H., Kim, C. S., Lee, Y. M., Kim, J. M. and Kim, J. S., 2011. Chlorogenic Acid inhibits the formation of advanced glycation end products and associated protein cross-linking. *Arch Pharm Res* **34**(3): 495-500.
- Klein, E. Y., 2013. Antimalarial drug resistance: a review of the biology and strategies to delay emergence and spread. *Int J Antimicrob Ag* **41**(4): 311-317.
- Mahmout, Y., Mianpeurem, T., Dolmazon, R., Bouchu, D. and Fenet, B., 2005. Amphiphile triterpenoids from *Hymenocardia acida* Tul. Phytoantimalarial and anti-inflammatory activities? *Phytochemistry* **7**: 61-66.
- Matsuda, H., Wang, T., Managi, H. and Yoshikawa, M., 2003. Structural requirements of flavonoids for inhibition of protein glycation and radical scavenging activities. *Bioorgan Med Chem* **11**(24): 5317-5323.
- Medicines-for-Malaria-Venture, 2016. Malaria & Medicines. Retrieved 13 December, 2016, from <http://www.mmv.org/malaria-medicines>.
- Meeprom, A., Sompong, W., Chan, C. B. and Adisakwattana, S., 2013. Isoferulic acid, a new anti-glycation agent, inhibits fructose- and glucose-mediated protein glycation *in vitro*. *Molecules* **18**(6): 6439-6454.
- Milne, R. and Brownstein, S., 2013. Advanced glycation end products and diabetic retinopathy. *Amino Acids* **44**(6): 1397-1407.
- Munch, G., Thome, J., Foley, P., Schinzel, R. and Riederer, P., 1997. Advanced glycation end products in ageing and Alzheimer's disease. *Brain Res Rev* **23**(1-2): 134-143.
- Nenna, A., Nappi, F., Avtaar Singh, S. S., Sutherland, F. W., Di Domenico, F., Chello, M. and Spadaccio, C., 2015. Pharmacologic approaches against advanced glycation end products (AGEs) in diabetic cardiovascular disease. *Res Cardiovasc Med* **4**(2): e26949.
- Nisar, M., Adzu, B., Inamullah, K., Bashir, A., Ihsan, A. and Gilani, A. H., 2007. Antinociceptive and antipyretic activities of the *Zizyphus oxyphylla* Edgew. leaves. *Phytother Res* **21**(7): 693-695.

- Pais, M., Marchand, J., Ratle, G. and Jarreau, F. X., 1968. Peptidic Alkaloids .6. Hymenocardine Alkaloid from *Hymenocardia Acida* Tul. *B Soc Chim Fr*(7): 2979-&.
- Panseeta, P., Lomchoey, K., Prabpai, S., Kongsaree, P., Suksamrarn, A., Ruchirawat, S. and Suksamrarn, S., 2011. Antiplasmodial and antimycobacterial cyclopeptide alkaloids from the root of *Ziziphus mauritiana*. *Phytochemistry* **72**(9): 909-915.
- Peng, X. F., Ma, J. Y., Chen, F. and Wang, M. F., 2011. Naturally occurring inhibitors against the formation of advanced glycation end-products. *Food Funct* **2**(6): 289-301.
- Peyroux, J. and Sternberg, M., 2006. Advanced glycation end products (AGEs): pharmacological inhibition in diabetes. *Pathol Biol* **54**(7): 405-419.
- Rahbar, S. and Figarola, J. L., 2003. Novel inhibitors of advanced glycation end products. *Arch Biochem Biophys* **419**(1): 63-79.
- Rahbar, S., Natarajan, R., Yerneni, K., Scott, S., Gonzales, N. and Nadler, J. L., 2000. Evidence that pioglitazone, metformin and pentoxifylline are inhibitors of glycation. *Clin Chim Acta* **301**(1-2): 65-77.
- Rauf, A., Ali, J., Khan, H., Mubarak, M. S. and Patel, S., 2016. Emerging CAM *Ziziphus nummularia* with *in vivo* sedative-hypnotic, antipyretic and analgesic attributes. *3 Biotech* **6**(11).
- Ray, S. D. and Dewanjee, S., 2015. Isolation of a new triterpene derivative and *in vitro* and *in vivo* anticancer activity of ethanolic extract from root bark of *Zizyphus nummularia* Aubrev. *Nat Prod Res* **29**(16): 1529-1536.
- Sadowska-Bartos, I. and Bartosz, G., 2015. Prevention of protein glycation by natural compounds. *Molecules* **20**(2): 3309-3334.
- Sasaki, K., Chiba, S. and Yoshizaki, F., 2014. Effect of natural flavonoids, stilbenes and caffeic acid oligomers on protein glycation. *Biomed Rep* **2**(5): 628-632.
- Sero, L., Sanguinet, L., Blanchard, P., Dang, B. T., Morel, S., Richomme, P., Seraphin, D. and Derbre, S., 2013. Tuning a 96-well microtiter plate fluorescence-based assay to identify AGE inhibitors in crude plant extracts. *Molecules* **18**(11): 14320-14339.
- Shah, A. H., Ageel, A. M., Tariq, M., Mossa, J. S. and Al-Yahya, M. A., 1986. Chemical constituents of the stem bark of *Zizyphus spina-christi*. *Fitoterapia* **58**(6): 452-454.
- Shahat, A. A., Pieters, L., Apers, S., Nazeif, N. M., Abdel-Azim, N. S., Vanden Berghe, D. and Vlietinck, A. J., 2001. Chemical and biological investigations on *Zizyphus spina-christi* L. *Phytother Res* **15**(7): 593-597.

- Silvan, J. M., Assar, S. H., Srey, C., del Castillo, M. D. and Ames, J. M., 2011. Control of the Maillard reaction by ferulic acid. *Food Chem* **128**(1): 208-213.
- Singh, B. and Pandey, V. B., 1995. An *N*-formyl cyclopeptide alkaloid from *Zizyphus nummularia* bark. *Phytochemistry* **38**(1): 271-273.
- Tschesche, R., Elgamal, M., Miana, G. A. and Eckhardt, G., 1975. Alkaloids from rhamnaceae-XXVI. Nummularine-D, -E and -F, new cyclopeptide alkaloids from *Zizyphus nummularia*. *Tetrahedron* **31**(23): 2944-2947.
- Tschesche, R., Khokhar, I., Spilles, C. and von Radloff, M., 1974. Peptide alkaloids from *Zizyphus spinachristi*. *Phytochemistry* **13**(8): 1633.
- Vinay, K., Abbas, A. K., Fausto, N. and Mitchel, R. N., 2007. Malaria. In: Robbins Basic pathology. 8th edition. Saunders Elsevier, Philadelphia, pp. 433,434.
- Vonthron-Senecheau, C., Weniger, B., Ouattara, M., Bi, F. T., Kamenan, A., Lobstein, A., Brun, R. and Anton, R., 2003. *In vitro* antiplasmodial activity and cytotoxicity of ethnobotanically selected Ivorian plants. *J Ethnopharmacol* **87**(2-3): 221-225.
- Voziyan, P. A., Khalifah, R. G., Thibaudeau, C., Yildiz, A., Jacob, J., Serianni, A. S. and Hudson, B. G., 2003. Modification of proteins *in vitro* by physiological levels of glucose - Pyridoxamine inhibits conversion of Amadori intermediate to advanced glycation end-products through binding of redox metal ions. *J Biol Chem* **278**(47): 46616-46624.
- Voziyan, P. A., Metz, T. O., Baynes, J. W. and Hudson, B. G., 2002. A post-amadori inhibitor pyridoxamine also inhibits chemical modification of proteins by scavenging carbonyl intermediates of carbohydrate and lipid degradation. *J Biol Chem* **277**(5): 3397-3403.
- Wada, R. and Yagihashi, S., 2005. Role of advanced glycation end products and their receptors in development of diabetic neuropathy. *Ann Ny Acad Sci* **1043**: 598-604.
- West, B. J., Deng, S. X., Uwaya, A., Isami, F., Abe, Y., Yamagishi, S. and Jensen, C. J., 2016. Iridoids are natural glycation inhibitors. *Glycoconjugate J* **33**(4): 671-681.
- West, B. J., Uwaya, A., Isami, F., Deng, S., Nakajima, S. and Jensen, C. J., 2014. Antiglycation activity of iridoids and their food sources. *Int J Food Sci* **2014**: 276950.
- World-Health-Organization, 2014. WHO traditional medicine strategy 2014-2023.
- World-Health-Organization, 2015. Guidelines for the treatment of malaria. 3rd edition.
- World-Health-Organization, 2016a. Fact Sheet: World Malaria Report 2016. Retrieved 13 December, 2016, from <http://www.who.int/malaria/media/world-malaria-report-2016/en/>.

World-Health-Organization, 2016b. Questions and answers on RTS,S/ASO1 malaria vaccine.

Retrieved 13 December, 2016, from

http://www.who.int/immunization/research/development/malaria_vaccine_qa/en/.

Xie, Y. X. and Chen, X. Q., 2013. Structures required of polyphenols for inhibiting advanced glycation end products formation. *Curr Drug Metab* **14**(4): 414-431.

Zong, H. L., Ward, M. and Stitt, A. W., 2011. AGEs, RAGE, and Diabetic Retinopathy. *Curr Diabetes Rep* **11**(4): 244-252.

CHAPTER 2

General experimental procedures

2.1 Chromatographic Methods

2.1.1 Solvents and reagents

All solvents, including acetonitrile, chloroform, isopropyl alcohol, methanol and methylene chloride were purchased from Acros Organics (Geel, Belgium) or from Fisher Scientific (Leicestershire, UK) and were analytical grade. All reagents, such as ammonia (25%), dimethyl sulfoxide (DMSO), formic acid ($\geq 98\%$) and hydrochloric acid (25%) were purchased from Acros Organics or Sigma-Aldrich (St. Louis, MO, USA). Solvents used for HPLC, i.e. methanol and acetonitrile were HPLC grade and were purchased from Fisher Scientific. Water was dispensed by a Milli-Q system from Millipore (Bedford, MA, USA) and was passed through a 0.22 μm membrane filter before usage.

2.1.2 Thin-layer chromatography

Analytical plates for thin-layer chromatography (TLC) were purchased from Merck (Darmstadt, Germany). Silica gel 60 F₂₅₄ plates (20 x 20 cm) were used for normal phase (NP) TLC.

Dragendorff reagent was prepared by combining a mixture A and a solution B. Mixture A was prepared by suspending 0.85 g bismuth subnitrate ($\text{Bi}_5\text{O}(\text{OH})_9(\text{NO}_3)_4$) in 40 mL water and 10 mL glacial acetic acid. Solution B was prepared by dissolving 8 g potassium iodide (KI) in 20 mL water.

Iodoplatinate reagent was prepared by combining a solution A and a solution B. Solution A was prepared by dissolving 100 mg of hydrogen hexachloroplatinate (IV) hydrate ($\text{H}_2\text{Cl}_6\text{Pt} \cdot \text{X H}_2\text{O}$) in 1 mL of water. Solution B was prepared by dissolving 6 g potassium iodide (KI) in 100 mL of water.

Cerium sulphate reagent was prepared by dissolving 1 g of cerium sulphate (CeSO_4) and 10 g of trichloroacetic acid in 100 mL sulfuric acid (15%). In order to improve the dissolution, the mixture was heated at 60 °C (Wagner and Bladt, 1996)

2.1.3 Flash chromatography

Flash chromatography was carried out on a Reveleris® iES system from Grace (Columbia, MD, USA) using the Reveleris® Navigator™ software. The system is comprised of a binary pump with four solvent selection, an ultraviolet (UV) detector, an evaporating light scattering

detector (ELSD) and a fraction collector. The ELSD carrier solvent was isopropyl alcohol. The column used was a pre-packed Flash Grace Reveleris[®] silica cartridge with a particle size of 40 µm. Samples were injected in dry form. Detection and collection were based on UV and ELSD. Eluate was collected in two trays of 96 tubes.

2.1.4 High-performance liquid chromatography

High-performance liquid chromatography (HPLC) analyses were carried out on an Agilent[®] 1200 series HPLC system, with degasser, quaternary pump, autosampler, thermostatic column compartment and diode array detector (DAD) (Agilent Technologies, Santa Clara, CA, USA). A silica based Luna C₁₈ (2) (250 × 4.6 mm, 5 µm) from Phenomenex (Torrence, CA, USA) was used to obtain separation. A suitable pre-column was installed to prolong the lifetime of the columns.

2.1.5 High-performance liquid chromatography – solid-phase extraction – nuclear magnetic resonance spectroscopy

Liquid chromatography – solid-phase extraction – nuclear magnetic resonance spectroscopy (LC-SPE-NMR) is a hyphenated technique, which combines a chromatographic (HPLC) system with a spectroscopic NMR system and an SPE system, which aids in the enrichment of the collected compounds. Two different HPLC-SPE-NMR configurations were used, one HPLC-PDA-SPE-NMR system, consisting of an Agilent[®] 1200 series HPLC system with an in-line solvent degasser, quaternary pump, autosampler, column compartment, and a diode-array detector (Agilent Technologies, Santa Clara, CA, USA). The other configuration was an HPLC-HRMS-PDA-SPE-NMR system, consisting of an Agilent[®] 1260 series HPLC system with built-in degasser, quaternary pump, autosampler, thermostatted column compartment and diode-array detector, where a flow splitter directed 1% of the eluate to a mass spectrometer (see 2.2.2).

In both configurations, the HPLC instrument is connected to a Bruker/Spark solid-phase extraction (SPE) system (Spark Holland, Emmen, The Netherlands) with HySphere Resin GP (general phase) cartridges (polydivinyl-benzene material with particle size 5 – 15 µm, dimensions 10 x 2 mm) to capture and collect the compounds. In order to improve the retention of the compounds eluting from the HPLC system on the GP cartridges, water is

added to the eluent stream coming from the HPLC. The water is pumped by a K-120 HPLC pump (Knauer, Berlin, Germany) at a flow rate two to three times as high as the flow rate applied in the chromatographic analysis. By performing multiple consecutive trappings, the same compounds were repeatedly captured on the same cartridges. The solvent residues were removed by drying the cartridges with nitrogen gas (N₂). The trapped compounds were eluted with deuterated solvent into 1.7 mm or 3 mm NMR tubes with a Gilson Liquid Handler 215 (Gilson, Middleton, WI, USA). A Phenomenex C₁₈ (2) Luna column (150 mm × 4.6 mm, 3 μm, 100 Å pore size) or a silica based C₁₈ XBridge column (250 mm × 4.6 mm, 5 μm) from Waters® (Milford, MA, USA) were used to obtain separation. The systems were controlled with Hystar version 3.2 software (Bruker Daltonik) and Prep Gilson ST Version 1.2 (Bruker Biospin).

2.1.6 Semi-preparative high-performance liquid chromatography

A semi-preparative HPLC system was used for the isolation of single compounds, and was comprised of a binary sample manager, injector and collector, a quaternary gradient module, a system fluidics organizer, an HPLC-pump, a DAD and a Micromass Quattro mass spectrometer with triple quadrupole detector (TQD), all supplied by Waters® (Milford, MA, USA). MassLynx version 4.1 was used to process the data. A Luna C₁₈ (2) 100 Å column (250 x 10 mm, 5 μm) was used, together with a suitable pre-column in order to prolong the lifetime of the column.

2.2 Spectroscopic Methods

2.2.1 Nuclear magnetic resonance spectroscopy

NMR spectra were recorded on two different instruments. The first spectrometer was a Bruker DRX-400 instrument (Rheinstetten, Germany), equipped with either a 3 mm broadband inverse (BBI) probe or a 5 mm dual ¹H/¹³C probe, using standard Bruker pulse sequences and operating at 400 MHz for ¹H and at 100 MHz for ¹³C. The spectra were processed with Topspin version 1.3.

The second one was a Bruker Avance III system (Rheinstetten, Germany), operating at 600 MHz for ¹H and at 150 MHz for ¹³C NMR spectra, equipped with a Bruker SampleJet

autosampler and a cryogenically cooled inverse triple-resonance 1.7 mm TCI probe (Bruker Biospin). Standard Bruker pulse sequences were used. Icon-NMR (version 4.2, Bruker Biospin) was used for controlling automated acquisition of NMR data (temperature equilibration to 300 K, optimization of lock parameters, gradient shimming, and setting of receiver gain). NMR data processing was performed with Topspin (version 3.1, Bruker Biospin).

Apart from ^1H - and ^{13}C -spectra, also distortionless enhancement by polarization transfer spectra (DEPT-135 and DEPT-90) were recorded. As for the 2D NMR experiments, correlation spectroscopy (COSY), heteronuclear single quantum coherence (HSQC) and heteronuclear multiple bond correlation (HMBC) NMR experiments were performed, revealing ^1H - ^1H , direct ^1H - ^{13}C and indirect ^1H - ^{13}C connections respectively.

Methanol- d_4 (99.8% D) and chloroform- d (99.8% D) were used as solvents and were purchased from Sigma-Aldrich.

2.2.2 Mass spectrometry

Throughout this research project, different mass spectrometers were used to obtain mass spectra:

- An Acquity ultra-performance liquid chromatography (UPLC) system, comprised of a binary solvent manager, sample manager, temperature-controlled column compartment, DAD and triple quadrupole detector (TQD) (Waters), operated with MassLynx 4.1. The mass spectrometer was operated in positive electrospray ionization (ESI+) mode, using MRM (multiple reaction monitoring).

- An Acquity UPLC system with XEVO® TQ-S mass spectrometer (Waters). Mass spectra were recorded in ESI+ mode, using MRM. Separation was achieved on an Acquity BEH SHIELD RP18 column from Waters® (100 x 2.1 mm; 1.7 μm).

- A micrOTOF-Q II mass spectrometer (Bruker Daltonik, Bremen, Germany) equipped with an ESI interface was part of the HPLC-HRMS-PDA-SPE-NMR system (see section 2.1.5).

- An Agilent 1290 series HPLC system with a sample manager, binary pump, temperature-controlled column compartment and quadrupole time-of-flight (QTOF) 6530 mass spectrometer (Santa Clara, CA, USA), equipped with an Agilent Jetstream source. The mass spectrometer was operated in ESI+ mode at a resolution of 20,000. Calibration and tuning was done with a tune mix (G1969-85000) and during acquisition the accuracy was monitored by using an ES-TOF reference mass solution kit (G1969-85001) from Agilent. MassHunter version B.06 software was used for data acquisition and processing.

- A UPLC system consisting of a CTC PAL™ autosampler (CTC Analytics, Zwingen, Swiss), an Accela™ quaternary solvent manager and a 'Hot Pocket' column oven (Thermo Fisher Scientific, Waltham, MA, USA) was used, connected to a Q Exactive™ mass spectrometer (Thermo Fisher Scientific), operated with heated electrospray ionization (HESI). The resolving power was set at 70,000 at full width at half maximum (FWHM). Separation was achieved on an Acquity BEH SHIELD RP18 column from Waters® (150 × 3.0 mm; 1.7 μm).

2.2.3 Optical rotation

The specific optical rotation was determined on a Jasco P-2000 polarimeter. The samples were dissolved in methanol or in methanol/water/formic acid (50:50:0.1). All measurements of the optical rotation were recorded at 589 nm with a path length of 50 mm and at 20 °C. For data handling, Spectramanager software was used.

2.3 Biological Methods

2.3.1 Antiplasmodial activity

The antiplasmodial activity of the isolated compounds was tested against *Plasmodium falciparum* K1, a strain which is (relatively) resistant to chloroquine. The parasite was maintained in continuous log phase growth in RPMI-1640 medium supplemented with 2% penicillin/streptomycin solution, 0.37 mM hypoxanthine, 25 mM HEPES (4-(2-hydroxyethyl)-1-piperazineethanesulfonic acid), 25 mM NaHCO₃, and 10% O⁺ human serum together with 4% human O⁺ erythrocytes. All cultures and assays were conducted at 37 °C under a microaerophilic atmosphere (4% CO₂, 3% O₂, and 93% N₂). The *in vitro* antimalarial activity was assessed using the lactate dehydrogenase assay. With this method, the conversion of lactate into pyruvate, which is catalyzed by the parasitic lactate dehydrogenase (LDH) enzyme and the coenzyme 3-acetyl pyridine adenine dinucleotide (APAD), is measured. Stock solutions of test compounds were prepared in DMSO at a concentration of 20 mM and diluted with culture medium before being added to asynchronous parasite cultures. Assays were performed in 96-well tissue culture plates, each well containing 10 µL of the test solution containing the test compound, together with 190 µL of the parasite inoculum (1% parasitemia, 2% hematocrit). After 72 h of incubation at 37 °C, plates were stored at –20 °C until further processing. After thawing, 20 µL of hemolyzed parasite suspension from each well was transferred into another plate together with 100 µL of Malstat reagent and 10 µL of a 1:1 mixture of phenazine ethosulfate (PES) (2 mg/mL) and nitroblue tetrazolium (NBT) (0.1 mg/mL). The plates were kept in the dark for 2 h, and the change in color was measured spectrophotometrically at 655 nm. The results were expressed as percentage reduction in parasitemia compared to control wells. IC₅₀ values were calculated from drug concentration-response curves. Chloroquine diphosphate was used as an antiplasmodial reference drug (Cos *et al.*, 2006; Mesia *et al.*, 2010).

2.3.2 Cytotoxicity

The cytotoxicity was determined on MRC-5 SV2 cells (human lung fibroblasts), which were cultured in MEM (minimum essential medium), supplemented with 20 mM L-glutamine, 16.5 mM NaHCO₃, 5% fetal calf serum. Cultures were kept at 37 °C and 5% CO₂. Assays were

performed in sterile 96-well tissue culture plates, each well containing 10 μL of test solution containing the test compound, together with 190 μL of cell suspension (3×10^4 cells/well). After 72 hours of incubation, 50 μL resazurine was added to each well and 4 h later, proliferation/viability was assessed fluorimetrically (λ_{ex} 550 nm, λ_{em} 590 nm). The % reduction in cell viability compared to the untreated controls was calculated and IC_{50} values were determined. Tamoxifen was used as reference drug (Cos *et al.*, 2006; Mesia *et al.*, 2010).

References

- Cos, P., Vlietinck, A. J., Vanden Berghe, D. and Maes, L., 2006. Anti-infective potential of natural products: How to develop a stronger *in vitro* 'proof-of-concept'. *J Ethnopharmacol* **106**(3): 290-302.
- Mesia, K., Cimanga, R. K., Dhooghe, L., Cos, P., Apers, S., Totte, J., Tona, G. L., Pieters, L., Vlietinck, A. J. and Maes, L., 2010. Antimalarial activity and toxicity evaluation of a quantified *Nauclea pobeguinii* extract. *J Ethnopharmacol* **131**(1): 10-16.
- Wagner, H. and Bladt, S., 1996. Appendix A: Spray Reagents. In: Plant Drug Analysis, a Thin Layer Chromatography Atlas. 2nd ed. Springer-Verlag, Berlin – Heidelberg – New York, pp. 359-364.

CHAPTER 3

Cyclopeptide alkaloids - review

Published online:

Emmy Tuentler, Vassiliki Exarchou, Sandra Apers, and Luc Pieters

Cyclopeptide alkaloids

Phytochem. Rev., **2016**, doi: 10.1007/s11101-016-9484-y.

3.1 Introduction

Cyclopeptide alkaloids are macrocyclic compounds, the ring system of which consists of a hydroxystyrylamine moiety, an amino acid and a β -hydroxy amino acid. This ring is substituted with one or two additional units. Although they occur in various plant families, they are most widely distributed in the Rhamnaceae family, notably the genus *Ziziphus* (although sometimes the spelling *Zizyphus* is applied, in this review *Ziziphus* is used throughout). Over the years they have been discussed in various reviews because of their intriguing chemical and biological properties. In 1997 a review on cyclopeptide alkaloids was published spanning the literature from January 1985 to December 1995 (Gournelis *et al.*, 1997). About ten years later, a review on plant cyclopeptides, including cyclopeptide alkaloids, was published covering the literature up to 2005 (Tan and Zhou, 2006). El-Seedi *et al.* (2007) published a review on cyclopeptide alkaloids treating the literature from 1995 till 2005. A chapter was devoted to cyclopeptide alkaloids from higher plants in the book series "The Alkaloids", covering the literature up to 2008, by Morel *et al.* (2009). Since then, no comprehensive review on the cyclopeptide alkaloids has been published anymore. In view of the limited accessibility of book chapters, the present review was conceived in order to discuss new findings and developments since 2005, i.e. covering the literature published from 2006 until now (last SciFinder® access on 27 September 2016).

3.2 Classification

The cyclopeptide alkaloids *sensu stricto* contain a 13-, 14- or sometimes 15-membered macrocyclic ring (Gournelis *et al.*, 1997; Joullié and Richard, 2004). In the 13-membered ring compounds, this macrocyclic ring is closed through an ether bridge in the *m*-position of the styrylamine unit, whereas in the 14-membered ring compounds the ring is closed in the *p*-position. As exemplified for 13-membered ring compounds in Figure 3.1, cyclopeptide alkaloids typically contain four building blocks (A, B, C and D) and in particular series of compounds a fifth building block E is present between A and B. "A" is a basic terminal amino acid, usually with a primary, monomethylated or dimethylated amino group; "B" is a β -

hydroxy amino acid; "C" is an amino acid taking part in the macrocyclic ring; "D" is the hydroxystyrylamine unit; and "E" (if present) is an amino acid. In this way, the macrocyclic ring contains two amide bonds and one ether linkage.

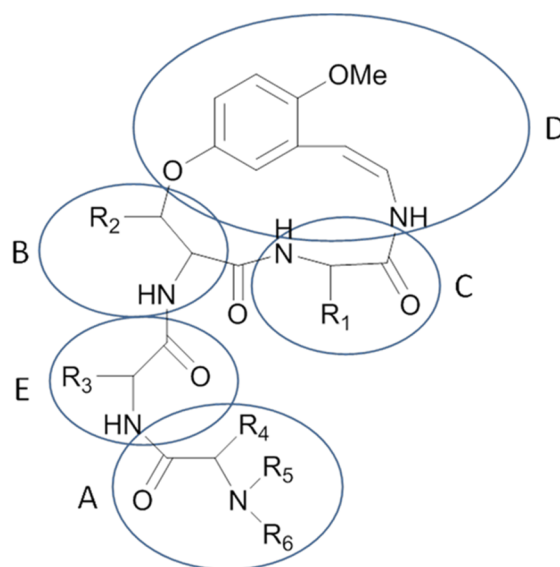


Fig. 3.1 General structure of 13-membered cyclopeptide alkaloids.

According to the size of the macrocyclic ring (13- or 14-membered) and the number of building blocks (4 or 5), cyclopeptide alkaloids can be classified as belonging to the 4(13), 5(13), 4(14) or 5(14) type. The 14-membered ring class is the largest one, and the 4(14) and 5(14) groups are subdivided according to the nature of the β -hydroxy amino acid (building block B). In this way, the 4(14) group has been subdivided into the frangulanine type (in which the β -hydroxy amino acid is leucine), the integerrine type (phenylalanine) and the amphibine-F type (proline). Similarly, the 5(14) group has been subdivided into the scutianine-A type (leucine or phenylalanine) and the amphibine-B type (proline). Accordingly, the 4(13) and 5(13) groups, with proline as β -hydroxy amino acid, are classified as the nummularine-C type and the ziziphine-A type, respectively. The 15-membered ring compounds are rather rare, and do not follow the general scheme of Figure 3.1. For instance, the macrocyclic ring of mucronine-A (Figure 3.2) consists of a hydroxystyrylamine unit and three amino acids. The basic amino acid (building block A), in this case with a dimethylamino group, is also part of the ring system. Mucronine-A is the prototype of the 4(15) class of cyclopeptide alkaloids.

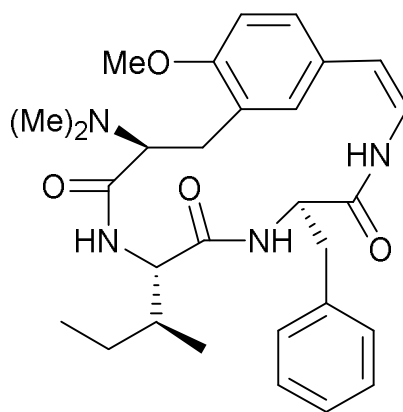


Fig. 3.2 Mucronine-A, a 15-membered cyclopeptide alkaloid.

The 14-membered cyclopeptide alkaloids have also been categorized according to the macrocyclic ring (El-Seedi *et al.*, 2005), substructure 1 covering the frangulanine, integerrine and scutianine-A type; substructure 2 covering the pandamine and hymenocardine type (see below); substructure 3 being a unique substructure represented by anorldianine; substructure 4 covering the amphibine-F type with proline; and substructure 5 covering the amphibine-B and -F type alkaloids without proline.

In addition to the cyclopeptide alkaloids *sensu stricto*, also linear peptide alkaloids, in which the macrocyclic ring system is broken, and neutral compounds, in which the basic amino acid (building block A) is missing, can be distinguished (Gournelis *et al.*, 1997). Some particular features of the neutral cyclopeptide alkaloids are discussed below in section 3.5. Although Tan and Zhou (2006) have proposed a classification system of plant cyclopeptides in which the cyclopeptide alkaloids (type I) are subdivided as types Ia1, Ia2, Ia3, Ib and Ic, in this review the classification system described above used in the previous reviews by Gournelis *et al.* (1997) and El-Seedi *et al.* (2007) was applied.

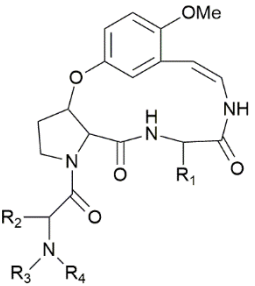
3.3 Structures of New Compounds

3.3.1 Cyclopeptide alkaloids of the 4(13) type (nummularine-C type)

Since 2006, a total of seven new cyclopeptide alkaloids of the 4(13) type have been reported, more in particular belonging to the nummularine-C type with proline as the β -hydroxy amino

acid (building block B) (Table 3.1). Sativanine-N and sativanine-O were obtained from stem bark of *Ziziphus sativa* Gaertn (Singh *et al.*, 2006). Sativanine-N (1) contains isoleucine both as ring-bound amino acid (building block C) and as basic terminal amino acid (building block A) with an unsubstituted primary amino group. In sativanine-O (2), two phenylalanine units are present instead, still with a primary amino group. From root bark and bark of *Ziziphus xylopyrus* (Retz.) Willd. (although originally referred to a *Zizyphus xylopyra*) four cyclopeptide alkaloids of the same type have been reported, all of them containing a phenylalanine unit as ring-bound amino acid (building block C). The basic terminal amino acid (building block A) is *N,N*-dimethyl-leucine in xylopyrine-A (3), *N,N*-dimethyl-phenylalanine in xylopyrine-B (4), *N,N*-dimethylvaline in xylopyrine-D (5), and valine in xylopyrine-E (6) (Singh *et al.*, 2007a; Pandey *et al.*, 2008a). A cyclopeptide related to xylopyrine-B, in which the A-unit is *N*-methyl-phenylalanine, was isolated from bark of *Ziziphus jujuba* Mill. and named jubanine-E (7), together with the known compound nummularine-K (Pandey *et al.*, 2008a; 2008d). The same compound was obtained from *Ziziphus joazeiro* Mart. and named joazerine, in addition to the known compound nummularine-M (Singh *et al.*, 2012a, 2012b).

Table 3.1 4(13) Cyclopeptide alkaloids (nummularine-C type).

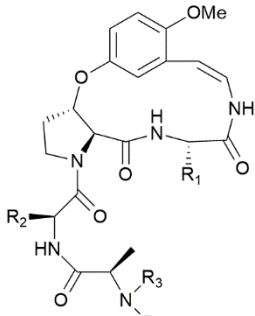
		1 Sativanine-N	R ₁ = R ₂	CH(CH ₃)CH ₂ CH ₃	R ₃ = R ₄	H
		2 Sativanine-O	R ₁ = R ₂	Benzyl	R ₃ = R ₄	H
		3 Xylopyrine-A	R ₁	Benzyl	R ₃ = R ₄	CH ₃
			R ₂	CH ₂ CH(CH ₃) ₂		
		4 Xylopyrine-B	R ₁ = R ₂	Benzyl	R ₃ = R ₄	CH ₃
		5 Xylopyrine-D	R ₁	Benzyl	R ₃ = R ₄	CH ₃
			R ₂	CH(CH ₃) ₂		
		6 Xylopyrine-E	R ₁	Benzyl	R ₃ = R ₄	H
			R ₂	CH(CH ₃) ₂		
		7 Jubanine-E	R ₁ = R ₂	Benzyl	R ₃	CH ₃
					R ₄	H

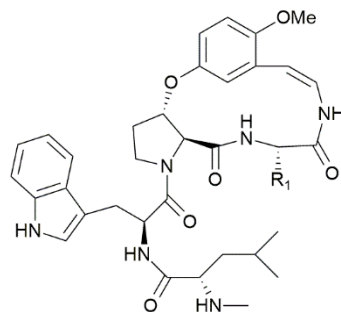
No.	Name	Plant origin	Family	Chem. formula	M _r	Reference
1	Sativanine-N	<i>Ziziphus sativa</i> Gaertn.	Rhamnaceae	C ₂₆ H ₃₈ N ₄ O ₅	486	Singh <i>et al.</i> (2006)
2	Sativanine-O			C ₃₂ H ₃₄ N ₄ O ₅	554	
3	Xylopyrine-A	<i>Ziziphus xylopyrus</i> (Retz.) Willd.	Rhamnaceae	C ₃₁ H ₄₀ N ₄ O ₅	548	Singh <i>et al.</i> (2007a)
4	Xylopyrine-B			C ₃₄ H ₃₈ N ₄ O ₅	582	Pandey <i>et al.</i> (2008a)
5	Xylopyrine-D			C ₃₀ H ₃₈ N ₄ O ₅	534	
6	Xylopyrine-E			C ₂₈ H ₃₄ N ₄ O ₅	506	
7	Jubanine-E	<i>Ziziphus jujuba</i> Mill.	Rhamnaceae	C ₃₃ H ₃₆ N ₄ O ₅	568	Pandey <i>et al.</i> (2008a)
7	Joazerine (= Jubanine-E)	<i>Ziziphus joazeiro</i> Mart.	Rhamnaceae	C ₃₃ H ₃₆ N ₄ O ₅	568	Singh <i>et al.</i> (2012a)

3.3.2 Cyclopeptide alkaloids of the 5(13) type (ziziphine-A type)

In the same time frame, also seven new cyclopeptide alkaloids of the 5(13) type, more in particular of the ziziphine-A type, again characterized by proline as the β -hydroxy amino acid (building block B), have been described (Table 3.2). Sativanine-M isolated from *Ziziphus sativa* bark contains isoleucine as building block C (ring-bound amino acid), valine as additional building block E, and an alanine derivative as basic terminal amino acid (building block A), i.e. *N*-formyl, *N*-methyl-alanine (8). Also nummularine-P was reported (Pandey *et al.*, 2008b). Five jubanines (F – J) (9 – 13) belonging to the same type have been obtained from roots of *Ziziphus jujuba*, in addition to the known compounds nummularine-B, daechuine-S3 and mucronine-K (Kang *et al.*, 2015). They all have isoleucine or valine as building blocks C or E in various combinations, and *N*-methyl- or *N,N*-dimethyl-alanine as basic terminal amino acid. Finally, mauritine-M (14) was reported from the root of *Ziziphus mauritiana* Lam. (Panseeta *et al.*, 2011). Mauritine-M contains *N*-methyl-leucine, proline, isoleucine and tryptophan as building blocks A, B, C and E, respectively (D being the hydroxystyrylamine unit).

Table 3.2 5(13) Cyclopeptide alkaloids (ziziphine-A type).

				
8 Sativanine-M	R ₁	CH(CH ₃)CH ₂ CH ₃	R ₃	CH ₃
	R ₂	CH(CH ₃) ₂	R ₄	CHO
(8: no relative configurations assigned)				
9 Jubanine-F	R ₁ = R ₂	CH(CH ₃) ₂	R ₃	CH ₃
			R ₄	H
10 Jubanine-G	R ₁	CH(CH ₃) ₂	R ₃	CH ₃
	R ₂	CH(CH ₃)CH ₂ CH ₃	R ₄	H
11 Jubanine-H	R ₁ = R ₂	CH(CH ₃)CH ₂ CH ₃	R ₃	CH ₃
			R ₄	H
12 Jubanine-I	R ₁	CH(CH ₃)CH ₂ CH ₃	R ₃ = R ₄	CH ₃
	R ₂	CH(CH ₃) ₂		
13 Jubanine-J	R ₁ = R ₂	CH(CH ₃)CH ₂ CH ₃	R ₃ = R ₄	CH ₃
14 Mauritine-M	R ₁	CH(CH ₃)CH ₂ CH ₃		

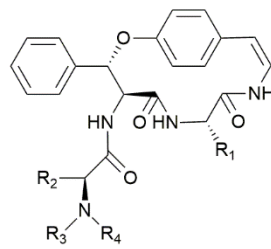


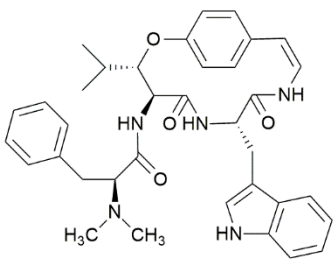
No.	Name	Plant origin	Family	Chem. formula	M _r	Reference
8	Sativanine-M	<i>Ziziphus sativa</i> Gaertn.	Rhamnaceae	C ₃₀ H ₄₃ N ₅ O ₇	585	Pandey <i>et al.</i> (2008b)
9	Jubanine-F	<i>Ziziphus jujuba</i> Mill.	Rhamnaceae	C ₂₈ H ₄₁ N ₅ O ₆	543	Kang <i>et al.</i> (2015)
10	Jubanine-G			C ₂₉ H ₄₃ N ₅ O ₆	557	
11	Jubanine-H			C ₃₀ H ₄₅ N ₅ O ₆	571	
12	Jubanine-I			C ₃₀ H ₄₅ N ₅ O ₆	571	
13	Jubanine-J			C ₃₁ H ₄₇ N ₅ O ₆	585	
14	Mauritine-M	<i>Ziziphus mauritiana</i> Lam.	Rhamnaceae	C ₃₈ H ₅₀ N ₆ O ₆	686	Panseeta <i>et al.</i> (2011)

3.3.3 Cyclopeptide alkaloids of the 4(14) type (integerrine and frangulanine type)

In addition to the xylopyrines discussed above, belonging to the 4(13) class, some other new xylopyrines have been isolated from root bark or bark of the same species (*Ziziphus xylopyrus*), showing a 4(14) structure, i.e. xylopyrines-C, -F, -G and -H (15 – 18), together with scutianine-C, nummularine-P, sativanine-H, franganine, frangufoline, amphibine-D and mauritine-A (Singh *et al.*, 2008a; Pandey and co-workers, 2008c; 2012). They all belong to the integerrine type, containing phenylalanine as building block B (Table 3.3). The basic terminal amino acid (unit A) is derived from phenylalanine, leucine or isoleucine, in which the amino-group can be primary, mono-methylated, or methylated and formylated. It should be noted that because of the formyl substitution, the nitrogen atom loses its basic properties. Xylopyrine-F was also reported as rugosanine-C from stem bark of *Ziziphus rugosa* Lam., in addition to nummularine-K, -M, -N, sativanine-C, mauritine-A, -D, and amphibine-B (Singh and co-workers, 2008; 2013). Together with mauritine-L (19) from the root of *Ziziphus mauritiana* altogether five new 4(14) type alkaloids of the integerrine type were identified since 2006. In addition, one new 4(14) cyclopeptide alkaloid of the frangulanine type, characterized by leucine as building block B, i.e. chamaedrine (20), was obtained from roots of *Melochia chamaedrys* A. St. Hill in addition to adouetine-X, frangufoline, scutianine-B and -C (Dias *et al.* 2007). The genus *Melochia* is now classified in the Malvaceae family (Emile *et al.*, 2007, Michalet *et al.*, 2008).

Table 3.3 4(14) Cyclopeptide alkaloids (integerrine- and frangulanine-type).





15 Xylopyrine-C	R ₁ = R ₂	Benzyl	R ₃	CH ₃	20 Chamaedrine
			R ₄	H	
16 Xylopyrine-F	R ₁ = R ₂	CH ₂ CH(CH ₃) ₂	R ₃ = R ₄	H	
17 Xylopyrine-G	R ₁	Benzyl	R ₃	CH ₃	
	R ₂	CH ₂ CH(CH ₃) ₂	R ₄	CHO	
18 Xylopyrine-H	R ₁	Benzyl	R ₃	CH ₃	
	R ₂	CH(CH ₃) ₂	R ₄	H	
19 Mauritine-L	R ₁ = R ₂	CH(CH ₃)CH ₂ CH ₃	R ₃	CH ₃	
			R ₄	H	

(**15** - **18**: no relative configurations assigned)

No.	Name	Plant origin	Family	Chem. formula	M _r	Reference
15	Xylopyrine-C	<i>Ziziphus xylopyrus</i> (Retz.) Willd.	Rhamnaceae	C ₃₆ H ₃₆ N ₄ O ₄	588	Singh <i>et al.</i> (2008a)
16	Xylopyrine-F			C ₂₉ H ₃₈ N ₄ O ₄	506	Pandey <i>et al.</i> (2008c)
17	Xylopyrine-G			C ₃₄ H ₃₈ N ₄ O ₅	582	Pandey <i>et al.</i> (2012)
18	Xylopyrine-H			C ₃₂ H ₃₆ N ₄ O ₄	540	
16	Rugosanine-C (= xylopyrine-F)	<i>Ziziphus rugosa</i> Lam.	Rhamnaceae	C ₂₉ H ₃₆ N ₄ O ₄	506	Singh <i>et al.</i> (2013)
19	Mauritine-L	<i>Ziziphus mauritiana</i> Lam.	Rhamnaceae	C ₃₀ H ₄₀ N ₄ O ₄	520	Panseeta <i>et al.</i> (2011)
20	Chamaedrine	<i>Melochia chamaedrys</i> A. St.Hill.	Malvaceae	C ₃₆ H ₄₁ N ₅ O ₄	607	Dias <i>et al.</i> (2007)

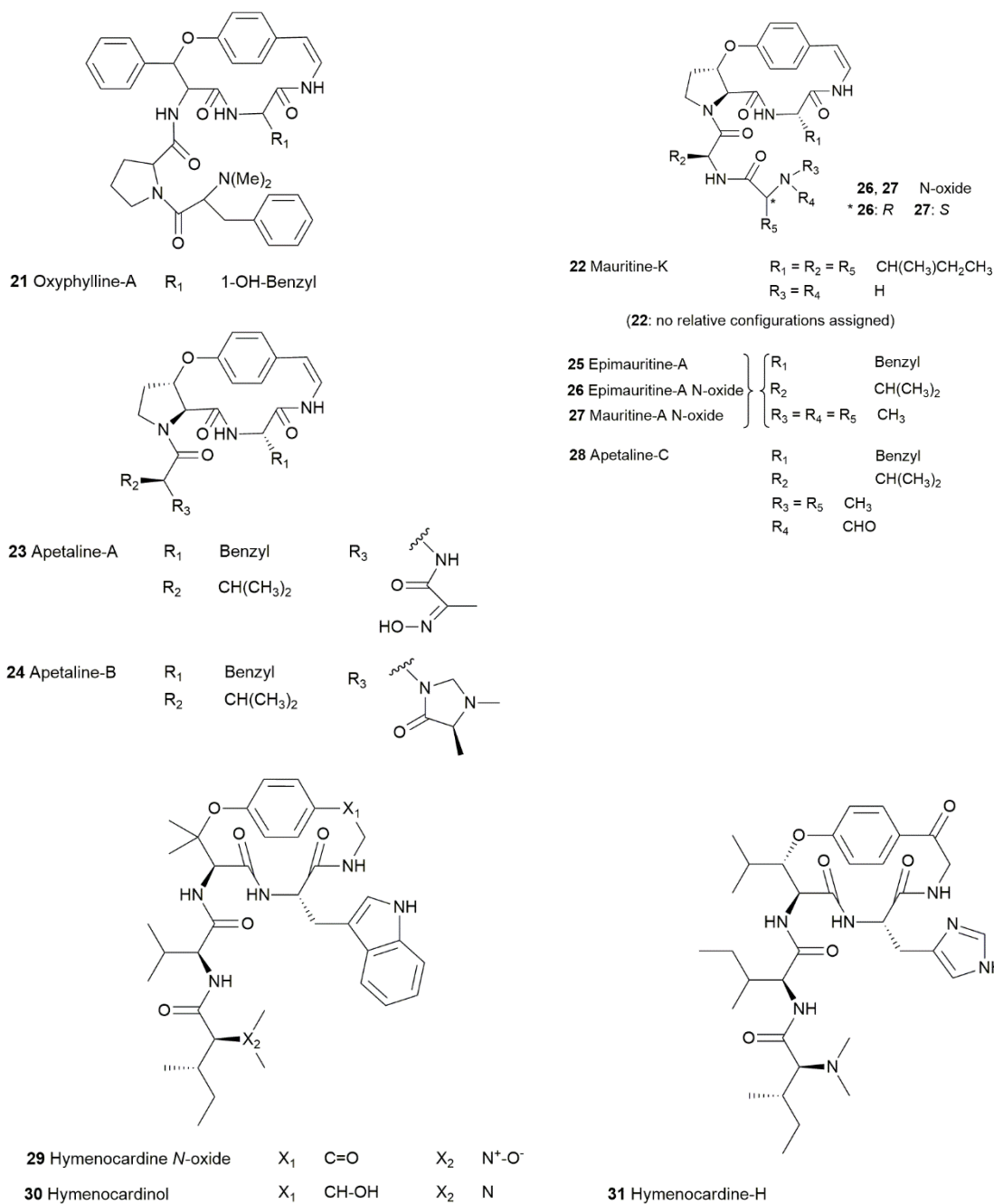
3.3.4 Cyclopeptide alkaloids of the 5(14) type

Only one new cyclopeptide alkaloid belonging to the scutianine-A type (with leucine or phenylalanine as the β -hydroxy amino acid unit (building block B) has been reported since 2006, i.e. oxyphylline-A (21) from stem bark of *Ziziphus oxyphylla* Edgew. (Table 3.4), together with nummularine-R (Inayat-Ur-Rahman *et al.*, 2007). The terminal basic amino acid (unit A) is *N,N*-dimethyl-phenylalanine, the additional intermediary amino acid (unit E) proline. In addition to sativanine-K, one 5(14)-type cyclopeptide alkaloid has been isolated from root bark of *Ziziphus mauritiana*, i.e. mauritine-K (22), in which the β -hydroxy amino acid unit (building block B) is proline (amphibine-B type), the basic terminal amino acid leucine (unit A),

the ring-bound amino acid (unit C) as well as the additional amino acid (unit E) leucine (Singh *et al.*, 2007b). Six new cyclopeptide alkaloids (23 – 28) belonging to the same amphibine-B type have been isolated from stems of *Ziziphus apetala* Hook. f. in addition to the known compounds mauritine-A and mauritine-F (Han *et al.*, 2011). Apetaline-A (23) and -B (24) consist of phenylalanine as the β -hydroxy amino acid (building block B) and the ring-bound amino acid (unit C), valine as additional amino acid (unit E), and an unusual terminal unit (A), i.e. 2-(hydroxylimino)-propanoic acid (which can be considered as an alanine derivative) in apetaline-A, and an imidizolidine-4-one structure (formed by bridging one methyl of *N,N*-dimethyl-alanine and the *N*-atom of the preceding valine unit) in apetaline-B. Another new compound was identified as epimauritine-A (25), being the C-34 epimer of mauritine-A (C-34 is the chiral carbon of the terminal alanine moiety). In addition, also epimauritine-A *N*-oxide (26) and mauritine-A *N*-oxide (27) were obtained. Apetaline-C (28) is similar to (epi)mauritine-A, but contains *N*-formyl, *N*-methylamine-alanine as terminal amino acid; the absolute configuration at C-34 could not be determined.

Recently, three new cyclopeptide alkaloids have been obtained from root bark of *Hymenocardia acida* Tul. (Phyllanthaceae) (Tuenter *et al.*, 2016). In addition to the known major compound hymenocardine, also hymenocardine *N*-oxide (29), hymenocardinol (30) and hymenocardine-H (31) were obtained. These cyclopeptide alkaloids do not contain the usual hydroxystyrylamine building block, but rather a *p*-hydroxyphenylethylamine unit: The -CH=CH- moiety is replaced by a -CH(OH)-CH₂- group in hymenocardinol (30). Hymenocardinol can be considered as the reduced analog of hymenocardine, possessing a hydroxyl- instead of a keto-functionality. Whereas hymenocardine and hymenocardinol consist of *N,N*-dimethyl-isoleucine, valine, tryptophan and valine as building blocks A, B, C and E, respectively, the new cyclopeptide alkaloid hymenocardine-H consist of *N,N*-dimethyl-isoleucine, leucine, histidine and isoleucine as building blocks A, B, C and E, respectively. Because of the presence of histidine, an unusual amino acid in cyclopeptide alkaloids, the name hymenocardine-H (31) was adopted for this compound.

Table 3.4 5(14) Cyclopeptide alkaloids.



No.	Name	Plant origin	Family	Chem. formula	M_r	Reference
21	Oxyphylline-A	<i>Ziziphus oxyphylla</i> Edgew.	Rhamnaceae	$\text{C}_{42}\text{H}_{45}\text{N}_5\text{O}_6$	715	Inayat-Ur-Rahman <i>et al.</i> (2007)
22	Mauritine-K	<i>Ziziphus mauritiana</i> Lam.	Rhamnaceae	$\text{C}_{31}\text{H}_{47}\text{N}_5\text{O}_5$	569	Singh <i>et al.</i> (2007b)
23	Apetaline-A	<i>Ziziphus apetala</i> Hook. f.	Rhamnaceae	$\text{C}_{30}\text{H}_{35}\text{N}_5\text{O}_6$	561	Han <i>et al.</i> (2011)
24	Apetaline-B			$\text{C}_{32}\text{H}_{39}\text{N}_5\text{O}_5$	573	
25	Epimauritine-A			$\text{C}_{32}\text{H}_{41}\text{N}_5\text{O}_5$	575	
26	Epimauritine-A N-oxide			$\text{C}_{32}\text{H}_{41}\text{N}_5\text{O}_6$	591	

No.	Name	Plant origin	Family	Chem. formula	M _r	Reference
27	Mauritine-A N-oxide			C ₃₂ H ₄₁ N ₅ O ₆	591	
28	Apetaline-C			C ₃₂ H ₃₉ N ₅ O ₆	589	
29	Hymenocardine N-oxide	<i>Hymenocardia acida</i> Tul.	Phyllanthaceae	C ₃₇ H ₅₀ N ₆ O ₇	690	Tuenter <i>et al.</i> (2016)
30	Hymenocardinol			C ₃₇ H ₅₂ N ₆ O ₆	676	
31	Hymenocardine-H			C ₃₄ H ₅₁ N ₇ O ₆	653	

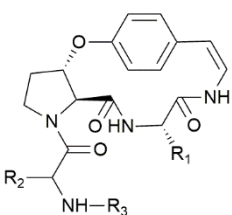
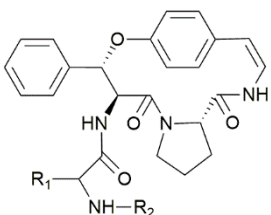
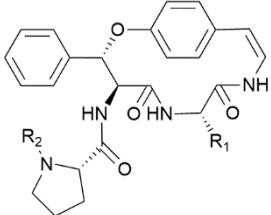
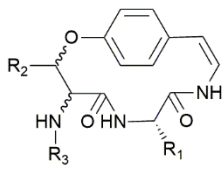

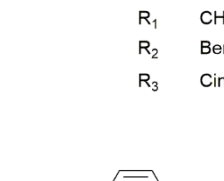
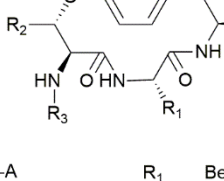
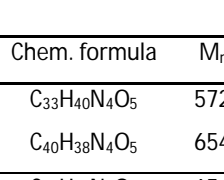
3.3.5 Neutral cyclopeptide alkaloids

Neutral cyclopeptide alkaloids follow the same structural pattern as the other cyclopeptide alkaloids, but the terminal basic amino acid known as building block A (Figure 3.1) is replaced by a substituent that does not contain a nitrogen atom (or that is not derived from an amino acid), e.g. an acyl group. It should be noted that the absence of the nitrogen atom in this substituent is a less ambiguous criterion than the absence of basic properties, since *N*-formylation destroys its basic character. Nevertheless, *N*-formyl containing cyclopeptide alkaloids as described above should not be classified as “neutral cyclopeptide alkaloids” to avoid confusion. Because the number of neutral cyclopeptide alkaloids is still rather small, there has been no particular need to distinguish subtypes, but obviously also here the same distinction between 13-, 14- and 15-membered ring types consisting of 4 or 5 building blocks (depending on the presence or absence of unit E) can be made. Two new neutral cyclopeptide alkaloids have been reported from the root of *Ziziphus oxyphylla* Edgew., i.e. oxyphylline-B (32) and oxyphylline-C (33) (Table 3.5), together with oxyphylline-D, nummularine-C and -R (Kaleem *et al.*, 2012). Oxyphylline-B consists of proline, isoleucine and valine as building blocks B, C and E, respectively; oxyphylline-C of phenylalanine, proline and again phenylalanine, respectively. In both compounds the “neutral” or rather nitrogen-lacking moiety is a cinnamoyl group. It should be noted that a compound obtained from *Ziziphus oxyphylla* that was named oxyphylline-D had already been reported before from *Sphaeranthus indicus* L. (Nisar *et al.*, 2010). Also hemsine-A was reported from *Z. oxyphylla* (Choudhary *et al.*, 2011). In amaiouine (34), isolated from leaves of *Amaioua guianensis* Aubl. (Rubiaceae), units B, C and E are phenylalanine, phenylalanine and proline, respectively, in which the proline-*N* is again substituted with a cinnamoyl residue (Laurindo de Oliveira *et al.*, 2009). Compounds 32 – 34 can therefore be considered as 5(14) neutral cyclopeptide alkaloids. Four new neutral

cyclopeptide alkaloids of the 4(14) type have been isolated from root bark of *Scutia buxifolia* Reiss. (Rhamnaceae) (Maldaner *et al.*, 2011), in addition to the known compounds scutianine-B, -C, -D and -E. Scutianene-E (35) and two of its diastereoisomers 3,4,28-*tris-epi*-scutianene-E (36) and 28-*epi*-scutianene-E (37) consist of β -hydroxy-phenylalanine as ring-bound amino acid (building block C), and leucine as building block B. A cinnamoyl moiety is directly attached to *N*-atom of the β -hydroxy-leucine unit. Similarly, in scutianene-L (38) isoleucine is the ring-bound amino acid (unit C), whereas the β -hydroxy-amino acid (unit B) is phenylalanine, the *N*-atom of which is substituted with a cinnamoyl group. A related 4(14) type compound, justicianene-A, was obtained from whole plant of *Justicia procumbens* L. (Acanthaceae), but interestingly a tyrosine moiety is present instead of a hydroxystyrylamine unit (Jin *et al.*, 2015). This adds evidence to the hypothesis that the hydroxystyrylamine unit is biogenetically derived from tyrosine (Gournelis *et al.*, 1997).

There may be some controversy whether or not these neutral cyclopeptides should be considered as alkaloids, since they are missing the peptidogenic amino acid with a mono- or dimethylated amino group exhibiting basic properties (unless in the case of formyl-substitution). However, many alkaloids devoid of a basic nitrogen are known, such as colchicine or piperine, and similarly also the neutral compounds discussed above could be termed "cyclopeptide alkaloids". Until 2011 only eight neutral cyclopeptide alkaloids have been reported: Scutianene-C (= scutianene-D), discarenes-C and -D, discarines-M and -N, lotusanine-B, sanjoinenine and amaiouine (Maldaner *et al.*, 2011). In the meantime, oxyphyllines-B and -C, scutianene-E and its 2 isomers, scutianene-L and justitiacene-A have been added to this list, bringing the total to 15 representatives. All of them contain a 14-membered macrocyclic ring. Remarkably, all recently isolated neutral cyclopeptide alkaloids as listed in Table 3.5 contained a cinnamoyl moiety as the *N*-acyl group. It has been proposed by Maldaner *et al.* (2011) to use the ending *ine* for cyclopeptide alkaloids *sensu stricto*, and to use *ene* for neutral compounds.

Table 3.5 Neutral cyclopeptides.

	32 Oxyphylline-B	R ₁	CH(CH ₃)CH ₂ CH ₃
		R ₂	CH(CH ₃) ₂
		R ₃	Cinnamoyl
	33 Oxyphylline-C	R ₁	Benzyl
		R ₂	Cinnamoyl
		R ₃	Cinnamoyl
	34 Amaouine	R ₁	Benzyl
		R ₂	Cinnamoyl
		R ₃	Cinnamoyl
	35 Scutianene-E	R ₁	1-OH-Benzyl (<i>L-threo</i>)
		R ₂	CH(CH ₃) ₂ (<i>L-erythro</i>)
		R ₃	Cinnamoyl
	36 3,4,28- <i>tris-epi</i> -Scutianene	R ₁	1-OH-Benzyl (<i>L-erythro</i>)
		R ₂	CH(CH ₃) ₂ (<i>D-erythro</i>)
		R ₃	Cinnamoyl
	37 28- <i>epi</i> -Scutianene	R ₁	1-OH-Benzyl (<i>L-erythro</i>)
		R ₂	CH(CH ₃) ₂ (<i>L-erythro</i>)
		R ₃	Cinnamoyl
	38 Scutianene-L	R ₁	CH(CH ₃)CH ₂ CH ₃
		R ₂	Benzyl (<i>D-threo</i>)
		R ₃	Cinnamoyl
	39 Justicianene-A	R ₁	Benzyl
		R ₂	CH(CH ₃) ₂
		R ₃	Cinnamoyl

No.	Name	Plant origin	Family	Chem. formula	M _r	Reference
32	Oxyphylline-B	<i>Ziziphus oxyphylla</i> Edgew.	Rhamnaceae	C ₃₃ H ₄₀ N ₄ O ₅	572	Kaleem <i>et al.</i> (2012)
33	Oxyphylline-C			C ₄₀ H ₃₈ N ₄ O ₅	654	
34	Amaiouine	<i>Amaioua guianensis</i> Aubl.	Rubiaceae	C ₄₀ H ₃₈ N ₄ O ₅	654	Laurindo de Oliveira <i>et al.</i> (2009)
35	Scutianene-E	<i>Scutia buxifolia</i> Reiss.	Rhamnaceae	C ₃₂ H ₃₃ N ₃ O ₅	539	Maldaner <i>et al.</i> (2011)
36	3,4,28- <i>tris-epi</i> -Scutianene-E			C ₃₂ H ₃₃ N ₃ O ₅	539	
37	28- <i>epi</i> -Scutianene-E			C ₃₂ H ₃₃ N ₃ O ₅	539	
38	Scutianene-L			C ₃₂ H ₃₂ N ₃ O ₄	523	
39	Justicianene-A	<i>Justicia procumbens</i> L.	Acanthaceae	C ₃₃ H ₃₆ N ₃ O ₆	570	Jin <i>et al.</i> (2015)

3.4 Distribution of Cyclopeptide Alkaloids

This review paper confirms that the Rhamnaceae family and especially the genus *Ziziphus* is by far the most important source of cyclopeptide alkaloids. Other plant families from which cyclopeptide alkaloids have been obtained during the past decade include the Acanthaceae, Malvaceae, Phyllanthaceae and Rubiaceae. The presence of the cyclopeptide alkaloids frangulanine and melonovine-A in *Christiana africana* DC. supported the reclassification of the genus *Christiana* from Tiliaceae to Malvaceae (Michalet *et al.*, 2008). Recently, UPLC/QTOF MS combined with an informatics platform was applied to the rapid characterization of Ziziphi Spinosae Semen, the dried seeds of *Ziziphus jujuba* Mill. var. *spinosa* (Bunge) Hu ex H.F.Chou, and to distinguish it from its adulterant Ziziphi Mauritiana Semen (Zhang *et al.*, 2016). With regard to cyclopeptide alkaloids, only ramosine-A, sanjoinine-A and lotusine-B were detected in Ziziphi Spinosae Semen, whereas a much wider range was present in Ziziphi Mauritiana Semen, including amphibine-D, lotusanine-A, lotusine-B, ramosine-A, sanjoinine, sanjoinine-A, -B, -D, -F, G1 and its 11-epimer, and -G2. Daechuine S10 has been obtained from roots of *Z. jujuba* Mill. var. *spinosa* (Meng *et al.*, 2013).

3.5 Configurational Studies and Total Synthesis

For some cyclopeptide alkaloids originally reported before 2006, the relative or absolute configuration has been investigated more recently. The relative configuration of oxyphylline-D, nummularine-C and -R was reported by Nisar *et al.* (2010). Single crystal X-ray diffraction of the 13-membered ring compound nummularine-B methiodide revealed all *S*-configurations of the amino acid residues (Panseeta *et al.*, 2011). The absolute configuration of franganine, isolated from root bark of *Discaria americana* Gillies & Hook. (Rhamnaceae), was established by NMR spectroscopy and X-ray diffraction analysis of tri-*N*-methylfranganine methiodide (Caro *et al.*, 2012). The absolute configuration of discarine-C, -D and myrianthine-A, three cyclopeptide alkaloids originally obtained from *Discaria febrifuga*, was determined by a combination of NMR studies, chiral GC (gas chromatography), and comparison of NMR data with those of synthetic tripeptides (Mostardeiro *et al.*, 2013).

Because of their diverse biological properties (see below), the cyclopeptide alkaloids and non-natural analogs have been of considerable interest to synthetic organic chemists. A two-step synthesis of *p*-cyclophanes (such as the 14-membered ring cyclopeptide alkaloids) by the combined use of a Ugi four-component reaction (Ugi-4CR) and an intramolecular S_NAr -based (aromatic nucleophilic substitution) macrocyclization reaction has been reported as a sequence allowing the introduction of at least 4 points of diversity (Cristau *et al.*, 2006). De Greef *et al.* (2006) have developed a flexible two-step route to macrocyclic ansapeptoids and peptides, in which the core structure is synthesized by a combination of a Ugi four-component reaction with bifunctional building blocks to form the dipeptoid part, followed by a suitable macrocyclization reaction. The synthesis of cyclopeptide alkaloids starting from amino acids as building blocks and using copper(I) catalysis to install the key structural elements was discussed by Evano (2008). The total synthesis of the cyclopeptide alkaloids paliurine-E and -F, ziziphine-N and -Q, abyssenine-A and mucronine-E was reported, involving an intramolecular amidation of vinyl iodide, which allowed to address simultaneously two synthetic challenges associated with cyclopeptide alkaloids: the formation of the enamide and macrocyclization (cycloenamidation reaction). Physical, spectroscopic and spectrometric characteristics of synthetic (-)-paliurine-F and mucronine-E corresponded in all respects to those reported for the natural products, thereby establishing their relative and absolute configurations (Toumi and co-workers, 2007; 2008a; 2008b; 2009). The total synthesis of abyssenine-B and mucronine-E was also reported by Wang *et al.* (2007) using a CuI/*N,N*-dimethylglycine-catalyzed coupling reaction of vinyl iodides with amides as the key step. The configuration of natural abyssenine-B and mucronine-E could tentatively be assigned as *S,S,S*. The total synthesis of ziziphine-N was also reported using a Mitsunobu reaction, followed by installation of the enamide part and ring closure (He *et al.*, 2007). More recently, Cu-mediated enamide formation in the total synthesis of complex peptide natural products was reviewed by Kuranaga *et al.* (2014).

3.6 Biological Activity

3.6.1 Activity on the central nervous system (CNS), analgesic and anti-inflammatory activity

As pointed out in previous reviews, many cyclopeptide alkaloids exert activity on the central nervous system (CNS) (Gournelis *et al.*, 1997; El-Seedi *et al.*, 2007). The cyclopeptide alkaloid fraction from *Ziziphi spinosi* semen, defined as the dried seed of *Ziziphus jujuba* Mill. var. *spinosa* (Rhamnaceae), and traditionally used as a tranquilizer, analgesic and anticonvulsant, was found to enhance pentobarbital-induced sleeping behavior in mice after oral administration. It was suggested that the enhancement of Cl^- influx by the cyclopeptide alkaloid fraction may play an important role in the potentiation of pentobarbital-induced sleeping behavior (Ma *et al.*, 2008). The observed effects were comparable to those of muscimol used as a positive control. The same alkaloid fraction also showed anxiolytic effects: it increased the time spent on the open arms and the number of open arm entries in the elevated plus-maze test. Significant effects were obtained at a dose of 8.0 mg/kg, whereas diazepam used as a positive control was administered at a dose of 2.0 mg/kg. In addition, the cyclopeptide alkaloid fraction increased the number of head-dips in the hole-board test (significant effect at 8.0 mg/kg), and increased the percentage of centre zone ambulatory time in the open-field box (significant effect at 2.0 mg/kg), again vs. diazepam active at a dose of 0.5 and 2.0 mg/kg, respectively. However, in contrast to diazepam, it did not affect locomotor activity, and it did not influence grip force. The cyclopeptide alkaloid fraction was found to increase Cl^- influx and to over-express γ -subunits of GABA_A receptors in cultured cerebellar granule cells (Han *et al.*, 2008). The fraction was prepared using a common liquid/liquid partitioning scheme for isolation of alkaloids. An initial partitioning step was performed between 5% hydrochloric acid and ether, followed by alkalization of the aqueous acid solution with NH_4OH to a pH of 9.0 and a second partitioning step with chloroform. The cyclopeptide alkaloid-containing chloroform fraction, was dried and was administered to mice as a suspension in 1% carboxymethylcellulose in physiological saline, but unfortunately it was not phytochemically characterized.

The cyclopeptide alkaloid fraction from leaves of *Ziziphus nummularia*, prepared using a liquid/liquid partitioning scheme as described in the previous paragraph, was evaluated after oral administration for its analgesic activity in the acetic acid-induced writhing, tail flick and hot plate tests; and for its anti-inflammatory activity against rat paw oedema, mouse peritonitis and cotton pellet granuloma. Although it was mentioned that the presence of cyclopeptide alkaloids was confirmed by identification tests, TLC and GC-MS analysis, there is no information on the composition of the extract. Anti-oedematogenic and anti-nociceptive effects were observed (Goyal *et al.*, 2013). In the anti-oedematogenic assays significant effects were observed in a dose range of 10-30 mg/kg vs. indomethacine used as a positive control at 10 mg/kg. Analgesic activity in the acetic acid-induced writhing test was observed in the same dose range vs. aspirin as a positive control at 100 mg/kg. In addition, analgesic effects were also observed in the tail flick and hot plate tests, used to evaluate centrally acting analgesics, vs. morphine at 5 mg/kg as a positive control. However, in an acute toxicity study, the LD₅₀ value was established as 200 mg/kg, leaving a rather narrow therapeutic range.

The potential antinociceptive effect of six (4)14-membered cyclopeptide alkaloids, all belonging to the frangulanine-type, was investigated in mice using the tail-flick test as a simple pain model. Test compounds were administered intrathecally into the spinal column (Trevisan *et al.*, 2009). Obviously, results obtained after intrathecal administration cannot be compared to those observed after oral administration as in the studies mentioned above. Franganine and adouetine-X showed antinociceptive effects; adouetine-X also exhibited a pronounced analgesic effect in a chronic neuropathic pain model in mice, but unfortunately no positive control was used. Adouetine-X was able to decrease the activities of Ca²⁺-ATPase and Na⁺/K⁺-ATPase *in vitro*.

Five cyclopeptide alkaloids isolated from *Ziziphus oxyphylla*, including oxyphyllines-B, -C, -D, nummularines-C and -R were evaluated in the acetic acid induced writhing and formalin induced flinching behavior tests after intraperitoneal administration. Especially oxyphylline-B and nummularine-R showed activity. Significant activities were already observed at a dose of 2.5 mg/kg, vs. diclofenac used as a positive control at 10 mg/kg. It was concluded that the peripheral analgesia was strongly augmented by their central effects (Kaleem *et al.*, 2013a).

In summary, it appears that there is increasing evidence for the CNS activities of particular cyclopeptide alkaloids at realistic doses. In view of the limited number of cyclopeptide alkaloids evaluated for their effects on the CNS, it has not been possible yet to establish clear structure-activity relationships.

It has been reported that traditional practitioners of Indian medicine extract the stem part of *Ziziphus jujuba* by a crude pyrolysis method and use the oil in the treatment of pain. A prototype pyrolyzer was applied to simulate this traditional method. FTIR (fourier transform infrared) and GC-MS analysis of the extracted oily substance obtained by both the traditional and the simulated process revealed the presence of various cyclic, nitrogenous, long-chain and heterocyclic compounds, which were believed to be the pyrolysates of various cyclopeptide alkaloids present in the stem of *Ziziphus jujuba* (Shanmugavasan *et al.*, 2011).

3.6.2 Antimicrobial activity

Mauritine-K, isolated from *Ziziphus mauritiana* Lam., exhibited antifungal activity (inhibition of spore germination) against some plant pathogenic fungi such as *Botrytis cinerea* at doses ranging from 200 to 1000 µg/mL, but since no positive control was used it is difficult to evaluate these results. Sativanine-K on the other hand was not active (Singh *et al.*, 2007b). Bioassay-guided fractionation of a leaf extract of *Melochia odorata* L.f. (Malvaceae) resulted in the isolation of frangulanine, which showed moderate antifungal activity against *Candida albicans* and *Saccharomyces cerevisiae*. The minimal amount of frangulanine needed to inhibit fungal growth on a TLC plate was 25 and 50 µg, respectively, compared to 2.5 and 5.0 µg for ketoconazole, respectively (Emile *et al.*, 2007).

Mauritine-L, -M, nummularine-H, -B and hemsine-A exhibited antiplasmodial activity against *Plasmodium falciparum* strain K1 with IC₅₀ values ranging from 3.7 to 10.3 µM, whereas dihydroartemisinin used as a positive control exhibited an IC₅₀ value of 4.2 nM (Panseeta *et al.*, 2011). Hymenocardine, its *N*-oxide, hymenocardine-H and hymenocardinol obtained from *Hymenocardia acida* showed antiplasmodial activity (strain K1) in a concentration range from 12.2 to 27.9 µM, vs. chloroquine used as a positive control with an IC₅₀ value of 0.2 µM. However, only moderate cytotoxicities were observed against human lung fibroblasts (MRC-5 cells), yielding favorable selectivity indices (Tuenter *et al.*, 2016).

Mauritine-M and nummularine-H showed antimycobacterial activity against *Mycobacterium tuberculosis* with MIC (minimal inhibitory concentration) values of 72.8 and 4.5 μM , respectively, whereas the standard drugs isoniazid and kanamycin sulfate showed MIC values of 0.4 and 4.2 μM , respectively. No cytotoxicity controls were carried out; therefore, the selectivity cannot be evaluated (Panseeta *et al.*, 2011). The synthetic cyclopeptide alkaloids paliurine-E and -F, ziziphine-N and -Q, abyssenine-A and mucronine-E were evaluated for cytotoxicity against the human HT1080 tumoral cell line, and for antibacterial activity against a methicillin-resistant strain of *Staphylococcus aureus*, *Bacillus anthracis* and *Escherichia coli*. No significant antibacterial activity was observed, whereas paliurine-F, abyssenine-A and mucronine-E were moderately cytotoxic, displaying IC_{50} values of 0.82, 1.03 and 0.68 mM, respectively. No positive controls were used (Toumi *et al.*, 2009).

Again, as mentioned above for the CNS activity, the number of cyclopeptide alkaloids evaluated for their antimicrobial effects is still too low to allow the establishment of clear structure-activity relationships. Nevertheless, it appears that the cyclopeptide alkaloids as a class can be considered as a promising source of new antimicrobial lead compounds, especially against some fungi, mycobacteria or protozoa, with favorable selectivity indices, in the absence of obvious cytotoxicity.

3.6.3 Other activities

Three cyclopeptide alkaloids isolated from *Ziziphus oxyphylla* Edgew., nummularine-C, -R and hemsine-A showed inhibition of α -glucosidase and anti-glycation activities, which may support local antidiabetic use. With regard to α -glucosidase inhibition, all compounds were more active than 1-deoxynojirimycin, used as a positive control. Hemsine-A was more active as anti-glycation agent than rutin, used as a positive control in this assay (bovine serum albumin - methyl glyoxal assay) (Choudhary *et al.*, 2011). Oxyphylline-D, nummularine-C and -R from the same species were found to be active as *in vitro* inhibitors of urease, catalyzing the production of ammonia and carbon dioxide from urea, which plays a role in various pathologies. All test compounds were more active than thiourea used as a positive control (Kaleem *et al.*, 2013b). Oxyphylline-B, -C, -D, nummularine-C and -R showed *in vitro* antioxidative (radical scavenging) potential (Kaleem *et al.*, 2015).

For all biological activities, it should be noted that publications dealing with extracts, e.g. *Ziziphus* extracts, were only included in this review if at least the presence of cyclopeptide alkaloids had been confirmed. Reports dealing with biological activities of completely uncharacterized extracts were not included in this review.

3.7 Conclusions

Although the number of cyclopeptide alkaloids is gradually increasing, it remains a relatively small class of natural products. All cyclopeptide alkaloids identified in the past decade follow the same structural patterns as outlined before. Remarkably, from the 39 compounds reported for the first time from nature in this time frame, 8 belong to the class of neutral cyclopeptide alkaloids, bringing the total of representative of this group to 15. It is proposed to use the term “neutral cyclopeptide alkaloid” only for those compounds containing a side chain that does not contain a nitrogen atom (or that is not derived from an amino acid), e.g. an acyl group. Indeed, the absence of the nitrogen atom in this substituent is a less ambiguous criterion than the absence of basic properties, since *N*-formylation of an amino acid-derived moiety results in loss of the basic character, but the latter compounds should not be considered as neutral cyclopeptide alkaloids. By analogy with the differentiation between 4(13), 5(13), 4(14) and 5(14) cyclopeptide alkaloids, it is proposed to distinguish two types of neutral cyclopeptide alkaloids, i.e. the 4(14) and the 5(14) type, in which the *N*-acyl moiety is considered as the 4th resp. the 5th building block.

When reviewing the literature it becomes obvious that on many occasions the relative or absolute configuration of all chiral centers has not been determined yet. This remains to be investigated in future chemical and spectroscopic work. A second observation is that relatively few compounds have pharmacologically been investigated, and that even fewer compounds have been the subject of systematic investigations to establish structure-activity relationships. Small libraries of cyclopeptide alkaloids should be constructed (by isolation or synthetically) in order to fill this gap.

References

- Caro, M. S. B., de Oliveira, L. H., Ilha, V., Burrow, R. A., Dalcol, I. I. and Morel, A. F., 2012. Absolute Configuration of Franganine. *J Nat Prod* **75**(6): 1220-1222.
- Choudhary, M. I., Adhikari, A., Rasheed, S., Marasini, B. P., Hussain, N., Kaleem, W. A. and Attaur-Rahman, 2011. Cyclopeptide alkaloids of *Ziziphus oxyphylla* Edgw as novel inhibitors of alpha-glucosidase enzyme and protein glycation. *Phytochem Lett* **4**(4): 404-406.
- Cristau, P., Vors, J. P. and Zhu, J. P., 2006. Rapid synthesis of cyclopeptide alkaloid-like paracyclophanes by combined use of Ugi-4CR and intramolecular S(N)Ar reaction. *Qsar Comb Sci* **25**(5-6): 519-526.
- de Greef, M., Abeln, S., Belkasmi, K., Domling, A., Orru, R. V. A. and Wessjohann, L. A., 2006. Rapid combinatorial access to macrocyclic ansapeptoids and ansapeptides with natural-product-like core structures. *Synthesis-Stuttgart*(23): 3997-4004.
- de Oliveira, P. L., Tanaka, C. M., Kato, L., da Silva, C. C., Medina, R. P., Moraes, A. P., Sabino, J. R. and de Oliveira, C. M., 2009. Amaiouine, a cyclopeptide alkaloid from the leaves of *Amaioua guianensis*. *J Nat Prod* **72**(6): 1195-1197.
- Dias, G. C. D., Gressler, V., Hoenzel, S. C. S. M., Silva, U. F., Dalcol, I. I. and Morel, A. F., 2007. Constituents of the roots of *Melochia chamaedrys*. *Phytochemistry* **68**(5): 668-672.
- El-Seedi, H. R., Larsson, S. and Backlund, A., 2005. Chemosystematic value of cyclopeptide alkaloids from *Heisteria nitida* (Olacaceae). *Biochem Syst Ecol* **33**(8): 831-839.
- El-Seedi, H. R., Zahra, M. H., Goransson, U. and Verpoorte, R., 2007. Cyclopeptide alkaloids. *Phytochemistry reviews* **6**: 143-165.
- Emile, A., Waikedre, J., Herrenknecht, C., Fourneau, C., Gantier, J. C., Hnawia, E., Cabalion, P., Hocquemiller, R. and Fournet, A., 2007. Bioassay-guided isolation of antifungal alkaloids from *Melochia odorata*. *Phytother Res* **21**(4): 398-400.
- Evano, G., 2008. Synthèse de produits naturels: Des acides amines et du cuivre(I) pour la synthèse d'alcaloïdes cyclopeptidiques. *Actualité Chimique* **322**: 20-26.
- Gournelis, D. C., Laskaris, G. G. and Verpoorte, R., 1997. Cyclopeptide alkaloids. *Nat Prod Rep* **14**(1): 75-82.

- Goyal, M., Ghosh, M., Nagori, B. P. and Sasmal, D., 2013. Analgesic and anti-inflammatory studies of cyclopeptide alkaloid fraction of leaves of *Zizyphus nummularia*. *Saudi J Biol Sci* **20**(4): 365-371.
- Han, H. S., Ma, Y., Eun, J. S., Hong, J. T. and Oh, K. W., 2008. Anxiolytic-Like Effects of Cyclopeptide fraction alkaloids of *Zizyphi Spinosi Semen*: Possible Involvement of GABA_A Receptors. *Biomol Ther* **16**(3): 261-269.
- Han, J., Ji, C. J., He, W. J., Shen, Y., Leng, Y., Xu, W. Y., Fan, J. T., Zeng, G. Z., Kong, L. D. and Tan, N. H., 2011. Cyclopeptide Alkaloids from *Ziziphus apetala*. *J Nat Prod* **74**(12): 2571-2575.
- He, G., Wang, J. and Ma, D. W., 2007. Highly convergent route to cyclopeptide alkaloids. Total synthesis of ziziphine N. *Org Lett* **9**(7): 1367-1369.
- Inayat-Ur-Rahman, Khan, M. A., Arfan, M., Akhtar, G., Khan, L. and Ahmad, V. U., 2007. A new 14-membered cyclopeptide alkaloid from *Zizyphus oxyphylla*. *Nat Prod Res* **21**(3): 243-253.
- Jin, H., Chen, L., Tian, Y., Li, B. and Dong, J. X., 2015. New cyclopeptide alkaloid and lignan glycoside from *Justicia procumbens*. *J Asian Nat Prod Res* **17**(1): 33-39.
- Joullie, M. M. and Richard, D. J., 2004. Cyclopeptide alkaloids: chemistry and biology. *Chem Commun*(18): 2011-2015.
- Kaleem, W. A., Muhammad, N., Khan, H., Rauf, A., Zia-ul-Haq, M., Qayum, M., Khan, A. Z., Nisar, M. and Obaidullah, 2015. Antioxidant potential of cyclopeptide alkaloids isolated from *Zizyphus oxyphylla*. *J Chem Soc Pakistan* **37**(3): 474-478.
- Kaleem, W. A., Muhammad, N., Qayum, M., Khan, H., Khan, A., Aliberti, L. and De Feo, V., 2013a. Antinociceptive activity of cyclopeptide alkaloids isolated from *Zizyphus oxyphylla* Edgew (Rhamnaceae). *Fitoterapia* **91**: 154-158.
- Kaleem, W. A., Nisar, M., Qayum, M., Zia-Ul-Haq, M., Adhikari, A. and De Feo, V., 2012. New 14-Membered cyclopeptide alkaloids from *Zizyphus oxyphylla* Edgew. *Int J Mol Sci* **13**(9): 11520-11529.
- Kaleem, W. A., Nisar, M., Qayum, M., Zia-Ul-Haq, M., Choudhary, M. I. and Ercisli, S., 2013b. Urease inhibitory potential of *Zizyphus oxyphylla* Edgew. extracts and isolated compounds. *Turk J Med Sci* **43**(4): 497-500.
- Kang, K. B., Ming, G., Kim, G. J., Ha, T. K. Q., Choi, H., Oh, W. K. and Sung, S. H., 2015. Jubanines F-J, cyclopeptide alkaloids from the roots of *Ziziphus jujuba*. *Phytochemistry* **119**: 90-95.

- Kuranaga, T., Sesoko, Y. and Inoue, M., 2014. Cu-mediated enamide formation in the total synthesis of complex peptide natural products. *Nat Prod Rep* **31**(4): 514-532.
- Ma, Y., Han, H., Nam, S. Y., Kim, Y. B., Hong, J. T., Yun, Y. P. and Oh, K. W., 2008. Cyclopeptide alkaloid fraction from *Zizyphi Spinosi Semen* enhances pentobarbital-induced sleeping behaviors. *J Ethnopharmacol* **117**(2): 318-324.
- Maldaner, G., Marangon, P., Ilha, V., Caro, M. S. B., Burrow, R. A., Dalcol, I. I. and Morel, A. F., 2011. Cyclopeptide alkaloids from *Scutia buxifolia* Reiss. *Phytochemistry* **72**(8): 804-809.
- Meng, Y. J., Zhang, Y. W., Jiang, H. Y., Bao, Y. L., Wu, Y., Sun, L. G., Yu, C. L., Huang, Y. X. and Li, Y. X., 2013. Chemical constituents from the roots of *Zizyphus jujuba* Mill. var. *spinosa*. *Biochem Syst Ecol* **50**: 182-186.
- Michalet, S., Payen-Fattaccioli, L., Beney, C., Cegiela, P., Bayet, C., Cartier, G., Nougoué-Tchamo, D., Tsamo, E., Mariotte, A. M. and Dijoux-Franca, M. G., 2008. New components including cyclopeptides from barks of *Christiana africana* DC. (Tiliaceae). *Helv Chim Acta* **91**(6): 1106-1117.
- Morel, A. F., Maldaner, G. and Ilha, V., 2009. Cyclopeptide alkaloids from higher plants. In: *The Alkaloids: chemical and biological perspectives*. Wiley, New York, pp. 79-141.
- Mostardeiro, M. A., Ilha, V., Dahmer, J., Caro, M. S. B., Dalcol, I. I., da Silva, U. F. and Morel, A. F., 2013. Cyclopeptide alkaloids: stereochemistry and synthesis of the precursors of discarines C and D and myrianthine A. *J Nat Prod* **76**(7): 1343-1350.
- Nisar, M., Kaleem, W. A., Adhikari, A., Ali, Z., Hussain, N., Khan, I., Qayum, M. and Choudhary, M. I., 2010. Stereochemistry and NMR data assignment of cyclopeptide alkaloids from *Zizyphus oxyphylla*. *Nat Prod Commun* **5**(8): 1205-1208.
- Pandey, M. B., Singh, A. K., Singh, J. P., Singh, V. P. and Pandey, V. B., 2008a. Three new cyclopeptide alkaloids from *Zizyphus* species. *J Asian Nat Prod Res* **10**(8): 709-713.
- Pandey, M. B., Singh, A. K., Singh, V. P. and Pandey, V. B., 2008b. Cyclopeptide alkaloids from *Zizyphus sativa* bark. *Nat Prod Res* **22**(3): 219-221.
- Pandey, M. B., Singh, J. P., Singh, A. K. and Singh, V. P., 2008c. Xylopyrine-F, a new cyclopeptide alkaloid from *Zizyphus xylopyra*. *J Asian Nat Prod Res* **10**(8): 725-728.
- Pandey, M. B., Singh, J. P., Singh, S. and Singh, A. K., 2008d. Constituents of *Zizyphus jujuba*. *J Indian Chem Soc* **85**(5): 555-556.
- Pandey, M. B., Singh, S., Malhotra, M., Pandey, V. B. and Singh, T. D., 2012. Two new 14-membered cyclopeptide alkaloids from *Zizyphus xylopyra*. *Nat Prod Res* **26**(9): 836-841.

- Panseeta, P., Lomchoey, K., Prabpai, S., Kongsaree, P., Suksamrarn, A., Ruchirawat, S. and Suksamrarn, S., 2011. Antiplasmodial and antimycobacterial cyclopeptide alkaloids from the root of *Ziziphus mauritiana*. *Phytochemistry* **72**(9): 909-915.
- Rai, N., Singh, S., Singh, V. P. and Pandey, V. B., 2008. Cyclopeptide alkaloids of *Zizyphus xylopyra*. *J Indian Chem Soc* **85**(3): 336-337.
- Shanmugavasan, A., Vaitheeswaran, K. S. R. and Ramachandran, T., 2011. Design and development of pyrolyser to extract medicinal oil from the stem of *Ziziphus jujuba*. *J Anal Appl Pyrol* **92**(1): 176-183.
- Singh, A., Pandey, M. B., Singh, J. P. and Singh, S., 2008b. Peptide alkaloids of *Zizyphus rugosa*. *J Indian Chem Soc* **85**(6): 658-659.
- Singh, A. K., Pandey, M. B., Singh, V. P. and Pandey, V. B., 2007b. Mauritine-K, A new antifungal cyclopeptide alkaloid from *Zizyphus mauritiana*. *J Indian Chem Soc* **84**(8): 781-784.
- Singh, A. K., Pandey, M. B., Singh, V. P. and Pandey, V. B., 2007a. Xylopyrine-A and xylopyrine-B, two new peptide alkaloids from *Zizyphus xylopyra*. *Nat Prod Res* **21**(12): 1114-1120.
- Singh, A. K., Pandey, M. B., Singh, V. P. and Pandey, V. B., 2008a. Xylopyrine-C, a new cyclopeptide alkaloid from *Zizyphus xylopyra*. *J Asian Nat Prod Res* **10**(8): 715-718.
- Singh, P. J., Raghubanshi, S. and Yudava, A., 2013. Cyclopeptide alkaloids of *Zizyphus rugosa*. *Chem Biol and Phys Sci* **3**: 994-997.
- Singh, S., Pandey, A. K., Yadava, A., Singh, P. and Singh, J. P., 2012a. Peptide alkaloids from *Zizyphus joazeiro*. *J Chem Biol And Phy Sci* **2**: 608-611.
- Singh, S., Pandey, M. B., Singh, J. P. and Pandey, V. B., 2006. Peptide alkaloids from *Zizyphus sativa* bark. *J Asian Nat Prod Res* **8**(8): 733-737.
- Singh, S., Yadav, A. and Singh, P., 2012b. Chemical constituents of *Zizyphus joazeiro*. *Int J Green and Herbal Chem* **1**: 18-20.
- Tan, N. H. and Zhou, J., 2006. Plant cyclopeptides. *Chem Rev* **106**(3): 840-895.
- Toumi, M., Couty, F. and Evano, G., 2007. Total synthesis of paliurine F. *Angew Chem Int Edit* **46**(4): 572-575.
- Toumi, M., Couty, F. and Evano, G., 2008b. Eight-step total synthesis of the cyclopeptide alkaloid mucronine E. *Synlett*(1): 29-32.
- Toumi, M., Couty, F. and Evano, G., 2008a. Total synthesis of the cyclopeptide alkaloid paliurine E. Insights into macrocyclization by ene-enamide RCM. *J Org Chem* **73**(4): 1270-1281.

- Toumi, M., Rincheval, V., Young, A., Gergeres, D., Turos, E., Couty, F., Mignotte, B. and Evano, G., 2009. A General route to cyclopeptide alkaloids: total syntheses and biological evaluation of paliurines E and F, ziziphines N and Q, abyssenine A, mucronine E, and analogues. *Eur J Org Chem*(20): 3368-3386.
- Trevisan, G., Maldaner, G., Velloso, N. A., Sant'Anna, G. D., Ilha, V., Gewehr, C. D. V., Rubin, M. A., Morel, A. F. and Ferreira, J., 2009. Antinociceptive effects of 14-membered cyclopeptide alkaloids. *J Nat Prod* **72**(4): 608-612.
- Tuenter, E., Exarchou, V., Balde, A., Cos, P., Maes, L., Apers, S. and Pieters, L., 2016. Cyclopeptide alkaloids from *Hymenocardia acida*. *J Nat Prod* **79**(7): 1746-1751.
- Wang, J., Schaeffler, L., He, G. and Ma, D. W., 2007. Total synthesis and stereochemistry assignment of 15-membered peptide alkaloids abyssenine B and mucronine E. *Tetrahedron Lett* **48**(38): 6717-6721.
- Zhang, F. X., Li, M., Qiao, L. R., Yao, Z. H., Li, C., Shen, X. Y., Wang, Y., Yu, K., Yao, X. S. and Dai, Y., 2016. Rapid characterization of *Ziziphi Spinosae Semen* by UPLC/Qtof MS with novel informatics platform and its application in evaluation of two seeds from *Ziziphus* species. *J Pharm Biomed Anal* **122**: 59-80.

CHAPTER 4

Hymenocardia acida

Published:

Emmy Tuentler, Vassiliki Exarchou, Aliou Baldé, Paul Cos, Louis Maes, Sandra Apers, and Luc Pieters

Cyclopeptide alkaloids from *Hymenocardia acida*

J. Nat. Prod., **2016**, 79 (7), pp 1746–1751.

4.1 Introduction

Hymenocardia acida Tul. is a shrub or small tree of about 6 m high that grows in the African Savannah. It belongs to the family of the Phyllanthaceae, although previously it was classified in the families of the Euphorbiaceae and Hymenocardiaceae (Pais *et al.*, 1968; Wurdack *et al.*, 2004; Starks *et al.*, 2014). Extracts of this plant have been used in traditional African medicine. For example, the leaves and roots are used to treat malaria, the roots are used against hypertension, and the plant may be employed as an antiseptic and to treat skin diseases. Another application is the use of decoctions of the leaves or roots to relieve pain (Vonthron-Senecheau *et al.*, 2003; Mahmoud *et al.*, 2005; Obidike *et al.*, 2011; Manga *et al.*, 2013). Previous phytochemical studies have shown the presence of alkaloids, anthocyanins, anthraquinones, cardiac glycosides, flavonoids, phenols, saponins, steroids, stilbenoids, tannins and triterpenoids (Mahmout *et al.*, 2005; Obidike *et al.*, 2011; Manga *et al.*, 2013). To date, one cyclopeptide alkaloid, hymenocardine, has been reported (Pais *et al.*, 1968).

The antiplasmodial activity and cytotoxicity of extracts from the leaves of *H. acida* has been shown by Vonthron-Senecheau (2003). Mahmoud *et al.* (2005) reported lupeol, lupeyl docosanoate and β -sitosterol to be present in *H. acida*, which showed antiplasmodial activity, related to their amphiphilic nature. Apart from this, little is known about its antiplasmodial constituents. In view of the traditional use of *Hymenocardia acida* against malaria, the occurrence of the cyclopeptide alkaloid hymenocardine (**1**) in the root bark, and the reported antiplasmodial activity of some cyclopeptide alkaloids such as ziziphines-N and -Q, mauritine-M, nummularine-H, and hemsine-A (Suksamrarn *et al.*, 2005; Panseeta *et al.*, 2011), it was decided to investigate in more detail the presence of potentially antiplasmodially active cyclopeptide alkaloids in the root bark of *H. acida*. Cyclopeptide alkaloids are polyamidic bases and they are considered as a relatively rare class of natural products. They are macrocyclic compounds, containing a 13-, 14- or 15-membered ring, and they can be classified according to their ring size. They consist of a styrylamine unit and three or four amino acids as common structural elements (Gournelis *et al.*, 1997; El-Seedi *et al.*, 2007).

4.2 Results and Discussion

The root bark of *H. acida* was extracted with 80% methanol and the crude extract was fractionated by liquid-liquid partitioning, followed by flash chromatography. The isolation of single compounds was performed with semi-preparative HPLC with DAD and ESIMS detection and in this way four cyclopeptide alkaloids were obtained (**1-4**) (Figure 4.1). Their structures were elucidated by 1D (^1H , ^{13}C , DEPT 135, DEPT 90) and 2D NMR experiments (COSY, HSQC, HMBC) and comparison to literature data, and were confirmed by HRESIMS.

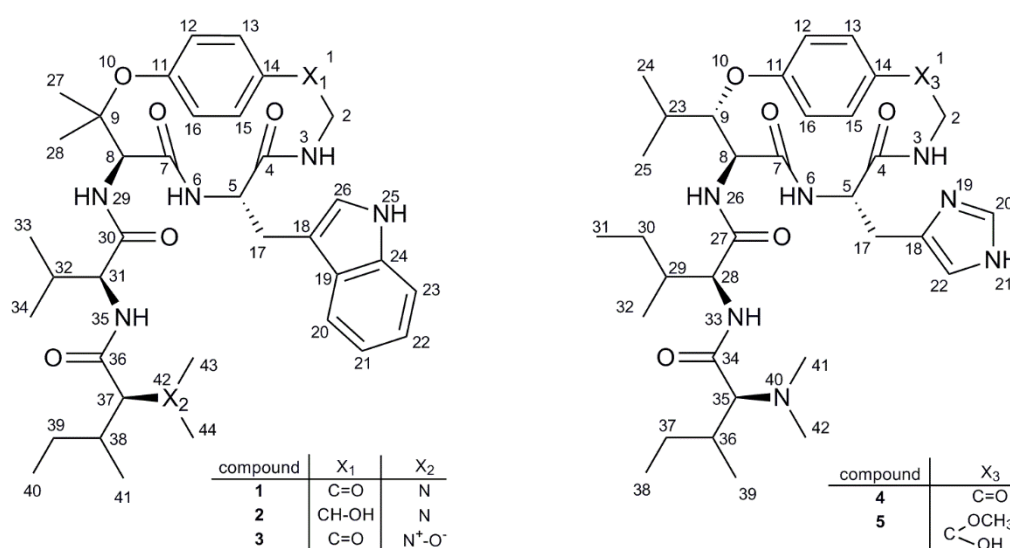


Fig. 4.1 Chemical structures of cyclopeptide alkaloids **1-4**, isolated from the root bark of *Hymenocardia acida*, and **5**, which was formed as an artefact.

Comparison of the NMR spectra of compound **1** with previously published data showed that this compound was hymenocardine, reported in *H. acida* earlier by Pais and co-workers (1968; 1979). The ^1H and ^{13}C NMR spectrum of compound **1** are displayed in Figures 4.2 and 4.3 respectively. ^1H and ^{13}C NMR chemical shift assignments for **1** are listed in Tables 4.1 and 4.2, respectively.

Fig 4.2 ^1H -NMR spectrum (400 MHz, methanol- d_4) of compound **1** (hymenocardine).

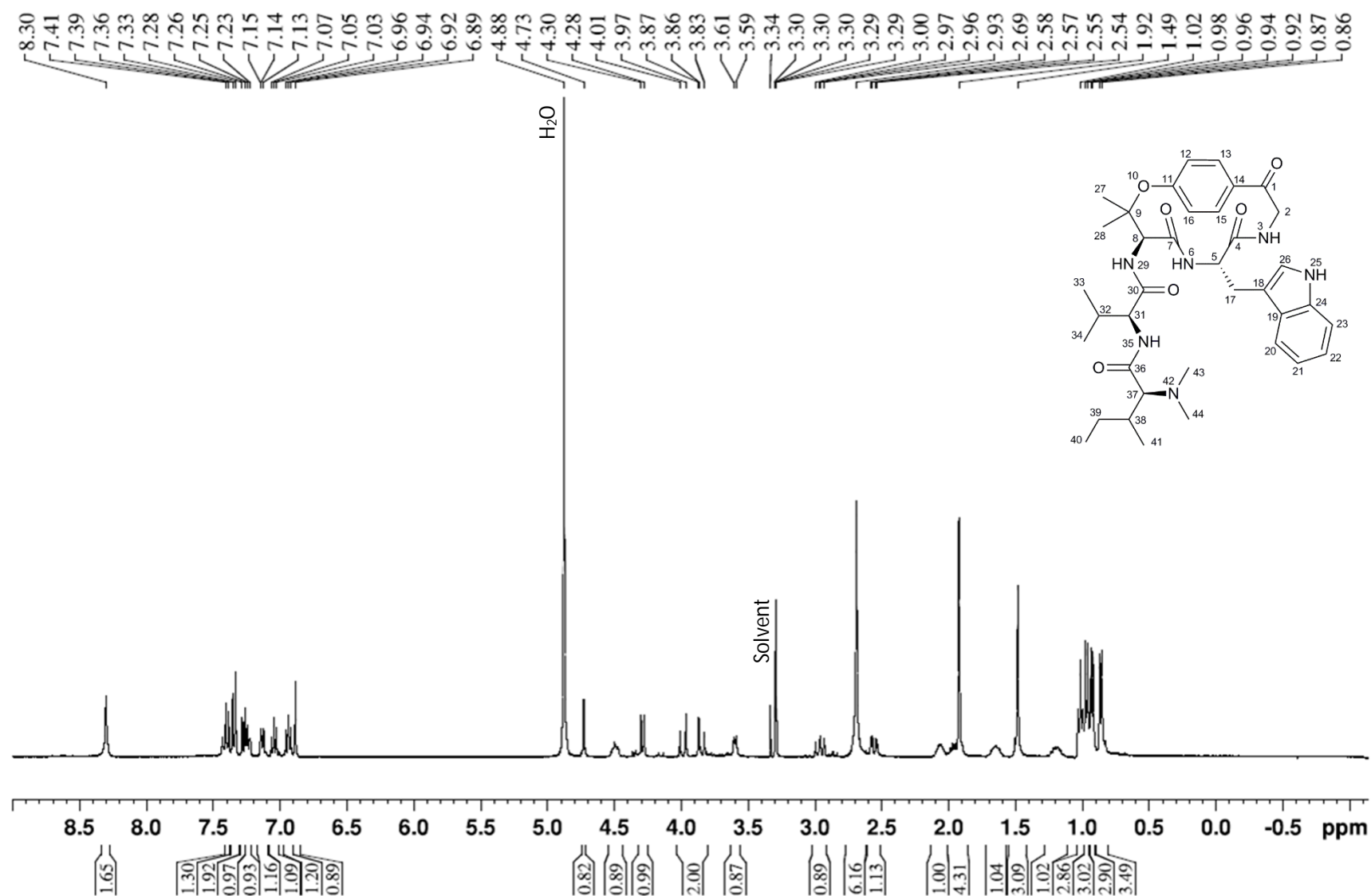
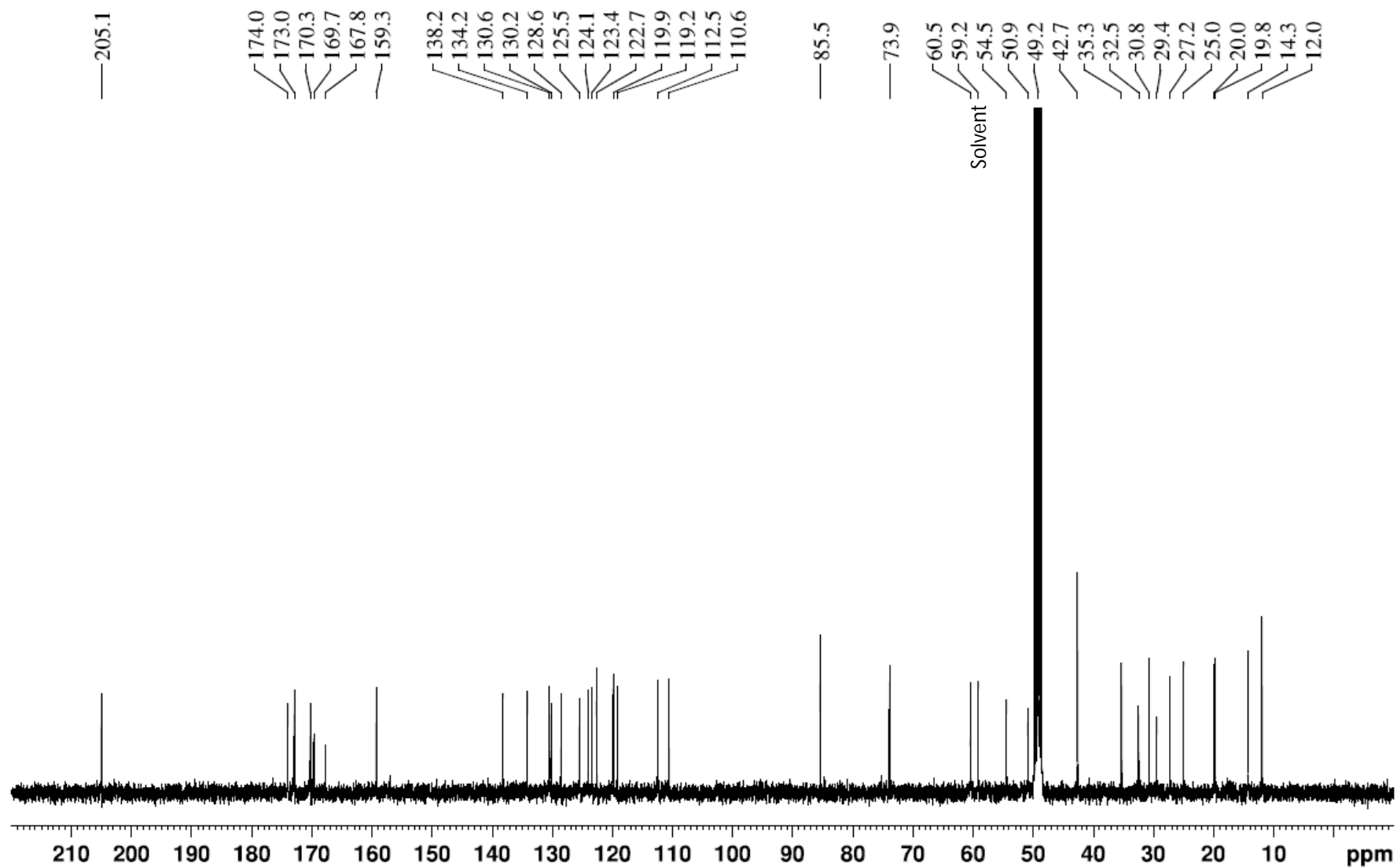


Fig. 4.3 ^{13}C -NMR spectrum (100 MHz, methanol- d_4) of compound **1** (hymenocardine).



The NMR spectra of compound **2** (Figures 4.4 and 4.5) showed a resemblance to those of compound **1**, but a carbon signal with δ_c 73.4 ppm that correlated with a proton at δ_H 5.01 ppm was present, while these signals were absent in the spectra of compound **1**. Moreover, the signal at 205.1 ppm in the ^{13}C NMR spectrum of compound **1**, corresponding to the carbonyl group at position C-1 was absent in the ^{13}C NMR spectrum of compound **2**. This could be explained by the presence of a hydroxy group instead of a carbonyl group at C-1. Thus, compound **2** was a reduced analog of compound **1** for which the name hymenocardinol was adopted. Although the reduced form of hymenocardine was obtained before after chemical modification of **1** with sodium borohydride (Pais *et al.*, 1968), this is the first report of compound **2** as a natural product.

According to its NMR spectra (Figures 4.6 and 4.7), also compound **3** was similar to compound **1**, but some of the signals corresponding to the terminal amino acid unit of the side chain showed more downfield chemical shifts. This could be observed for the two *N*-methyl groups, which resonated at δ_c 55.3 ppm/ δ_H 3.46 ppm and δ_c 56.9 ppm/ δ_H 3.32 ppm, respectively, whereas in compound **1** the values for both methyl groups were δ_c 42.7 ppm/ δ_H 2.69 ppm. Similarly, the CH group substituted by the *N*-dimethyl group was shifted to δ_c 82.4 ppm/ δ_H 3.90 ppm for compound **3**, compared to δ_c 73.9 ppm/ δ_H 3.60 ppm for compound **1**. A similar pattern was reported by Han *et al.* (2011) for cyclopeptide alkaloids containing an *N*-oxide group. Thus, compound **3** was identified as hymenocardine *N*-oxide. Although it is not uncommon that cyclopeptide alkaloids are isolated as *N*-oxides, together with tertiary amines (Han *et al.*, 2011), the possibility that the *N*-oxides are artefacts formed during drying, extraction, or isolation cannot completely be excluded.

Fig. 4.4 ^1H -NMR spectrum (400 MHz, methanol- d_4) of compound **2** (hymenocardinol).

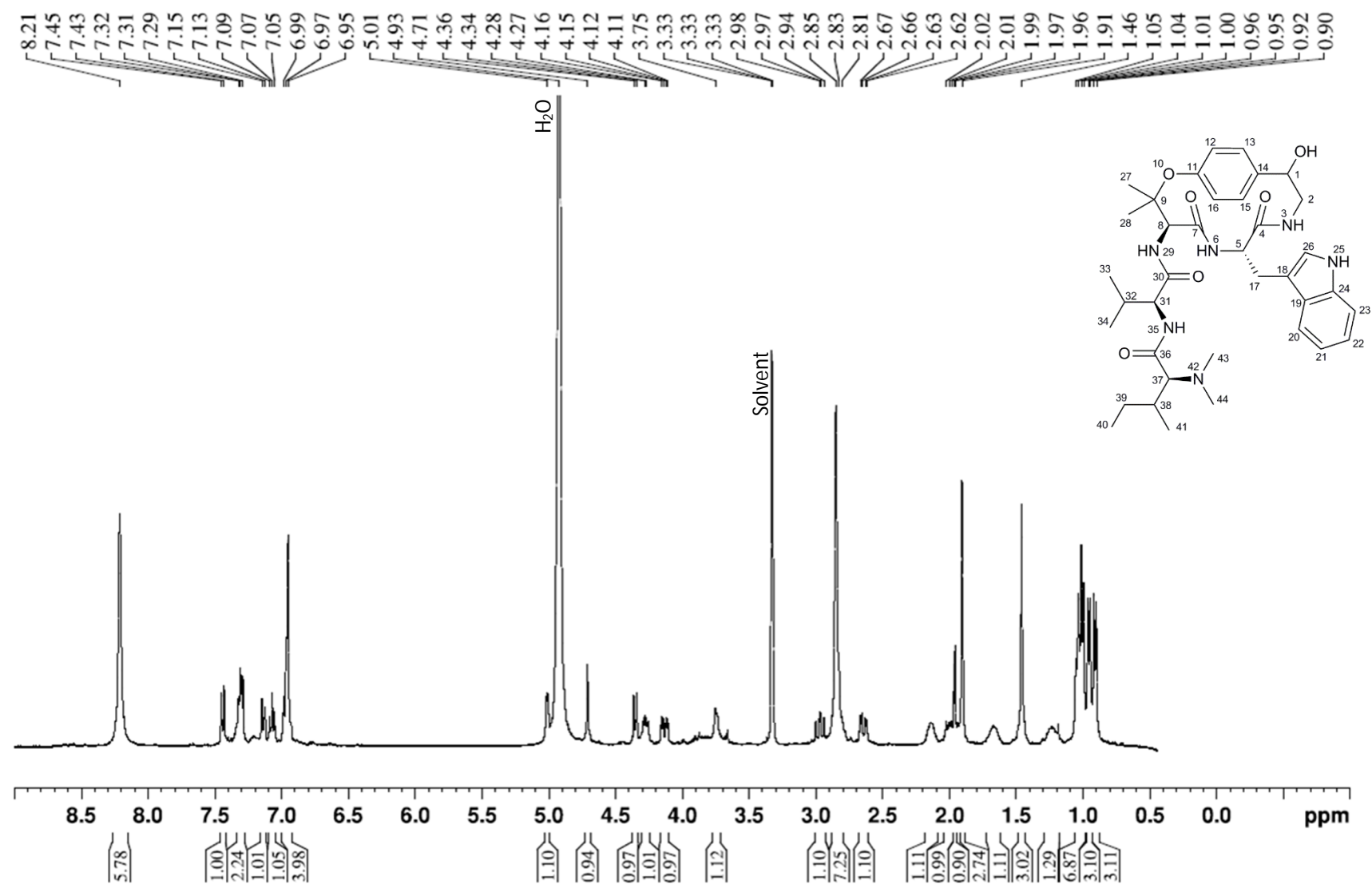


Fig. 4.5 ^{13}C -NMR spectrum (100 MHz, methanol- d_4) of compound **2** (hymenocardinol).

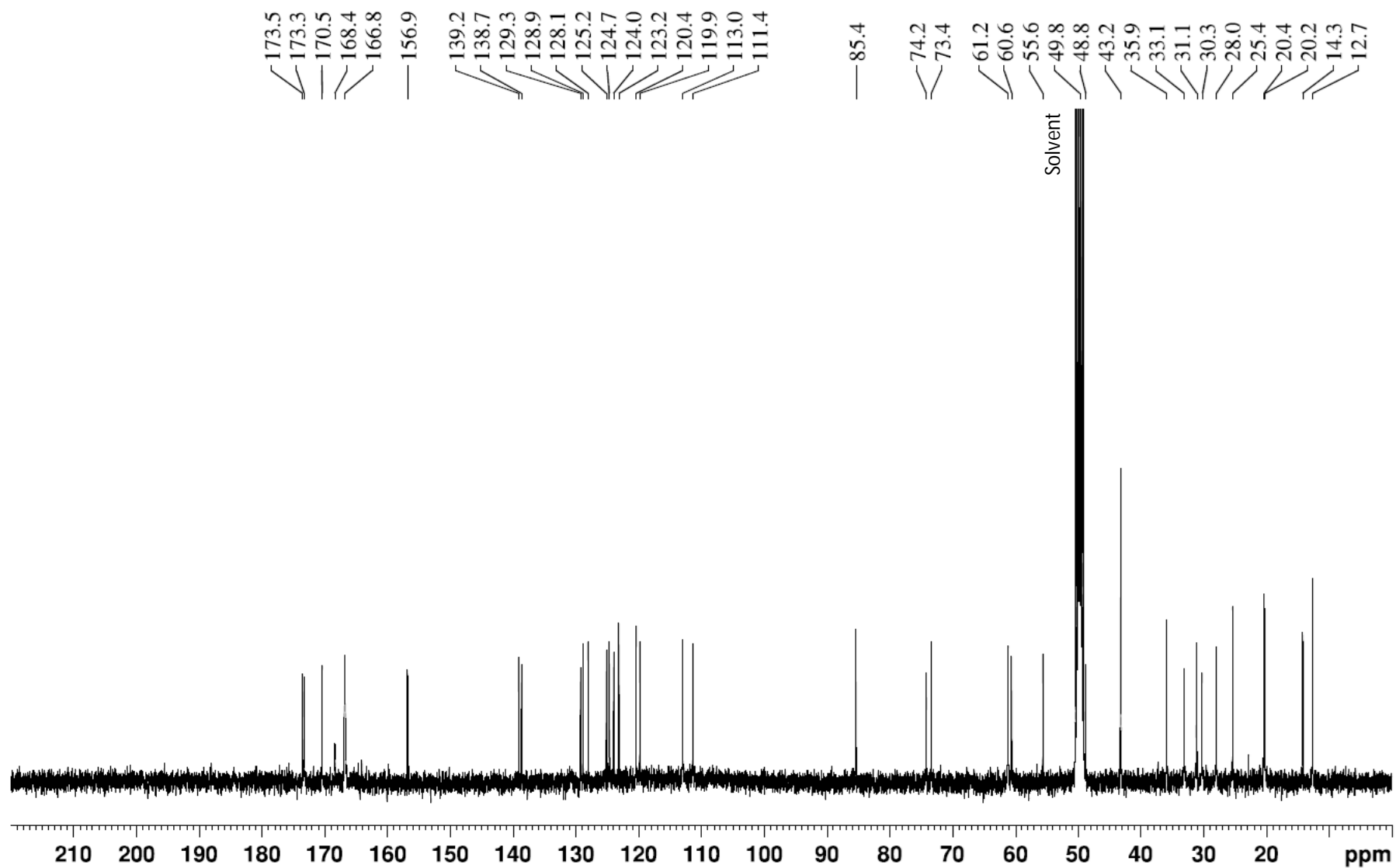


Fig. 4.6 ^1H -NMR spectrum (400 MHz, methanol- d_4) of compound **3** (hymenocardine *N*-oxide).

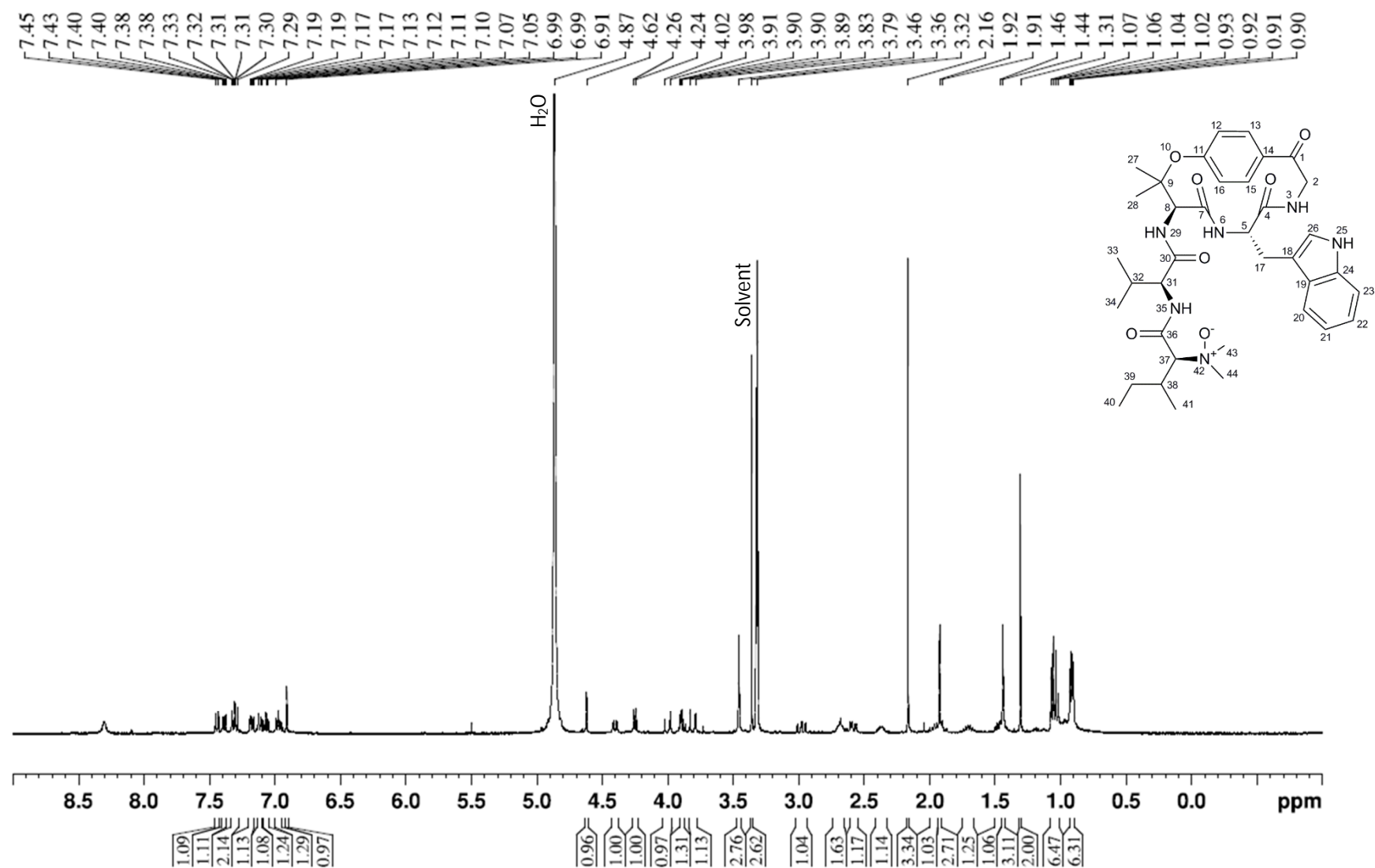
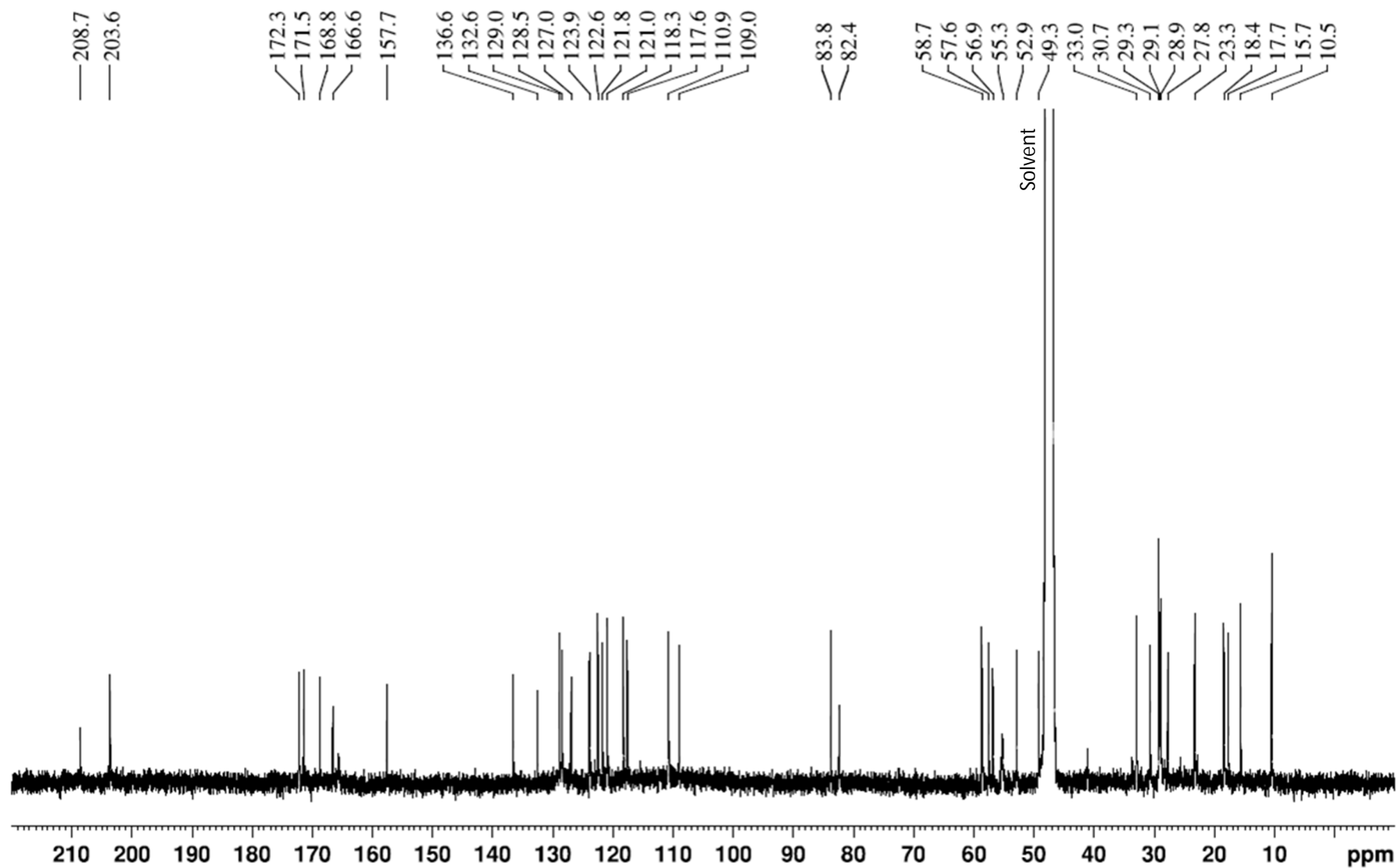


Fig. 4.7 ^{13}C -NMR spectrum (100 MHz, methanol- d_4) of compound **3** (hymenocardine *N*-oxide).



In contrast to the previous two compounds, compound **4** was structurally not closely related to hymenocardine (**1**), as deduced from the NMR spectra. (See Figures 4.8 – 4.11 for ^1H and 2D spectra). The structure of this compound was elucidated based on its 2D-NMR spectra (COSY, HSQC, and HMBC). Instead of a β -hydroxyvaline unit, present as one of the ring-bound amino acids in compounds **1-3**, this compound was found to contain a β -hydroxyleucine moiety, and in the side chain isoleucine was present instead of valine. Moreover, the 14-membered ring also contained a histidine moiety, whereas a tryptophan moiety was present in compounds **1-3**. The presence of histidine was confirmed by comparison with published NMR data for this amino acid (Ye *et al.*, 1993). To the best of our knowledge, this is the first report of a cyclopeptide alkaloid containing a histidine moiety. Because of the presence of this amino acid, compound **4** was named hymenocardine-H.

^1H and ^{13}C NMR chemical shift assignments for compounds **1-4** are listed in Tables 4.1 and 4.2, respectively. For compounds **1-3**, ^{13}C NMR spectra were recorded in methanol- d_4 and the spectra were recorded in DMSO- d_6 for **4**. When NMR spectra in methanol- d_4 were recorded for compound **4**, an artefact (compound **5**) was detected, which was identified as the hemiacetal form of **4**, formed after reaction with the solvent (methanol- d_4). This was deduced from the presence of a signal at 105.5 ppm in the ^{13}C NMR spectrum, while there was no signal for the carbonyl C-atom at C-1, which would have a chemical shift of more than 200 ppm. ^1H and ^{13}C NMR spectra of compound **5** are displayed in Figures 4.12 and 4.13, respectively.

Fig. 4.8 ^1H -NMR spectrum (400 MHz, $\text{DMSO}-d_6$) of compound **4** (hymenocardine-H).

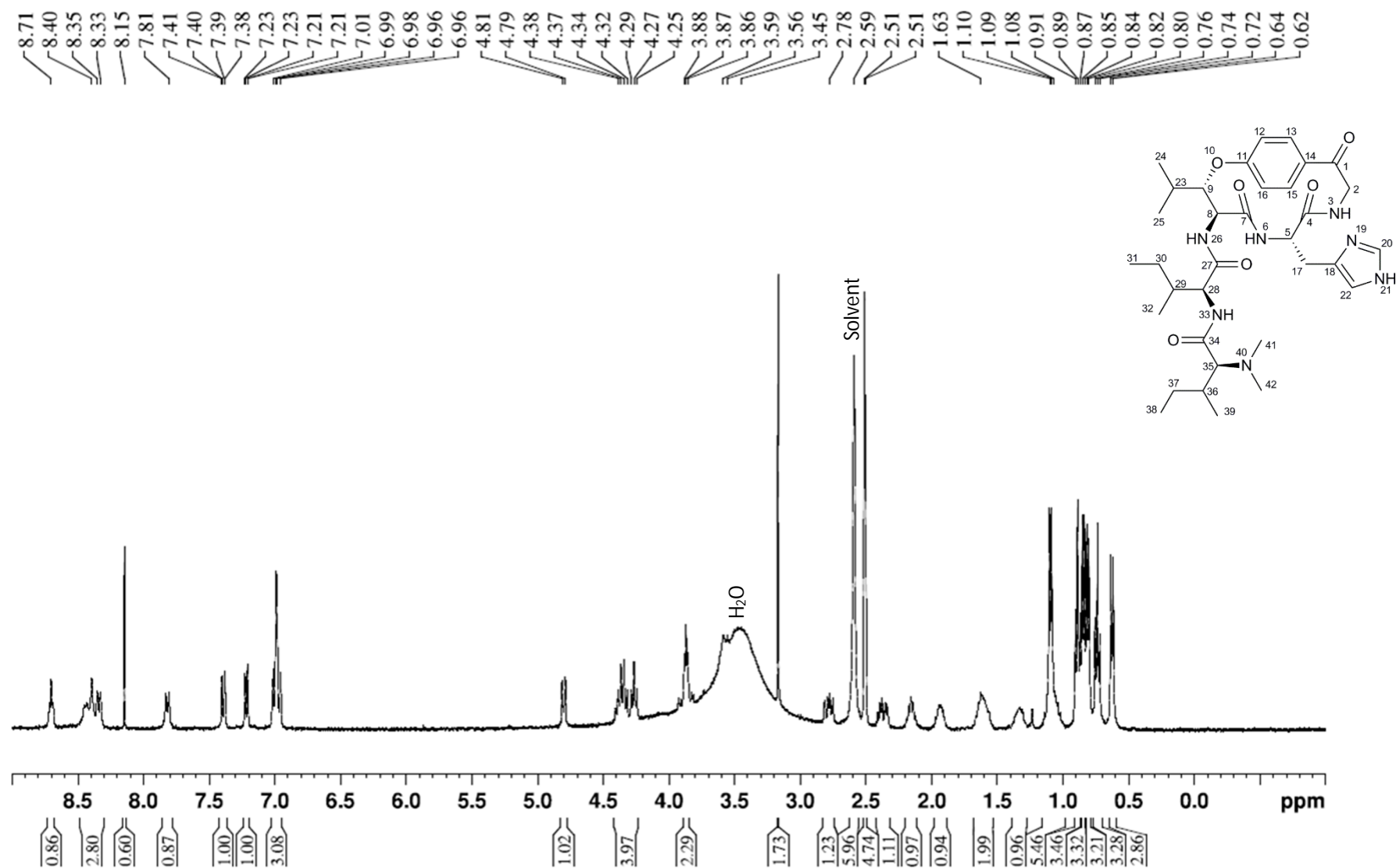


Fig. 4.9 HSQC spectrum (DMSO- d_6) of compound **4** (hymenocardine-H).

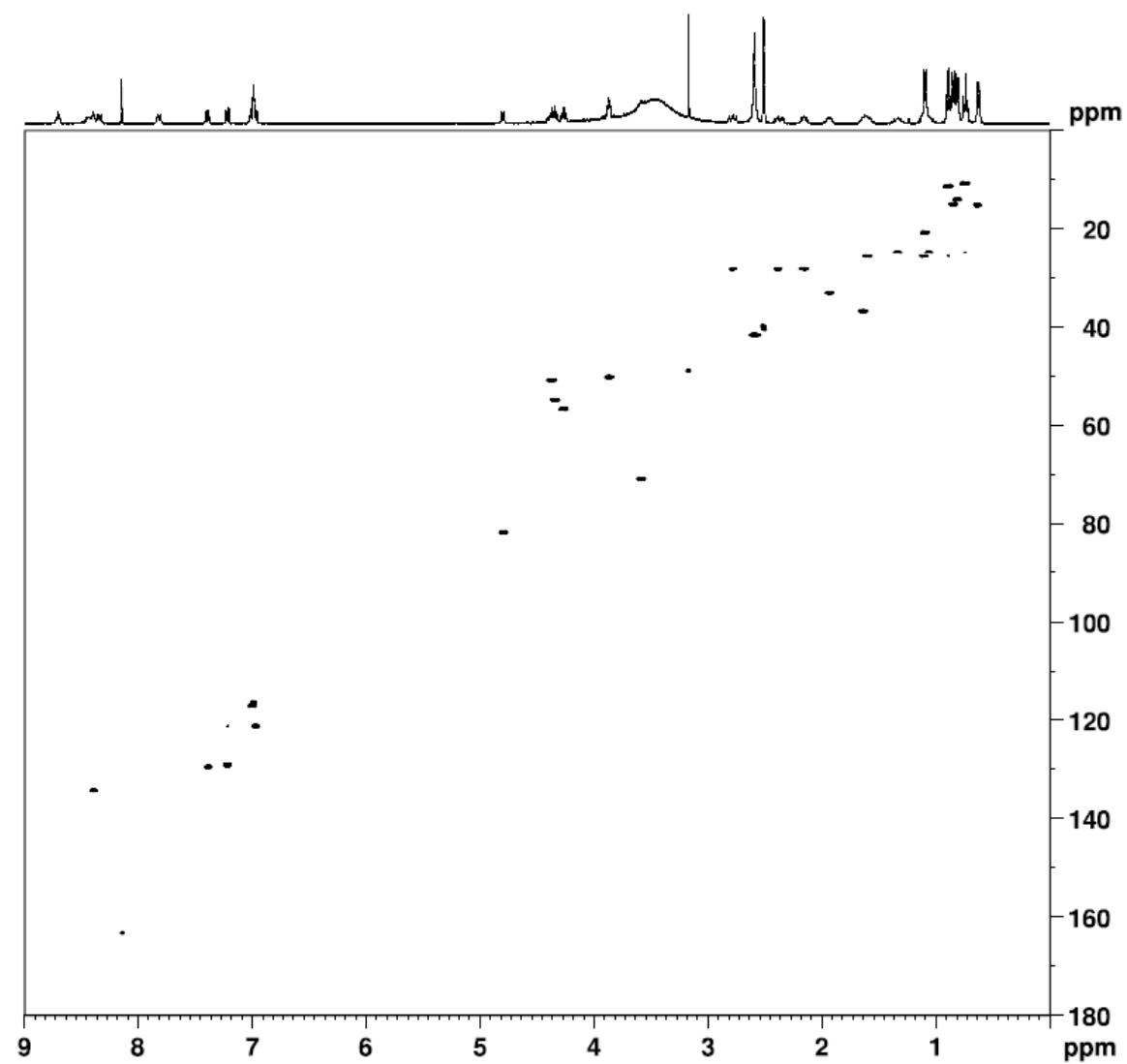


Fig. 4.10 HMBC spectrum (DMSO- d_6) of compound **4** (hymenocardine-H).

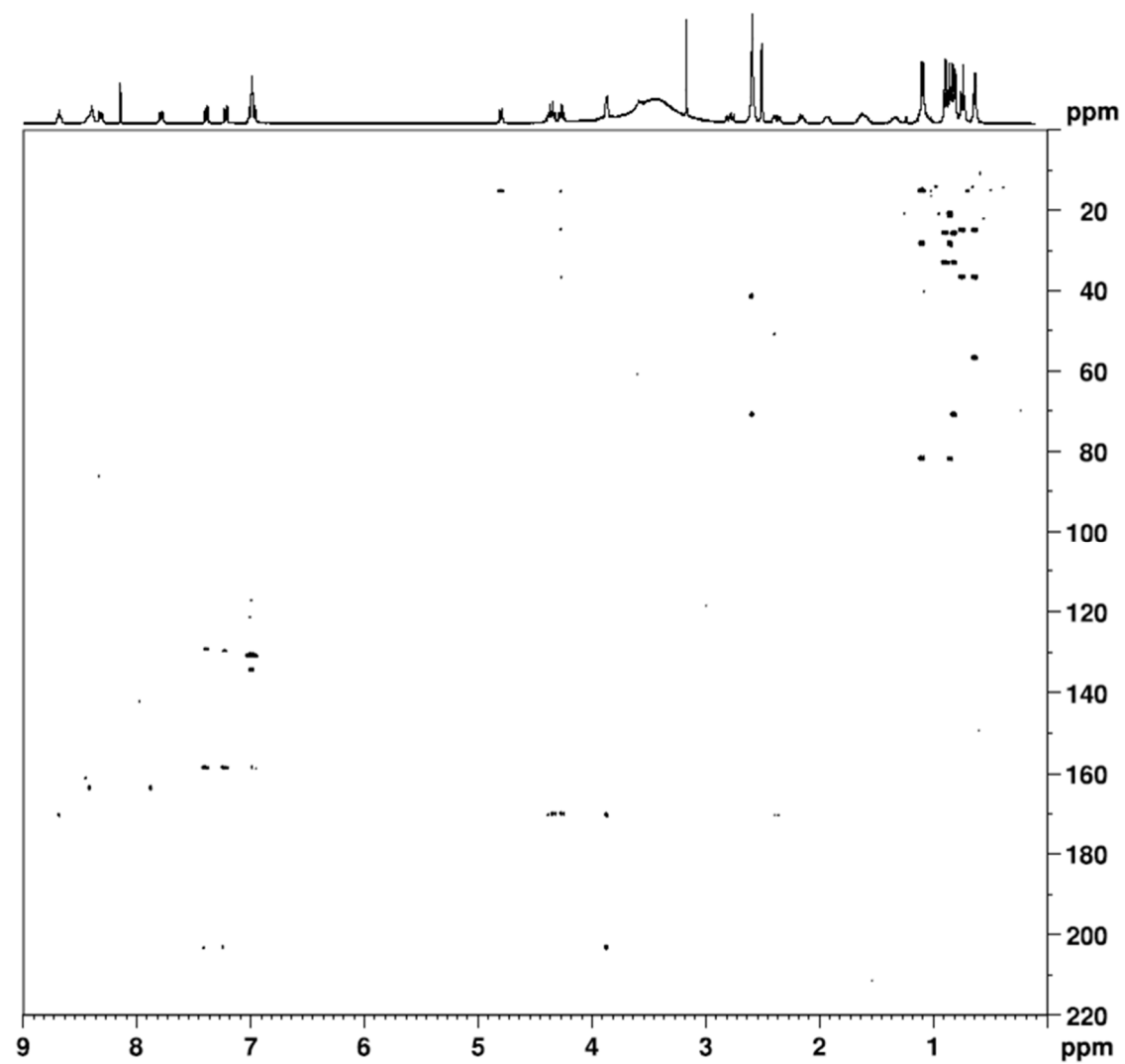


Fig. 4.11 COSY spectrum (DMSO- d_6) of compound **4** (hymenocardine-H).

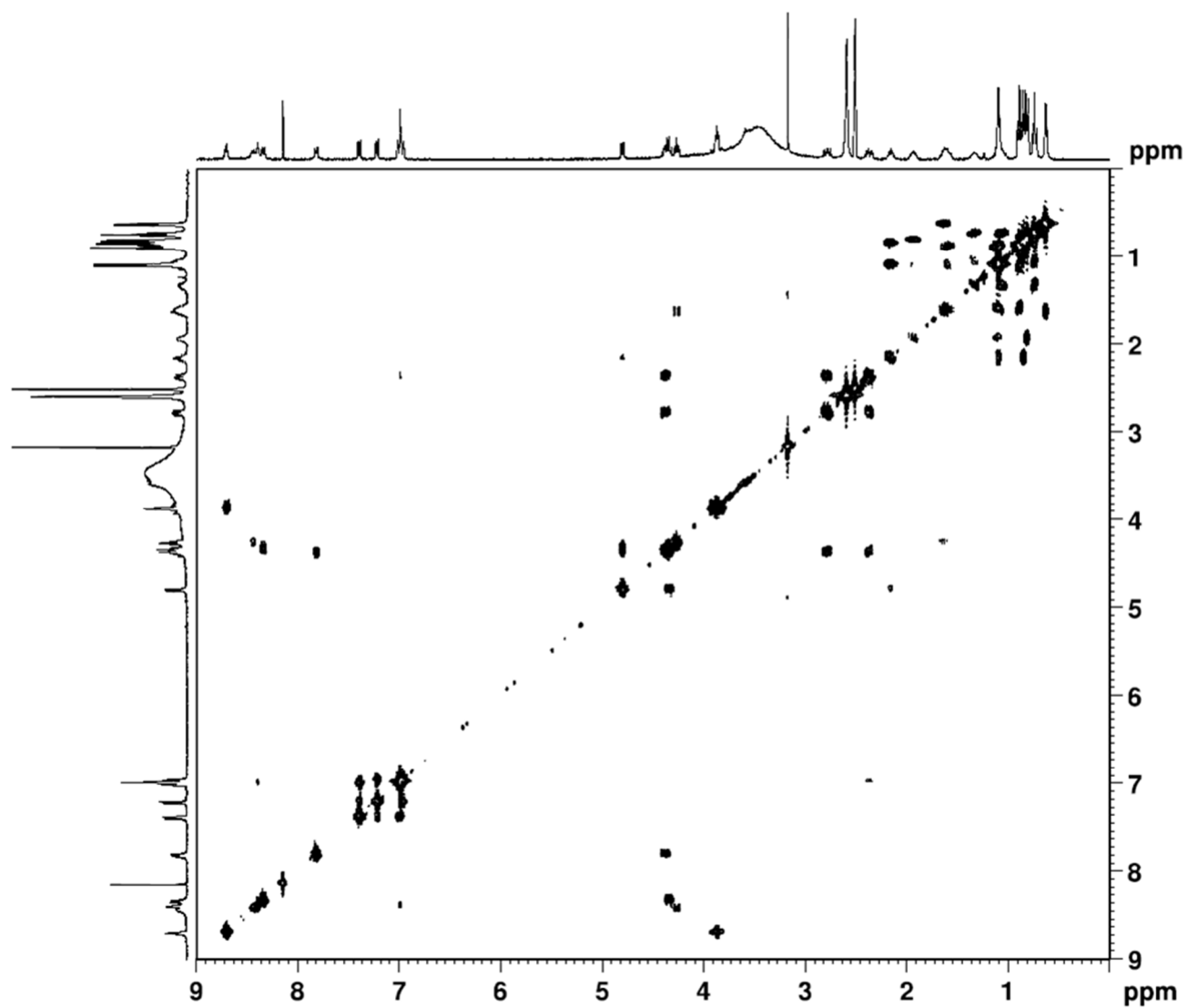


Fig. 4.12 ^1H -NMR spectrum (400 MHz, methanol- d_4) of compound **5** (hymenocardine-H hemi-acetal).

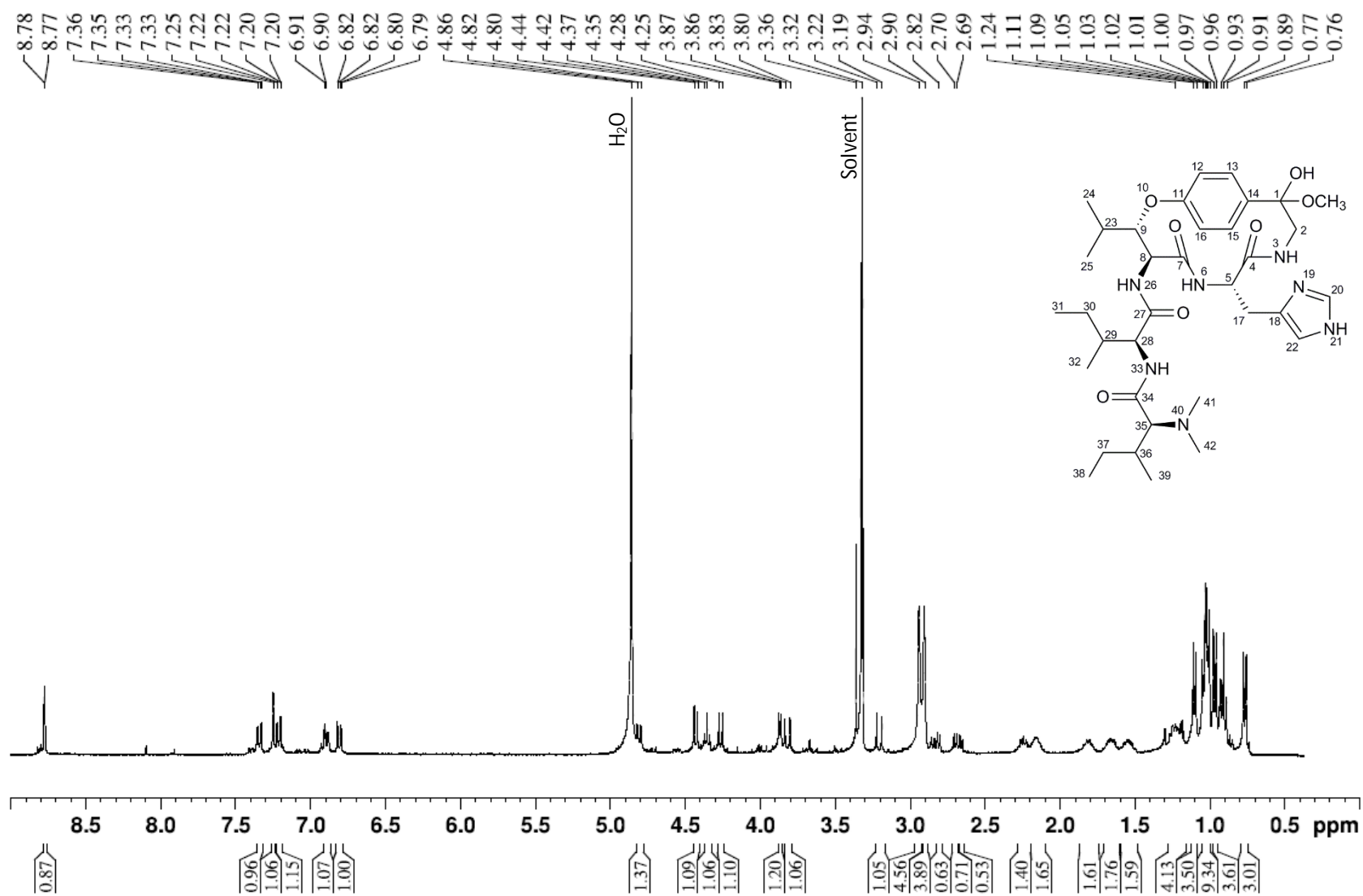
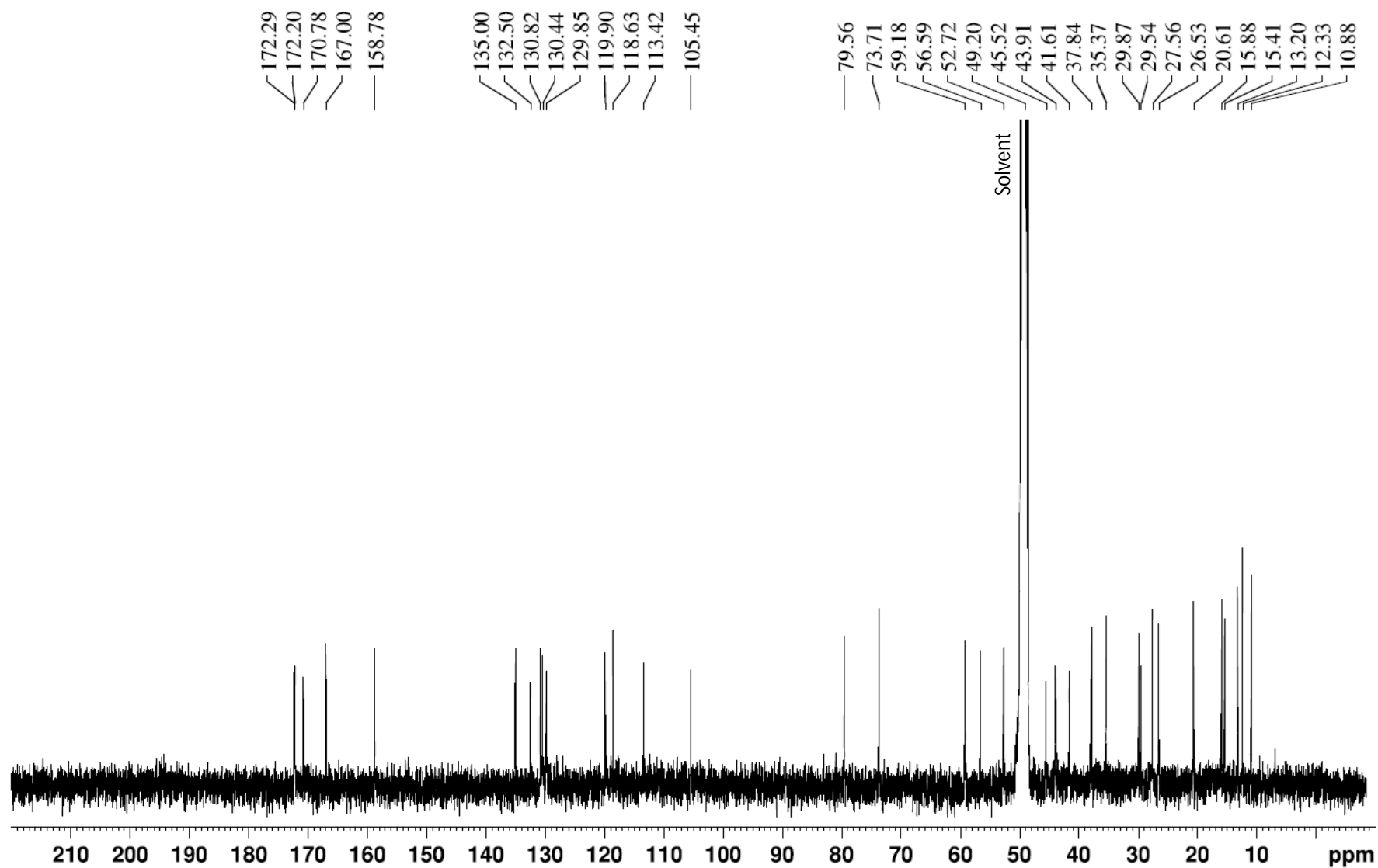


Fig. 4.13 ^{13}C -NMR spectrum (100 MHz, methanol- d_4) of compound **5** (hymenocardine-H hemi-acetal).



Amino acids that occur in Nature are usually present in the L-configuration. Also in cyclopeptide alkaloids, this configuration is found in the vast majority and only rarely the D-configuration has been reported, for example, in scutianine-E, isolated from *Scutia buxifolia* (Morel *et al.*, 2005). The configuration of hymenocardine (**1**) has been described in 1968 by Pais *et al.*, and indeed the L-configuration was found for the tryptophan, the valine, and the *N*-dimethylisoleucine units present in this cyclopeptide alkaloid. Conforming to the already reported configuration of hymenocardine and the occurrence of the L-form in almost all cyclopeptide alkaloids, the L-configuration was adopted for the amino acid moieties present in compounds **1-4**. For hymenocardine-H (**4**) the absolute configuration of the β -hydroxy amino acid, β -hydroxyleucine, was established as L-*erythro* based on the available NMR data. The coupling constant of the doublet corresponding to H-9 was 8.5 Hz, indicative of an *erythro* configuration. In addition, the chemical shifts of C-9 and C-8 were 81.8 ppm and 54.9 ppm, respectively, both suggestive for the L-amino acid form (Abu-Zarga *et al.*, 1995; Gournelis *et al.*, 1997).

Table 4.1 ¹H NMR spectroscopic data [δ_{H} in ppm, multiplicity (J in Hz)] for compounds **1-5**.^a

position	1	2	3	4	5
1	-	5.01, d (4.0)	-	-	-
2a	3.85, d (17.0)	2.84 ^b	3.81, d (17.0)	3.86 ^j	3.21, d (13.8)
2b	3.99, d (17.0)	4.13, dd (14.1, 5.1)	4.00, d (17.0)	3.88 ^j	3.82, d (13.8)
3 (N-H)	n.o.	n.o.	n.o.	8.71, t (5.4)	n.o.
5	4.53, m	4.28, m	4.40, dd (10.8, 4.5)	4.38 ^j	4.35, m
6 (N-H)	n.o.	n.o.	n.o.	7.81, d (9.5)	n.o.
8	4.73, s	4.71, s	4.62, s	4.43 ^j	4.43, d (9.4)
9	-	-	-	4.80, d (8.5)	4.81, dd (9.4, 2.0)
12	7.24, d (8.9)	7.14, d (8.4)	7.18, dd (8.3, 2.2)	7.01 ^k	6.90, dd (8.9, 2.7)
13	7.34, d (8.9)	7.32 ^c	7.39, dd (8.2, 2.1)	7.39, d (8.5)	7.34, dd (8.7, 2.2)
15	7.34, d (8.9)	6.95 ^d	7.31 ^f	7.22, dd (8.5, 2.0)	7.21, dd (8.6, 2.2)
16	7.14, dd (9.6, 2.1)	6.97 ^d	7.12, dd (8.4, 2.3)	6.97 ^k	6.81, dd (8.6, 2.5)
17a	2.56, dd (14.1, 4.3)	2.64, dd (14.3, 4.7)	2.58, dd (14.1, 4.6)	2.38, m	2.70, d (7.0)
17b	2.96, dd (14.0, 11.3)	2.97, dd (14.3, 10.4)	2.98, dd (14.0, 10.9)	2.78, dd (15.7, 9.2)	2.82, d (7.0)
20	7.40, d (8.2)	7.44, d (8.0)	7.44, d (7.9)	8.39, m	8.78, d (1.4)
21	6.94, dd (8.0, 7.6)	6.99 ^d	6.99, ddd (8.2, 7.5, 1.0)	8.40 ^l	N-H, n.o.
22	7.05, dd (8.2, 7.6)	7.07, dd (8.0, 7.5)	7.07, ddd (8.0, 7.6, 1.0)	6.99 ^k	7.25, s
23	7.27, d (8.2)	7.30 ^c	7.30 ^f	2.16, m	2.24, m
24	-	-	-	1.09 ^m	1.10, d (7.0)
25	N-H, n.o.	N-H, n.o.	N-H, n.o.	0.85, d (6.7)	0.97, d (7.0)
26	6.89, s	6.95 ^d	6.91, s	8.34, d (9.7)	N-H, n.o.
27	1.92, s	1.91, s	1.44, s	-	-
28	1.49, s	1.46, s	1.92, s	4.27 ^j	4.26, d (9.4)
29	N-H, n.o.	N-H, n.o.	N-H, n.o.	1.63, m	1.80, m
30a	-	-	-	1.06 ^m	1.24 ⁿ
30b	-	-	-	1.33, m	1.54, m
31	4.29, d (9.0)	4.35, d (8.6)	4.25, d (7.7)	0.74, t (7.4)	0.91, t (7.4)
32	1.97, m	2.00, m	1.96, m	0.63, d (6.8)	0.77, d (6.9)
33	0.86, d (6.7)	0.91, d (6.7)	0.92 ^g	8.43 ^l	N-H, n.o.
34	0.93, d (6.7)	0.96, d (6.7)	0.91 ^g	-	-
35	N-H, n.o.	N-H, n.o.	N-H, n.o.	3.57 ^p	3.87, d (4.9)
36	-	-	-	1.93, m	2.16, m
37a	3.60, d (6.6)	3.75, m	3.90, m	1.11 ^m	1.23 ⁿ
37b	-	-	-	1.60, m	1.66, m
38	2.06, m	2.13, m	2.37, m	0.89, t (7.3)	1.04 ^o
39a	1.20, m	1.23, m	1.46, m	0.81, d (6.6)	1.02 ^o
39b	1.65, m	1.67, m	1.71, m	-	-
40	1.02, t (7.4)	1.03 ^e	1.04 ^h	-	-
41	0.97, d (6.6)	1.00 ^e	1.06 ^h	2.59, s	2.90, s
42	-	-	-	2.51, m	2.94, s
43	2.69, s	2.85, s ^b	3.46, s	-	-
44	2.69, s	2.85, s ^b	3.32 ^q	-	-

^aSpectra were recorded at 400 MHz. Solvent for compounds **1-3** and **5**: methanol-*d*₄, compound **4**: DMSO-*d*₆. n.o.: not observed. ^{b-o}Overlapping signals. ^pOverlapping with residual water signal.

^qOverlapping with methanol signal.

Table 4.2 ^{13}C NMR spectroscopic data (δ_{C} in ppm, type) for compounds **1-5**.^a

position	1	2	3	4	5
1	205.1, C	73.4, CH	203.6, C	203.2, C	105.5, C
2	50.9, CH ₂	48.8, CH ₂	49.3, CH ₂	50.2, CH ₂	45.5, CH ₂
4	174.0, C	173.3, C	172.3, C	170.3, C	170.8, C
5	54.5, CH	55.6, CH	52.9, CH	50.9, CH	52.7, CH
7	170.3, C	170.5, C	168.8, C	170.2, C	172.3, C
8	59.2, CH	60.6, CH	57.6, CH	54.9, CH	56.6, CH
9	85.5, C	85.4, C	83.8, C	81.8, CH	79.6, CH
11	159.3, C	156.9, C	157.7, C	158.6, C	158.8, C
12	125.5, CH	124.0, CH	123.9, CH	117.2, CH	113.4, CH
13	130.6, CH	128.1, CH	129.0, CH	129.5, CH	130.8, CH
14	134.2, C	139.2, C	132.6, C	130.6, C	132.5, C
15	130.2, CH	128.9, CH	128.5, CH	129.1, CH	129.9, CH
16	123.4, CH	125.2, CH	121.8, CH	121.2, CH	119.9, CH
17	29.4, CH ₂	30.3, CH ₂	27.8, CH ₂	28.3, CH ₂	29.5, CH ₂
18	110.6, C	111.4, C	109.0, C	163.4, C	130.4, C
19	128.6, C	129.3, C	127.0, C	-	-
20	119.2, CH	119.9, CH	117.6, CH	134.3, CH	135.0, CH
21	119.9, CH	120.4, CH	118.3, CH	-	-
22	122.7, CH	123.2, CH	121.0, CH	116.5, CH	118.6, CH
23	112.5, CH	113.0, CH	110.9, CH	28.2, CH	29.9, CH
24	138.2, C	138.7, C	136.6, C	20.8, CH ₃	20.6, CH ₃
25	-	-	-	15.1, CH ₃	15.4, CH ₃
26	124.1, CH	124.7, CH	122.6, CH	-	-
27	25.0, CH ₃	25.4, CH ₃	29.1, CH ₃	169.8, C	172.2, C
28	30.8, CH ₃	31.1, CH ₃	23.3, CH ₃	56.8, CH	59.2, CH
29	-	-	-	36.8, CH	37.8, CH
30	173.0, C	173.6, C	171.5, C	24.9, CH ₂	26.5, CH ₂
31	60.5, CH	61.2, CH	58.7, CH	10.8, CH ₃	10.9, CH ₃
32	32.5, CH	33.1, CH	30.7, CH	15.3, CH ₃	15.9, CH ₃
33	20.0, CH ₃	20.4, CH ₃	18.4, CH ₃	-	-
34	19.8, CH ₃	20.2, CH ₃	17.7, CH ₃	169.9, C	167.0, C
35	-	-	-	70.9, CH	73.7, CH
36	169.7, C	168.4, C	166.6, C	33.2, CH	35.4, CH
37	73.9, CH	74.2, CH	82.4, CH	25.6, CH ₂	27.6, CH ₂
38	35.3, CH	35.9, CH	33.0, CH	11.5, CH ₃	12.3, CH ₃
39	27.2, CH ₂	28.0, CH ₂	28.9, CH ₂	14.1, CH ₃	13.2, CH ₃
40	12.0, CH ₃	12.7, CH ₃	10.5, CH ₃	-	-
41	14.3, CH ₃	14.3, CH ₃	15.7, CH ₃	40.2, CH ₃	43.9, CH ₃
42	-	-	-	41.6, CH ₃	41.6, CH ₃
43	42.7, CH ₃	43.2, CH ₃	55.3, CH ₃		
44	42.7, CH ₃	43.2, CH ₃	56.9, CH ₃		

^aSpectra were recorded at 100 MHz. Solvent for compounds **1-3** and **5**: methanol-*d*₄, compound **4**: DMSO-*d*₆.

The antiplasmodial activity against *Plasmodium falciparum* strain K1 and cytotoxicity against MRC-5 cells (human fetal lung fibroblast cells) were determined for compounds **1-4** (Table 4.3). All four compounds showed antiplasmodial activity with IC₅₀ values ranging between 12.2 and 27.9 μ M. Compound **1** was the only compound that showed cytotoxicity with an IC₅₀ value of 51.1 \pm 17.2 μ M, and for the other compounds no cytotoxicity was observed in a concentration up to 64.0 μ M (IC₅₀ > 64.0 μ M).

Table 4.3. Antiplasmodial activity against *P. falciparum* strain K1 and cytotoxicity against MRC5-Cells (IC₅₀ μ M) for compounds **1-4**, obtained from root bark of *Hymenocardia acida*.

compound	<i>P. falciparum</i> K1	MRC-5
1	16.4 \pm 6.8	51.1 \pm 17.2
2	17.5 \pm 8.7	> 64.0
3	12.2 \pm 6.6	> 64.0
4	27.9 \pm 16.5	> 64.0
chloroquine	0.2 \pm 0.1	-

From previous results by Suksamrarn *et al.* (2005) and Panseeta *et al.* (2011), it has been shown that all known cyclopeptide alkaloids with antiplasmodial activity contain a β -hydroxy proline unit, although this amino acid unit was also present in some inactive compounds. Moreover, the importance of both the methoxy group in the styrylamine moiety and the methylation of the terminal nitrogen atom was suggested.

Compounds **1-4** do not contain a β -hydroxyproline moiety nor a methoxy group, but they do possess methylated terminal nitrogen atoms. It can be concluded that the presence of the β -hydroxyproline and the methoxy group might be an indication for antiplasmodial activity, but that these functional groups are not indispensable and cyclopeptide alkaloids with other functional groups can also show antiplasmodial activity. Based on the results of the limited set of compounds that was tested, the terminal *N*-methyl groups could be crucial for the antiplasmodial activity. In view of the moderate *in vitro* antiplasmodial activity of the isolated cyclopeptide alkaloids, it is not clear to what extent these constituents explain the traditional use of *H. acida* against malaria.

4.3 Materials and Methods

4.3.1 General experimental procedures

See Chapter 2, general experimental procedures, sections 2.1, chromatographic methods, and 2.2, spectroscopic methods.

4.3.2 Plant material

The root bark of *Hymenocardia acida* was collected in December 2012 in Dubréka, Guinea-Conakry. A specimen of this plant is maintained at the Research and Valorization Center on Medicinal Plants in Dubréka (voucher code 62HK530).

4.3.3 Extraction and isolation

A crude extract was prepared from 2.7 kg of the dried and milled root bark of *H. acida* by means of percolation with 80% CH₃OH/20% H₂O (83 L in total). After evaporation of the solvent and freeze-drying, 356.9 g of crude extract remained. The crude extract was redissolved in 50% CH₃OH/50% H₂O and acidified to pH <3 with 2 M HCl. Then, a liquid-liquid partition was performed with CHCl₃. Next, the pH of the CH₃OH/H₂O/H⁺ phase was increased to > 9 by addition of NH₄OH (25%), followed by a second liquid-liquid partition with CHCl₃. Thus, the plant material was divided into three fractions: CHCl₃ (I), CHCl₃ (II), and CH₃OH/H₂O (pH > 9). TLC analysis of these three fractions was performed with CHCl₃-CH₃OH-NH₄OH (60:30:10) as the mobile phase and the plates were observed under UV light (254 and 366 nm) and under visible light after spraying with Dragendorff and iodoplatinate reagents.

The TLC analysis indicated that alkaloids were only present in the CHCl₃ (II) phase (8.27 g). Further fractionation of this phase was performed by flash chromatography on a GraceResolv 120 g silica column. The solvents CH₂Cl₂ (A), EtOAc (B) and CH₃OH (C) were used as follows: 0 min 100% A, 0% B, 0% C, changing linearly to 0% A and 100% B at 40 min; then a linear change to 50% B/50% C in a 20 min time span, which was retained between 60 and 80 min; from 80 to 100 min a linear change to 100% C; finally, this condition was maintained until 115 min. The flow rate was 13 mL/min and for detection ELSD and UV absorption at 254 nm and 366 nm were used. Throughout the whole experiment, the eluent was collected in test tubes, based

on the ELSD and UV absorption intensity. Together with TLC analysis, which was performed as described above, test tubes that showed a similar pattern were combined. This resulted in 12 fractions.

Fractions 11 and 12 were selected based on their TLC profiles (CH_2Cl_2 - CH_3OH - NH_4OH , 95:5:2) and were submitted to semi-preparative HPLC. The system was operated with a C_{18} Luna column (250 mm x 10.0 mm, particle size, 5 μm) from Phenomenex (Utrecht, The Netherlands) and a C_{18} guard column (10 mm x 10 mm, particle size, 5 μm) from Grace (Hesperia, CA, USA). Linear gradients with H_2O + 0.1% formic acid (A) and acetonitrile (B) were applied. For fraction 11: 0 to 5 min 20% B, 25 min 30% B, 40-45 min 100% B. For fraction 12: 0 to 5 min 20% B, 20 min 25% B, 35 min 45% B, 40-45 min 100% B. The flow rate was 3.0 mL/min. Sample concentration 25 mg/mL; injection volume fraction 11: 400 μL , fraction 12: 200 μL . The DAD spectrum was recorded from 200 nm to 450 nm and mass spectra were taken in the ESI+ mode, MS scan range: m/z 150 to 750. $V_{\text{capillary}}$ 3.00 kV, V_{cone} 50 V, $V_{\text{extractor}}$ 3 V, $V_{\text{RF Lens}}$ 0.2 V, T_{source} 135 $^{\circ}\text{C}$, $T_{\text{Desolvation}}$ 400 $^{\circ}\text{C}$, desolvation gas flow 750 L/h, cone gas flow 50 L/h. Automatic collection was triggered taking into account the signal intensity of various ions. For fraction 11: m/z 659 or m/z 675, which resulted in hymenocardine (**1**) and hymenocardinol (**2**). For fraction 12: m/z 654; m/z 675 or m/z 691. From this fraction hymenocardine (**1**) was isolated together with hymenocardine *N*-oxide (**3**) and hymenocardine-H (**4**).

Hymenocardine (1): yellowish powder (561 mg); $[\alpha]_D$ -106.8 (c 0.5, CH₃OH); UV λ_{\max} 201, 263 nm; ¹H NMR (methanol-*d*₄, 400 MHz) and ¹³C NMR (methanol-*d*₄, 100 MHz), see Tables 4.1 and 4.2, respectively; HRESIMS *m/z* 675.3893 [M+H]⁺; 697.3705 [M+Na]⁺ and 713.3444 [M+K]⁺ (calcd. for C₃₇H₅₁N₆O₆, 675.3865).

Hymenocardinol (2): yellowish powder (39 mg); $[\alpha]_D$ -75.6 (c 0.5, CH₃OH); UV λ_{\max} 201, 221, 278 nm; ¹H NMR (methanol-*d*₄, 400 MHz) and ¹³C NMR (methanol-*d*₄, 100 MHz), see Tables 4.1 and 4.2, respectively; HRESIMS *m/z* 677.4079 [M+H]⁺; 699.3898 [M+Na]⁺ and 715.3641 [M+K]⁺ (calcd. for C₃₇H₅₃N₆O₆, 677.4027).

Hymenocardine N-oxide (3): yellowish powder (5 mg); $[\alpha]_D$ -100.7 (c 0.4, CH₃OH); UV λ_{\max} 204, 220, 263 nm; ¹H NMR (methanol-*d*₄, 400 MHz) and ¹³C NMR (methanol-*d*₄, 100 MHz), see Tables 4.1 and 4.2, respectively; HRESIMS *m/z* 691.3855 [M+H]⁺ and 713.3605 [M+Na]⁺ (calcd for C₃₇H₅₂N₆O₇, 691.3814).

Hymenocardine-H (4): white powder (12 mg); $[\alpha]_D$ -55.5 (c 0.9 CH₃OH); UV λ_{\max} 206, 266 nm; ¹H NMR (DMSO-*d*₆, 400 MHz) and ¹³C NMR (DMSO-*d*₆, 100 MHz), see Tables 4.1 and 4.2, respectively; HRESIMS *m/z* 654.4018 [M+H]⁺; 676.3837 [M+Na]⁺ and 692.3620 [M+K]⁺ (calcd for C₃₄H₅₁N₇O₆, 654.3974).

4.3.4 Antiplasmodial and cytotoxic activities

The antiplasmodial activity and cytotoxic activities were determined as described in chapter 2, general experimental procedures, section 2.3, biological activity testing. The means and standard deviations of six and four experiments were calculated for compounds **1** and **2** and compounds **3** and **4**, respectively.

References

- Abu-Zarga, M., Sabri, S., Alaboudi, A., Ajaz, M. S., Sultana, N. and Attaurrahman, 1995. New cyclopeptide alkaloids from *Ziziphus lotus*. *J Nat Products* **58**(4): 504-511.
- El-Seedi, H. R., Zahra, M. H., Goransson, U. and Verpoorte, R., 2007. Cyclopeptide alkaloids. *Phytochem Rev* **6**(1): 143-165.
- Gournelis, D. C., Laskaris, G. G. and Verpoorte, R., 1997. Cyclopeptide alkaloids. *Nat Prod Rep* **14**(1): 75-82.
- Han, J., Ji, C. J., He, W. J., Shen, Y., Leng, Y., Xu, W. Y., Fan, J. T., Zeng, G. Z., Kong, L. D. and Tan, N. H., 2011. Cyclopeptide Alkaloids from *Ziziphus apetala*. *J Nat Prod* **74**(12): 2571-2575.
- Mahmout, Y., Mianpeurem, T., Dolmazon, R., Bouchu, D. and Fenet, B., 2005. Amphiphile triterpenoids from *Hymenocardia acida* Tul. Phytoantimalarial and anti-inflammatory activities? *Phytochemistry* **7**: 61-66.
- Manga, F. N., El Khattabi, C., Fontaine, J., Berkenboom, G., Duez, P., Noyon, C., Van Antwerpen, P., Nzunzu, J. L. and Pochet, S., 2013. Vasorelaxant and antihypertensive effects of methanolic extracts from *Hymenocardia acida* Tul. *J Ethnopharmacol* **146**(2): 623-631.
- Morel, A. F., Maldaner, G., Ilha, V., Missau, F., Silva, U. F. and Dalcol, I. I., 2005. Cyclopeptide alkaloids from *Scutia buxifolia* Reiss and their antimicrobial activity. *Phytochemistry* **66**(21): 2571-2576.
- Obidike, I. C., Aboh, M. I. and Salawu, O. A., 2011. Microbiological and mucociliary properties of the ethanol extract of *Hymenocardia acida* on selected respiratory clinical isolates. *J Diet Suppl* **8**(1): 1-11.
- Pais, M., Jarreau, F. X., Gonzalezsierra, M., Mascaretti, O. A., Ruveda, E. A., Chang, C. J., Hagaman, E. W. and Wenker, E., 1979. Carbon-13 NMR analysis of cyclic peptide alkaloids. *Phytochemistry* **18**(11): 1869-1872.
- Pais, M., Marchand, J., Ratle, G. and Jarreau, F. X., 1968. N° 453. – Alcaloïdes peptidiques. VI (1). – L'hymenocardine, alcaloïde de l'*Hymenocardia acida* Tul (Hymenocardiacees). *B Soc Chim Fr*(7): 2979-2984.

- Panseeta, P., Lomchoey, K., Prabpai, S., Kongsaree, P., Suksamrarn, A., Ruchirawat, S. and Suksamrarn, S., 2011. Antiplasmodial and antimycobacterial cyclopeptide alkaloids from the root of *Ziziphus mauritiana*. *Phytochemistry* **72**(9): 909-915.
- Starks, C. M., Williams, R. B., Norman, V. L., Rice, S. M., O'Neil-Johnson, M., Lawrence, J. A. and Eldridge, G. R., 2014. Antibacterial chromene and chromane stilbenoids from *Hymenocardia acida*. *Phytochemistry* **98**: 216-222.
- Suksamrarn, S., Suwannapoch, N., Aunchai, N., Kuno, M., Ratananukul, P., Haritakun, R., Jansakul, C. and Ruchirawat, S., 2005. Ziziphine N, O, P and Q, new antiplasmodial cyclopeptide alkaloids from *Ziziphus oenoplia* var. *brunoniana*. *Tetrahedron* **61**(5): 1175-1180.
- Vonthron-Senecheau, C., Weniger, B., Ouattara, M., Bi, F. T., Kamenan, A., Lobstein, A., Brun, R. and Anton, R., 2003. In vitro antiplasmodial activity and cytotoxicity of ethnobotanically selected Ivorian plants. *J Ethnopharmacol* **87**(2-3): 221-225.
- Wurdack, K. J., Hoffmann, P., Samuel, R., De Bruijn, A., Van der Bank, M. and Chase, M. W., 2004. Molecular phylogenetic analysis of Phyllanthaceae (Phyllanthoideae Pro Parte, Euphorbiaceae sensu lato) using plastid RBCL DNA sequences. *Am J Bot* **91**(11): 1882-1900.
- Ye, C. H., Fu, R. Q., Hu, J. Z., Hou, L. and Ding, S. W., 1993. Carbon-13 chemical shift anisotropies of solid amino acids. *Magn Reson Chem* **31**(8): 699-704.

CHAPTER 5

Ziziphus oxyphylla

Published:

Emmy Tuentler, Rizwan Ahmad, Kenn Foubert, Adnan Amin, Maria Orfanoudaki, Paul Cos, Louis Maes, Sandra Apers, Luc Pieters, and Vassiliki Exarchou

Isolation and structure elucidation by LC-DAD-MS and LC-DAD-SPE-NMR of cyclopeptide alkaloids from the roots of *Ziziphus oxyphylla* and evaluation of their antiplasmodial activity

J. Nat. Prod., **2016**, 79 (11), pp 2865–2872.

5.1 Introduction

Cyclopeptide alkaloids are polyamidic, basic compounds that are distributed widely in various plant families, including the Asteraceae, Celastraceae, Euphorbiaceae, Menispermaceae, Pandaceae, Rubiaceae, Sterculiaceae, and Urticaceae, but most prominently in the Rhamnaceae, and especially the genus *Ziziphus*. Typically, their structures contain a 13-, 14-, or 15-membered macrocycle, formed by a stryrylamine unit, a common amino acid, and a β -hydroxy-amino acid. Moreover, a side chain consisting of one (i.e., a total of four building blocks) or two (a total of five building blocks) additional amino acids is attached to this ring. In this manner, the 4(13)-, 4(14)-, 5(13)-, and 5(14)-cyclopeptide alkaloid subclasses are distinguished (Gournelis *et al.*, 1997; Morel *et al.*, 2009).

Ziziphus oxyphylla Edgew. (Rhamnaceae) is a small- to medium-sized tree that grows in the northern regions of Pakistan. The fruits are used as a common food, and in traditional medicine different parts of the plant are applied in a wide range of pathological conditions, for example, to treat inflammation, microbial infections, fever or pain, allergy, and diabetes. Previous investigations have already shown *in vivo* antipyretic effects of a methanolic extract of *Z. oxyphylla* leaves and antinociceptive activities of methanolic extracts of the leaves and roots of this plant (Nisar *et al.*, 2007; Kaleem *et al.*, 2013), but the active compounds are not known. Phytochemical tests revealed the presence of alkaloids, anthraquinones, flavonoids, glycosides, phenols, saponins and tannins (Inayat-ur-Rahman *et al.*, 2007) and so far seven cyclopeptide alkaloids were isolated and identified from roots and stem (bark) of this species, i.e. hemsine-A, nummularines-C and -R, and oxyphyllines-A, -B, -C and -D (Inayat-ur-Rahman *et al.*, 2007; Choudhary *et al.*, 2011; Kaleem *et al.*, 2012). Cyclopeptide alkaloids isolated from various sources have been reported to exhibit antibacterial, antifungal, antiplasmodial and sedative activities (Han *et al.*, 1989; Morel *et al.*, 2005; Sing *et al.*, 2007; Morel *et al.*, 2008; Ma *et al.*, 2008); antiplasmodial activity more in particular for ziziphines-N and -Q (Suksamrarn *et al.*, 2005), hemsine-A, mauritine-M and nummularine-H (Panseeta *et al.*, 2011), hymenocardine, hymenocardinol and hymenocardine *N*-oxide (Tuenter *et al.*, 2016). Therefore, in the present work, the roots of *Z. oxyphylla* were selected for the targeted

isolation of cyclopeptide alkaloids, to evaluate their antiplasmodial activity, and to establish structure-activity relationships.

5.2 Results and Discussion

Cyclopeptide alkaloids were isolated and identified from two different batches of roots of *Z. oxyphylla*, collected at different locations in Pakistan in different years. Whereas for the first batch a general liquid-liquid partition and fractionation scheme was followed, a more alkaloid-specific fractionation procedure was used for the second batch to increase the number of alkaloids detected. The isolation of single compounds was performed by semi-preparative HPLC with DAD and ESIMS detection together with LC-DAD-SPE-NMR and all together nine different cyclopeptide alkaloids were identified (Figure 5.1). Their structures were elucidated by a 1D (^1H , ^{13}C , DEPT 135, DEPT 90) and 2D NMR experiments (COSY, HSQC, HMBC), mass spectrometry, and by comparison to literature data.

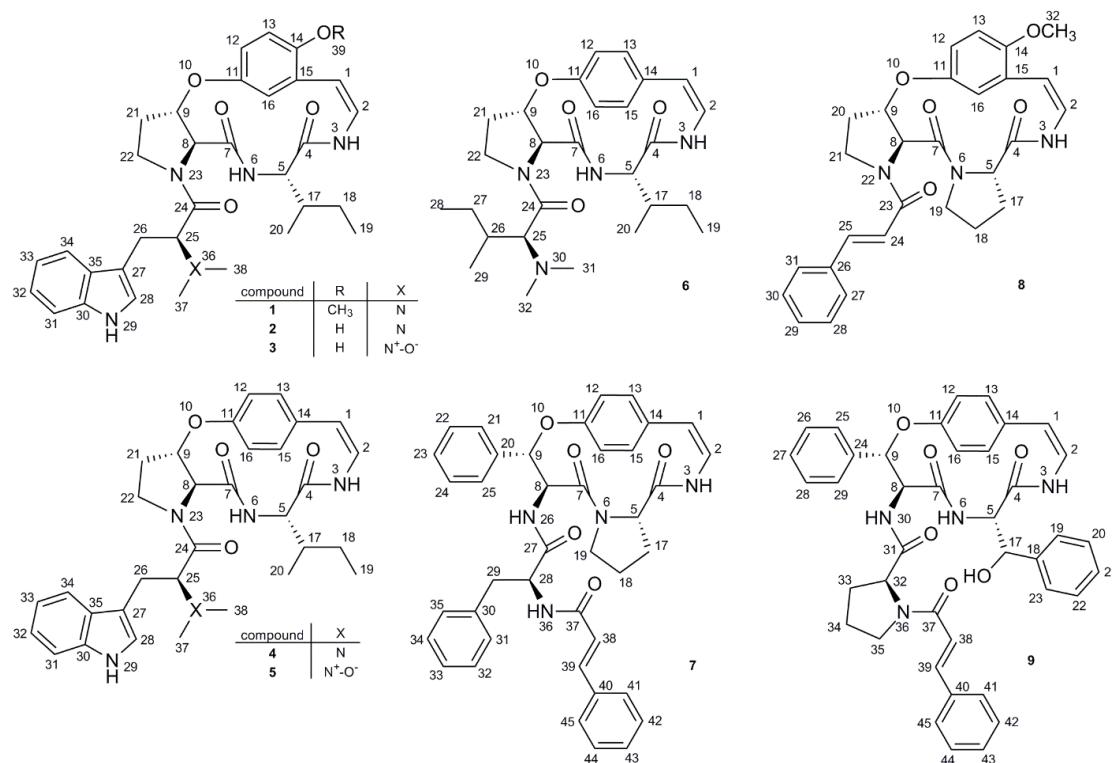


Fig. 5.1 Chemical structures of cyclopeptide alkaloids 1-9, isolated from the roots of *Ziziphus oxyphylla*.

The NMR data of compound **1** (Figures 5.2 and 5.3) were in agreement with previously reported assignments for nummularine-R (Nisar *et al.*, 2010). ^1H and ^{13}C NMR chemical shift assignments for **1** are listed in Tables 5.1 and 5.2, respectively. This cyclopeptide alkaloid has been previously isolated from *Z. oxyphylla* and was found to be present in both batches. Compound **2** showed very similar NMR spectra (Figures 5.4 and 5.5), but the characteristic signals of C-39 (56.7 ppm) and H-39 (3.77 ppm), indicative for the methoxy group attached to the styrylamine moiety of compound **1**, were absent in the spectra of compound **2**. The ESIMS data showed a base peak at m/z 611 $[\text{M}+\text{Na}]^+$ for compound **1** and at m/z 597 $[\text{M}+\text{Na}]^+$ for compound **2**. The accurate mass of compound **2** was found to be 574.3031 daltons $[\text{M}+\text{H}]^+$, in accordance with a molecular formula of $\text{C}_{32}\text{H}_{40}\text{N}_5\text{O}_5$. Taking into account both the NMR and MS data, it was concluded that compound **2** contains a hydroxy group instead of a methoxy group at position C-14. Thus, this compound was assigned as *O*-desmethylnummularine-R. Furthermore, the *N*-oxide of compound **2**, *O*-desmethylnummularine-R *N*-oxide (**3**), was also obtained in the present investigation. Indeed, from the NMR data (Figures 5.6 – 5.9) it was deduced that two *N*-methyl groups were present, indicated by signals at δ_{C} 57.1 ppm/ δ_{H} 3.49 ppm and δ_{C} 53.7 ppm/ δ_{H} 3.39 ppm, whereas in compound **2** both *N*-methyl groups occurred at δ_{C} 42.6 ppm/ δ_{H} 2.92 ppm. Also, C-25 showed a downfield shift of almost 10 ppm when compared to compound **2** (76.3 ppm vs. 67.2 ppm). These findings are in agreement with previously reported NMR assignments for cyclopeptide alkaloid *N*-oxides (Han *et al.*, 2011; Tuentner *et al.*, 2016). In addition, the HRESIMS peak at m/z 590.3002 $[\text{M}+\text{H}]^+$ corresponded to the proposed structure ($\text{C}_{32}\text{H}_{40}\text{N}_5\text{O}_6$). Compounds **2** and **3** were only detected in the second batch of plant material investigated.

Fig. 5.2 ^1H NMR spectrum (400 MHz, methanol- d_4) of compound **1** (nummularine-R).

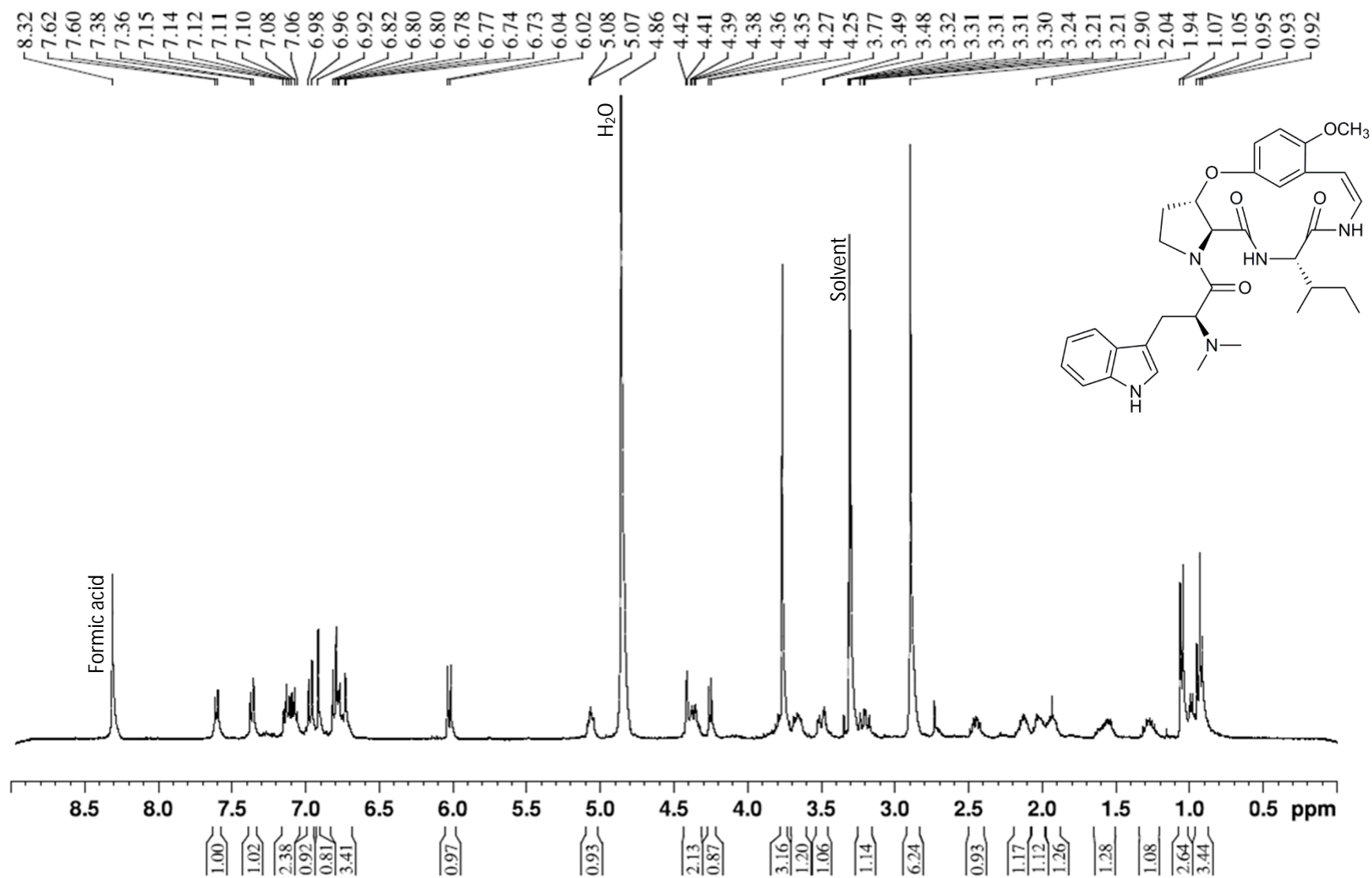


Fig. 5.3 ^{13}C spectrum (100 MHz, methanol- d_4) of compound **1** (nummularine-R).

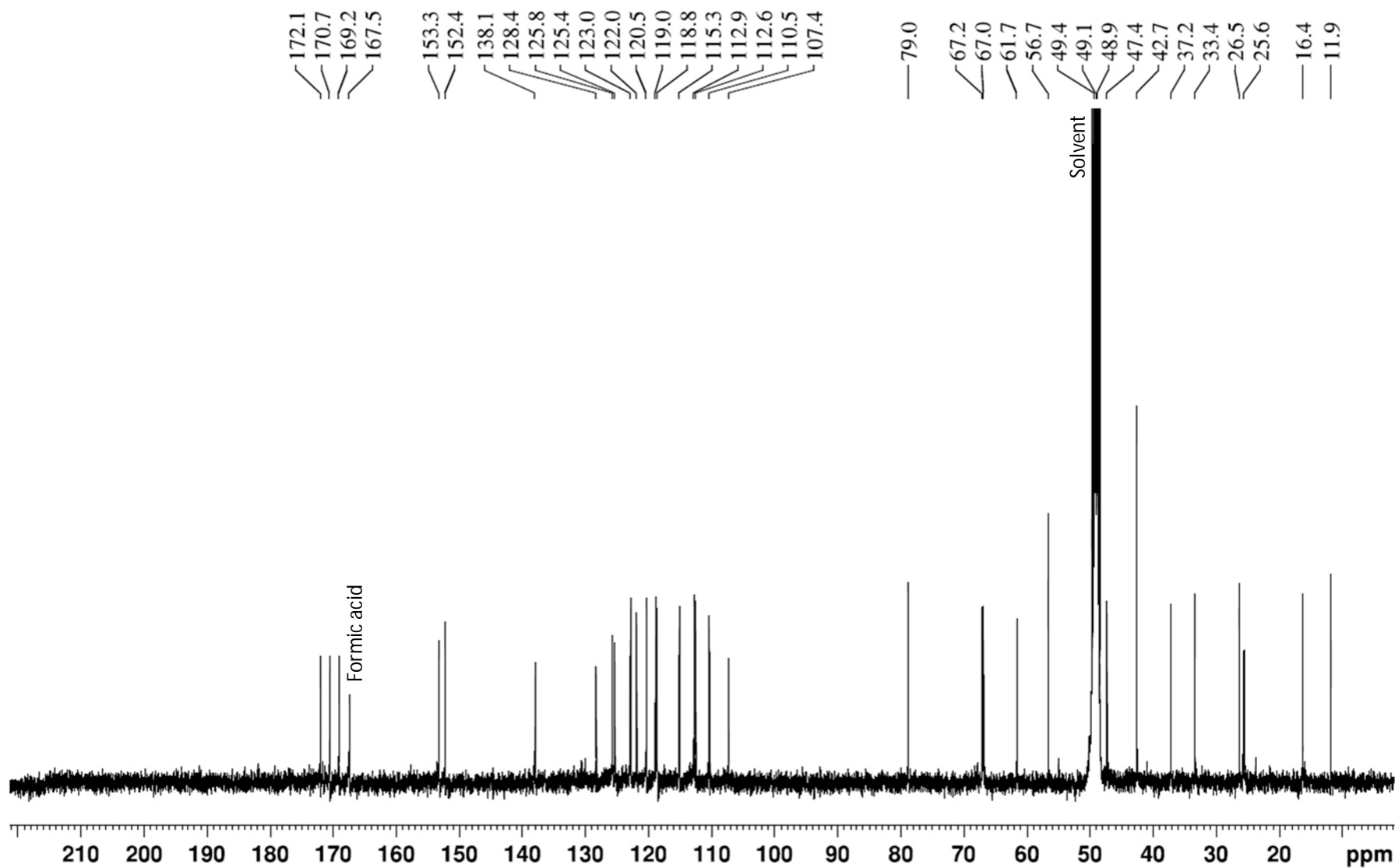


Fig. 5.4 ^1H NMR spectrum (400 MHz, methanol- d_4) of compound **2** (*O*-desmethyl-nummularine-R).

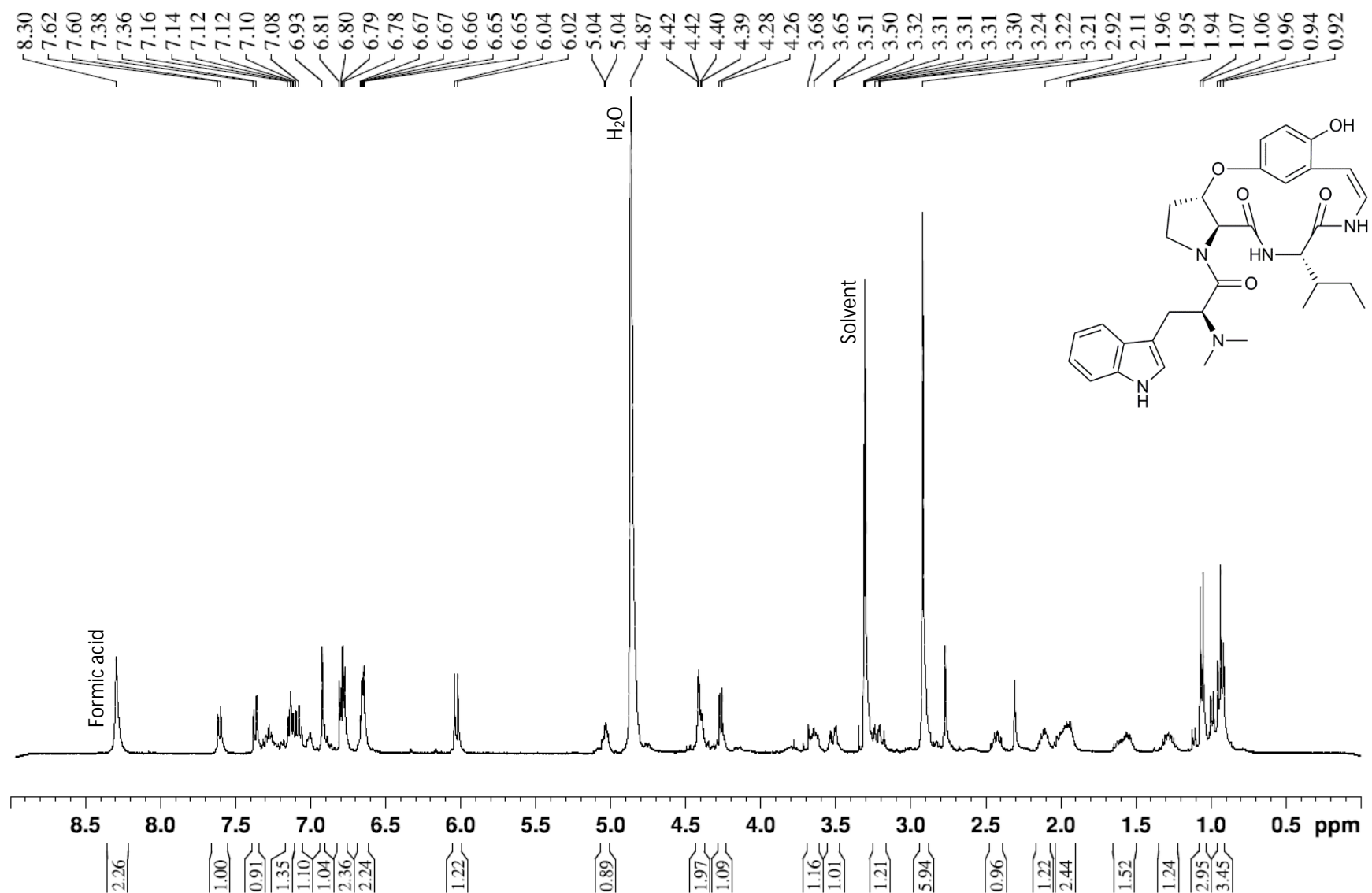


Fig. 5.5 ^{13}C spectrum (100 MHz, methanol- d_4) of compound **2** (*O*-desmethyl-nummularine-R).

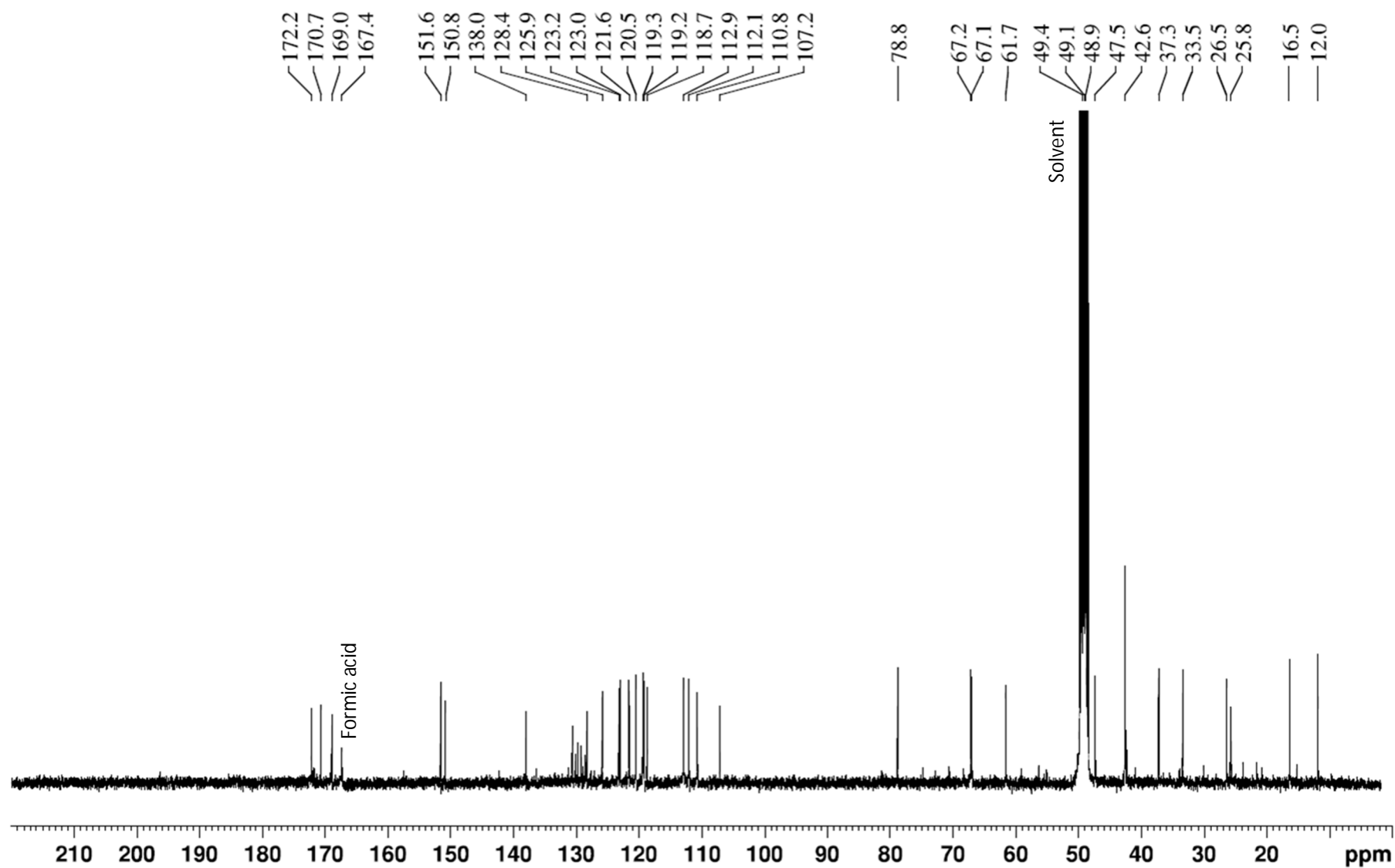


Fig. 5.6 ^1H NMR spectrum (400 MHz, methanol- d_4) of compound **3** (*O*-desmethylnummularine-R *N*-oxide).

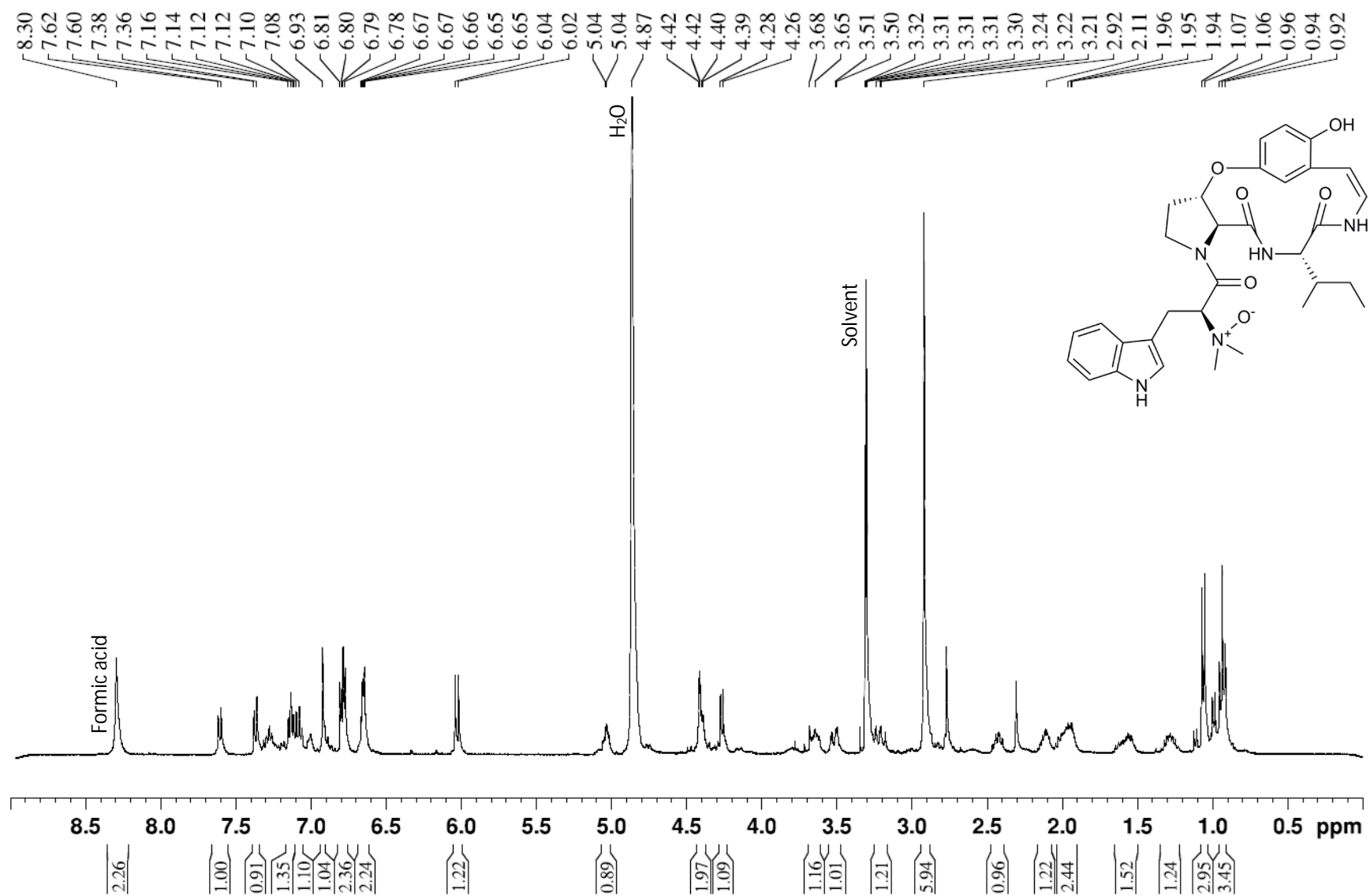


Fig. 5.7 HSQC spectrum (methanol- d_4) of compound **3** (*O*-desmethylnummularine-R *N*-oxide).

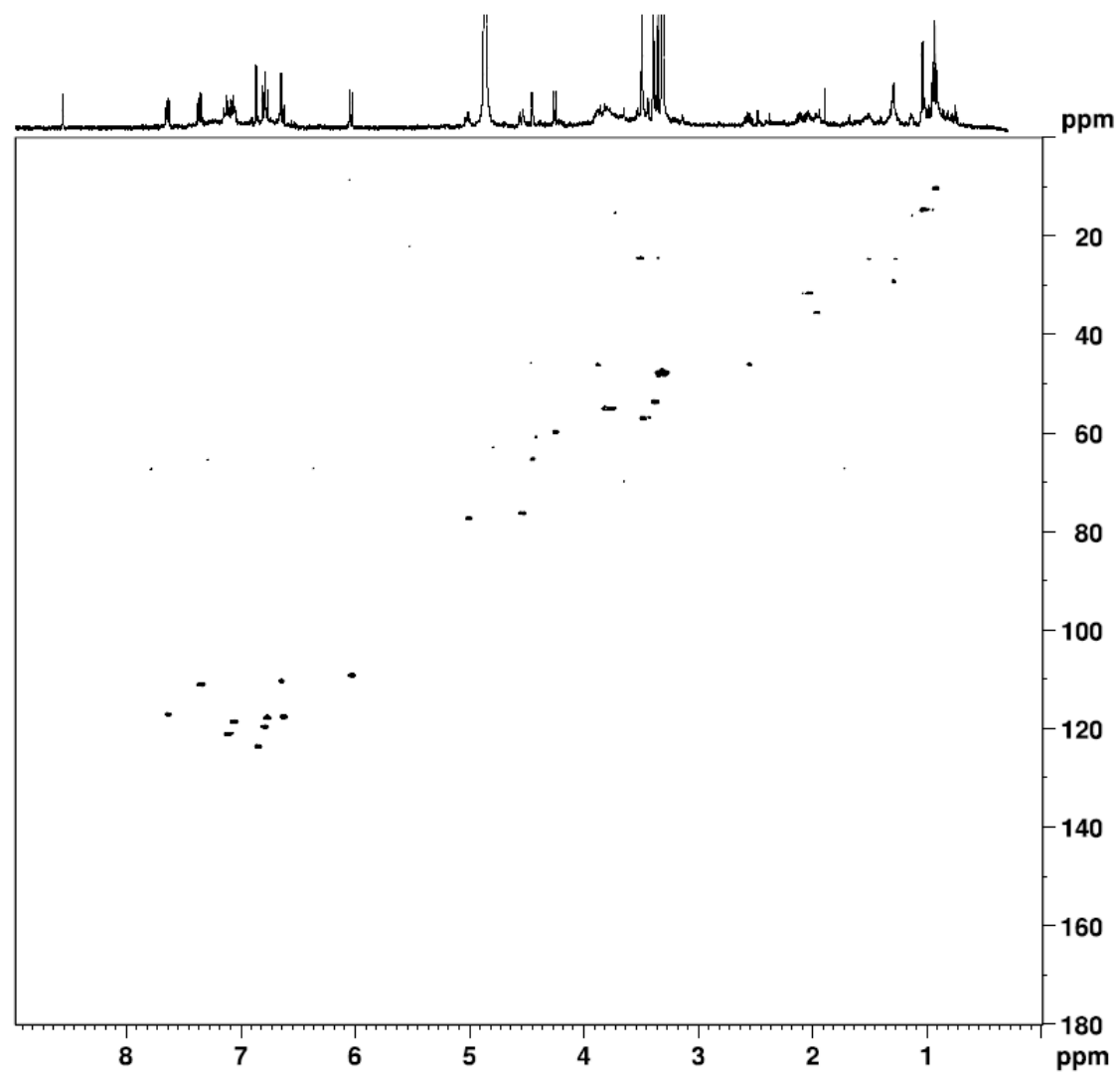


Fig. 5.8 HMBC spectrum (methanol- d_4) of compound **3** (*O*-desmethylnummularine-R *N*-oxide).

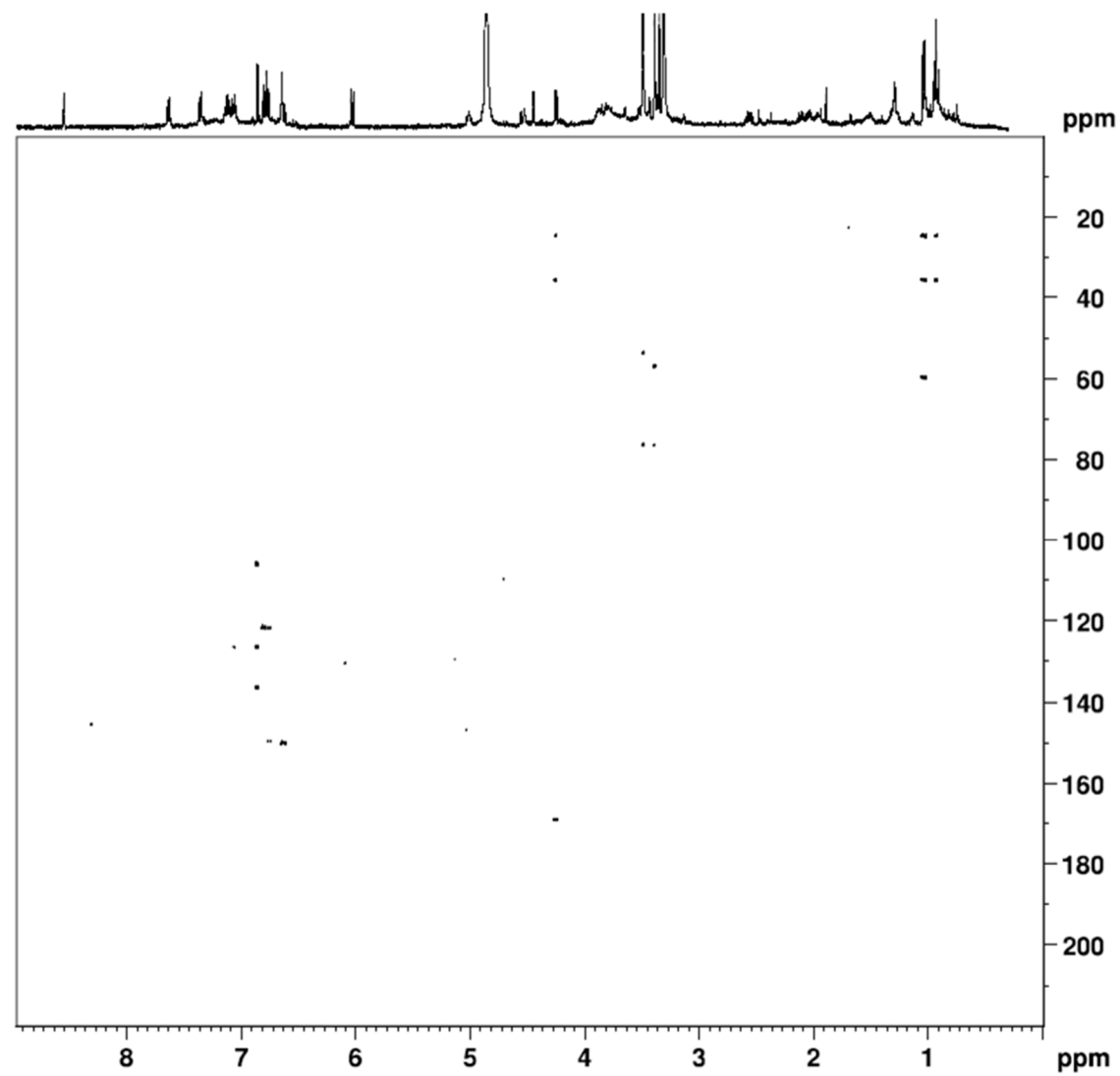
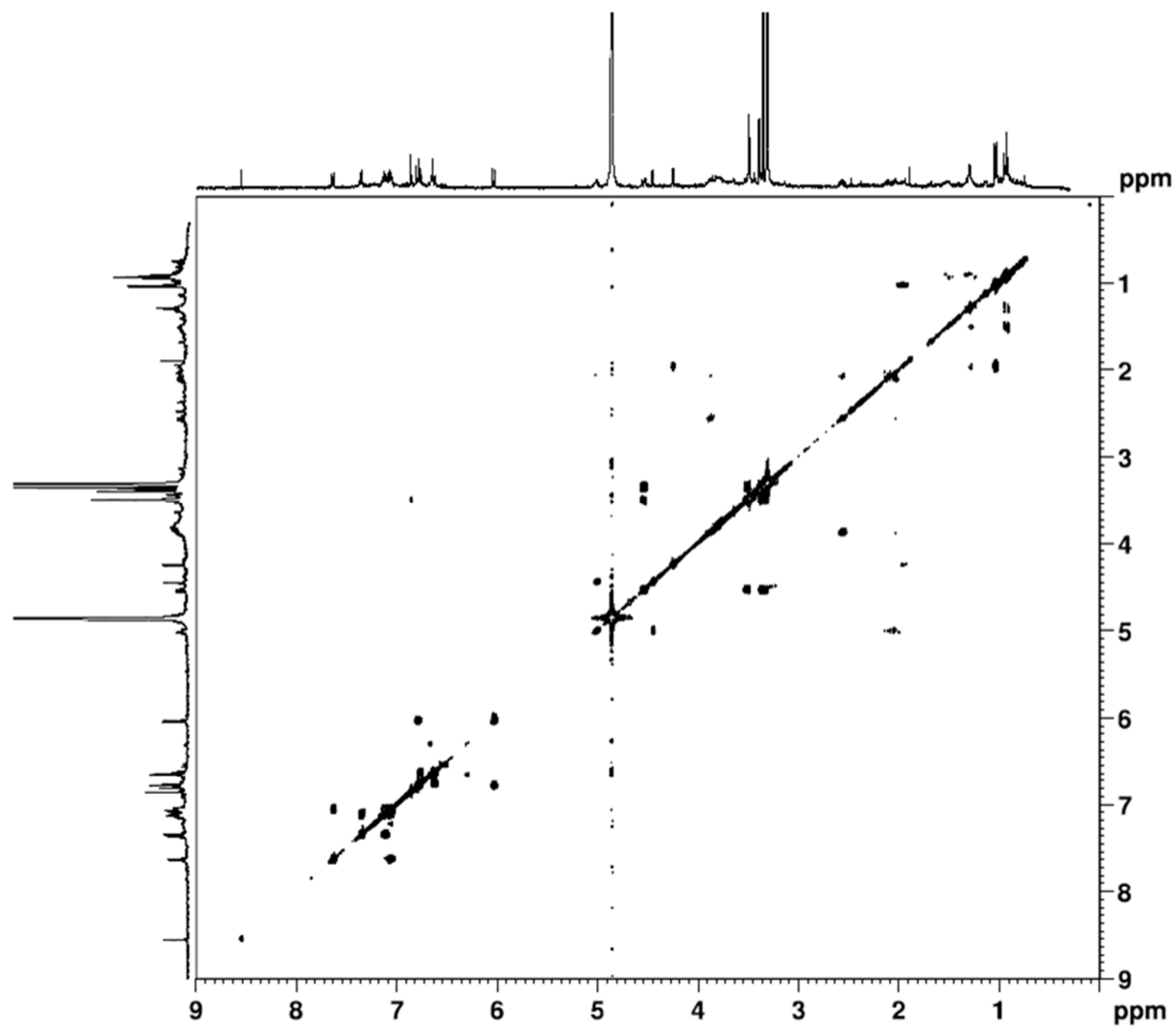


Fig. 5.9 COSY spectrum (methanol- d_4) of compound **3** (*O*-desmethylnummularine-R *N*-oxide).



Comparison of the NMR spectra of compound **4** (Figures 5.10 and 5.11) with previously published assignments showed that this compound is hemsine-A, previously isolated from *Z. oxyphylla* (Choudhary *et al.*, 2011). Also hemsine-A *N*-oxide was isolated (compound **5**), as deduced from the NMR data (Figures 5.12 – 5.15). HRESIMS supported the proposed structures. Both these compounds could only be isolated by following the more alkaloid-specific fractionation method used for the second batch of plant material. Hemsine-A *N*-oxide (compound **5**) is reported here for the first time and although it is not uncommon that cyclopeptide alkaloids are isolated as *N*-oxides, together with tertiary amines (Han *et al.*, 2011), the possibility that the *N*-oxides are artefacts formed during drying, extraction, or isolation cannot completely be excluded.

Compound **6** was identified as ramosine-A, mainly based on the NMR data (Figures 5.16 and 5.17). This cyclopeptide alkaloid was previously reported from *Paliurus ramosissimus* (Lin *et al.*, 2003), but this is the first time it has been isolated from *Z. oxyphylla* (batch 2). Compound **7** was reported in *Z. oxyphylla* by Kaleem *et al.* (2012) and was isolated from the first batch of plant material. The NMR data (Figures 5.18 and 5.19) are in agreement with previously reported assignments for oxyphylline-C.

Fig. 5.10 ^1H NMR spectrum (400 MHz, methanol- d_4) of compound **4** (Hemsine-A).

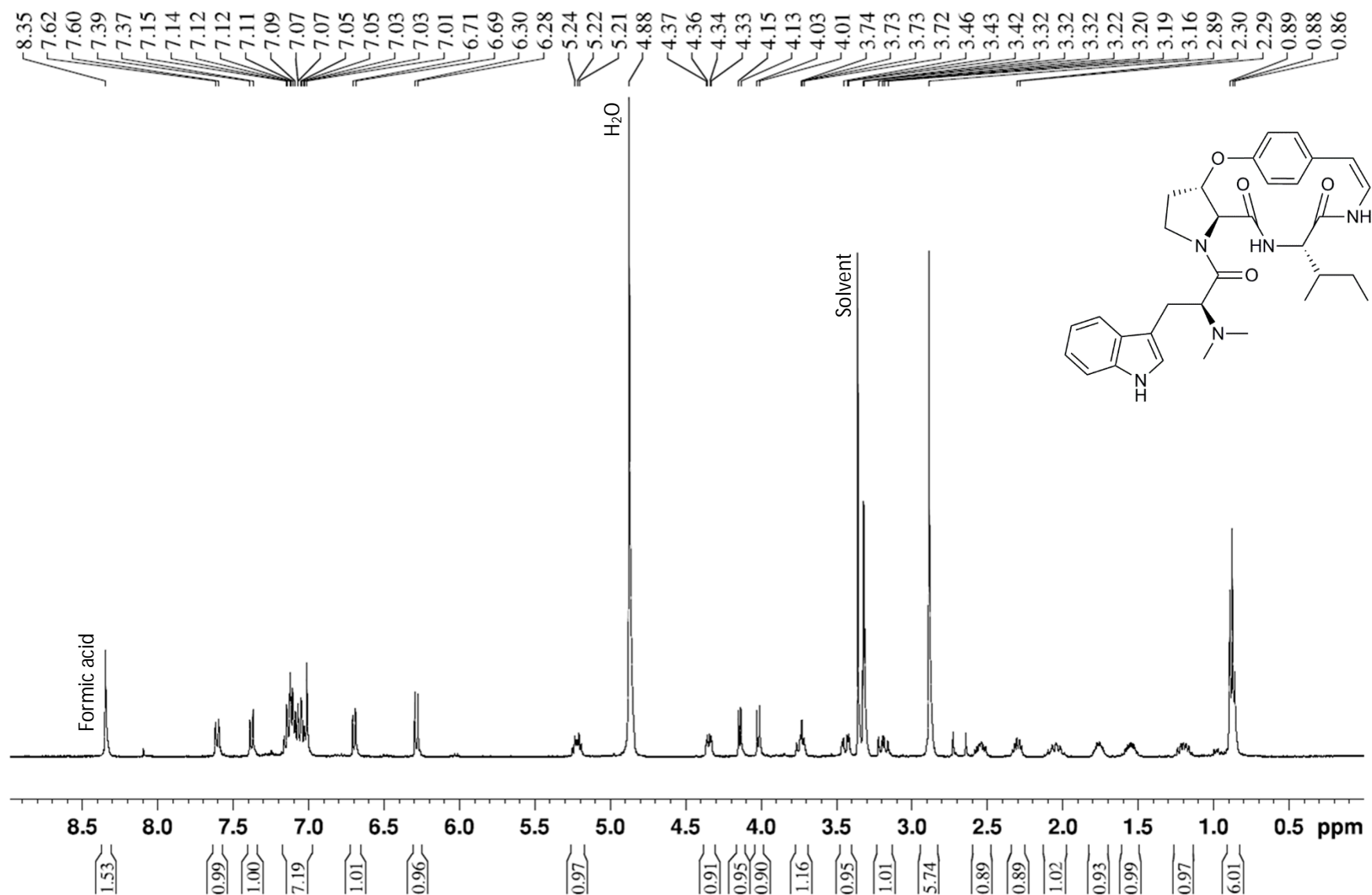


Fig. 5.11 ^{13}C NMR spectrum (100 MHz, methanol- d_4) of compound **4** (Hemsine-A).

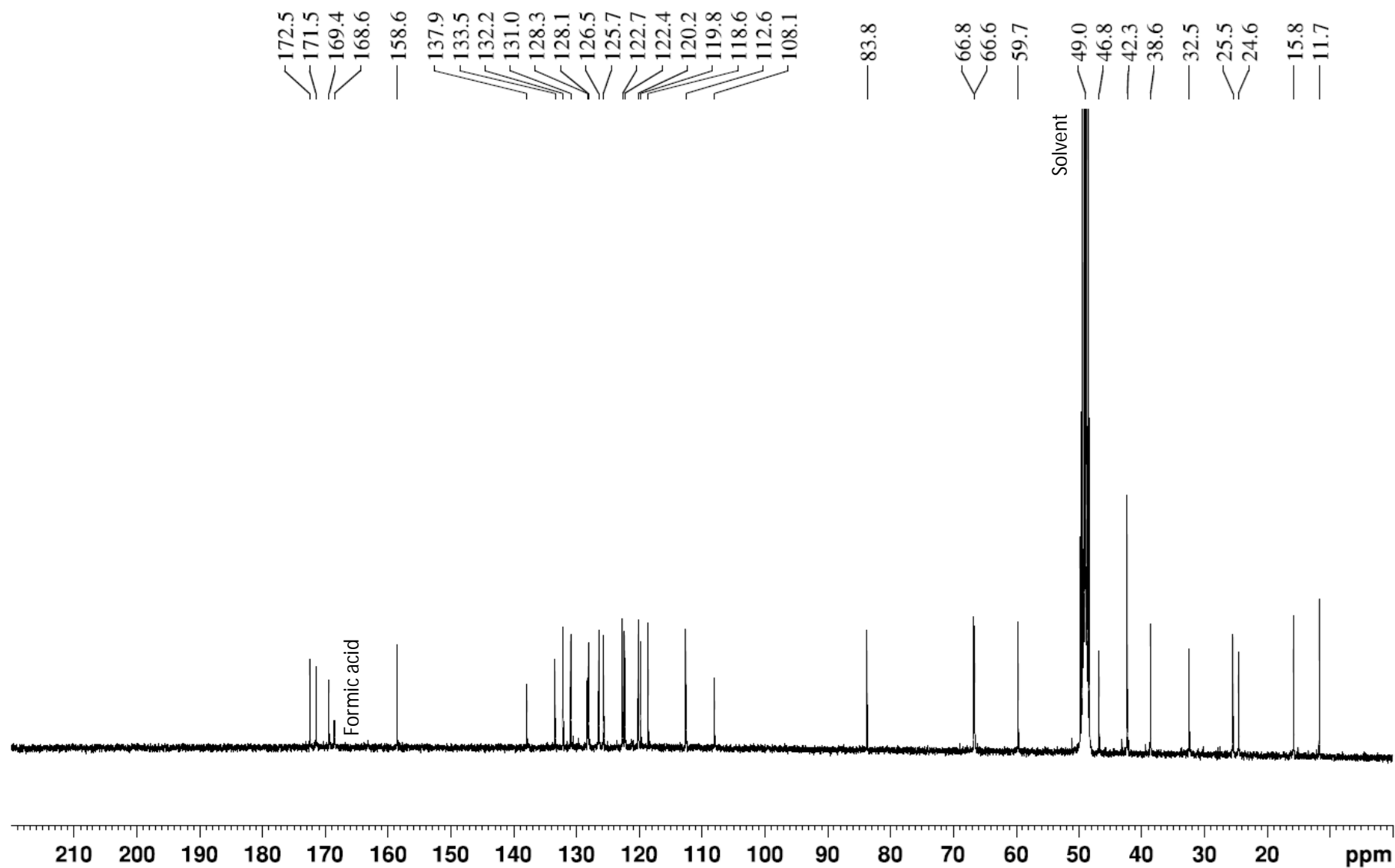


Fig. 5.12. ^1H NMR spectrum (400 MHz, methanol- d_4) of compound **5** (Hemsine-A *N*-oxide).

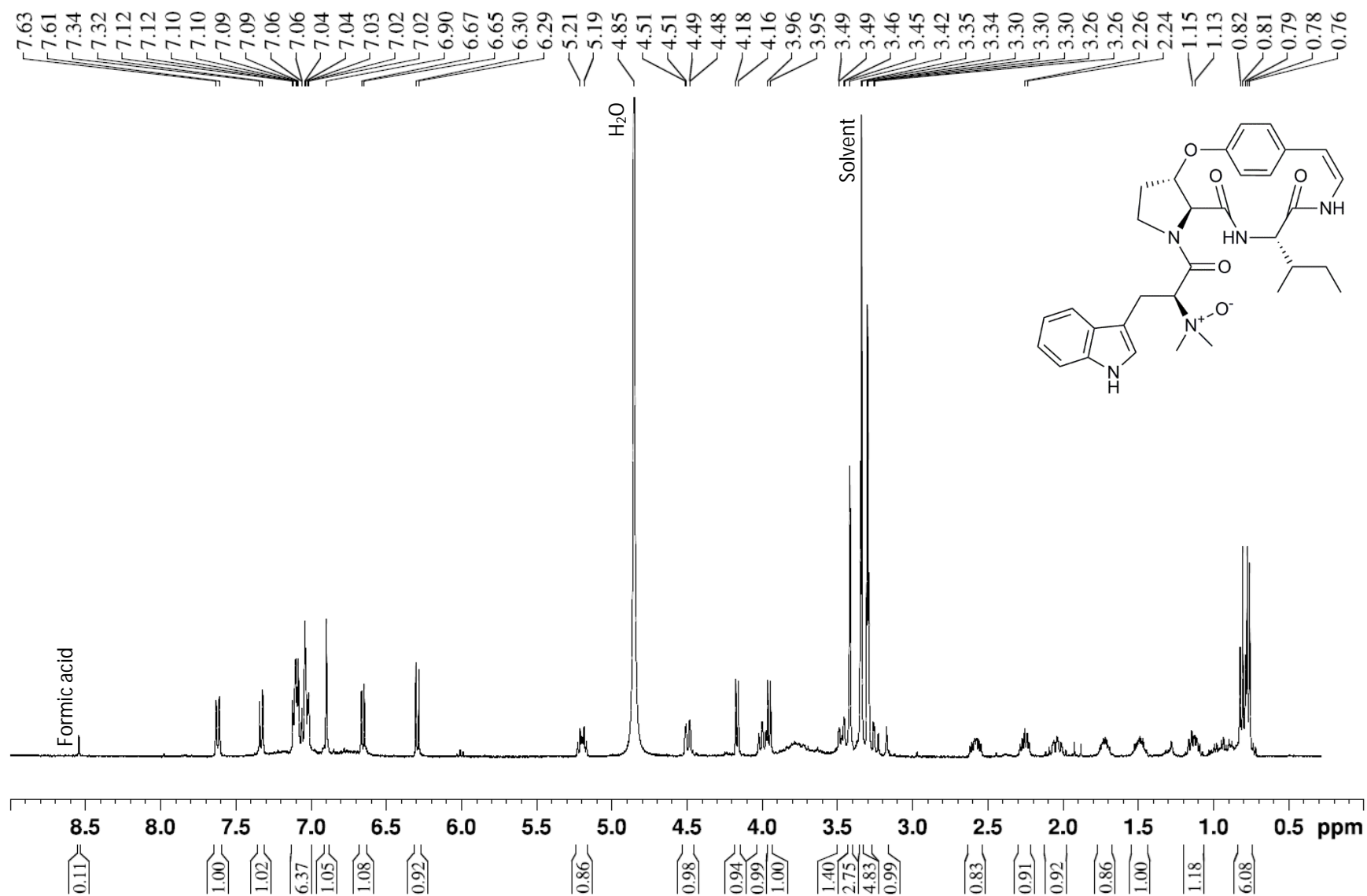


Fig. 5.13 HSQC spectrum (methanol- d_4) of compound **5** (Hemsine-A *N*-oxide).

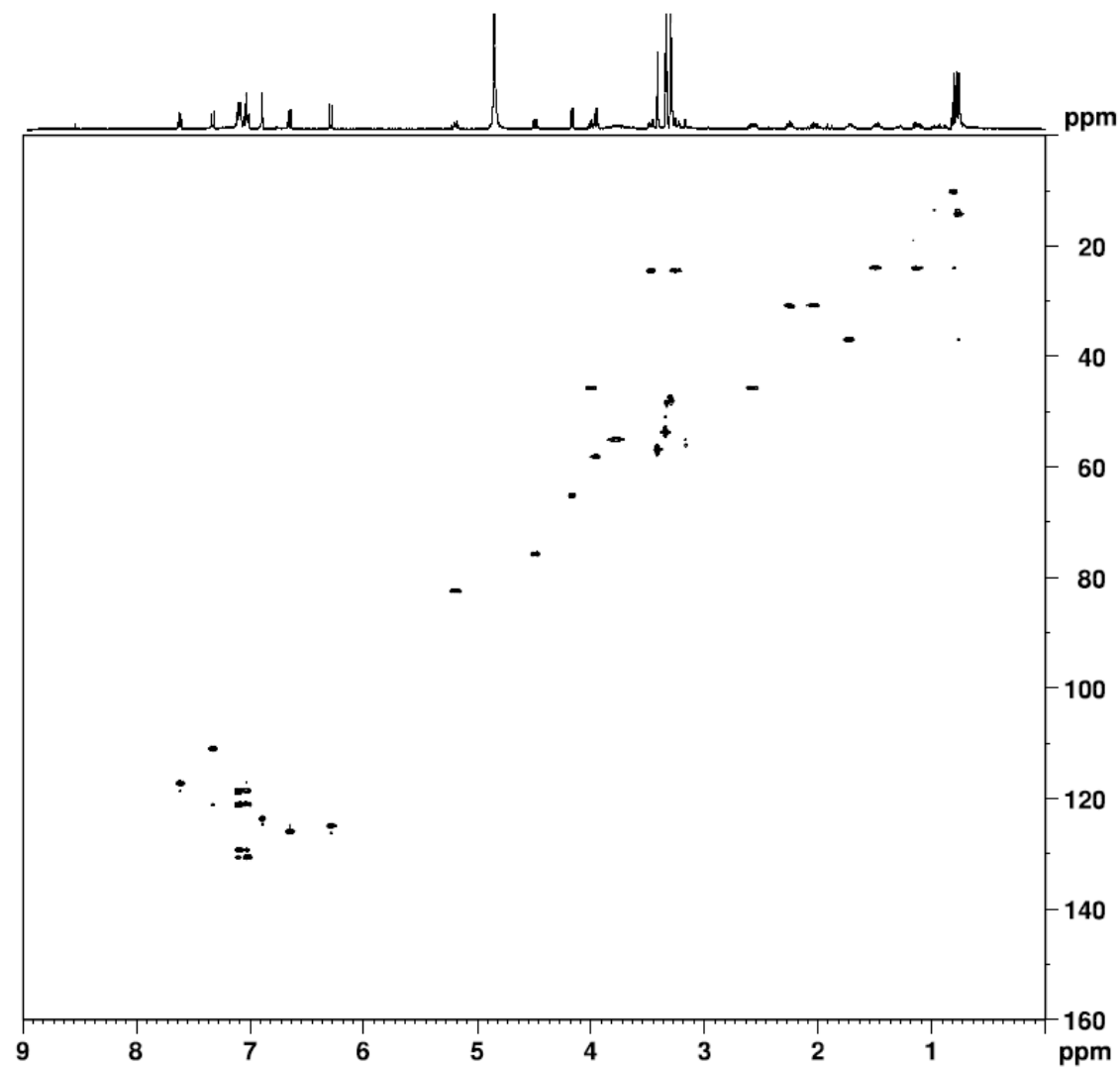


Fig. 5.14 HMBC spectrum (methanol- d_4) of compound **5** (Hemsine-A *N*-oxide).

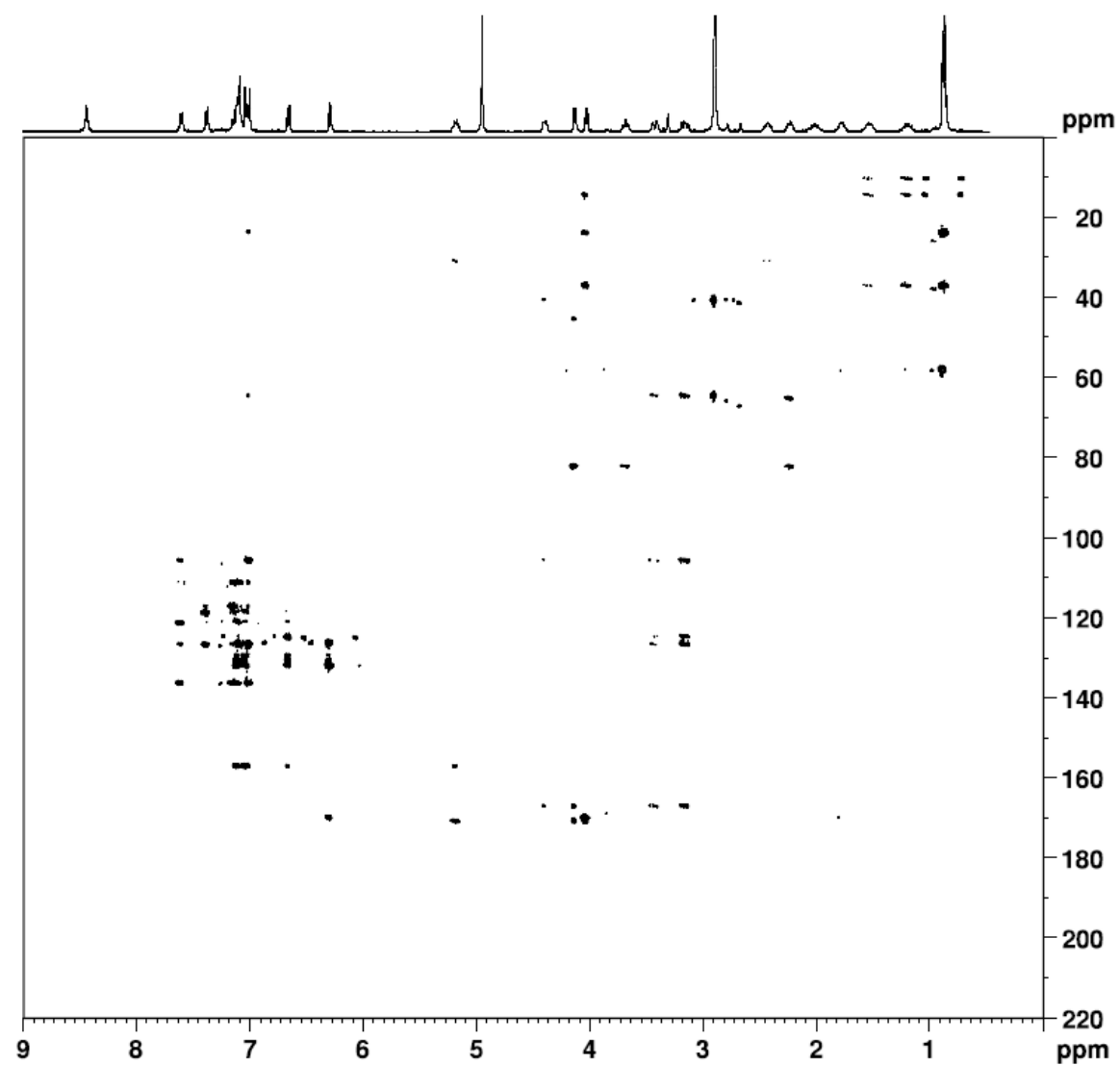


Fig. 5.15 COSY spectrum (methanol- d_4) of compound **5** (Hemsine-A *N*-oxide).

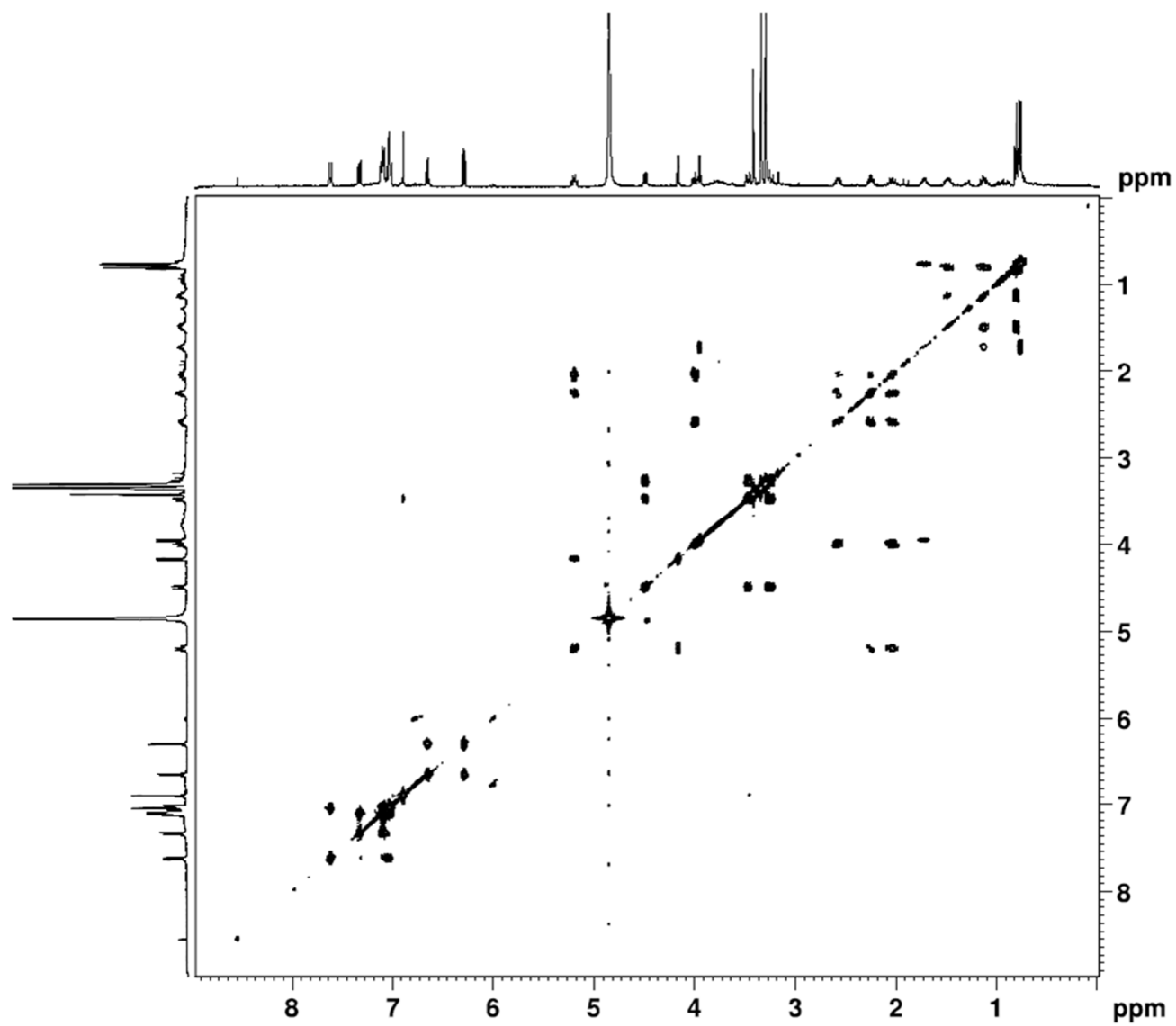


Fig. 5.16 ^1H NMR spectrum (400 MHz, methanol- d_4) of compound **6** (Ramosine-A).

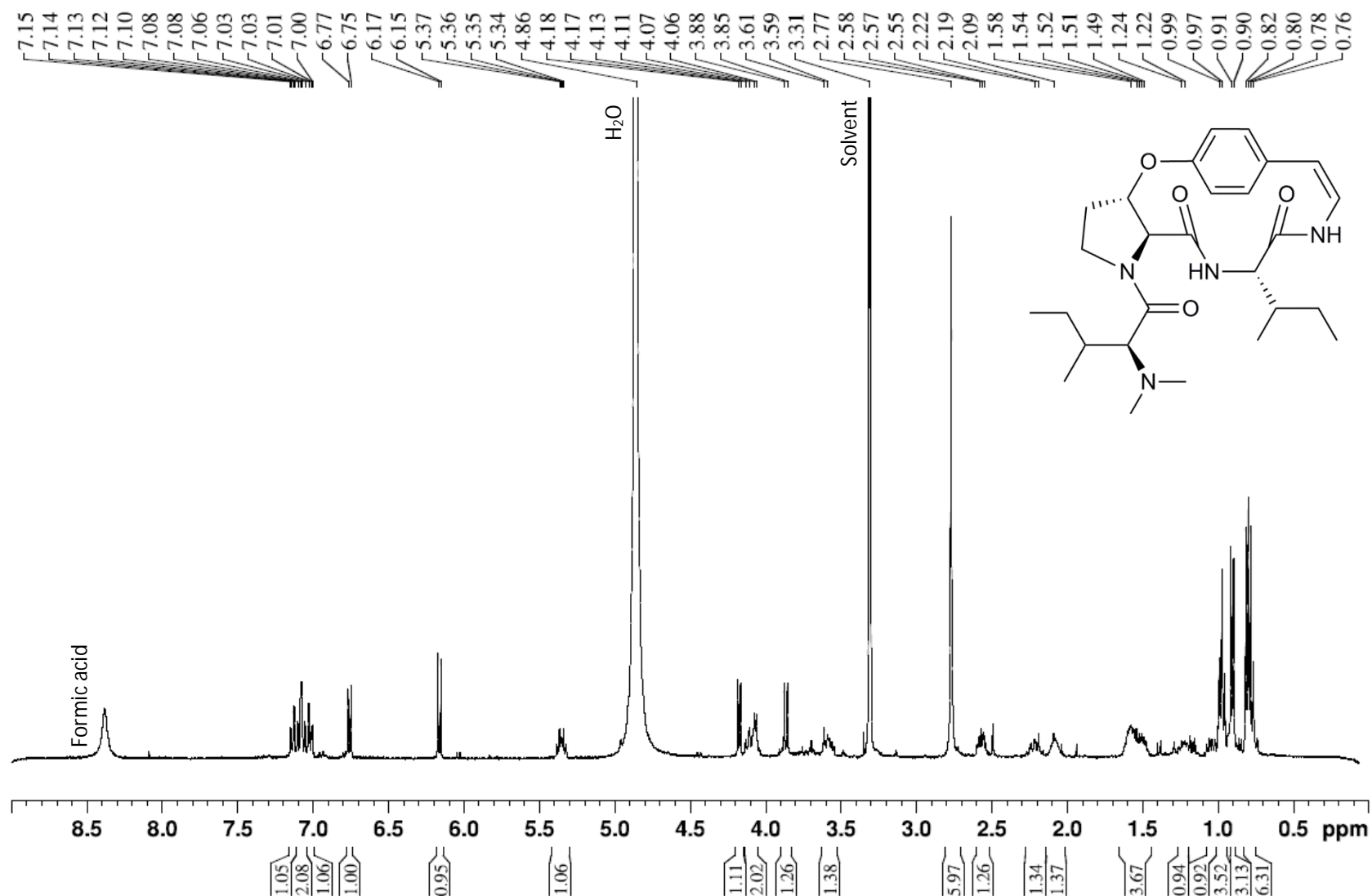


Fig. 5.17 ^{13}C NMR spectrum (100 MHz, methanol- d_4) of compound **6** (Ramosine-A).

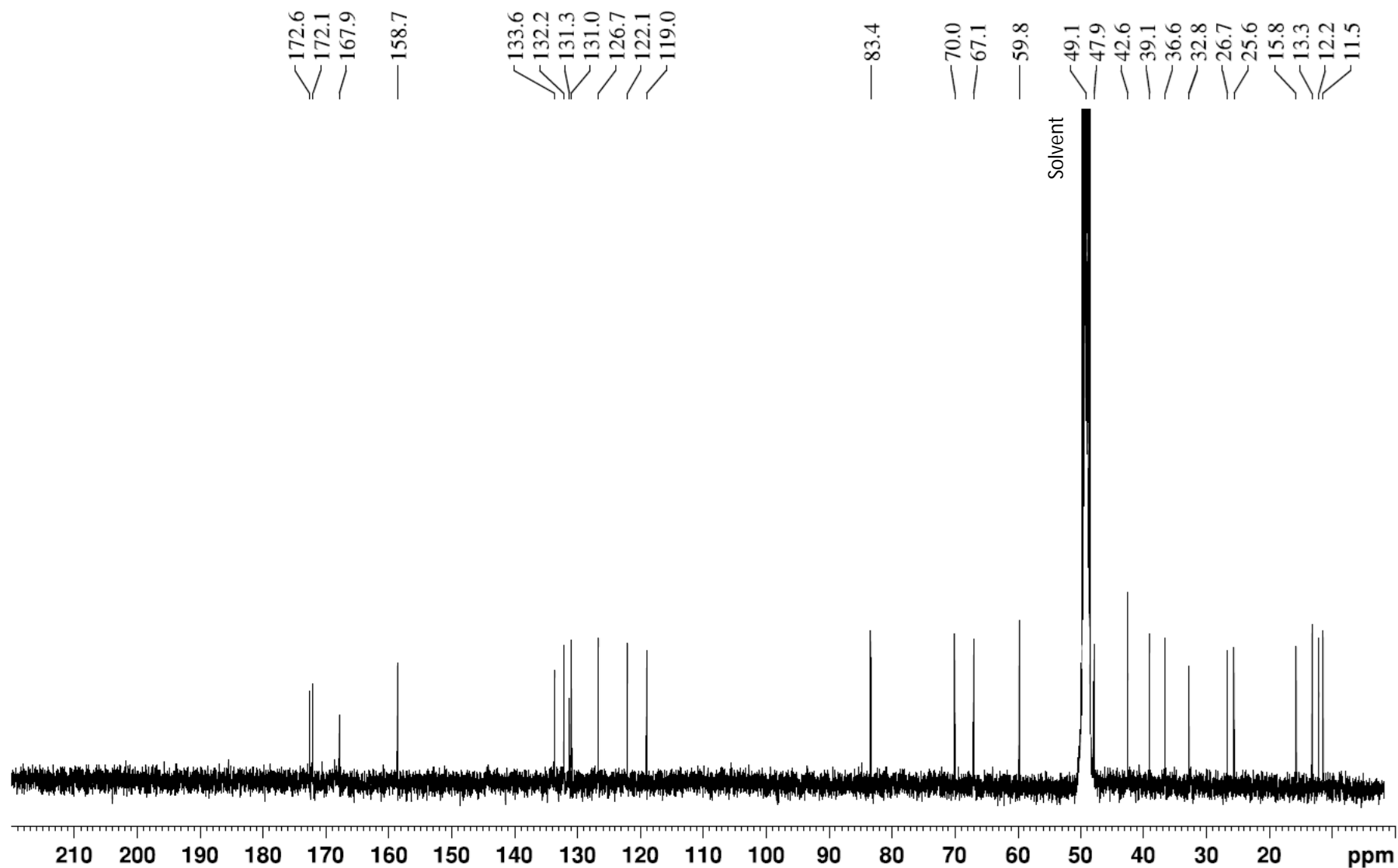


Fig. 5.18 ^1H NMR spectrum (400 MHz, chloroform-*d*) of compound **7** (Oxyphylline-C).

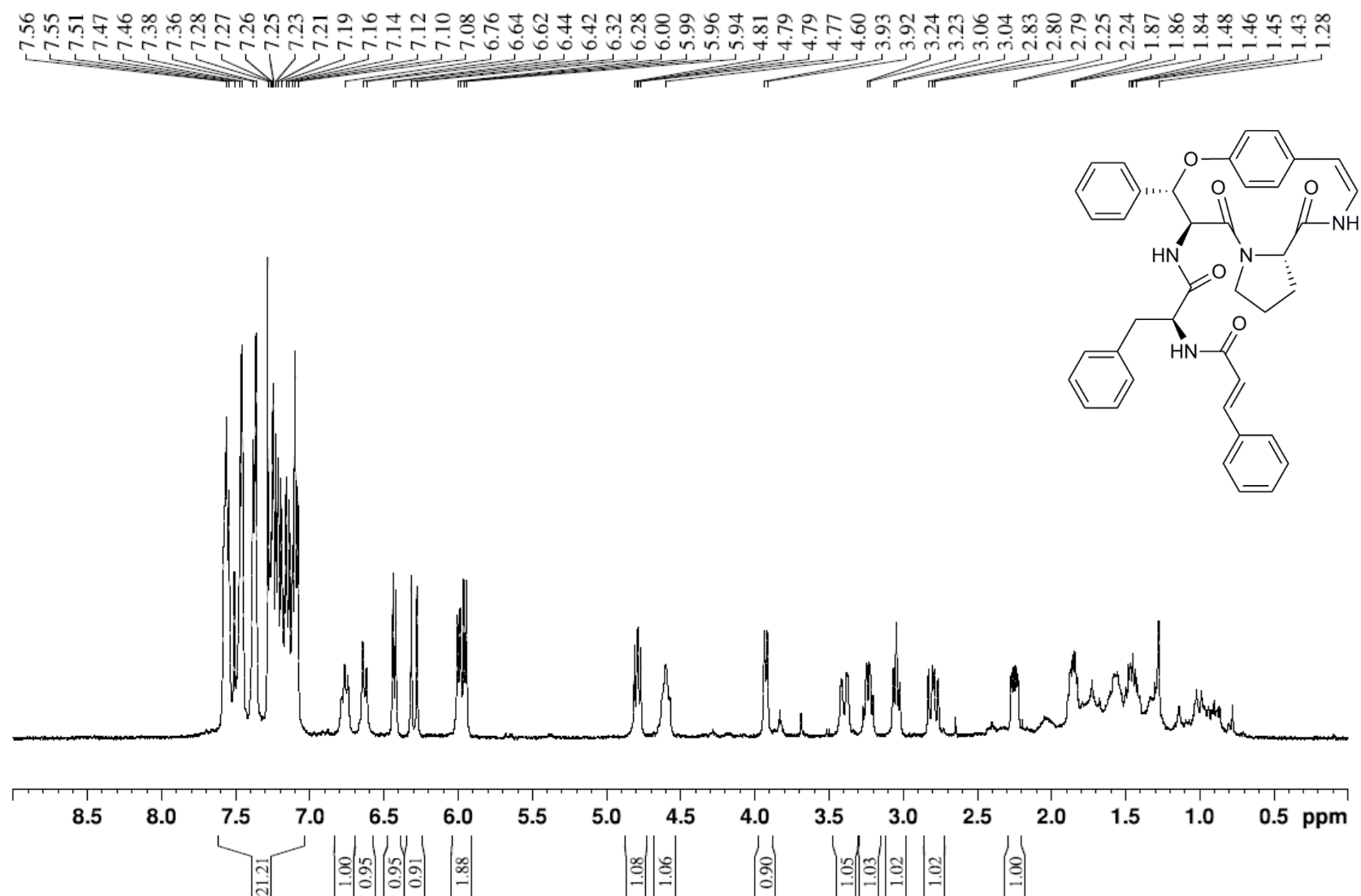
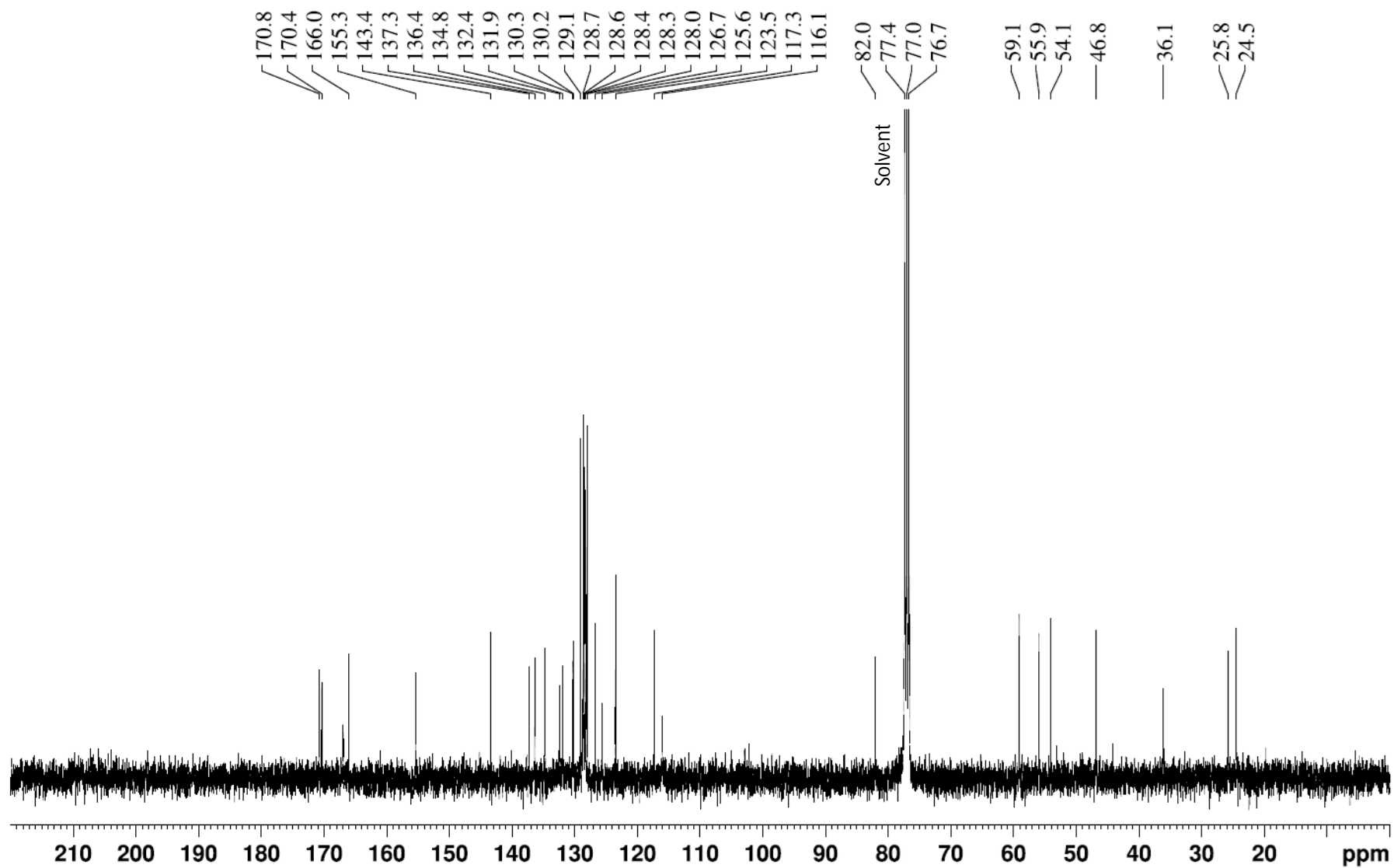


Fig. 5.19 ^{13}C NMR spectrum (100 MHz, chloroform-*d*) of compound **7** (Oxyphylline-C).



Compound **8** was identified as a new cyclopeptide alkaloid based on its 1D (Figures 5.21 and 5.22) and 2D NMR spectra in combination with HRESIMS measurements. It belonged to the subclass of cyclopeptide alkaloids containing a 13-membered ring composed of a 2-methoxystyrylamine moiety and two proline amino acids. A typical signal in the ^1H NMR spectrum of many cyclopeptide alkaloids is the peak due to the β -proton of the β -hydroxylated ring-bound amino acid (H-9). In the case of compound **8**, this signal appeared as a multiplet at 5.37 ppm. In the COSY spectrum, this proton showed cross peaks with a doublet at 4.56 ppm, assigned to H-8, and to a CH_2 group (2.58 ppm/2.38 ppm, H-20). This CH_2 group was connected to another CH_2 group (4.07 ppm/3.85 ppm, H-21) as evident from COSY interactions. Based on these observations and comparison with previously reported NMR assignments, it was concluded that a β -hydroxyproline moiety is present as one of the ring-bound amino acids. In addition, a second proline amino acid unit could be identified. In the COSY spectrum the signal at 4.69 ppm (dd, $J = 9.4$ Hz; 3.5 Hz), corresponding to the α -proton of this amino acid (H-5), showed clear cross peaks with a CH_2 group at 2.31 ppm/2.05 ppm (H-17). This CH_2 group, in turn, was found to be connected to a second CH_2 unit (2.05 ppm/1.87 ppm, H-18), which again is linked to a third CH_2 group (4.47 ppm/3.38 ppm, H-19), substituted by an N -atom closing the five-membered ring of this second proline moiety. The whole ^1H NMR spectrum integrated for 29 protons, 13 of which showed a chemical shift value between 5.5 and 9.0 ppm. Only one of them, the doublet at 8.47 ppm, did not show a cross peak in the HSQC spectrum, and was assigned to the NH-proton of the styrylamine moiety (H-3). The styrylamine double bond with $\delta_{\text{C-1}}$ 106.6 ppm / $\delta_{\text{H-1}}$ 5.99 ppm (d, 8.8 Hz) and $\delta_{\text{C-2}}$ 121.7 ppm / $\delta_{\text{H-2}}$ 6.98 ppm was assigned a *cis* conformation, as deduced from the J value of the H-1 doublet (8.8 Hz). HMBC correlations of H-1 with C-16 and H-16 with C-1, H-2 with C-15, H-13 with C-11 and H-12/H-16 with C-14, indicated that the aromatic ring is substituted at positions C-11 and C-15, bearing a methoxy group ($\delta_{\text{C-32}}$ 56.0 ppm / $\delta_{\text{H-32}}$ 3.83 ppm, s) at position C-14. The key HMBC correlations for the structure elucidation of compound **8** are shown in Figure 5.20. Closure of the macrocyclic ring through 1,3-substitution of the aromatic moiety is typical for 13-membered ring cyclopeptide alkaloids. The fourth and last building block was identified as a cinnamoyl moiety. The aromatic protons occurred at 7.40 ppm (H-28, H-29, H-30) and 7.54 ppm for H-27 and H-31, with $\delta_{\text{C-29}}$ 130.1 ppm and C-28 and C-30 both at 128.9 ppm, and C-27 and C-31 both at 128.0 ppm. The double bond ($\delta_{\text{H-24}}$ 6.76 ppm, d (15.6 Hz) / $\delta_{\text{C-24}}$ 117.1 ppm and $\delta_{\text{H-25}}$ 7.69 ppm, d (15.5 Hz) / $\delta_{\text{C-24}}$ 143.4 ppm) showed a *trans* geometry and its linkage to the carbonyl group (C-23)

could be established through HMBC-interactions of H-24 and H-25 with C-23; H-25 was also correlated with C-27/C-31. Accordingly, the structure of compound **8** was assigned as shown, and the trivial name oxyphylline-E is proposed. HRESIMS analysis in the positive ion mode resulted in the detection of m/z 488.2220 $[M+H]^+$ and 510.2054 $[M+Na]^+$, in agreement with the molecular formula $C_{28}H_{30}N_3O_5$ (calcd m/z 488.2180) and $C_{28}H_{29}N_3O_5Na$ (calcd m/z 510.1999), respectively.

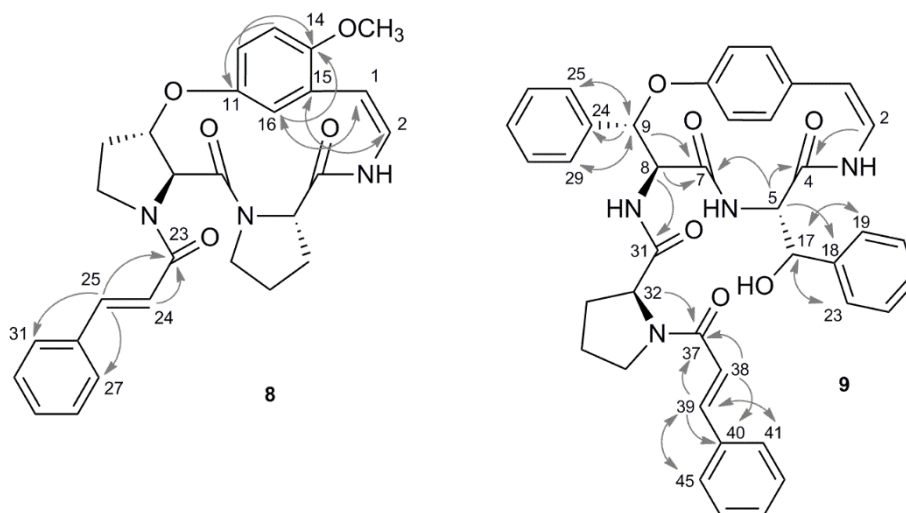


Fig. 5.20. Key HMBC Correlations for oxyphylline-E (**8**) and oxyphylline-F (**9**).

From the NMR spectra of compound **9** (Figures 5.23 – 5.24), it was concluded that it contains a 14-membered ring consisting of a styrylamine unit and two β -hydroxy-phenylalanine amino acid moieties. The side chain consisted of a proline and a cinnamoyl moiety. As for compound **8**, the signal of H-9 appearing at δ_H 5.66 ppm (δ_C 82.5 ppm) could be used as a starting point for the structure elucidation. From COSY interactions, this proton could be linked to H-8 at 4.56 ppm. In contrast to compound **8**, however, no interactions with a CH_2 group were observed. Instead, the HMBC spectrum showed cross peaks with carbon atoms belonging to an aromatic system, δ_{C-24} 139.1 ppm, with C-25 and C-29 both resonating at δ_C 129.6 ppm. Further inspection of the COSY and HMBC spectra led to the identification of β -hydroxy-phenylalanine as one of the ring-bound amino acids. Both H-8 and H-9 showed HMBC interactions with a carbon signal at 171.0 ppm, corresponding to the carbonyl group at C-7. A proton at δ_H 4.30 ppm (d, 9.5 Hz) also showed a cross peak in the HMBC spectrum with C-7, and was assigned to the α -proton of the other ring-bound amino acid (H-5). The H-5 proton showed a COSY correlation to a proton at 4.66 ppm (d, J = 9.4 Hz), assigned to H-17. Analysis

of the HMBC and COSY spectra then led to the identification of a second phenyl ring. Since the integration of the signal at 4.66 ppm (H-17) accounted for only one proton and given its downfield shift compared to the β -protons in phenylalanine and comparison to literature data (Tschesche and co-workers, 1974; 1977), it could be concluded that C-17 is hydroxylated. Therefore, this amino acid unit was also identified as β -hydroxy-phenylalanine. Through HMBC correlations of H-5 (at 4.30 ppm) and H-2 (at 6.17 ppm) with the carbonyl group at C-4 (δ_c 171.7 ppm), a link with the stryrylamine moiety could be established. This was supported by the relatively weak long-distance correlation in HMBC of H-1 (δ_H 6.86 ppm) with C-4. As in compound **8**, the double bond was assigned a *cis* conformation given the *J* value of 7 Hz, but, in contrast to compound **8**, the aromatic ring did not contain a methoxy group and showed a *para*-substitution in positions 11 and 14 to close a 14-membered macrocyclic ring.

In addition, H-8 also correlated with a carbonyl group at 170.2 ppm in the HMBC spectrum assigned to C-31. The same carbonyl group also correlated with a proton at 4.10 ppm, assigned to H-32. The COSY spectrum revealed the connection of H-32 to a CH₂ group (δ_H 2.14 ppm, m/1.55 ppm, m, H-33), which, in turn was connected to a second CH₂ group (δ_H 1.78 ppm, m/1.41 ppm, m, H-34), and finally a third CH₂ group (δ_H 3.00 ppm, t (8.8 Hz)/3.30 ppm, m, H-35), leading to the identification of this amino acid substituent as proline. The H-32 proton correlated with another carbonyl group in the HMBC spectrum (δ_c 168.0, C-37). The latter correlation allowed the position of the terminal cinnamoyl moiety to be established, since it showed two more correlations with two doublets (δ_H 6.65 ppm and 7.60 ppm), coupled to each other with a *J* value of 15.5 Hz, indicative of a *trans* alkene bond. Further inspection of the COSY and HMBC spectra allowed a phenyl ring to be identified, thus completing the cinnamoyl moiety. The key HMBC correlations of compound **9** are shown in Figure 5.20. HRESIMS analysis in the (+)-ESIMS mode gave *m/z* 671.2885 [M+H]⁺ and 693.2698 [M+Na]⁺, which were in agreement with a molecular formula of C₄₀H₃₉N₄O₆, (calcd *m/z* 671.3228) and C₄₀H₃₈N₄O₆Na (calcd *m/z* 693.2684), respectively. For compound **9**, the name oxyphylline-F was adopted. Compound **8** was isolated from batch 1, whereas compound **9** was found in both batches of plant material.

Fig. 5.21 ^1H NMR spectrum (400 MHz, chloroform- d) of compound **8** (Oxyphylline-E).

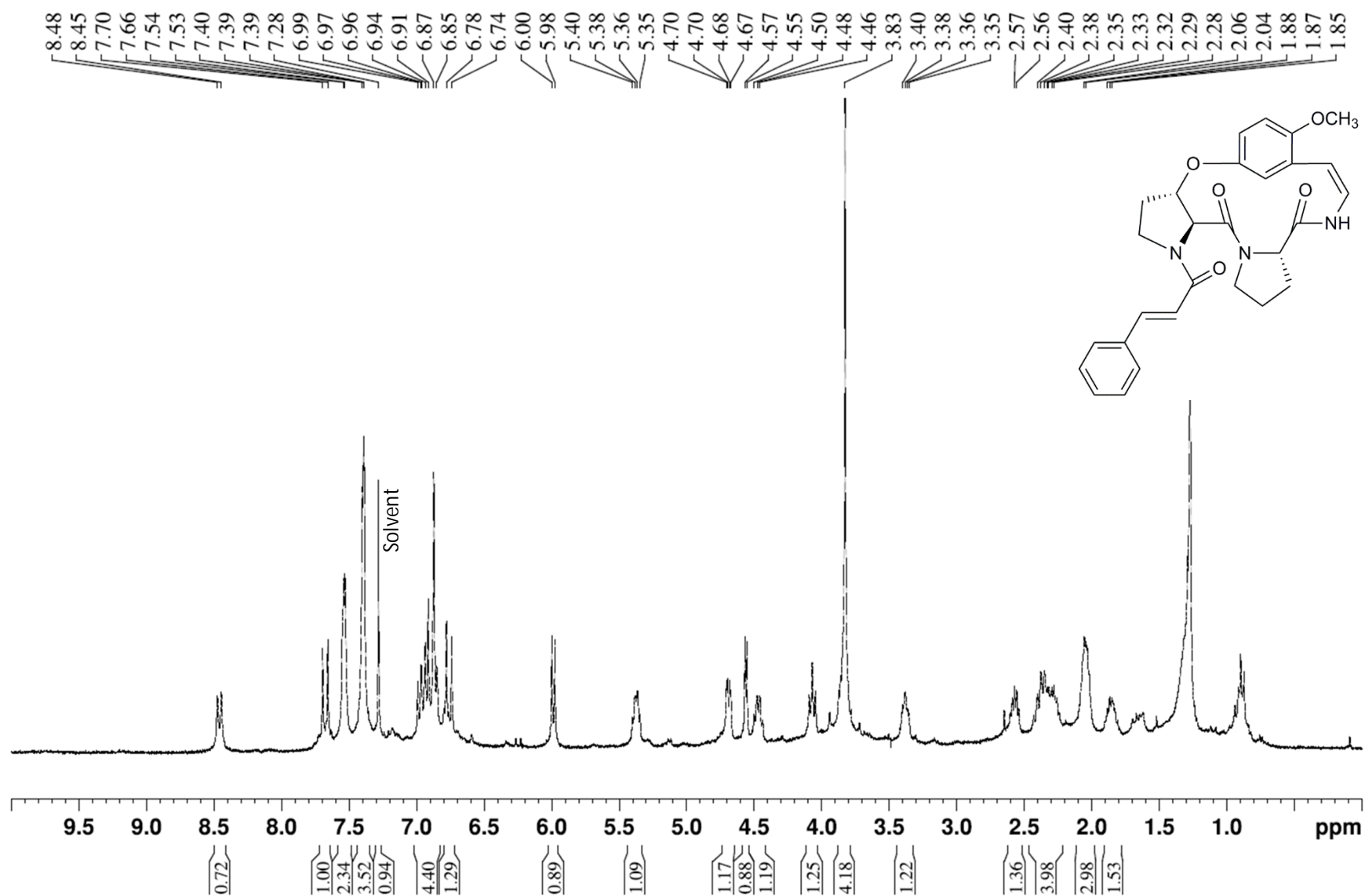


Fig. 5.22 ^{13}C NMR spectrum (100 MHz, chloroform-*d*) of compound **8** (Oxyphylline-E).

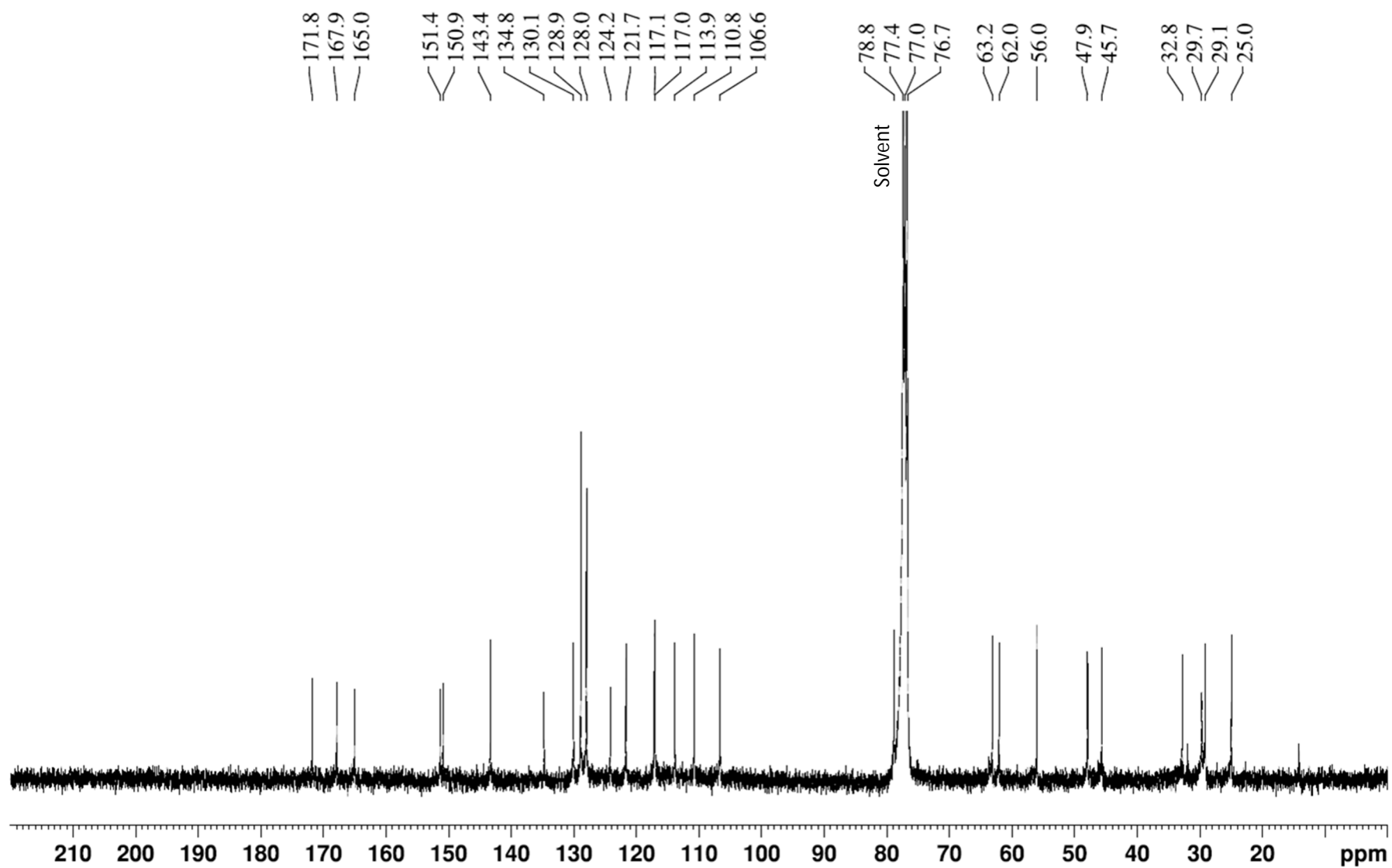


Fig. 5.23 ^1H NMR spectrum (400 MHz, methanol- d_4) of compound **9** (Oxyphylline-F).

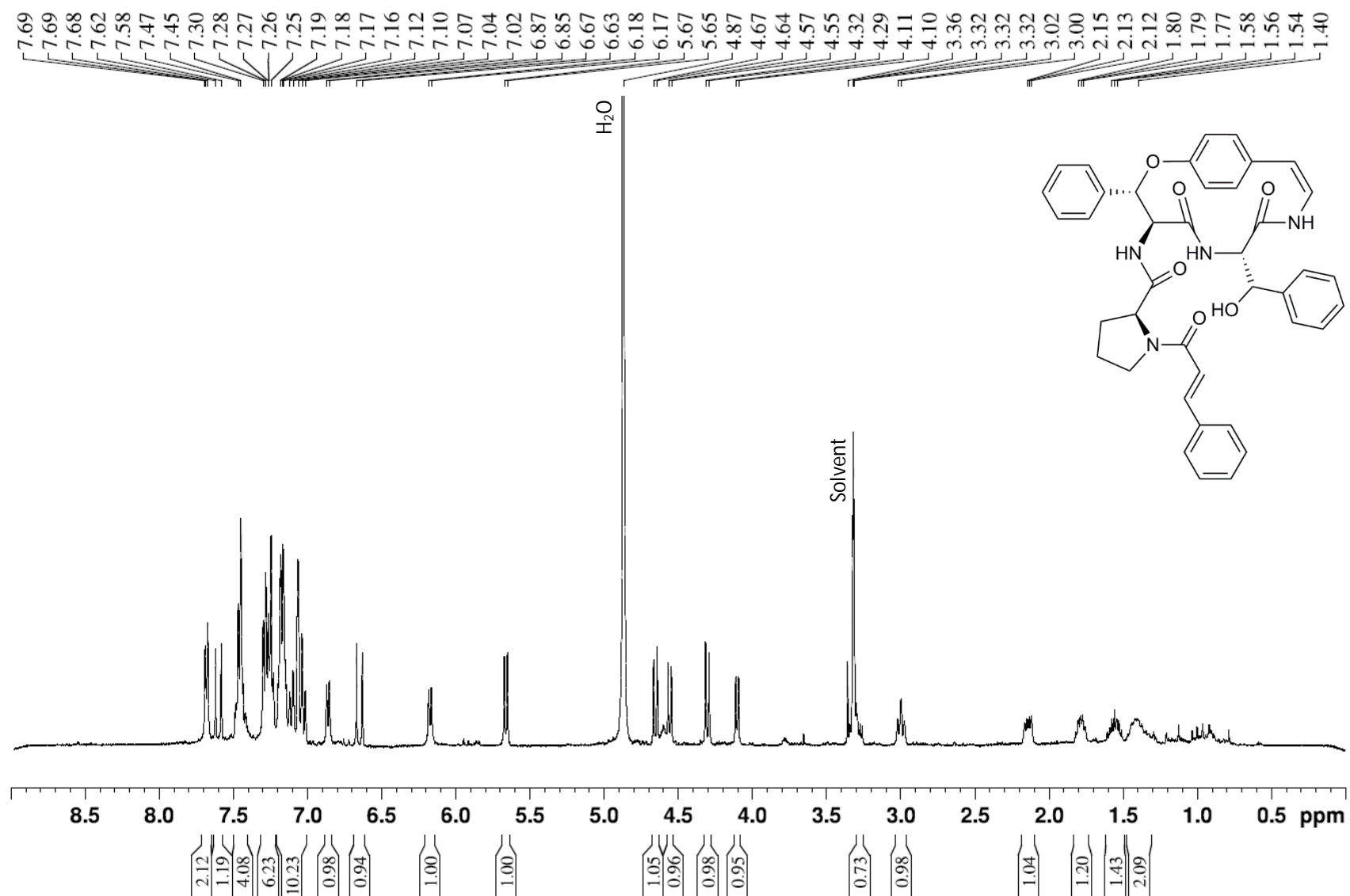
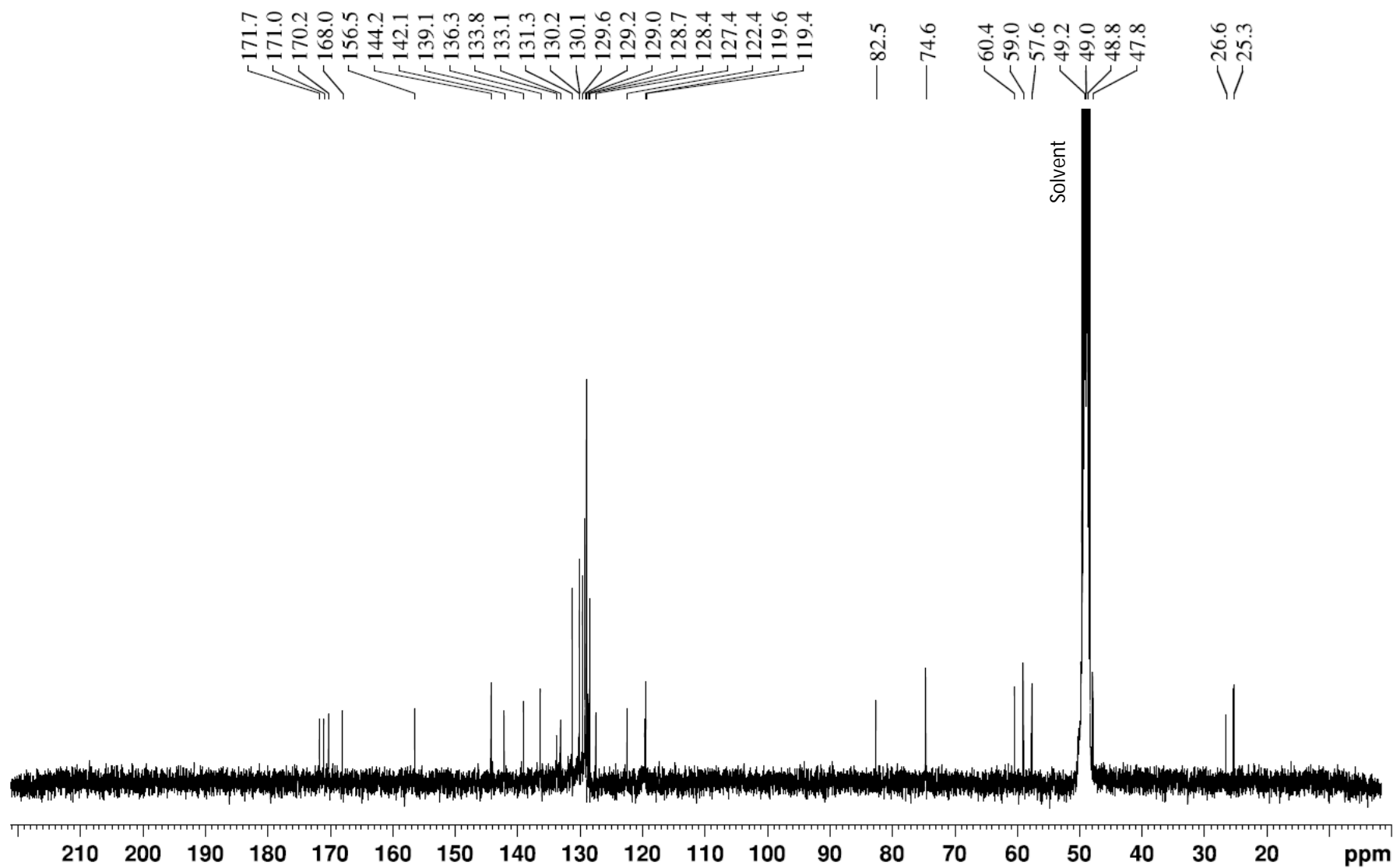


Fig. 5.24 ^{13}C NMR spectrum (100 MHz, methanol- d_4) of compound **9** (Oxyphylline-F).



Nummularine-R (**1**) and its derivatives **2** and **3** belong to the group of 4(13)-cyclopeptide alkaloids and hemsine-A (**4**), its *N*-oxide (**5**) and ramosine-A (**6**) to the 4(14)-group. Oxyphyllines-C (**7**), -E (**8**) and -F (**9**) are so-called neutral cyclopeptide alkaloids, in which the basic amino acid in the side chain is missing, and instead contain a cinnamoyl moiety (Gournelis *et al.*, 1997). Neutral cyclopeptide alkaloids are relatively rare. Until now, only fifteen representatives have been reported and all of them were found to contain a 14-membered macrocyclic ring. Oxyphylline-E is thus the first 13-membered neutral cyclopeptide alkaloid.

Amino acids that occur in Nature are usually present in the L-configuration. Also in cyclopeptide alkaloids, this configuration is found in the vast majority and only rarely the D-configuration has been reported, for example, in scutianine-E, isolated from *Scutia buxifolia* (Morel *et al.*, 2005). The configuration of nummularine-R (**1**) has been described in 2010 by Nisar *et al.*, based on values for coupling constants and NOESY interactions, and the L-configuration was adopted for the three amino acid units present in this cyclopeptide alkaloid (Nisar *et al.*, 2010). The L-configuration was also reported for hemsine-A (**4**) and ramosine-A (**6**) (Lin *et al.*, 2003). In oxyphylline-C (**8**), the two ring-bound amino acid units were found to be present in the L-configuration as well (Kaleem *et al.*, 2012). Conforming to the already reported configurations of these cyclopeptide alkaloids, the same configuration was adopted here and the L-configuration was also adopted for the closely structurally related compounds, *O*-desmethylnummularine-R (**2**), *O*-desmethylnummularine-R *N*-oxide (**3**), hemsine-A *N*-oxide (**5**), oxyphylline-E (**8**) and oxyphylline-F (**9**). For the β -hydroxy-proline unit in oxyphylline-E (**8**), the same relative configuration was adopted for C-9, as reported for other cyclopeptide alkaloids, based on similar ^1H NMR chemical shifts and coupling patterns. The *J* value of the α - and β -proton of the β -hydroxy-phenylalanine unit in compound **7** and the corresponding unit in compound **9** can be used to distinguish the *erythro* form from the *threo* form. In case of the *erythro* form, a *J* value of 8 Hz is typical, while the *threo* form exhibits a smaller *J* value of approximately 2 Hz (Gournelis *et al.*, 1997). For oxyphylline-C, the L-*erythro*-form has been reported before (J_{8-9} 7.2 Hz) (Kaleem *et al.*, 2012). Here, both oxyphylline-C (**7**) and the new compound, oxyphylline-F (**9**) were found to contain L-*erythro*- β -hydroxy-phenylalanine, since they showed a J_{8-9} of 7.2 and 8.4 Hz, respectively. Moreover, a J_{5-17} of 9.5 Hz and J_{17-5} of 9.4 Hz

suggest that the other β -hydroxy-phenylalanine unit in compound **9** is also present in the L-*erythro* form.

^1H and ^{13}C NMR chemical shift assignments for compounds **1–9** were based on 1D and 2D NMR experiments and are listed in Tables 5.1 and 5.2, respectively. For compounds **1–6** and **9** the NMR spectra were recorded in methanol- d_4 . For compounds **7** and **8** chloroform- d was used.

Table 5.1 ¹H NMR spectroscopic data [δ_{H} in ppm, multiplicity (*J* in Hz)] for compounds **1-9**.^a

position	1	2	3	4	5	6	7	8	9
1	6.03, d (8.9)	6.03, d (8.9)	6.03, d (9.0)	6.70, d (7.6)	6.66, d (7.5)	6.76, d (7.5)	6.43, d (7.5)	5.99, d (8.8)	6.86, d (7.3)
2	6.80 ^b	6.80 ^b	6.79 ^b	6.29, d (7.6)	6.29, d (7.5)	6.16, d (7.5)	6.76, t (8.4)	6.98 ^b	6.17, d (7.4)
3 (N-H)	n.o.	n.o.	n.o.	n.o.	n.o.	n.o.	6.63, d (9.8)	8.47, d (11.8)	n.o.
5	4.26, d (6.5)	4.27, d (6.5)	4.25, d (6.0)	4.02, d (7.1)	3.95, d (7.0)	3.86, d (8.4)	3.92, d (7.3)	4.69, dd (9.4, 3.5)	4.30, d (9.5)
8	4.42, d (3.2)	4.42 ^b	4.45, d (3.0)	4.14, d (6.5)	4.17, d (6.4)	4.17, d (6.8)	4.78, dd (9.7, 7.2)	4.56, d (5.5)	4.56, d (8.4)
9	5.07, m	5.04, m	5.02, m	5.22, m	5.20, m	5.35, m	5.95, d (7.2)	5.37, m	5.66, d (8.4)
12	6.79 ^b	6.65 ^b	6.62 ^b	7.11 ^b	7.10 ^b	7.13, dd (8.4, 2.4)	7.10 ^b	6.87 ^b	7.10 ^b
13	6.97, d (9.1)	6.79 ^b	6.77 ^b	7.05 ^b	7.03 ^b	7.06 ^b	7.26 ^b	6.93 ^b	7.03 ^b
15	-	-	-	7.10 ^b	7.09 ^b	7.08 ^b	7.37 ^b	-	7.06 ^b
16	6.73 ^b	6.66 ^b	6.65 ^b	7.05 ^b	7.03 ^b	7.02, dd (8.2, 2.4)	7.14 ^b	6.88 ^b	7.07 ^b
17a	1.94, m	1.95, m ^b	1.97, m	1.76, m	1.72, m	1.59 ^b	1.46, m	2.05, m ^b	4.66, d (9.4)
17b	-	-	-	-	-	-	2.25, m	2.31, m	-
18a	1.27, m	1.28, m	1.28, m	1.20, m	1.13, m	1.05, m	1.58, m	1.87, m	-
18b	1.57, m	1.56, m	1.51, m	1.54, m	1.49, m	1.51 ^b	1.85, m	2.05, m ^b	-
19a	0.93, t (7.4)	0.94, t (7.5)	0.93, t (7.3)	0.87 ^b	0.81, t (7.5)	0.78 ^b	3.04, t (8.7)	3.38, m	7.25 ^b
19b	-	-	-	-	-	-	3.24, m	4.47, m	-
20a	1.06, d (6.9)	1.06, d (6.9)	1.03, d (6.9)	0.88 ^b	0.77, d (6.8)	0.81 ^b	-	2.38, m	7.17 ^b
20b	-	-	-	-	-	-	-	2.58, m	-
21a	2.03, m	2.00 ^b	2.04, m	2.04, m	2.04, m	2.22, m	7.37 ^b	3.85, m ^b	7.16 ^b
21b	2.13, m	2.11, m	2.10, m	2.30, m	2.25, m	2.57, m	-	4.07, t (9.3)	-
22a	2.46, m	2.42, m	2.56, m	2.54, m	2.59, m	3.59, m	7.20 ^b	-	7.17 ^b
22b	3.67, m	3.65, m	3.88, m	3.73, m	4.00, t (9.5)	4.10 ^b	-	-	-
23	-	-	-	-	-	-	7.19-7.28 ^d	-	7.25 ^b

position	1	2	3	4	5	6	7	8	9
24	-	-	-	-	-	-	7.20 ^b	6.76, d (15.6)	-
25	4.37, m	4.41 ^b	4.54, dd (11.8, 2.7)	4.35, dd (9.8, 4.1)	4.50, dd (11.2, 2.7)	4.07 ^b	7.37 ^b	7.68, d (15.5)	7.29 ^b
26a	3.21, dd (13.6, 10.6)	3.21, dd (14.1, 10.6)	3.36 ^c	3.19, dd (14.6, 9.6)	3.26 ^c	2.08, m	7.55 ^b	-	7.16 ^b
26b	3.50, dd (14.2, 3.9)	3.52, dd (14.1, 3.7)	3.53 ^b	3.44, dd (14.6/4.0)	3.47, dd (13.6, 2.6)	-	-	-	-
27a	-	-	-	-	-	1.23, m	-	7.54 ^b	7.24 ^b
27b	-	-	-	-	-	1.57 ^b	-	-	-
28	6.92, s	6.93, s	6.86, s	7.01 ^b	6.90, s	0.97, t (7.3)	4.60, m	7.40 ^b	7.16 ^b
29a	N-H, n.o.	NH, n.o.	NH, n.o.	NH, n.o.	NH, n.o.	0.91, d (6.7)	2.79, dd (15.5, 10.6)	7.40 ^b	7.29 ^b
29b	-	-	-	-	-	-	3.39, d (15.5)	-	-
30	-	-	-	-	-	-	-	7.40 ^b	NH, n.o.
31	7.37, d (7.9)	7.37, d (7.8)	7.36, d (7.9)	7.38, d (7.9)	7.33, d (8.0)	2.77, s	7.09 ^b	7.54 ^b	-
32	7.13, t (7.5)	7.14, t (7.5)	7.13, t (7.1)	7.15 ^b	7.09 ^b	2.77, s	7.24 ^b	3.83, s	4.10, d (7.4)
33a	7.08, t (7.5)	7.08, t (7.4)	7.06, t (7.6)	7.10 ^b	7.04 ^b	-	7.14 ^b	-	1.55, m
33b	-	-	-	-	-	-	-	-	2.14, m
34a	7.61, d (7.9)	7.61, d (7.8)	7.64, d (7.9)	7.61, d (7.9)	7.62, d (7.7)	-	7.24 ^b	-	1.41, m
34b	-	-	-	-	-	-	-	-	1.78, m
35a	-	-	-	-	-	-	7.09 ^b	-	3.00, t (8.8)
35b	-	-	-	-	-	-	-	-	3.30 ^d
36	-	-	-	-	-	-	5.99, d (7.7)	-	-
37	2.90, s	2.92, s	3.49, s	2.88, s	3.42, s	-	-	-	-
38	2.90, s	2.92, s	3.39, s	2.88, s	3.35, s	-	6.30, d (15.4)	-	6.65, d (15.5)
39	3.77, s	OH, n.o.	OH, n.o.	-	-	-	7.53, d (15.3)	-	7.60, d (15.5)
40	-	-	-	-	-	-	-	-	-
41	-	-	-	-	-	-	7.56 ^b	-	7.68, d (7.3)

position	1	2	3	4	5	6	7	8	9
42							7.46 ^b		7.45 ^b
43							7.45 ^b		7.44 ^b
44							7.46 ^b		7.45 ^b
45							7.56 ^b		7.68, d (7.3)
46									OH, n.o.

^aSpectra were recorded at 400 MHz. Solvent for compounds **1-6, 9**: methanol-*d*₄; solvent for compounds **7** and **8**: chloroform-*d*; n.o.: not observed.

^bOverlapping signals. ^cOverlapping with residual solvent signal. ^dCould not be assigned unequivocally, due to overlapping of aromatic signals.

Table 5.2 ^{13}C NMR spectroscopic data (δ_{C} in ppm, type) for compounds **1-9**.^a

position	1	2	3	4	5	6	7	8	9
1	110.5, CH	110.8, CH	109.3, CH	128.1, CH	127.6, CH	131.3, CH	116.1, CH	106.6, CH	133.8, CH
2	122.0, CH	121.6, CH	119.7, CH	126.5, CH	126.5, CH	126.7, CH	125.6, CH	121.7, CH	127.4, CH
4	170.7, C	170.7, C	169.1, C	171.5, C	171.5, C	172.1, C	170.4, C	171.8 or 167.9 ^c	171.7, C
5	61.7, CH	61.7, CH	59.8, CH	59.7, CH	59.7, CH	59.8, CH	59.1, CH	62.1, CH	59.0, CH
7	172.1, C	172.2, C	n.o.	172.5, C	172.7, C	172.6, C	170.8, C	171.8 or 167.9 ^c	171.0, C
8	67.0, CH	67.1, CH	65.4, CH	66.8, CH	66.9, CH	67.1, CH	55.9, CH	63.2, CH	57.6, CH
9	79.0, CH	78.8, CH	77.4, CH	83.8, CH	84.0, CH	83.4, CH	82.0, CH	78.9, CH	82.5, CH
11	152.4, C	151.6, C	149.7, C	158.6, C	158.6, C	158.7, C	155.3, C	150.9, C	156.5, C
12	119.0, CH	119.2, CH	117.7, CH	119.8, CH	120.2, CH	119.0, CH	130.3, CH	117.0, CH	119.6, CH
13	115.3, CH	119.3, CH	117.9, CH	132.2, CH	132.2, CH	132.2, CH	123.5, CH	113.9, CH	131.3, CH
14	153.3, C	150.8, C	150.0, C	133.5, C	133.4, C	133.6, C	132.4, C	151.4, C	133.1, C
15	125.4, C	123.2, C	121.7, C	131.0, CH	130.9, CH	131.0, CH	123.5, CH	124.2, C	130.2, CH
16	112.6, CH	112.1, CH	110.4, CH	122.4, CH	122.6, CH	122.1, CH	131.9, CH	110.8, CH	122.4, CH
17	37.2, CH	37.3, CH	35.6, CH	38.6, CH	38.6, CH	39.1, CH	25.8, CH ₂	29.1, CH ₂	74.6, CH
18	26.5, CH ₂	26.5, CH ₂	24.7, CH ₂	25.5, CH ₂	25.5, CH ₂	25.6, CH ₂	24.5, CH ₂	25.0, CH ₂	142.1, C
19	11.9, CH ₃	12.0, CH ₃	10.4, CH ₃	11.7, CH ₃	11.7, CH ₃	11.5, CH ₃	46.8, CH ₂	48.0, CH ₂	128.4, CH
20	16.4, CH ₃	16.5, CH ₃	14.8, CH ₃	15.8, CH ₃	15.8, CH ₃	15.8, CH ₃	137.3, C	32.8, CH ₂	129.0, CH
21	33.4, CH ₂	33.5, CH ₂	31.6, CH ₂	32.5, CH ₂	32.3, CH ₂	32.8, CH ₂	128.3, CH	45.7, CH ₂	128.7, CH
22	47.4, CH ₂	47.5, CH ₂	46.2, CH ₂	46.8, CH ₂	47.4, CH ₂	47.9, CH ₂	128.4, CH	-	129.0, CH
23	-	-	-	-	-	-	128.0-129.0 ^b	165.1, C	128.4, CH
24	169.2, C	169.0, C	n.o.	169.4, C	167.8, C	167.9, C	128.4, CH	117.1, CH	139.1, C
25	67.2, CH	67.2, CH	76.3, CH	66.6, CH	77.4, CH	70.0, CH	128.3, CH	143.4, CH	129.6, CH
26	25.6, CH ₂	25.8, CH ₂	24.5, CH ₂	24.6, CH ₂	26.0, CH ₂	36.6, CH	-	134.8, C	129.0, CH
27	107.4, C	107.2, C	106.0, C	108.1, C	107.8, C	26.7, CH ₂	166.9, C	128.0, CH	129.0, CH
28	125.8, CH	125.9, CH	123.7, CH	125.7, CH	125.3, CH	12.2, CH ₃	54.1, CH	128.9, CH	129.0, CH
29	-	-	-	-	-	13.3, CH ₃	36.1, CH ₂	130.1, CH	129.6, CH
30	138.1, C	138.0, C	136.5, C	137.9, C	137.9, C	-	136.4, C	128.9, CH	-
31	112.9, CH	112.9, CH	111.2, CH	112.6, CH	112.5, CH	42.6, CH ₃	128.6, CH	128.0, CH	170.2, C

position	1	2	3	4	5	6	7	8	9
32	123.0, CH	123.0, CH	121.2, CH	122.7, CH	122.7, CH	42.6, CH ₃	128.7, CH	56.0, CH ₃	60.4, CH
33	120.5, CH	120.5, CH	118.7, CH	120.2, CH	120.1, CH		126.7, CH		26.6, CH ₂
34	118.8, CH	118.7, CH	117.2, CH	118.6, CH	118.8, CH		128.7, CH		25.3, CH ₂
35	128.4, C	128.4, C	126.4, C	128.3, C	128.0, C		128.6, CH		47.8, CH ₂
37	42.7, CH ₃	42.6, CH ₃	57.1, CH ₃	42.3, CH ₃	58.4, CH ₃		166.0, C		168.0, C
38	42.7, CH ₃	42.6, CH ₃	53.7, CH ₃	42.3, CH ₃	55.3, CH ₃		117.3, CH		119.6, CH
39	56.7, CH ₃						143.4, CH		144.2, CH
40							134.8, C		136.3, C
41							128.0, CH		129.2, CH
42							129.1, CH		130.1, CH
43							130.1, CH		131.3, CH
44							129.1, CH		130.1, CH
45							128.0, CH		129.2, CH

^aSpectra were recorded at 100 MHz. Solvent for compounds **1-6, 9**: methanol-*d*₄; solvent for compounds **7** and **8**: chloroform-*d*; n.o.: not observed.

^bCould not be assigned unequivocally, due to overlapping of aromatic signals. ^cMay be interchanged.

The antiplasmodial activity against *Plasmodium falciparum* strain K1 and cytotoxicity for MRC-5 cells (human fetal lung fibroblast cells) were determined in triplicate for compounds **1**, **2**, **4**, **6** and **9** and the results are displayed in Table 5.3. The quantities of the other compounds isolated were insufficient for such testing.

Table 5.3 Antiplasmodial Activity against *P. falciparum* Strain K1 and Cytotoxicity against MRC5-cells (IC₅₀ µM) for five cyclopeptide alkaloids obtained from the roots of *Ziziphus oxyphylla*.

compound	<i>P. falciparum</i> K1	MRC-5
1	3.2 ± 2.6	30.6 ± 4.0
2	7.1 ± 1.6	> 64.0
4	13.6 ± 9.3	> 64.0
6	> 32.0	> 64.0
9	7.4 ± 3.0	31.2 ± 1.4
chloroquine	0.3 ± 0.2	-

Nummularine-R (**1**), *O*-desmethylnummularine-R (**2**) and oxyphylline-F (**9**) showed the most potent antiplasmodial activity (IC₅₀ values of 3.2, 7.1 and 7.4 µM, respectively), but only compound **2** did not show cytotoxicity at the highest test concentration of 64.0 µM and thus seems the most promising. For hemsine-A (**4**), an IC₅₀ value of 13.6 µM was found; the antiplasmodial activity of this compound has been reported before (IC₅₀ 7.3 µM) (Suksamrarn *et al.*, 2005).

Suksamrarn *et al.* (2005) described the possible importance of the methoxy group in position 2 of the styrylamine unit of cyclopeptide alkaloids for resultant antiplasmodial activity, but from the present study it can be concluded that cyclopeptide alkaloids with a 2-hydroxystyrylamine moiety, like compound **2**, are also active. Moreover, it was hypothesized that a mono- or dimethylated terminal *N*-atom is crucial for the activity (Suksamrarn *et al.*, 2005; Panseeta *et al.*, 2011), but this is in contradiction with the activity that was found herein for the new compound oxyphylline-F (**9**), which contains a terminal cinnamoyl moiety and no *N*-(di)methyl group. Based on the structural features and IC₅₀ values found for nummularine-R (**1**), *O*-desmethylnummularine-R (**2**), hemsine-A (**4**) and ramosine-A (**6**), it might be hypothesized that the tryptophan moiety in the side chain is important for antiplasmodial

activity. Compound **9**, however, does not contain a tryptophan unit and also showed antiplasmodial activity, which led to the conclusion that a tryptophan unit may play a role in mediating antiplasmodial activity, but is not indispensable. Interestingly, oxyphylline-F (**9**) is the first neutral cyclopeptide alkaloid for which the *in vitro* antiplasmodial activity has been reported. Apparently, it is not possible yet to determine a clear structure-activity relationship for the antiplasmodial activity of cyclopeptide alkaloids, since only a limited set of compounds has been evaluated so far. Evaluation of more cyclopeptide alkaloids will be necessary before clear structure-activity relationships can be established.

5.3 Materials and Methods

5.3.1 General experimental procedures

See chapter 2, general experimental procedures, sections 2.1, chromatographic methods, and 2.2, spectroscopic methods.

5.3.2 Plant material

Two different batches of roots from *Ziziphus oxyphylla* were collected in Pakistan. Batch 1 (1.5 kg) was collected in September and October 2009 in the Swat Valley, northern Pakistan. The identification was done by Prof. Dr. Mansoor Ahmad and a voucher specimen (0012-2009/AZ) was deposited at the Laboratory of Pharmacognosy, Research Institute of Pharmaceutical Sciences, University of Karachi, Pakistan. Batch 2 (2.9 kg) was collected in July and August 2012 in the city of Upper Dir, District Upper Dir, KPK Province, Pakistan. This identification was performed by Dr. Muhammad Zafar and a voucher specimen (5698-IK) was deposited at the Herbarium of Pakistan, Quaid-i-Azam University, Islamabad, Pakistan.

5.3.3 Extraction and isolation

The plant material of both batches was dried and milled before extraction. Batch 1 was macerated in methanol for 10 days and this was repeated three times with fresh solvent. The macerate was filtered and the solvent was evaporated under reduced pressure and at 40 °C until dryness. This resulted in 509 g of crude extract, of which 100 g was suspended in 200 mL

80% methanol and sequentially partitioned with *n*-hexane, chloroform, ethyl acetate, and *n*-butanol. A part of the chloroform fraction (3.3 g of 14 g) was submitted to flash chromatography for further fractionation. A GraceResolv 120 g silica column was used with the following solvents: dichloromethane (A), ethyl acetate (B) and methanol (C) and a flow rate of 40 mL/min. The gradient was as follows: 0 min 100% A, 0% B and C, changed stepwise to 0% A, 100% B and 0% C at 89 min. This condition was kept for 4 min. Then, a stepwise change to 0% A, 25% B and 75% C was applied in 24 min and this final condition was kept for 4 min. For detection, ELSD and UV absorption at 254 nm and 366 nm were used. Throughout the whole experiment the eluent was collected in test tubes, based on the ELSD and UV absorption intensity. Based on the obtained chromatograms in combination with a TLC analysis of the collected eluates, performed on normal-phase plates with 10% methanol in chloroform as the mobile phase, and observation of the results as described before, test tubes that showed a similar pattern were combined. This resulted in 14 fractions.

A crude extract of batch 2 was prepared by means of percolation with 80% methanol (105 L in total). After evaporation of the solvent and freeze-drying, 380 g of crude extract were obtained. The crude extract was dissolved in 50% methanol/50% water and was acidified to pH <3 with 2 M HCl. Then, a liquid-liquid partition was performed with dichloromethane. Next, the pH of the acidified phase was increased to >9 by the addition of NH₄OH (25%), followed by a second liquid-liquid partition with dichloromethane. Thus, the plant material was divided into three fractions: CH₂Cl₂ (I), CH₂Cl₂ (II), and CH₃OH/H₂O (pH >9) (III). TLC analysis of these three fractions was performed as described before. The TLC indicated that alkaloids were only present in the CH₂Cl₂ (II) phase (3.06 g). Further fractionation of this phase was performed by means of flash chromatography. The same type of column and solvents were used as for batch 1. The flow rate and settings of the detector were also identical. The gradient was as follows: 0 min 100% A, 0% B and C, changed stepwise to 0% A, 100% B and 0% C at 39 min. This condition was kept for 3.5 min. Then, a stepwise change to 0% A, 25% B and 75% C was accomplished in 64 min and this final condition was kept for 15 min. The ELSD and UV absorption signal in combination with TLC analysis, which was performed as described above, were used in order to combine test tubes with a similar content. This resulted in 23 fractions.

On the basis of TLC analysis [mobile phase CH₂Cl₂-CH₃OH (90:10)], fractions 4, 10, 11 and 12 from batch 1 and fractions 11, 12, 16 and 23 from batch 2 were submitted for semi-preparative HPLC. The system was operated with a C₁₈ Luna column (250 mm x 10.0 mm, particle size 5 µm) from Phenomenex (Utrecht, the Netherlands) and a C₁₈ guard column (10 mm x 10 mm, particle size 5 µm) from Grace (Hesperia, CA, USA). As mobile phase, H₂O or H₂O + 0.1% formic acid (A) and acetonitrile (B) were used. Linear gradients were applied and the flow rate was set at 3.0 mL/min. More detailed information about the HPLC conditions used for the isolation of each compound is given in Table 5.4. The DAD spectrum was recorded from 200 nm to 450 nm and mass spectra were taken in (+)-ESIMS mode, with MS scan range: *m/z* 150 to 850. *V*_{capillary} 3.00 kV, *V*_{cone} 50 V, *V*_{extractor} 3 V, *V*_{RF-Lens} 0.2 V, *T*_{source} 135 °C, *T*_{Desolvation} 400 °C, desolvation gas flow 750 L/h, cone gas flow 50 L/h. Interesting peaks were selected based on the UV-spectrum and the *m/z* value of each peak. The collection of the eluate was triggered as long as the intensity of selected *m/z* values exceeded the set threshold. The specific settings for the collection of each cyclopeptide alkaloid are shown in Table 5.4.

Table 5.4. Conditions applied in the semi-preparative isolation of nine cyclopeptide obtained from the roots of *Ziziphus oxyphylla*.

batch, fraction	C _{sample} (mg/mL), solvent	V _{inj} (μL)	mobile phase	gradient	compound	m/z	isolated amount (mg)
1, 4	10.0	500	H ₂ O (A)	0-5 min 55% B, 40-45 min 100% B	7	488 [M+H] ⁺	*
	methanol		ACN (B)		8	655 [M+H] ⁺	*
1, 10	15.0	100	H ₂ O + 0.1% FA (A)	0-5 min 30% B, 35 min 35% B, 40-45 min 100% B	1	588 [M+H] ⁺	20
	methanol		ACN (B)				
1, 11	20.0	250	H ₂ O (A)	0-5 min 50% B, 15-20 min 100% B	9	693 [M+Na] ⁺	34
	methanol		ACN (B)				
1, 12	20.0	250	H ₂ O (A)	0-5 min 50% B, 15-20 min 100% B	9	693 [M+Na] ⁺	17
	methanol		ACN (B)				
2, 11	25.0	400	H ₂ O + 0.1% FA (A)	0-5 min 25% B, 25 min 45% B, 30-35 min 100% B	1	611 [M+Na] ⁺	26
	methanol		ACN (B)		2	597 [M+Na] ⁺	28
2, 12	25.0	400	H ₂ O + 0.1% FA (A)	0-5 min 20% B, 25 min 35% B, 35-40 min 100% B	4	581 [M+Na] ⁺	198
	methanol		ACN (B)		6	508 [M+Na] ⁺	4
2, 16	25.0	400	H ₂ O + 0.1% FA (A)	0-5 min 20% B, 35 min 35% B, 40-45 min 100% B	9	694 [M+Na] ⁺	4
	methanol		ACN (B)				
2, 23	16.65	200	H ₂ O + 0.1% FA (A)	0-5 min 30% B, 25 min 35% B, 35 min 60% B, 40-45 min 100% B	3	529 [M-C ₂ H ₆ NO] ⁺	1
	methanol		ACN (B)		5	485 [M-C ₂ H ₆ NO-28] ⁺ and 513 [M-C ₂ H ₆ NO] ⁺	4

*Mixture, further purified by LC-SPE-NMR. FA = formic acid

^1H NMR spectra of each collected subfraction were recorded, giving an indication of the purity and the type of compound(s) present. Whenever the ^1H NMR spectrum appeared to represent a single compound, additional ^{13}C NMR and/or 2D NMR spectra (COSY, HSQC, HMBC) were recorded. From the ^1H NMR spectrum of the two samples isolated from batch 1, fraction 4, it could be concluded that these samples contained more than just one compound, but signals characteristic for cyclopeptide alkaloids could be seen. In order to further purify these two samples, LC-DAD-SPE-NMR was applied. For sample 1-4-1, water (A) and acetonitrile (B) were used as the mobile phase in the following gradient: 0 to 5 min 50% B, 20 min 65% B, 22 to 27 min 100% B. The flow rate was 0.8 mL/min and a Luna C_{18} column (250 x 4.6 mm, particle size, 5 μm ; pore size, 100 Å) was used as the stationary phase. The sample with a concentration of 10 mg/mL was injected in 7 consecutive runs, 15 μL per injection. For sample 1-4-3, the same HPLC conditions were applied, but the gradient was as follows: 0 to 5 min 56% B, 20 min 66% B, 25 to 30 min, 100% B. The sample with a concentration of 10 mg/mL was injected in 14 consecutive runs, 20 μL per injection. The eluting compounds were multitrapped on SPE cartridges, which were then dried with nitrogen gas. The adsorbed compounds (**7** and **8** for sample 1-4-3 and sample 1-4-1, respectively) were eluted into 3 mm NMR tubes using methanol- d_4 .

Nummularine-R (**1**): yellow powder (46 mg); $[\alpha]_{\text{D}} -244.7$ (c 0.5, CH_3OH); UV λ_{max} 219, 270, 318 nm; ^1H NMR (methanol- d_4 , 400 MHz) and ^{13}C NMR (methanol- d_4 , 100 MHz), see Tables 5.1 and 5.2 respectively; (+)-ESIMS m/z 589 $[\text{M}+\text{H}]^+$; 611 $[\text{M}+\text{Na}]^+$.

O-Desmethylnummularine-R (**2**): yellow powder (28 mg); $[\alpha]_{\text{D}} -295.5$ (c 0.6, CH_3OH); UV λ_{max} 222, 268, 320 nm; ^1H NMR (methanol- d_4 , 400 MHz) and ^{13}C NMR (methanol- d_4 , 100 MHz), see Tables 5.1 and 5.2 respectively; HRESIMS m/z 574.3031 $[\text{M}+\text{H}]^+$ (calcd for $\text{C}_{32}\text{H}_{40}\text{N}_5\text{O}_5$, 574.3024).

O-Desmethylnummularine-R N-oxide (**3**): yellow powder (1 mg); UV λ_{max} 202, 269, 319 nm; ^1H NMR (methanol- d_4 , 400 MHz) and ^{13}C NMR (methanol- d_4 , 100 MHz), see Tables 5.1 and 5.2 respectively; HRESIMS m/z 590.3002 $[\text{M}+\text{H}]^+$ (calcd for $\text{C}_{32}\text{H}_{40}\text{N}_5\text{O}_6$, 590.2973).

Hemsine-A (4): yellow oil (198 mg); $[\alpha]_D$ -81.3 (c 0.5, CH₃OH); UV λ_{\max} 221, 280 (shoulder) nm; ¹H NMR (methanol-*d*₄, 400 MHz) and ¹³C NMR (methanol-*d*₄, 100 MHz), see Tables 5.1 and 5.2 respectively; HRESIMS *m/z* 558.3097 [M+H]⁺ (calcd for C₃₂H₄₀N₅O₄, 558.3097).

Hemsine-A N-oxide (5): yellow powder (6 mg); $[\alpha]_D$ -65.7 (c 0.6, CH₃OH); UV λ_{\max} 218, 280 (shoulder) nm; ¹H NMR (methanol-*d*₄, 400 MHz) and ¹³C NMR (methanol-*d*₄, 100 MHz), see Tables 5.1 and 5.2 respectively; HRESIMS *m/z* 574.3036 [M+H]⁺ (calcd for C₃₂H₄₀N₅O₅, 574.3024).

Ramosine-A (6): yellow powder (4 mg); $[\alpha]_D$ -139.7 (c 0.4, CH₃OH); UV λ_{\max} low end absorption; ¹H NMR (methanol-*d*₄, 400 MHz) and ¹³C NMR (methanol-*d*₄, 100 MHz), see Tables 5.1 and 5.2 respectively; (+)-ESIMS *m/z* 508 [M+Na]⁺.

Oxyphylline-C (7): ¹H NMR (chloroform-*d*, 400 MHz): and ¹³C NMR (chloroform-*d*, 100 MHz), see Tables 5.1 and 5.2 respectively; (+)-ESIMS *m/z* 655 [M+H]⁺.

Oxyphylline-E (8): ¹H-NMR (chloroform-*d*, 400 MHz): and ¹³C-NMR (chloroform-*d*, 100 MHz), see Tables 5.1 and 5.2 respectively; HRESIMS *m/z* 488.2220 [M+H]⁺, 510.2054 [M+Na]⁺ (calcd for C₂₈H₃₀N₃O₅, 488.2180, calcd for C₂₈H₂₉N₃O₅Na 510.1999).

Oxyphylline-F (9): yellowish powder (41 mg); $[\alpha]_D$ -117.9 (c 0.5, CH₃OH); UV λ_{\max} low end, 284 nm; ¹H NMR (methanol-*d*₄, 400 MHz) and ¹³C NMR (methanol-*d*₄, 100 MHz), see Tables 5.1 and 5.2 respectively; HRESIMS *m/z* 671.2885 [M+H]⁺, 693.2698 [M+Na]⁺ (calcd for C₄₀H₃₉N₄O₆, 671.3228, calcd for C₄₀H₃₈N₄O₆Na 693.2684).

5.3.4 Antiplasmodial and cytotoxic activities

The antiplasmodial and cytotoxic activity determinations of the selected isolated components were performed as described in chapter 2, general experimental procedures, section 2.3, biological activity testing. The means and standard deviations of three experiments were calculated for compounds **1**, **2**, **4**, **6** and **9**.

References

- Choudhary, M. I., Adhikari, A., Rasheed, S., Marasini, B. P., Hussain, N., Kaleem, W. A. and Attar-Rahman, 2011. Cyclopeptide alkaloids of *Ziziphus oxyphylla* Edgw as novel inhibitors of alpha-glucosidase enzyme and protein glycation. *Phytochem Lett* **4**(4): 404-406.
- Gournelis, D. C., Laskaris, G. G. and Verpoorte, R., 1997. Cyclopeptide alkaloids. *Nat Prod Rep* **14**(1): 75-82.
- Han, B. H., Park, M. H. and Park, J. H., 1989. Chemical and pharmacological studies on sedative cyclopeptide alkaloids in some rhamnaceae plants. *Pure Appl Chem* **61**(3): 443-448.
- Han, J., Ji, C. J., He, W. J., Shen, Y., Leng, Y., Xu, W. Y., Fan, J. T., Zeng, G. Z., Kong, L. D. and Tan, N. H., 2011. Cyclopeptide Alkaloids from *Ziziphus apetala*. *J Nat Prod* **74**(12): 2571-2575.
- Inayat-Ur-Rahman, Khan, M. A., Arfan, M., Akhtar, G., Khan, L. and Ahmad, V. U., 2007. A new 14-membered cyclopeptide alkaloid from *Zizyphus oxyphylla*. *Nat Prod Res* **21**(3): 243-253.
- Kaleem, W. A., Muhammad, N., Qayum, M., Khan, H., Khan, A., Aliberti, L. and De Feo, V., 2013. Antinociceptive activity of cyclopeptide alkaloids isolated from *Ziziphus oxyphylla* Edgew (Rhamnaceae). *Fitoterapia* **91**: 154-158.
- Kaleem, W. A., Nisar, M., Qayum, M., Zia-Ul-Haq, M., Adhikari, A. and De Feo, V., 2012. New 14-Membered cyclopeptide alkaloids from *Zizyphus oxyphylla* Edgew. *Int J Mol Sci* **13**(9): 11520-11529.
- Lin, H. Y., Chen, C. H., Liu, K. C. S. C. and Lee, S. S., 2003. 14-membered cyclopeptides from *Paliurus ramosissimus* and *P. hemsleyanus*. *Helv Chim Acta* **86**(1): 127-138.
- Ma, Y., Han, H., Nam, S. Y., Kim, Y. B., Hong, J. T., Yun, Y. P. and Oh, K. W., 2008. Cyclopeptide alkaloid fraction from *Zizyphi Spinosi Semen* enhances pentobarbital-induced sleeping behaviors. *J Ethnopharmacol* **117**(2): 318-324.
- Morel, A. F., Araujo, C. A., da Silva, U. F., Hoelzel, S. C., Zachia, R. and Bastos, N. R., 2002. Antibacterial cyclopeptide alkaloids from the bark of *Condalia buxifolia*. *Phytochemistry* **61**(5): 561-566.
- Morel, A. F., Maldaner, G. and Ilha, V., 2009. Cyclopeptide alkaloids from higher plants. In: The Alkaloids. ed. Elsevier, London, pp. 79-141.

- Morel, A. F., Maldaner, G., Ilha, V., Missau, F., Silva, U. F. and Dalcol, I. I., 2005. Cyclopeptide alkaloids from *Scutia buxifolia* Reiss and their antimicrobial activity. *Phytochemistry* **66**(21): 2571-2576.
- Nisar, M., Adzu, B., Inamullah, K., Bashir, A., Ihsan, A. and Gilani, A. H., 2007. Antinociceptive and antipyretic activities of the *Zizyphus oxyphylla* Edgew. leaves. *Phytother Res* **21**(7): 693-695.
- Nisar, M., Kaleem, W. A., Adhikari, A., Ali, Z., Hussain, N., Khan, I., Qayum, M. and Choudhary, M. I., 2010. Stereochemistry and NMR data assignment of cyclopeptide alkaloids from *Zizyphus oxyphylla*. *Nat Prod Commun* **5**(8): 1205-1208.
- Panseeta, P., Lomchoey, K., Prabpai, S., Kongsaree, P., Suksamrarn, A., Ruchirawat, S. and Suksamrarn, S., 2011. Antiplasmodial and antimycobacterial cyclopeptide alkaloids from the root of *Zizyphus mauritiana*. *Phytochemistry* **72**(9): 909-915.
- Singh, A. K., Pandey, M. B., Singh, V. P. and Pandey, V. B., 2007. Mauritine-K, A new antifungal cyclopeptide alkaloid from *Zizyphus mauritiana*. *J Indian Chem Soc* **84**(8): 781-784.
- Suksamrarn, S., Suwannapoch, N., Aunchai, N., Kuno, M., Ratananukul, P., Haritakun, R., Jansakul, C. and Ruchirawat, S., 2005. Ziziphine N, O, P and Q, new antiplasmodial cyclopeptide alkaloids from *Zizyphus oenoplia* var. *brunoniana*. *Tetrahedron* **61**(5): 1175-1180.
- Tschesche, R. and Ammermann, E., 1974. Alkaloide aus Rhamnaceen, XXIII - Scutianin-C, -D und -E, drei weitere cyclopeptidalkaloide aus *Scutia buxifolia* Reiss. *Chem. Ber.* **107**: 2274-2283.
- Tschesche, R., Hillebrand, D., Wilhelm, H., Ammermann, E. and Eckhardt, G., 1977. Hysodricanin-A, mauritin-H, scutianin-F und aralionin-C, vier weitere cyclopeptidalkaloide aus *Zizyphus*, *Scutia* und *Araliorhamnus*. *Phytochemistry* **16**: 1025-1028.
- Tuenter, E., Exarchou, V., Balde, A., Cos, P., Maes, L., Apers, S. and Pieters, L., 2016. Cyclopeptide Alkaloids from *Hymenocardia acida*. *J Nat Prod* **79**(7): 1746-1751.

CHAPTER 6

Ziziphus nummularia

&

Ziziphus spina-christi

Published:

Emmy Tuenter, Kenn Foubert, Dan Staerk, Sandra Apers, and Luc Pieters

Isolation and structure elucidation of cyclopeptide alkaloids from *Ziziphus nummularia* and *Ziziphus spina-christi* by HPLC-DAD-MS and HPLC-PDA-(HRMS)-SPE-NMR

Phytochemistry, **2017**, 138, pp 163-169.

6.1 Introduction

Cyclopeptide alkaloids are polyamidic compounds, consisting of a 13-, 14- or 15 membered ring and a side chain, which has either a basic or a neutral character, depending on the presence of a terminal nitrogen atom. The macrocycle is typically composed of a styrylamine unit, a common amino acid and a β -hydroxy-amino acid, whereas the side chain consists of one or two more moieties. Based on these characteristics, the cyclopeptide alkaloids are classified in the 4(13), 4(14), 5(13) or 5(14) subclasses, and compounds from each subclass can be further characterized and classified by their β -hydroxy-amino acid. Their occurrence has been reported in a wide range of families, including the Asteraceae, Celastraceae, Euphorbiaceae, Menispermaceae, Pandaceae, Rubiaceae, Sterculiaceae and Urticaceae, but they are most widely distributed in the Rhamnaceae, and more specifically in the genus *Ziziphus* (Gournelis *et al.*, 1997; Inayat-Ur-Rahman *et al.*, 2001; El-Seedi *et al.*, 2007).

Ziziphus nummularia (Burm.f.) Wight & Arn. (Rhamnaceae) is a thorny shrub that grows in India and Pakistan. It is widely used in ethnomedicine, for example, the fruit and root are used to treat diarrhea, and the leaves as an antipyretic and against pain and inflammation. Phytochemical analysis has revealed the presence of flavonoids, phenolic acids, tannins, sterols, saponins, pectin, glycosides and triterpenoic acids. (Goyal *et al.*, 2013; Ray and Dewanjee, 2015; Rauf *et al.*, 2016). In addition, it is a rich source of cyclopeptide alkaloids, with almost 30 different compounds reported until now (Tschesche *et al.*, 1975; Dwivedi *et al.*, 1987; Singh and Pandey, 1995).

Ziziphus spina-christi (L.) Desf. (Rhamnaceae) is a shrub or tree, growing in areas with a sub-tropical climate, for example, Egypt, Saudi Arabia, Iraq, Iran and Pakistan. It is used for various medicinal purposes: fruits of this species are used in cases of dysentery and to treat bronchitis and cough, and a decoction of the bark and fresh fruit is used to promote the healing of fresh wounds. It is also used in some inflammatory conditions and against pain. Previous studies indicated that *Z. spina-christi* contained flavonoids, tannins, sterols, saponins, and triterpenoids (Shahat *et al.*, 2001; Farmani *et al.*, 2016). In addition, eleven different

cyclopeptide alkaloids were reported from its stem bark and/or root bark (Tschesche *et al.*, 1974; Shah *et al.*, 1986; Abdel-galil and El-Jissry, 1991).

Most phytochemical research, and in particular the isolation and structure elucidation of cyclopeptide alkaloids from these two *Ziziphus* species was performed decades ago. Nowadays, more sophisticated and more sensitive techniques, such as HPLC-PDA-(HRMS)-SPE-NMR (Wubshet *et al.*, 2015), are available, allowing the identification of minor compounds in plant extracts. Continuing our research program on cyclopeptide alkaloids (Tuenter *et al.*, 2016), it was decided to investigate *Z. nummularia* and *Z. spina-christi* for the presence of yet unknown compounds.

6.2 Results and Discussion

The bark of *Z. nummularia* and *Z. spina-christi* was extracted with 80% methanol and the crude extracts were fractionated by liquid-liquid partitioning, followed by flash chromatography. The purification of single compounds was performed with either HPLC-PDA-HRMS-SPE-NMR or semi-preparative HPLC with DAD and ESIMS detection. Seven cyclopeptide alkaloids were obtained (**1-7**), two from *Z. nummularia* (**1**, **2**) and five from *Z. spina-christi* (**3-7**). Their structures (Figure 6.1) were elucidated by 1D and 2D NMR experiments and comparison with literature data, and confirmed by (HR)ESIMS. ¹H and ¹³C NMR chemical shift assignments for compounds **1-7** are listed in Tables 6.1 and 6.2, respectively.

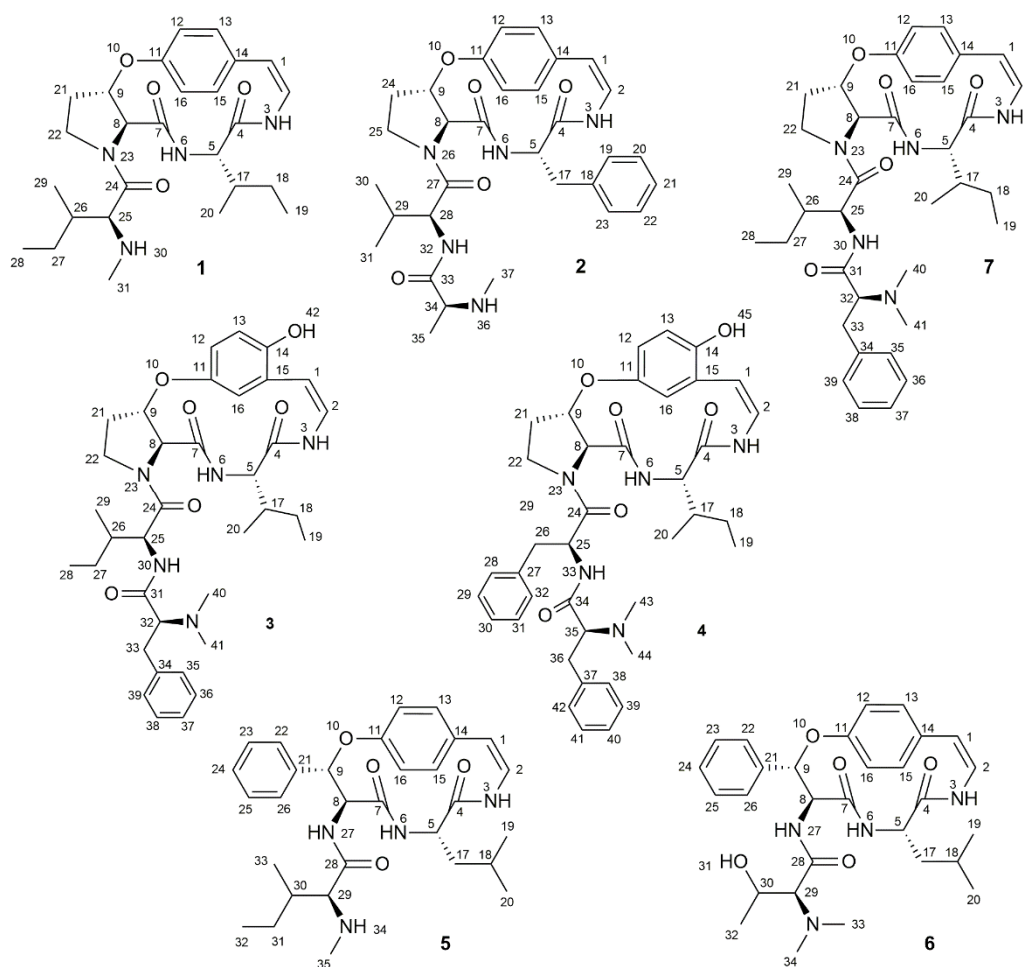


Fig. 6.1 Chemical structures of compounds **1-7**, isolated from the stem bark of *Ziziphus nummularia* (**1** and **2**) and *Ziziphus spina-christi* (**3-7**).

The NMR data of compound **1** (Figures 6.2 – 6.5 and Tables 6.1 and 6.2) showed great similarity with the NMR data previously reported for ramosine-A (Lin *et al.*, 2003). Ramosine-A contains a *para*-cyclophane. In the ^1H spectrum of **1**, four aromatic proton signals, of which two doublets of doublets, with J -values typical for an o,m -coupling pattern, and two overlapping signals (also appearing as doublets of doublets with J -values typical for an o,m -coupling pattern) were present. This was in agreement with the *para*-cyclophane (14-membered ring type) and not the 13-membered ring type (*meta*-cyclophane). In cyclopeptide alkaloids, the chemical shift value of H-9, the β -proton of the β -hydroxy-amino acid moiety, is very characteristic, and can be found between 5.00 and 5.50 ppm in a vast majority of compounds. In this case, a multiplet was present at 5.37 ppm. In the COSY spectrum, three cross peaks were observed for this proton signal, more specifically with H-8 (δ 4.20 ppm, d), H-21A (δ 2.22 ppm, m) and H-21B (δ 2.58 ppm, m). The proton signals of the CH_2 -group in position 21 also

showed cross peaks to H-22A (δ 3.58 ppm) and H-22B (δ 4.06 ppm). H-22A/H-22B did not show other correlations in the COSY spectrum. These data are in agreement with previously reported data for β -hydroxyproline in cyclopeptide alkaloids (more specifically in ramosine-A). The presence of two more amino acids, both isoleucine moieties, could be established based on the NMR data. Based on the HMBC spectrum, the ring-bound amino acid could be distinguished from the isoleucine in the side chain, since the *N*-methyl proton signal at 2.62 ppm (H-31) showed a cross peak to the α -carbon of the latter (C-25, δ 64.8 ppm). In contrast to ramosine-A, however, the signal that could be assigned to the *N*-methyl protons (δ_{H} 2.62 ppm, s) integrated for only three protons, whereas in ramosine-A a dimethylated terminal nitrogen atom was present. Moreover, HRESIMS showed a protonated molecule at m/z 471.2997, matching with a molecular formula of $\text{C}_{26}\text{H}_{39}\text{N}_4\text{O}_4$ $[\text{M}+\text{H}]^+$, while the molecular formula of ramosine-A is $\text{C}_{27}\text{H}_{40}\text{N}_4\text{O}_4$. Therefore, it could be concluded that the nitrogen atom of the terminal amino acid moiety of compound **1** contains only a single methyl group, and this compound was named nummularine-U (*N*-desmethyldramosine-A), being reported here for the first time.

The spectroscopic data of compound **2** (Figures 6.6 and 6.7) are in agreement with the assignments previously reported for mauritine-F (Cristau *et al.*, 2005).

Compound **1** belongs to the 4(14) subclass of cyclopeptide alkaloids, while compound **2** is of the 5(14) subclass. Both contain proline as the ring-bound β -hydroxy-amino acid, and therefore compound **1** can be classified as an amphibine-F type, and compound **2** as an amphibine-B type (Inayat-Ur-Rahman *et al.*, 2001). Close to 30 cyclopeptide alkaloids were reported in *Z. nummularia*, displaying a wide variety of structural characteristics. Approximately half of the reported alkaloids are composed of four moieties and the other half of five moieties. The 4(14) and 5(13) subclasses represent each around 40%, while only few cyclopeptide alkaloids belonging to the 5(14) and 4(13) types have been identified. Besides compound **1**, only one other compound belonging to the amphibine-F type has been reported in this species, namely, nummularine-F (Tschesche *et al.*, 1975). Interestingly, all compounds that are built up of five moieties contain a β -hydroxyproline moiety. Eleven cyclopeptide alkaloids of the zizyphine-A type (5(13), β -hydroxyproline) have been identified and besides mauritine-F, only two other amphibine-B type (5(14), β -hydroxyproline) alkaloids have been reported: mauritine-A and mauritine-D (Dwivedi *et al.*, 1987; Singh *et al.*, 1995).

Fig. 6.2 ^1H NMR spectrum (400 MHz, methanol- d_4) of compound **1** (nummularine-U).

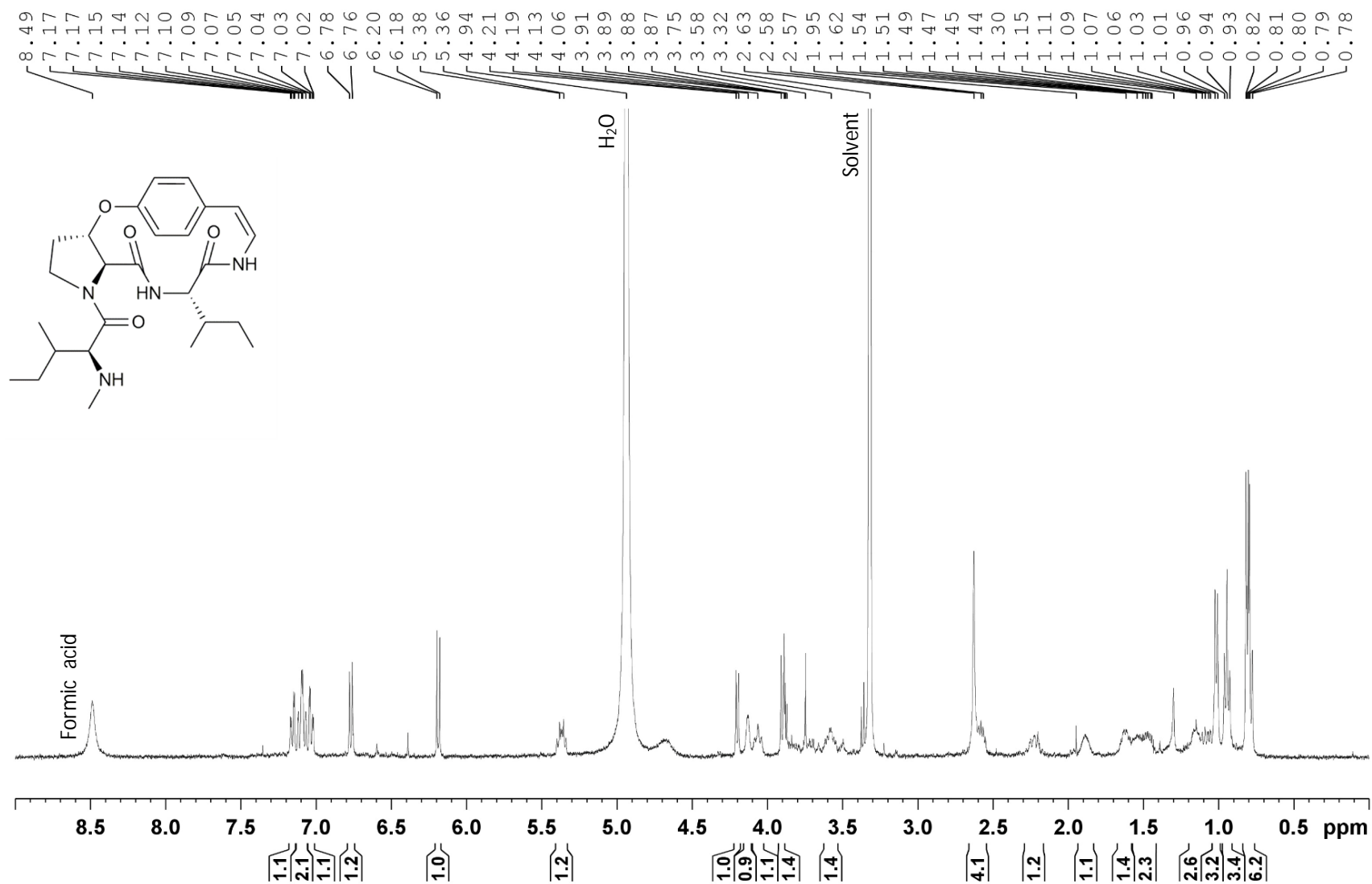


Fig. 6.3 HSQC spectrum (methanol- d_4) of compound **1** (nummularine-U).

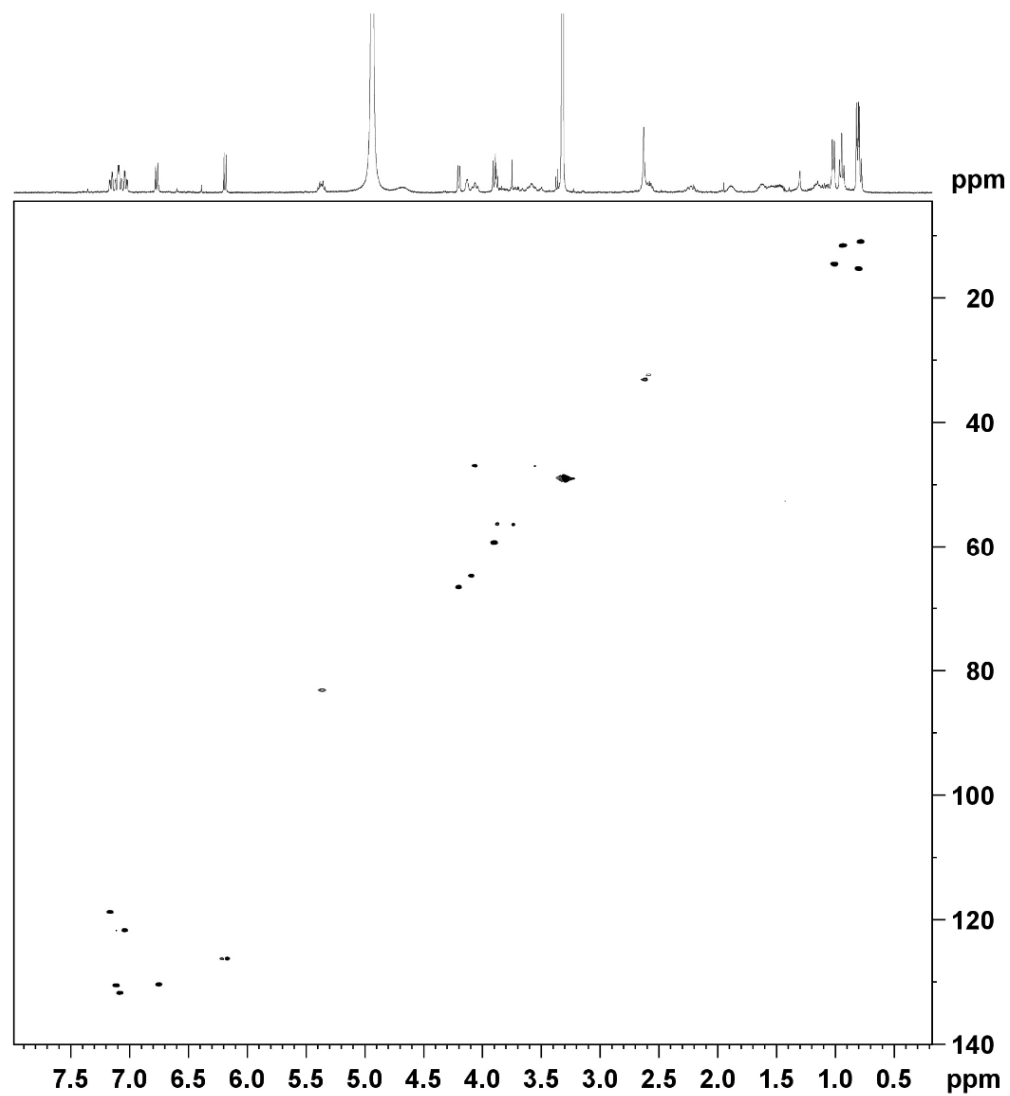


Fig. 6.4 HMBC spectrum (methanol- d_4) of compound **1** (nummularine-U).

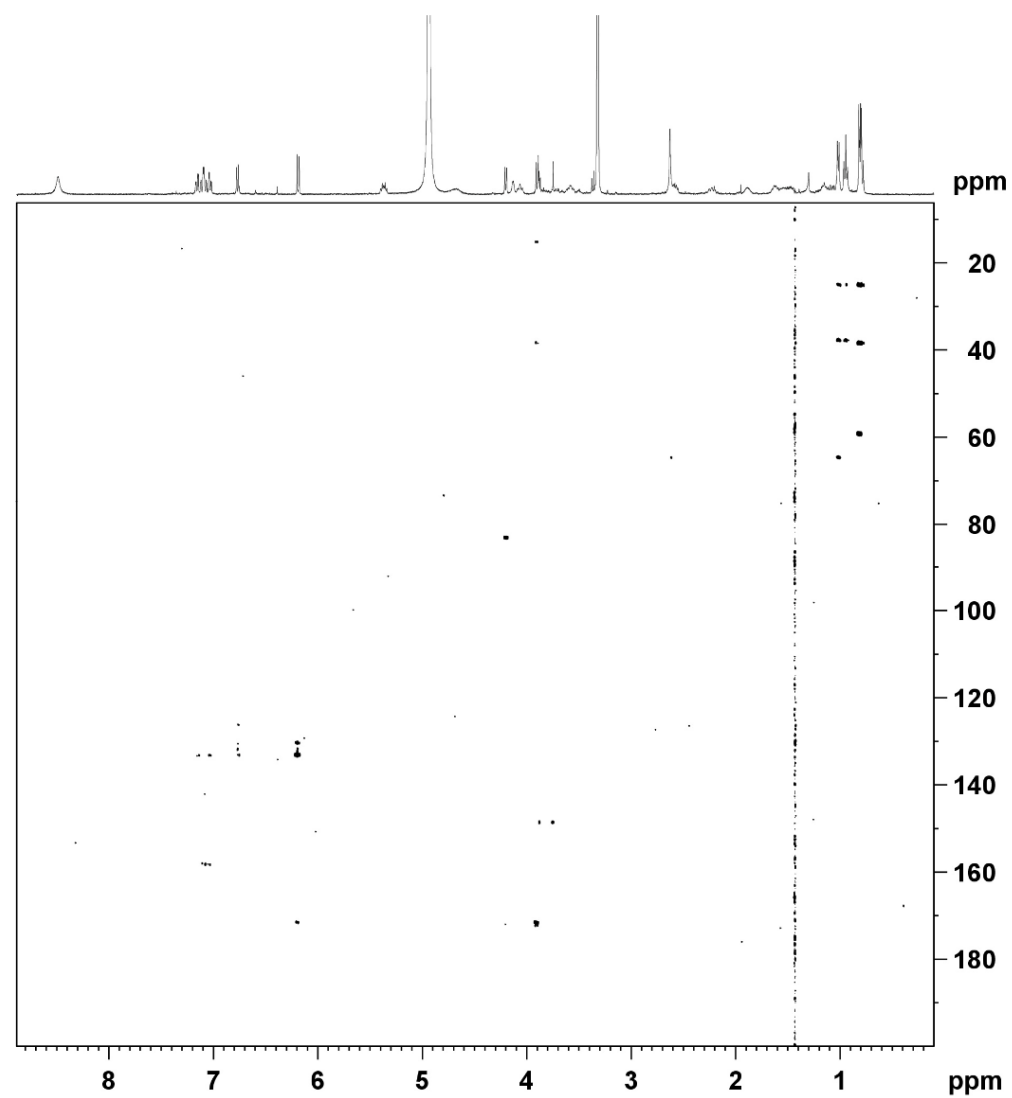


Fig. 6.5 COSY spectrum (methanol- d_4) of compound **1** (nummularine-U).

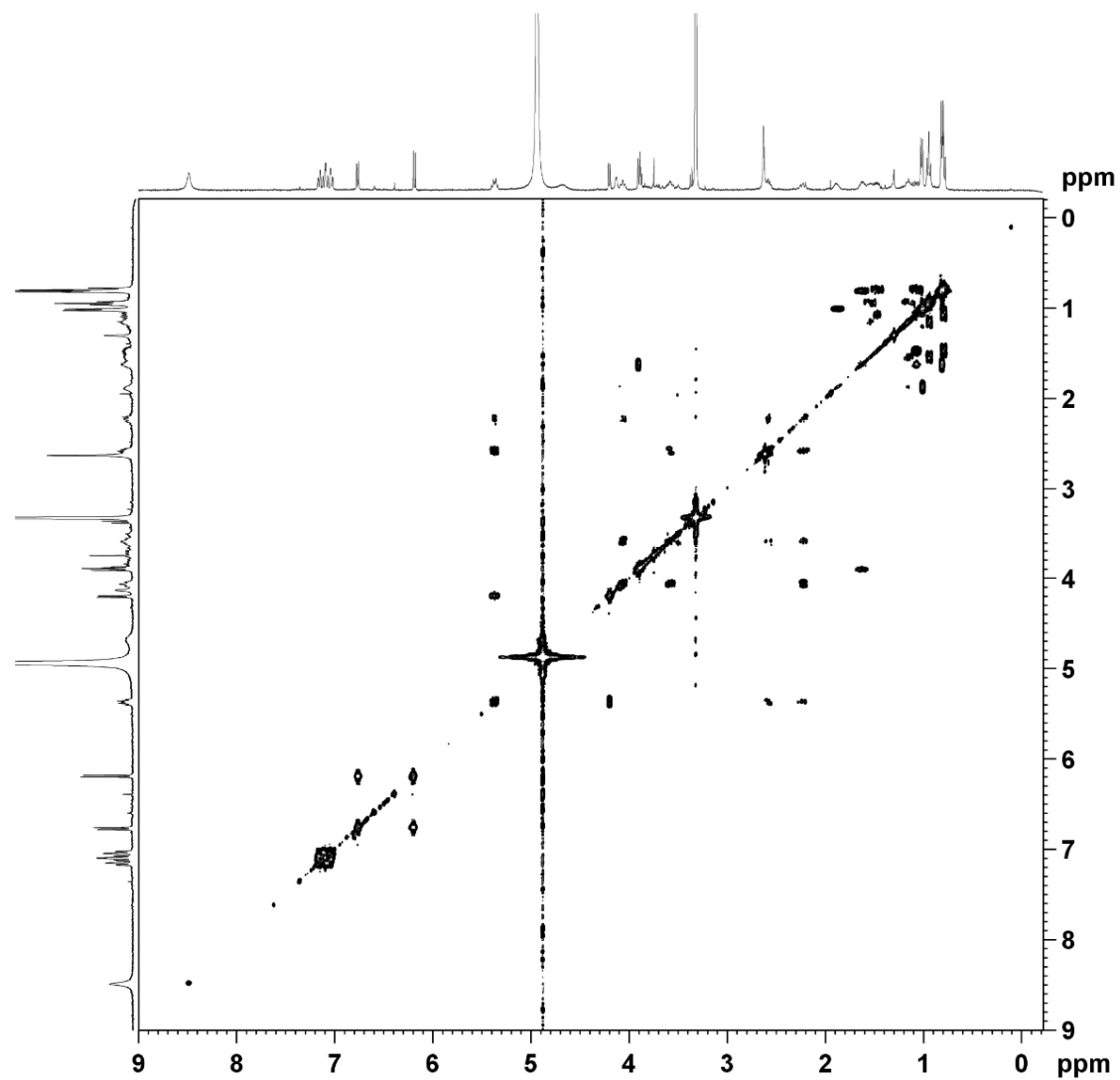


Fig. 6.6 ^1H NMR spectrum (400 MHz, methanol- d_4) of compound **2** (mauristine-F).

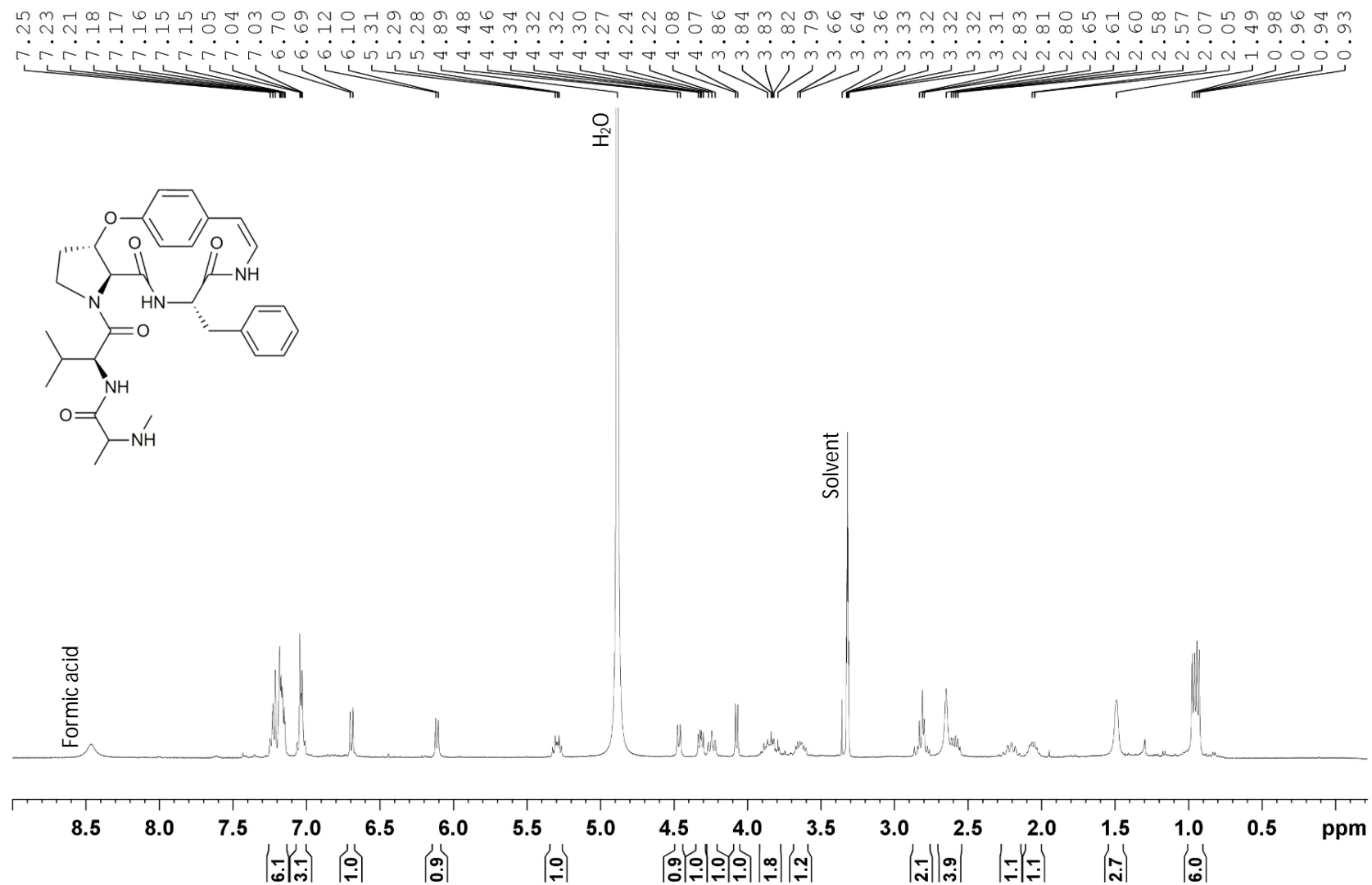
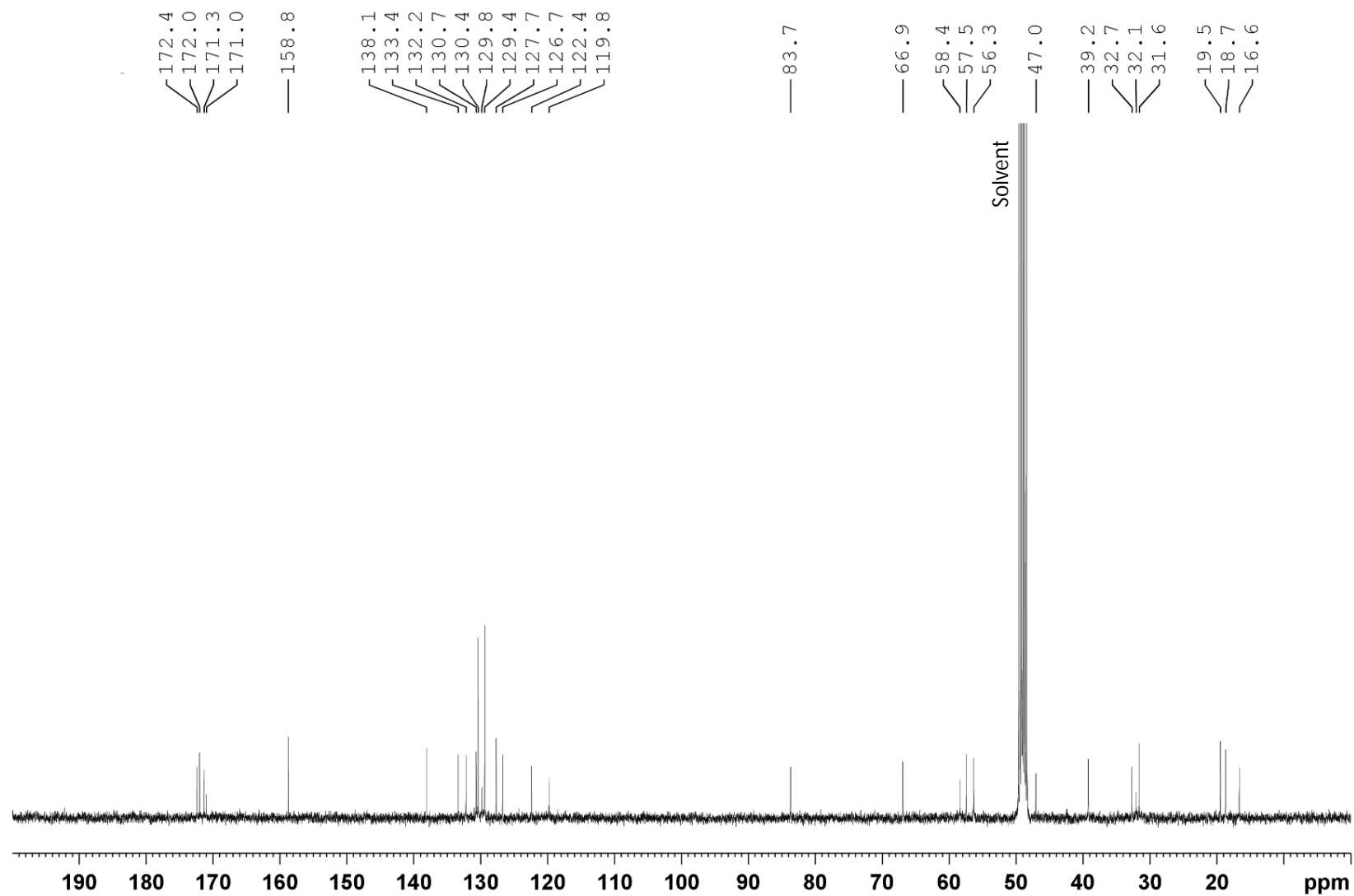


Fig. 6.7 ^{13}C NMR spectrum (100 MHz, methanol- d_4) of compound **2** (mauritine-F).



Compounds **3** and **4** were both purified by HPLC-PDA-SPE-NMR, and their HRESIMS measurements showed protonated molecules at m/z 648.3780 ($C_{36}H_{50}O_6N_5$, $[M+H]^+$) and m/z 682.3555 ($C_{39}H_{48}O_6N_5$, $[M+H]^+$), respectively. Their NMR spectra (Figures 6.8 – 6.15) showed the typical pattern of cyclopeptide alkaloids, and allowed to identify some amino acid moieties, which were reported before for paliurine-C and jubanine-A (Tschesche *et al.*, 1976; Lin *et al.*, 2000). These compounds both contain a 13-membered ring, consisting of a 2-methoxystyrylamine, an isoleucine and a β -hydroxyproline moiety, but differ in their side chain. Paliurine-C contains an additional isoleucine and a terminal *N*-dimethylated phenylalanine amino acid moiety, whereas jubanine-A has two phenylalanine moieties, the terminal one being *N*-dimethylated.

For the structure elucidation of compound **3**, H-9 could again be used as the starting point. This proton had a chemical shift of 5.27 ppm and showed cross peaks to δ_H 2.28 and 2.59 ppm (H-21A and H-21B, respectively) and to δ_H 4.37 (H-8). As in compounds **1** and **2**, the β -hydroxy-amino acid was identified as a β -hydroxyproline, as deduced from the COSY and HMBC data. As for the terminal amino acid moiety, the protons of the *N*-dimethyl group showed a cross peak in the HMBC spectrum to C-32 at 71.5 ppm. H-32 (δ_H 3.31 ppm) in turn was connected to a CH_2 -group (δ_H 2.94 ppm and 3.05 ppm, H-33A and H-33B), as deduced from the COSY spectrum. The HMBC spectrum showed correlations of these protons with δ_C 139.0 and 130.2 ppm, signals typical for an aromatic moiety. Indeed, further inspection of the COSY and HMBC spectrum led to the identification of a benzyl structure, and the terminal amino acid was identified as *N,N*-dimethylphenylalanine. Based on the 2D NMR spectra of compound **3**, two more amino acid moieties could be identified, being both isoleucine moieties. Due to overlap of the signals of C-7 and C-31 in the HMBC spectrum, it was not possible to determine which NMR signals should be assigned to the ring-bound isoleucine moiety and which to the isoleucine amino acid in the side chain. However, comparison with the ^{13}C chemical shifts, previously reported for paliurine-C (Lin *et al.*, 2000), allowed to discriminate both sets of signals. Especially the chemical shift value of the α -carbon of the amino acid is characteristic, since the α -carbon of the ring-bound isoleucine moiety was reported to have a more downfield shift (δ_C 60.2 ppm), compared to the α -carbon of the amino acid in the side chain (δ_C 53.8 ppm). Lin *et al.* (2000) also investigated the configuration of the α -carbon atoms in the intermediate and terminal amino acid of paliurines-A, -B, -C, -D and -F, by comparison with

^{13}C NMR data of comparable dipeptides. The chemical shift values observed in our study for compound **3** were closest to the values reported for the LL form of the dipeptide, indicating the same configuration for both amino acid moieties in the side chain.

For compound **4**, the β -hydroxy amino acid was identified as β -hydroxyproline and the terminal amino acid as *N,N*-dimethylphenylalanine, in the same way as described for compound **3**. The ^1H spectrum showed the characteristic pattern for a 1,2,4-trisubstituted benzene (δ 6.76, dd, 8.9 and 2.9 Hz, H-12; δ 6.84, d, 8.9 Hz, H-13; δ 6.71, d, 2.9 Hz, H-16), typically found for cyclopeptide alkaloids with a 13-membered ring (*meta*-cyclophane), substituted in position 14 (for compound **3**, the same moiety was identified, based on the 2D data). HMBC cross peaks of both H-2 and H-5 with C-4 allowed to determine the α -proton of the ring-bound amino acid, and further inspection of the 2D spectra led to the identification of this amino acid as an isoleucine moiety. Another amino acid could be identified as a phenylalanine moiety, which could only be positioned as the intermediate amino acid in the side chain.

Thus, according to the NMR data, the structures of compound **3** and **4** matched to a great extent with those of paliurine-C and jubanine-A, respectively. However, in the ^1H -NMR and HSQC spectra of compounds **3** and **4**, no signal corresponding to the methoxy group could be observed. This led to the conclusion that the two compounds that were purified here, possessed a 2-hydroxystyrylamine instead of a 2-methoxystyrylamine moiety. This hypothesis was in agreement with the obtained HRESIMS data. Compounds **3** and **4** have, to the best of our knowledge, not been reported before, and are named spinanine-B (*O*-desmethylpaliurine-C) and spinanine-C (*O*-desmethyljubanine-A).

Fig. 6.8 ^1H NMR spectrum (with suppression of the water signal) (600 MHz, methanol- d_4) of compound **3** (spinanine-B).

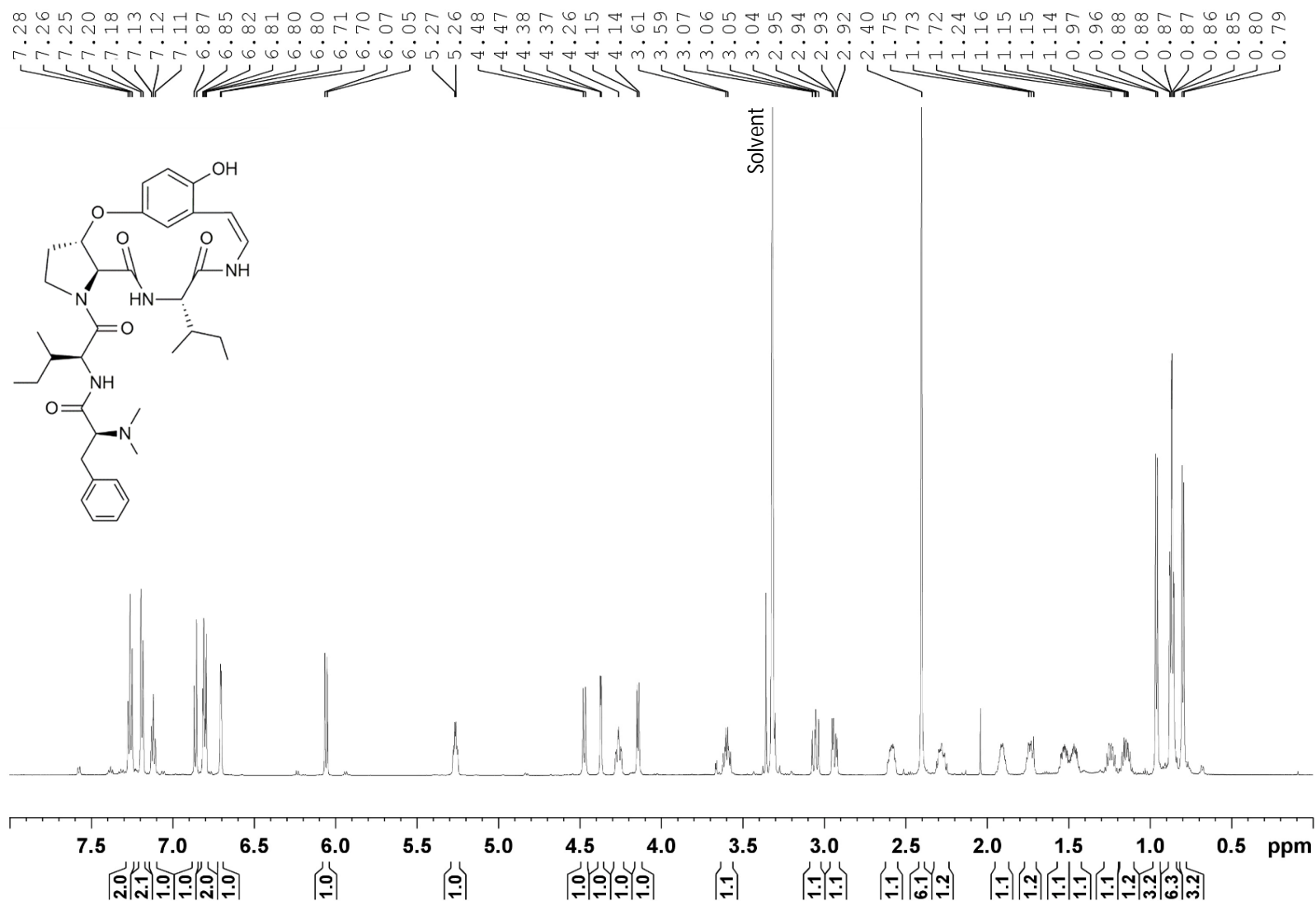


Fig. 6.9 HSQC spectrum (methanol- d_4) of compound **3** (spinanine-B).

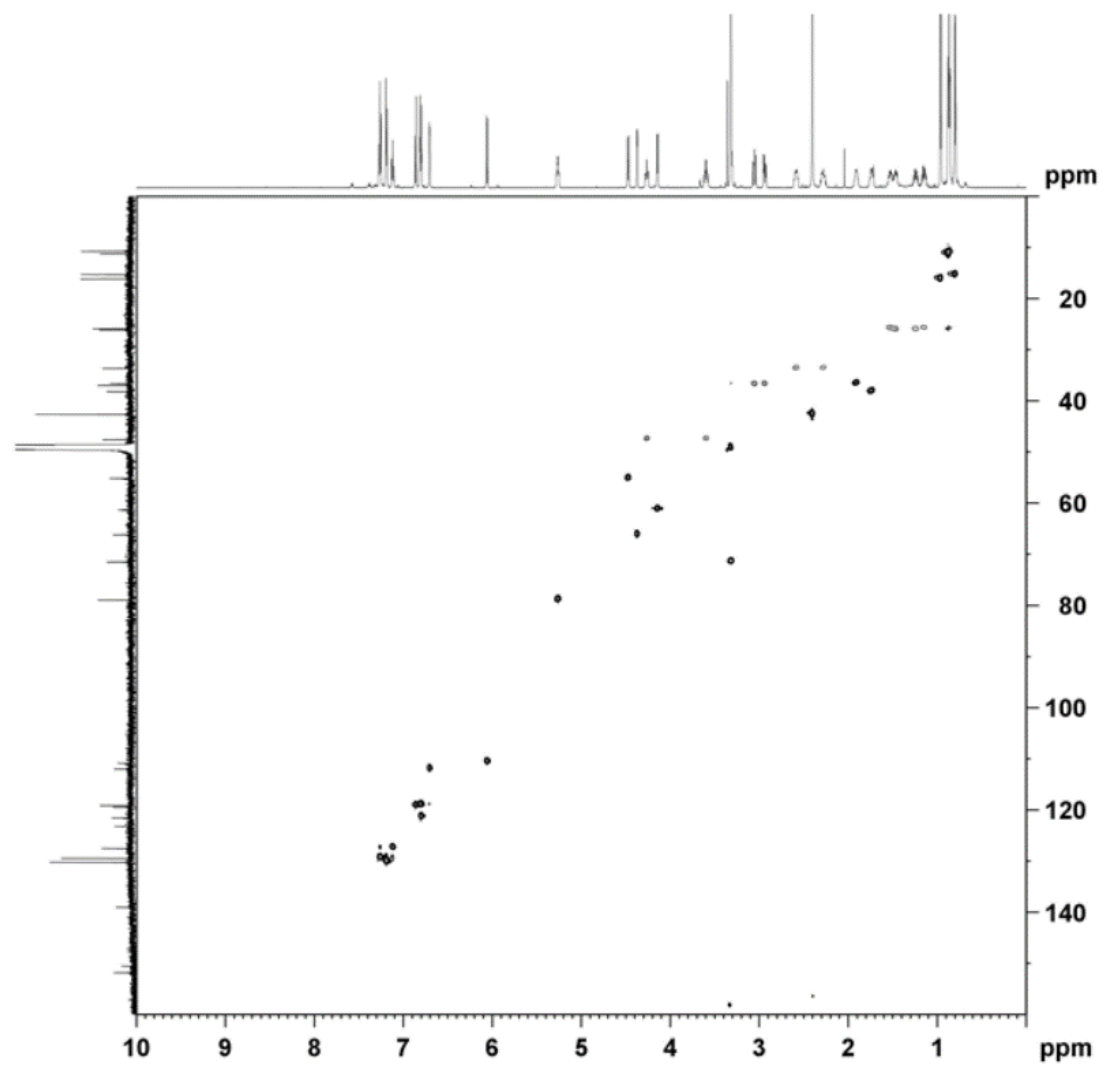


Fig. 6.10 HMBC spectrum (methanol- d_4) of compound **3** (spinanine-B).

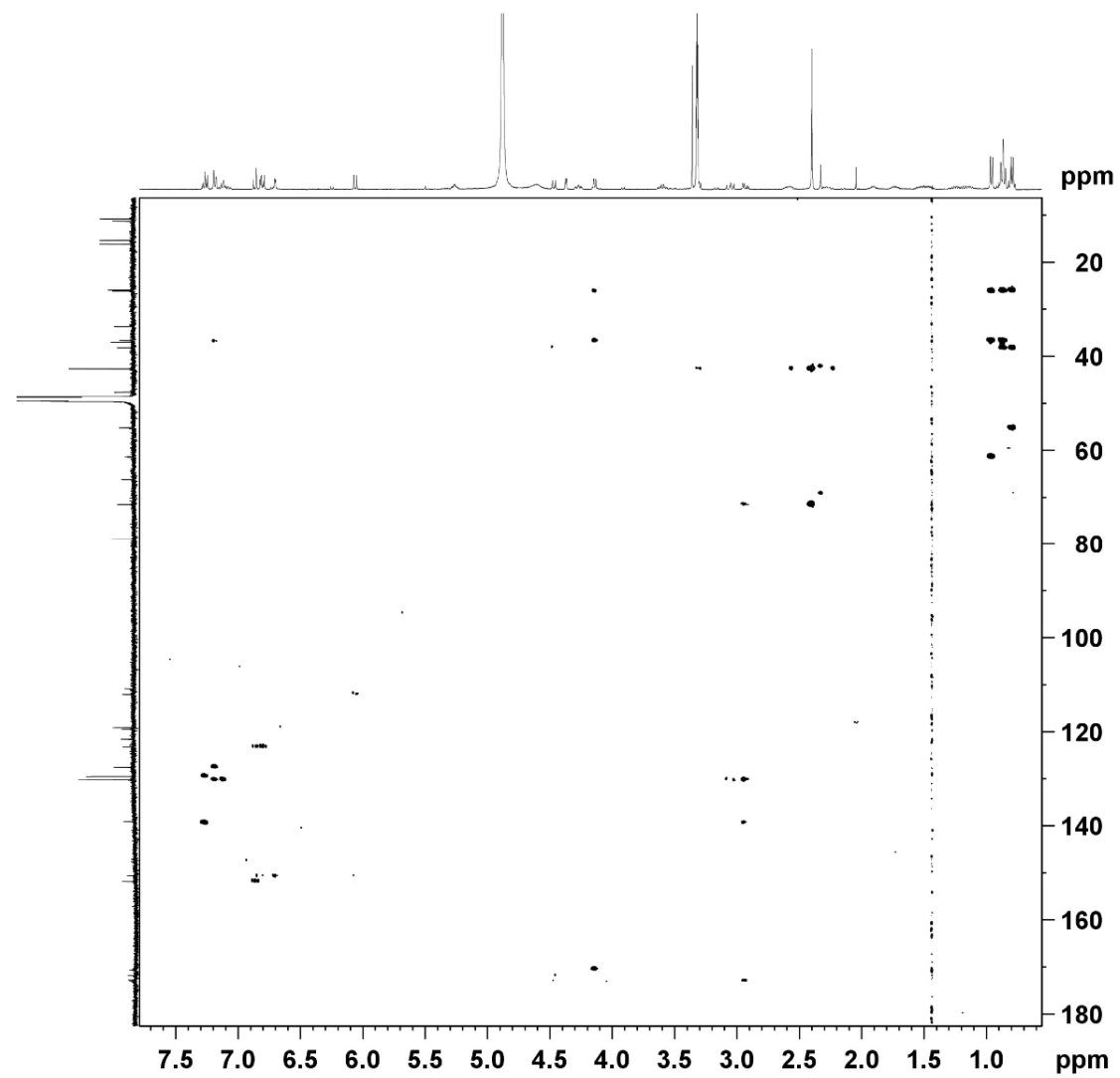


Fig. 6.11 COSY spectrum (methanol- d_4) of compound **3** (spinanine-B).

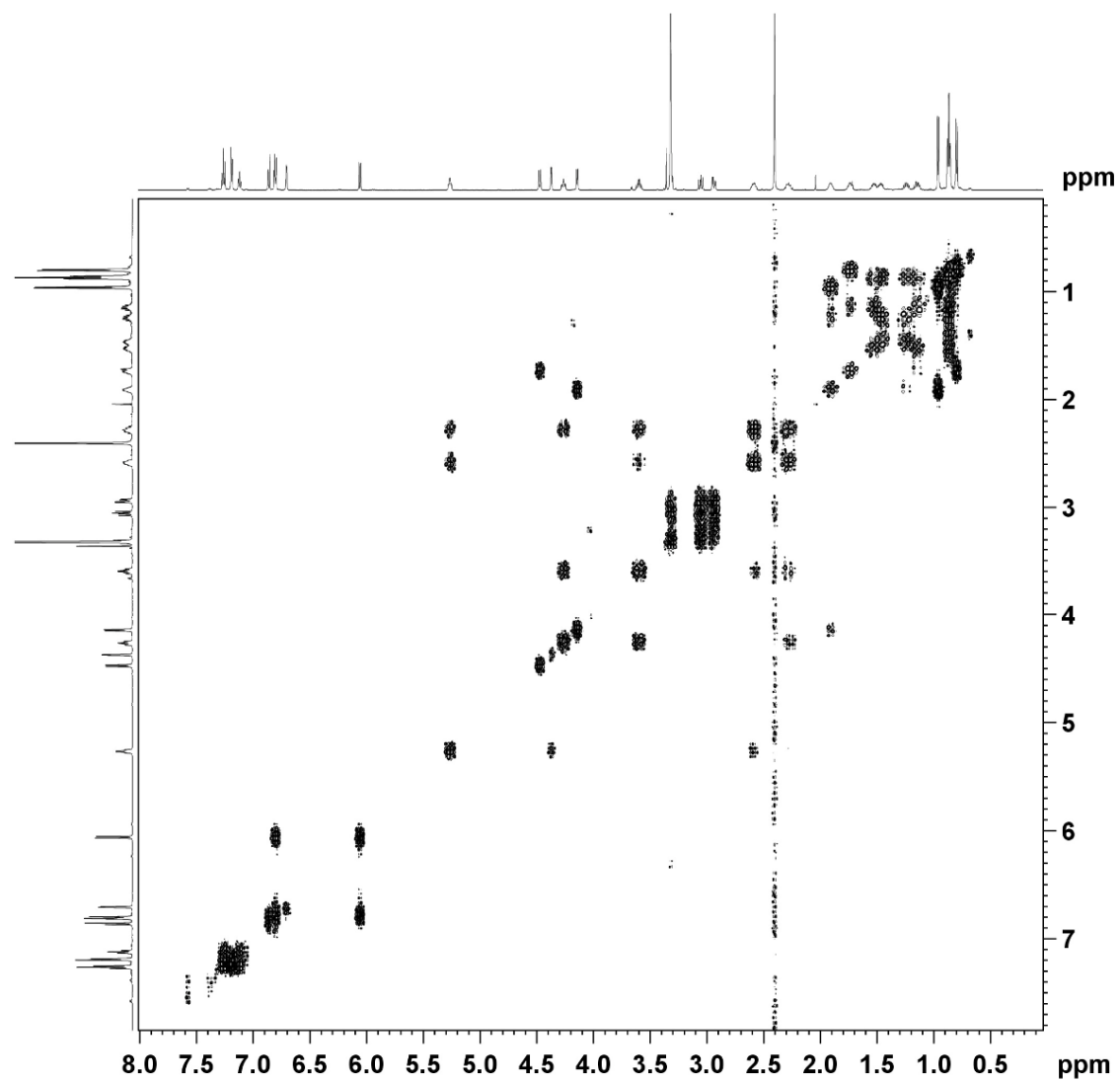


Fig. 6.12 ^1H NMR spectrum (600 MHz, methanol- d_4) of compound **4** (spinanine-C).

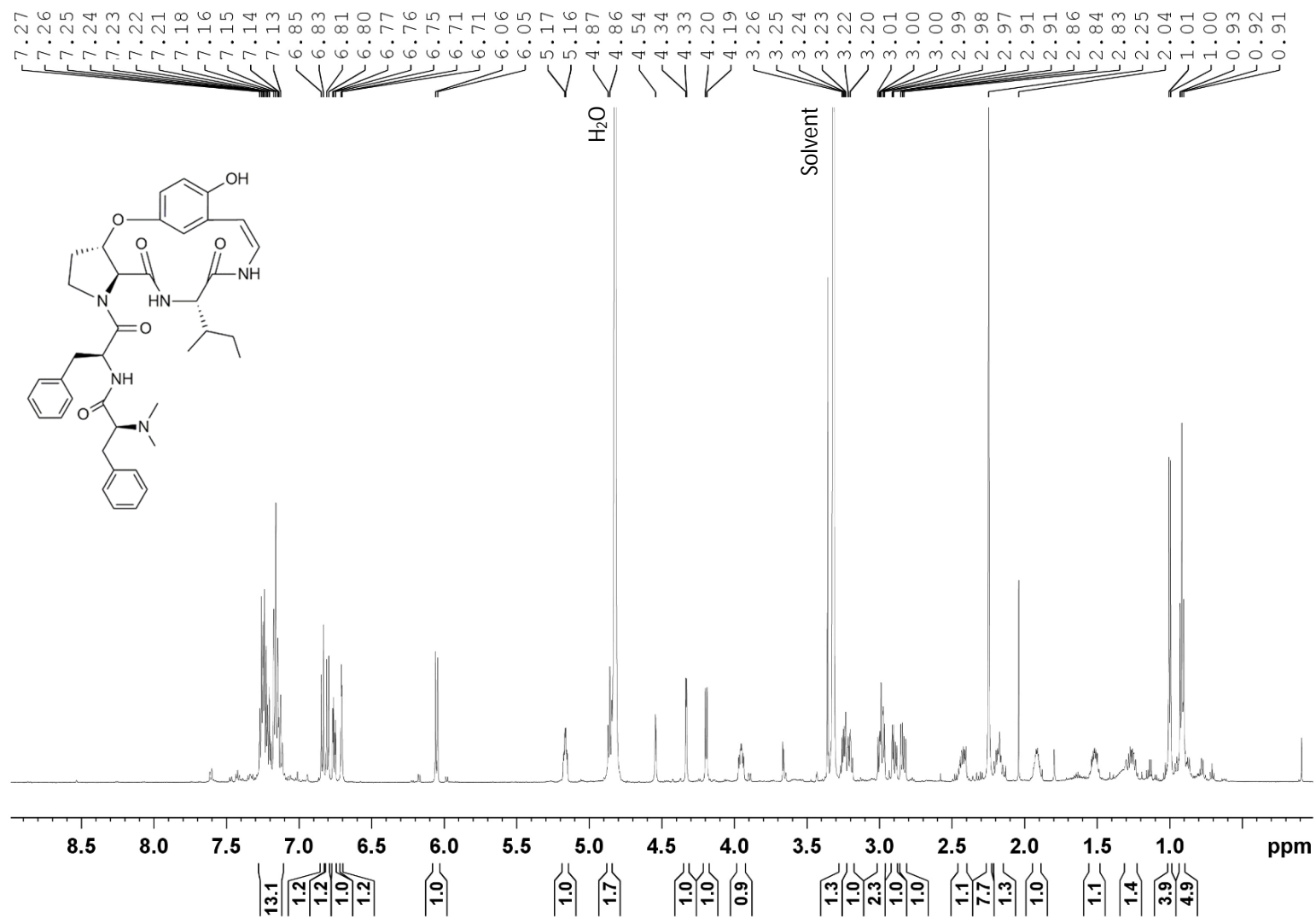


Fig. 6.13 HSQC spectrum (methanol- d_4) of compound **4** (spinanine-C).

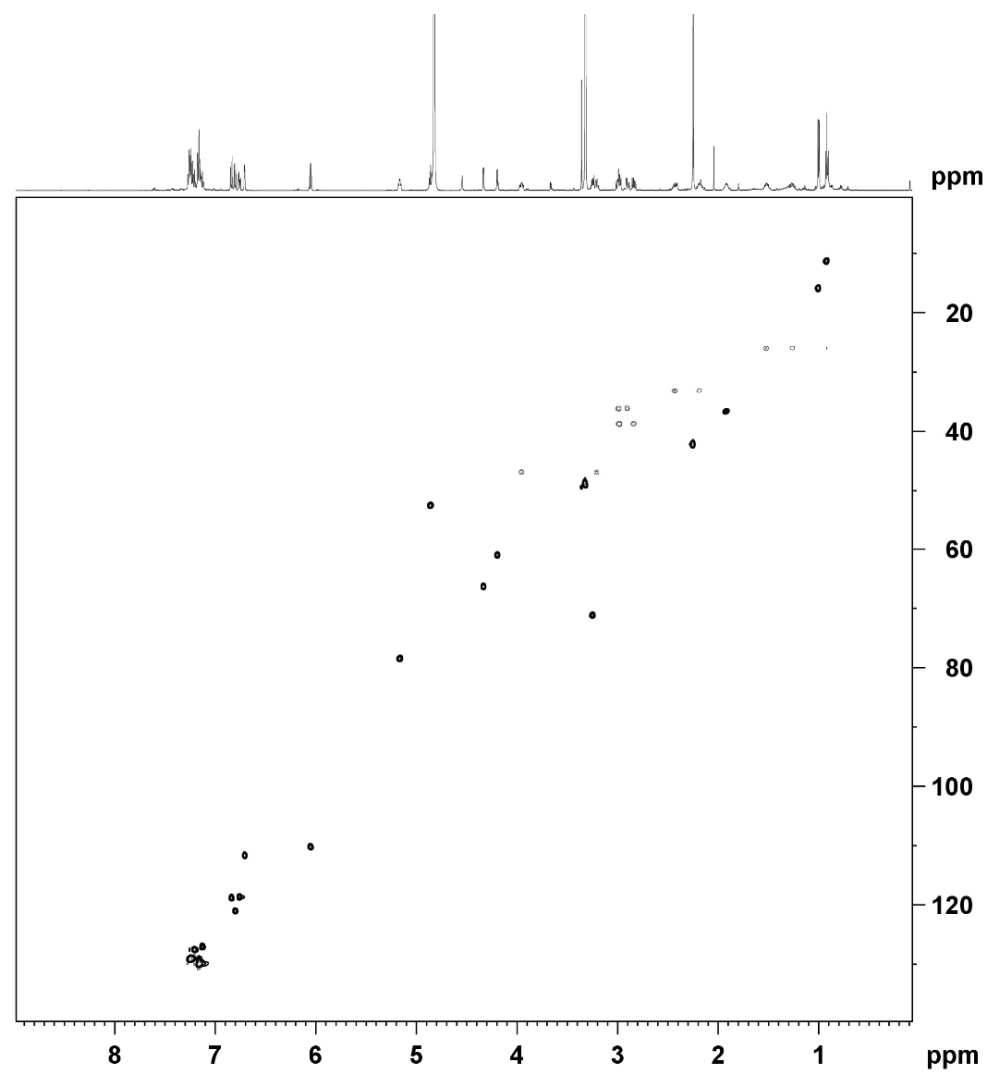


Fig. 6.14 HMBC spectrum (methanol- d_4) of compound **4** (spinanine-C).

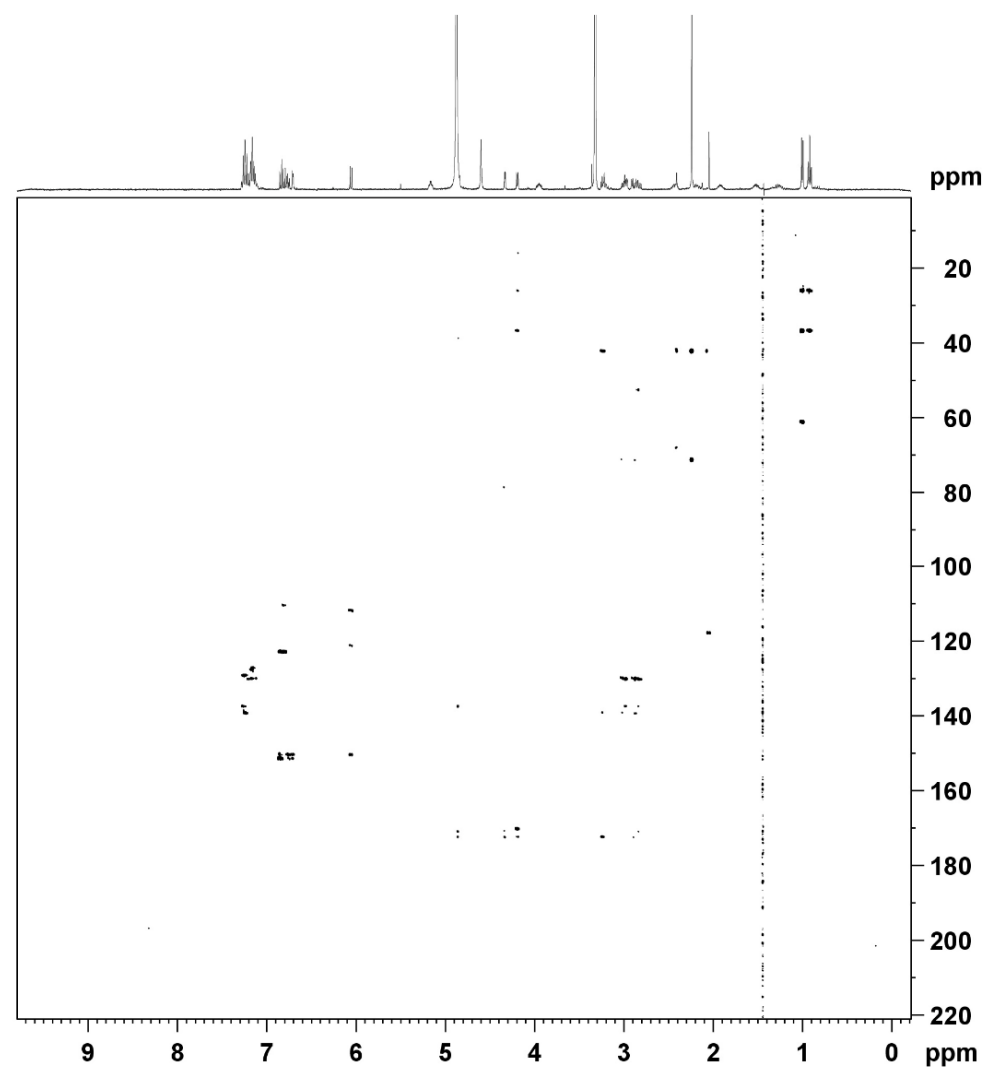
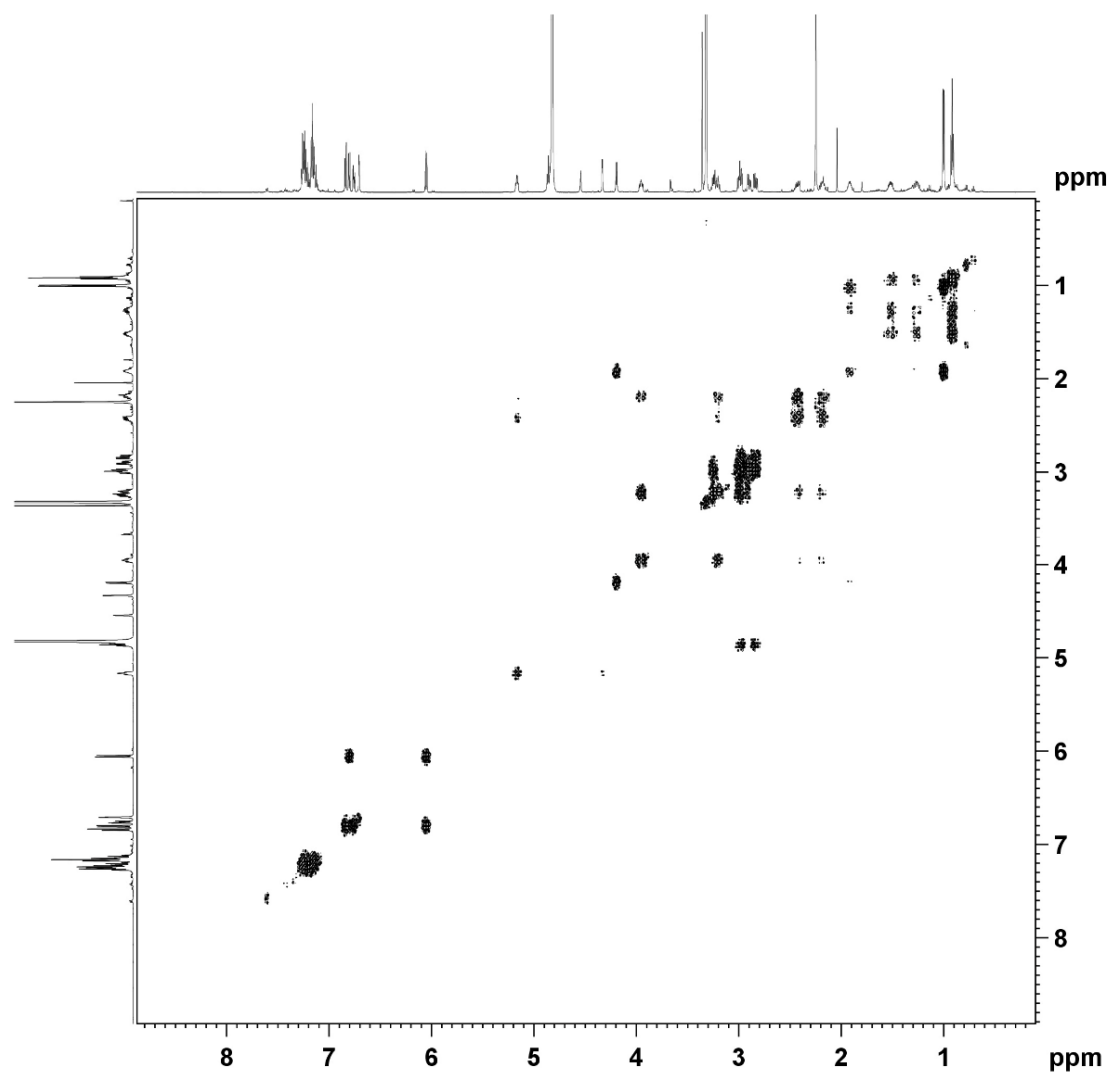


Fig. 6.15 COSY spectrum (methanol- d_4) of compound **4** (spinanine-C).



Furthermore, three other compounds were identified in *Z. spina-christi*: nummularine-D (**5**), nummularine-E (**6**) and amphibine-D (**7**), by comparison with reported spectral data (Tschesche *et al.*, 1972; Tschesche *et al.*, 1975). Their NMR spectra are shown in Figures 6.16 – 6.22. These compounds were reported before from other sources, but this is the first time they have been identified in *Z. spina-christi*.

The absolute configuration of nummularine-D and -E has not been reported before. However, from the NMR data of the ring-bound β -hydroxy-amino acid, β -hydroxyphenylalanine, the configuration of this moiety could be deduced. The C-8/C-9 chemical shifts were 56.8/80.9 ppm and 56.7/81.2 ppm, respectively, for compounds **5** and **6**, and the *J* values of H-9 were close to 8 Hz. These data indicated that the β -hydroxyphenylalanine moiety is present in the *L-erythro* form (Gournelis *et al.*, 1997). The configuration of the two amino acid moieties in the side chain of amphibine-D (**7**) could be deduced by comparing the ^{13}C chemical shift values to those reported by Lin *et al.* (2000) for the Leu(OMe)-Phe(NMe₂) dipeptide. Our values are consistent with those reported for the LL-dipeptide, which led to the conclusion that in amphibine-D both the isoleucine amino acid moiety and the phenylalanine amino acid moiety are present in their L-configuration. Considering the fact that the vast majority of cyclopeptide alkaloids are composed of L-amino acids, the L-configuration was also adopted for the other amino acids present in cyclopeptide alkaloids **1-7** reported here, although this could not be confirmed by experimental evidence for all chiral centers (Figure 6.1).

Up to now, three articles were published describing the isolation and identification of eleven cyclopeptide alkaloids from (stem) bark of *Z. spina-christi* (Tschesche *et al.*, 1974; Shah *et al.*, 1986; Abdel-galil and El-Jissry, 1991). The majority of the reported compounds have a 14-membered ring, while only three compounds with a 13-membered ring have been identified. These three compounds, i.e. amphibine-H, jubanine-A and zizyphine-F, all contain a β -hydroxyproline moiety and consist of five moieties, similar to spinanine-B (**3**) and spinanine-C (**4**). Thus, they all belong to the zizyphine-A type. Six 4(14) cyclopeptide alkaloids were reported displaying a wider variety: two frangulanine type compounds (with a β -hydroxyleucine moiety), three amphibine-F type compounds (with a β -hydroxyproline) and only one integerrine type, containing β -hydroxyphenylalanine. In the present work, two more compounds of the integerrine type were identified: nummularine-D (**5**) and nummularine-E

(6). The other two cyclopeptide alkaloids that reported in *Z. spina-christi* belong to the amphibine-B type (5(14) cyclopeptide alkaloids with a β -hydroxyproline moiety), which is also true for amphibine-D (7).

Fig. 6.16 ^1H NMR spectrum (600 MHz, methanol- d_4) of compound **5** (nummularine-D).

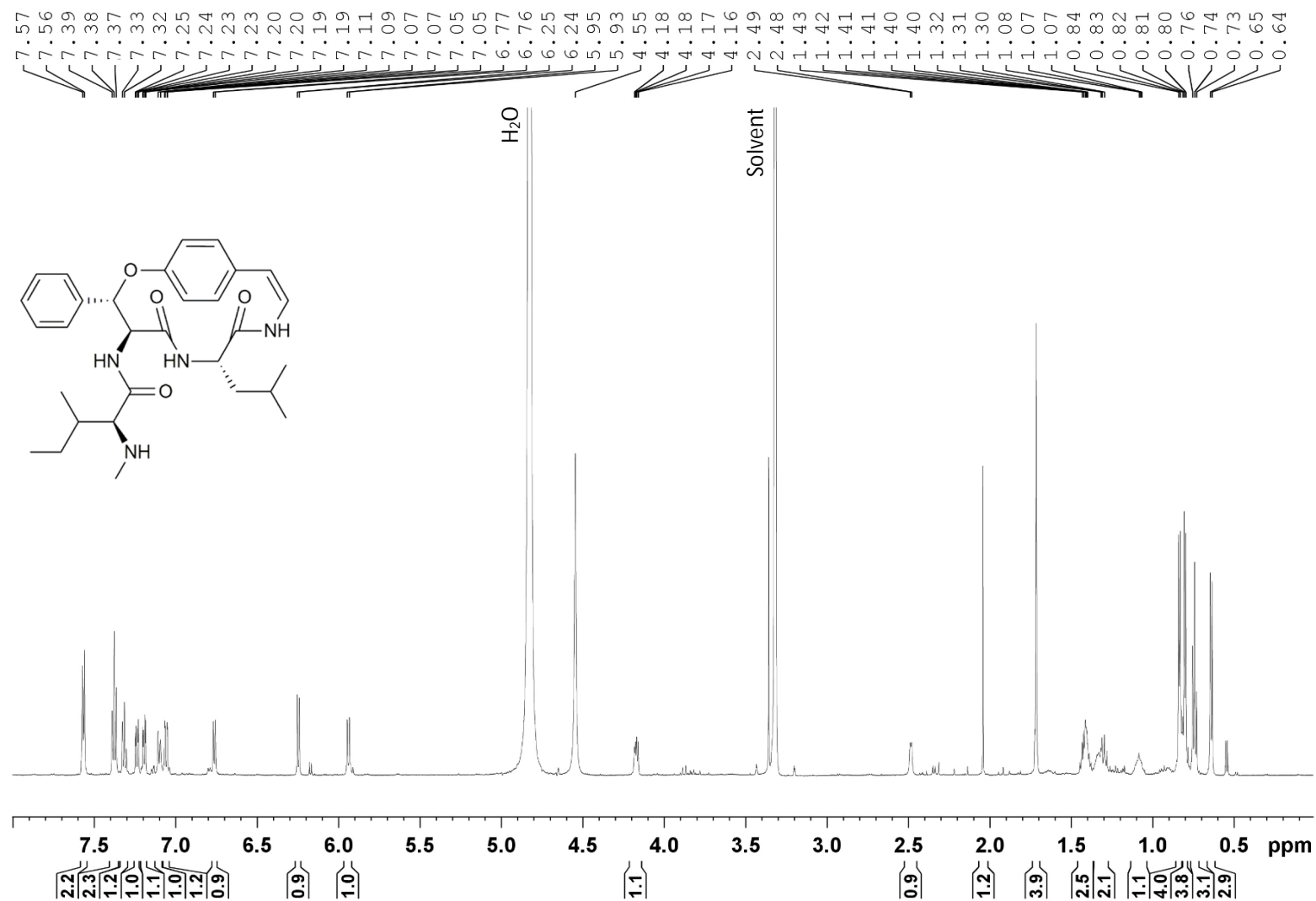


Fig. 6.17 HSQC spectrum (methanol-*d*₄) of compound **5** (nummularine-D).

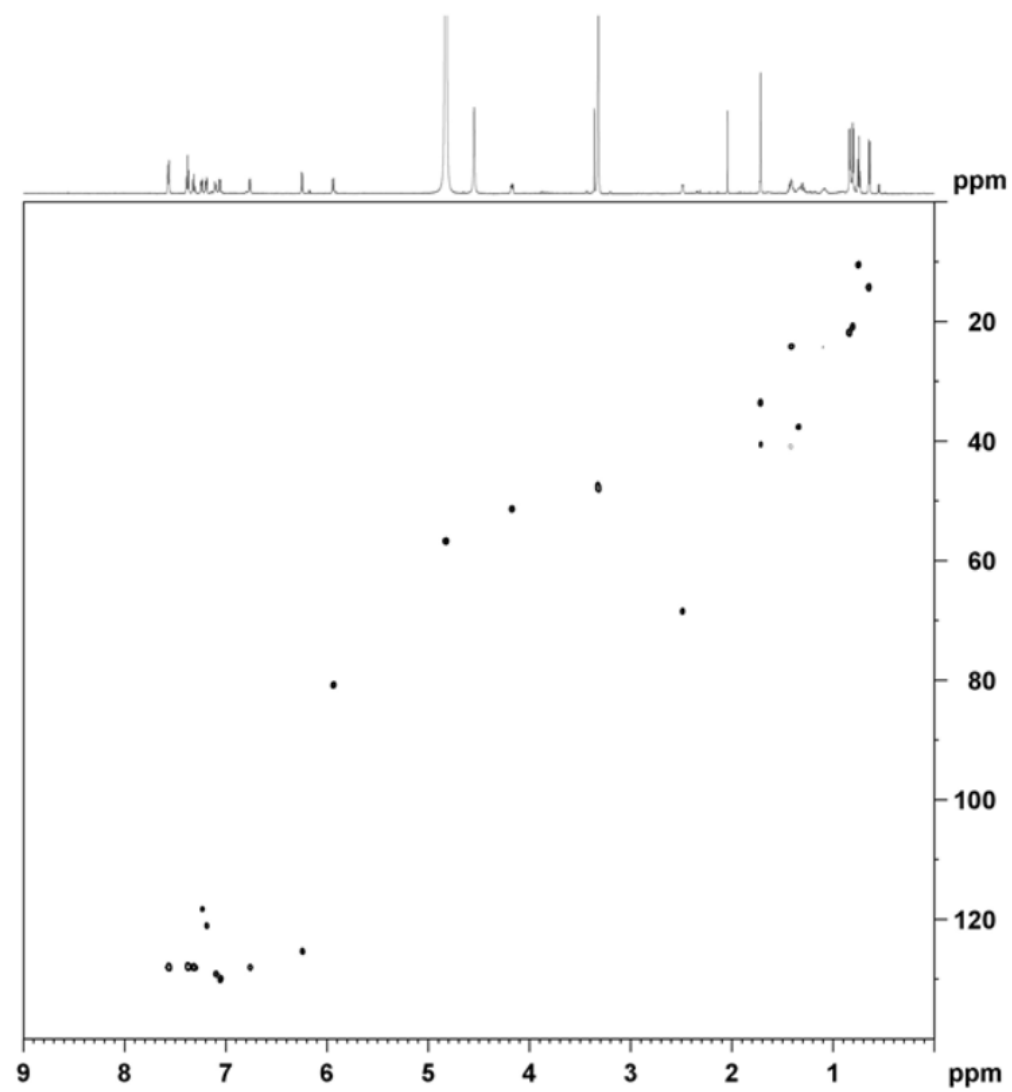


Fig. 6.18 COSY spectrum (methanol- d_4) of compound **5** (nummularine-D).

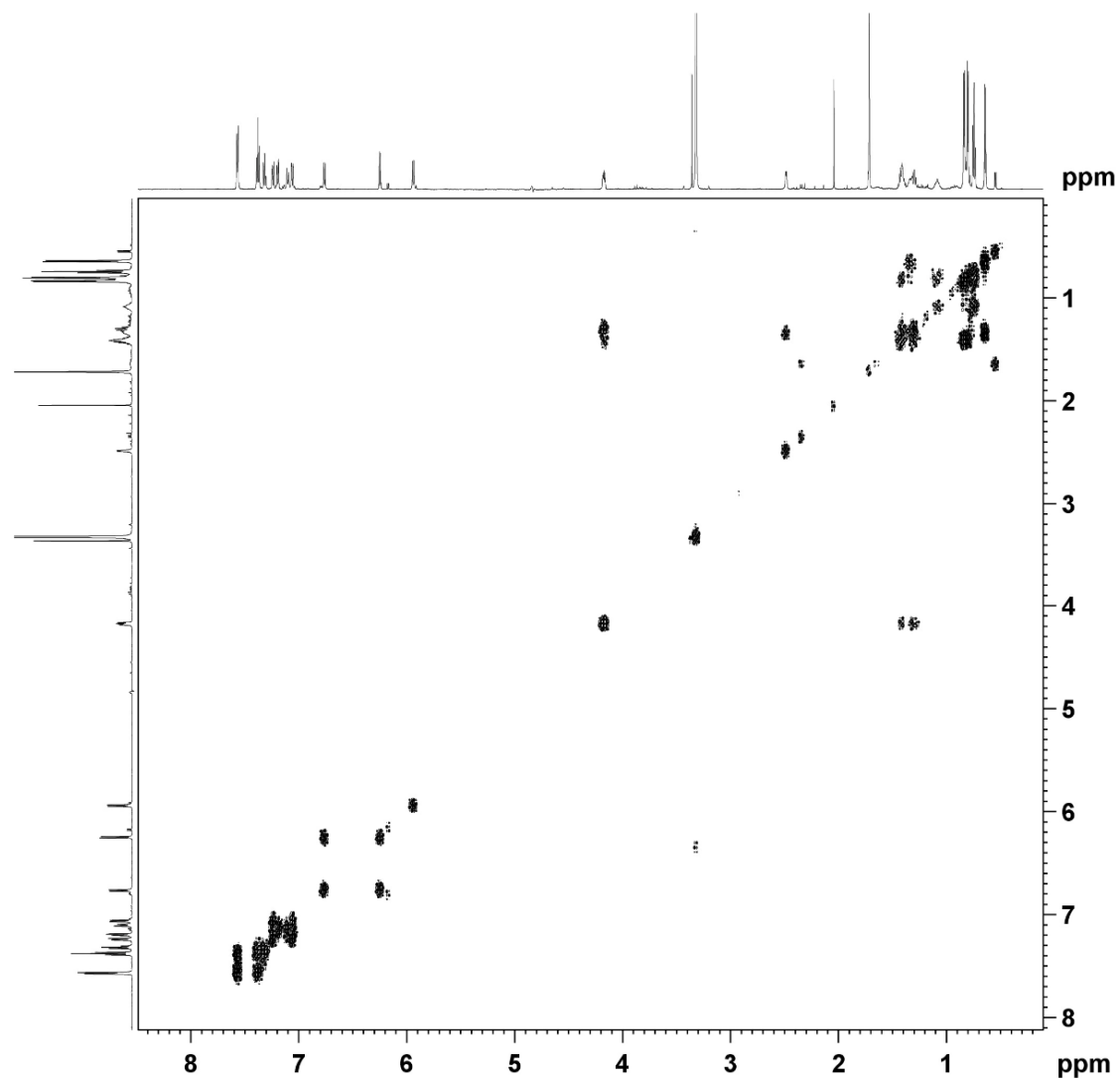


Fig. 6.19 ^1H NMR spectrum (with suppression of the methanol signal) (600 MHz, methanol- d_4) of compound **6** (nummularine-E).

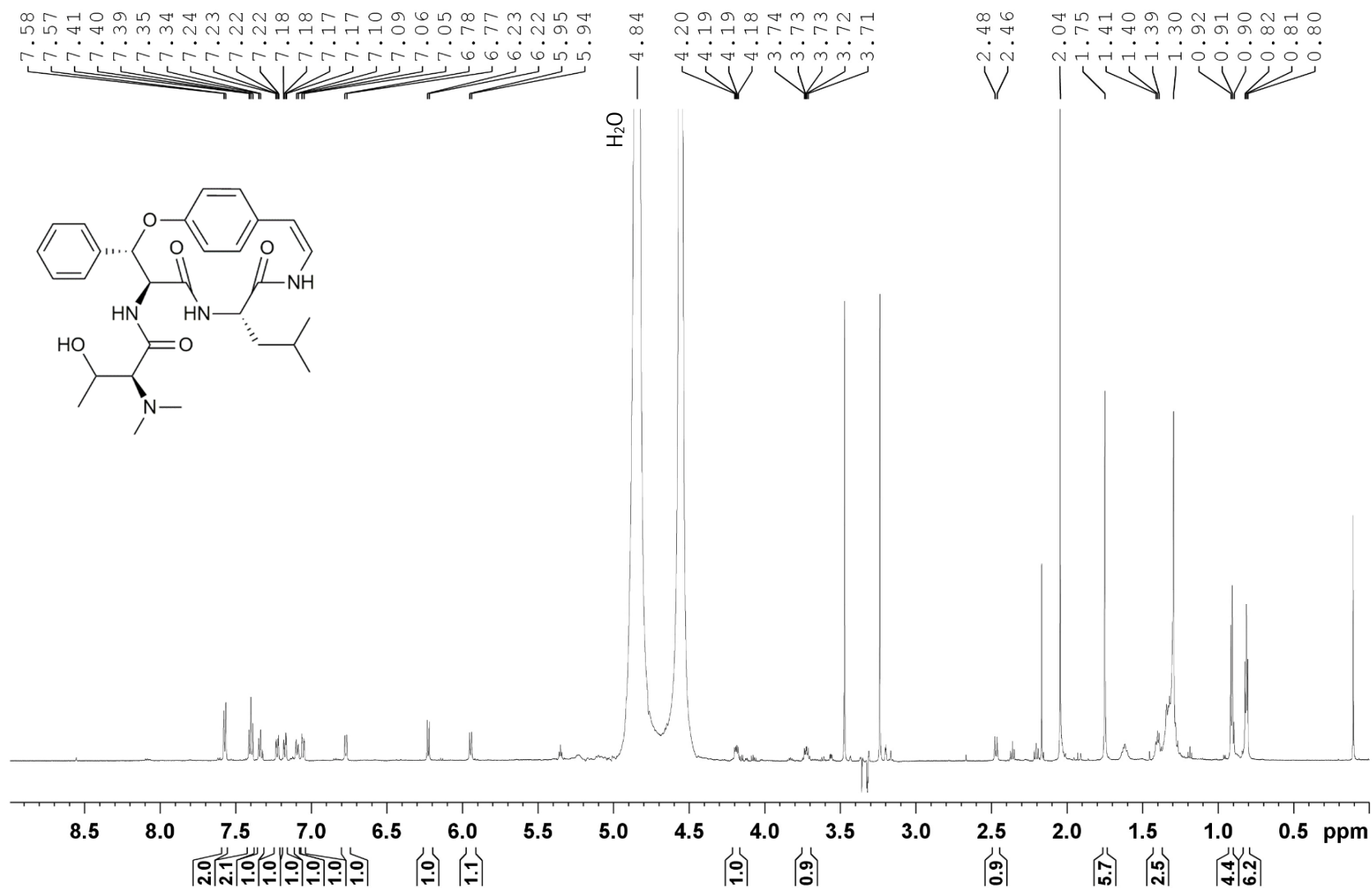


Fig. 6.20 ^{13}C NMR spectrum (100 MHz, methanol- d_4) of compound **6** (nummularine-E).

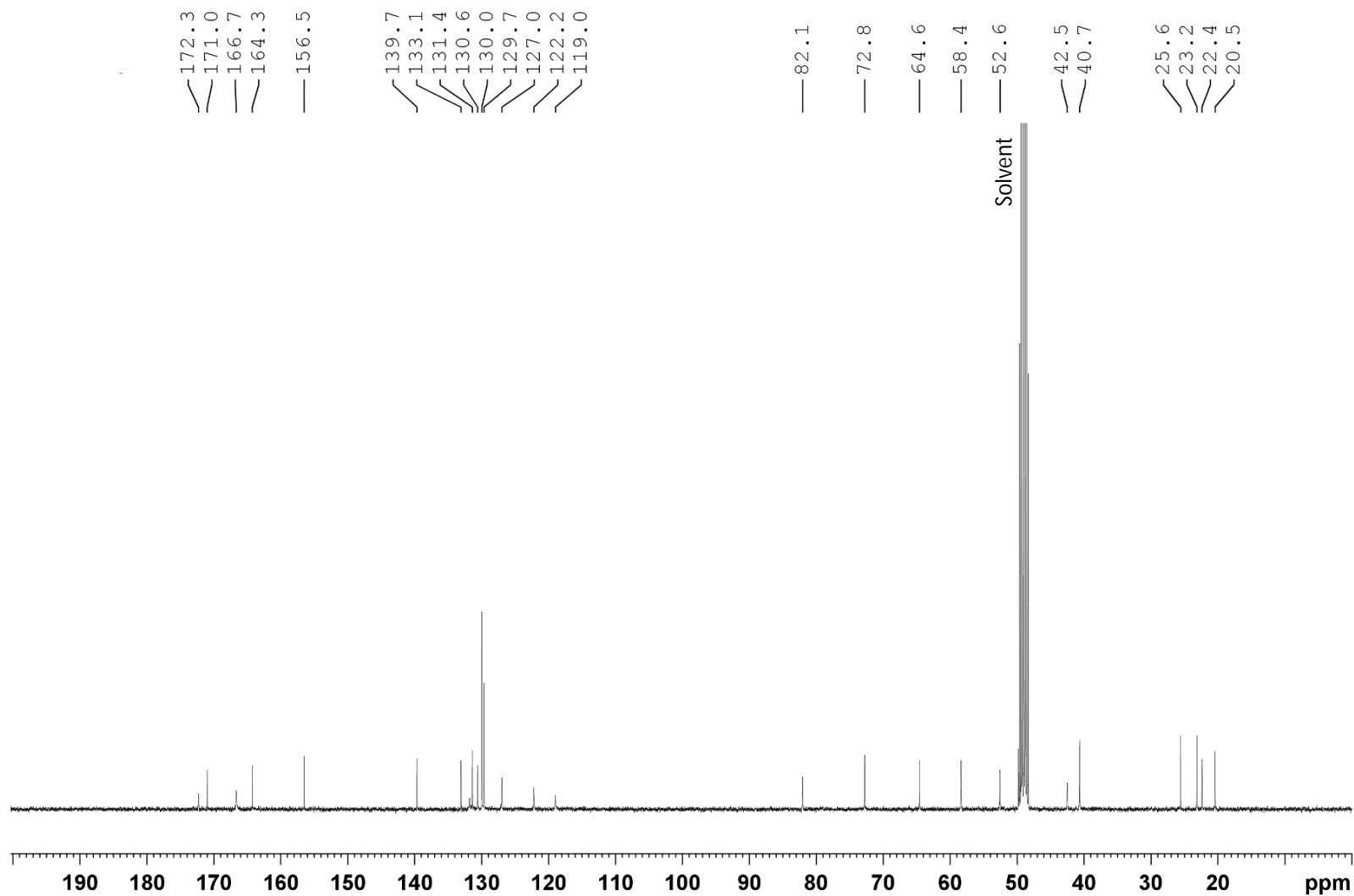


Fig. 6.21 ^1H NMR spectrum (400 MHz, methanol- d_4) of compound **7** (amphibine-D).

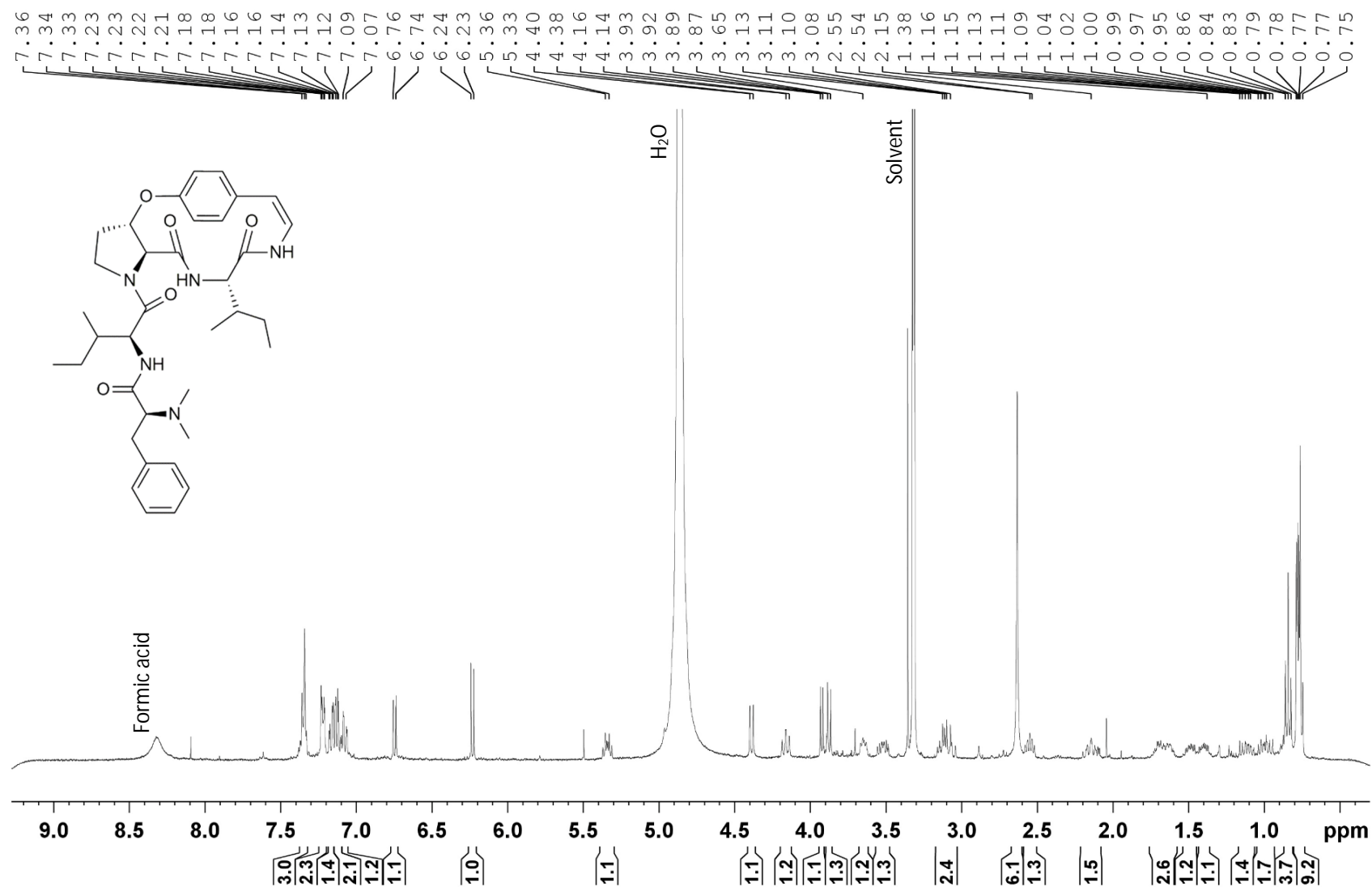


Fig. 6.22 ^{13}C NMR spectrum (100 MHz, methanol- d_4) of compound **7** (amphibine-D).

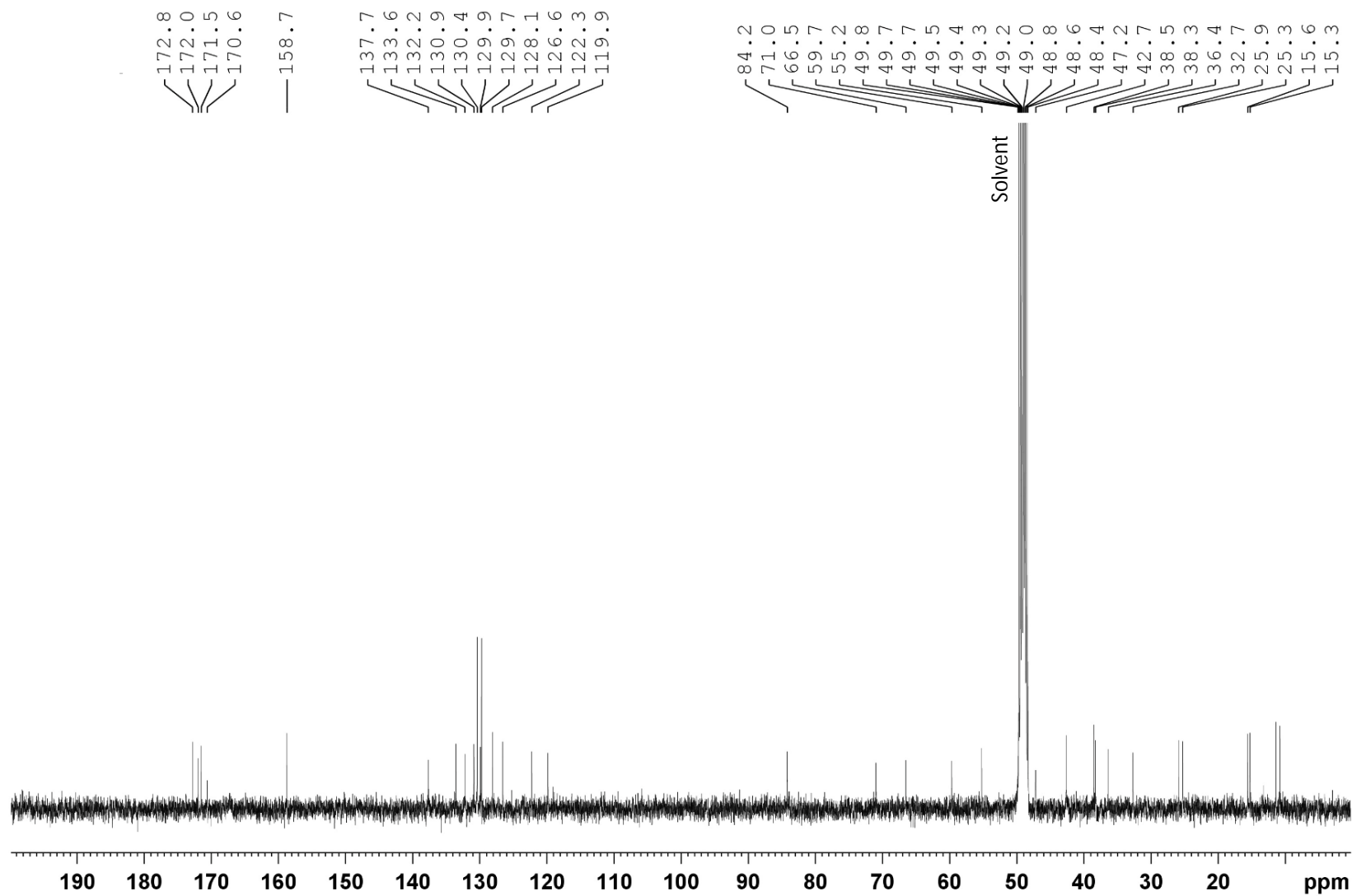


Table 6.1 ¹H NMR spectroscopic data (δ_H in ppm, multiplicity (*J* in Hz)) for compounds **1-7**.

position	1	2	3	4	5	6	7
1	6.77, d (7.5)	6.70, d (7.5)	6.06, d (9.0)	6.05, d (8.9)	6.76, d (7.5)	6.78, d (7.5)	6.75, d (7.5)
2	6.19, d (7.5)	6.11, d (7.5)	6.80, d (9.0)	6.80, d (9.0)	6.25, d (7.5)	6.23, d (7.5)	6.24, d (7.5)
3 (N-H)	n.o.	n.o.	n.o.	n.o.	n.o.	n.o.	n.o.
5	3.91, d (8.0)	4.32, dd (8.3, 5.2)	4.15, d (6.7)	4.20, d (6.6)	4.18, m	4.19, dd (9.2, 5.0)	3.87, d (8.1)
6 (N-H)	n.o.	n.o.	n.o.	n.o.	n.o.	n.o.	n.o.
8	4.20, d (6.6)	4.08, d (6.7)	4.37, d (3.3)	4.34, d (3.0)	4.83 ^a	4.87 ^s	3.95, d (6.5)
9	5.37, m	5.30, m	5.27, m	5.18, m	5.94, d (8.2)	5.95, d (8.0)	5.35, m
12	7.16, dd (8.5, 2.2)	7.16 ^a	6.81 ^a	6.76, dd (8.9, 2.9)	7.20, dd (8.4, 2.5)	7.18, dd (8.2, 2.5)	7.17, dd (8.4, 2.1)
13	7.08 ^a	7.02 ^a	6.86, d (8.9)	6.84, d (8.9)	7.10, d (8.4)	7.09, d (8.2)	7.08, dd (8.4, 2.1)
14	-	-	-	-	-	-	-
15	7.11 ^a	7.03 ^a	-	-	7.05, dd (8.5, 1.8)	7.05, dd (8.4, 1.8)	7.14 ^a
16	7.03, dd (8.2, 2.2)	7.03 ^a	6.71, d (2.7)	6.71, d (2.9)	7.24, dd (8.5, 2.5)	7.23, dd (8.4, 2.5)	7.12 ^a
17A	1.62, m	2.82, m	1.91, m	1.92, m	1.30, m	1.30 ^a	1.62, m
17B	-	-	-	-	1.41, m	1.40 ^a	-
18A	1.07, m	-	1.24, m	1.26, m	1.41, m	1.40 ^a	0.99, m
18B	1.47, m	-	1.47, m	1.52, m	-	-	1.40, m
19	0.79, t (7.5)	7.17 ^a	0.87, t (7.4)	0.92, t (7.4)	0.84, d (6.3)	0.81, d (5.4)	0.77 ^a
20	0.81, d (6.8)	7.23 ^a	0.96, d (6.9)	1.00, d (6.9)	0.80, d (6.3)	0.82, d (5.4)	0.78 ^a
21A	2.22, m	7.18 ^a	2.28, m	2.18, m	-	-	2.14, m
21B	2.58, m	-	2.59, m	2.43, m	-	-	2.56, m
22A	3.58, m	7.23 ^a	3.60, m	3.21, m	7.57, d (7.5)	7.58, d (7.5)	3.52, m
22B	4.06, m	-	4.26, m	3.95, m	-	-	4.17, dd (10.4, 9.0)

position	1	2	3	4	5	6	7
23	-	7.17 ^a	-	-	7.38, t (7.5)	7.40, t (7.5)	-
24A	-	2.21, m	-	-	7.31, t (7.5)	7.33, t (7.5)	-
24B	-	2.58, m	-	-	-	-	-
25A	4.10, m	3.62, m	4.48, d (8.9)	4.87, t (7.4)	7.38, t (7.5)	7.40, t (7.5)	4.39, d (9.0)
25B	-	4.25, t (9.4)	-	-	-	-	-
26A	1.89, m	-	1.74, m	2.84, dd (13.6, 7.1)	7.57, d (7.5)	7.58, d (7.5)	1.7, m
26B	-	-	-	2.99, dd (13.6, 7.1)	-	-	-
27A	1.15, m	-	1.15, m	-	N-H, n.o.	N-H, n.o.	1.10, m
27B	1.54, m	-	1.53, m	-	-	-	1.49, m
28	0.94, t (7.2)	4.47, d (7.5)	0.87, t (7.4)	7.10-7.30 ^b	-	-	0.85, t (7.5)
29	1.02, d (6.8)	2.05, m	0.80, d (6.8)	7.10-7.30 ^b	2.49, d (5.4)	2.47, d (9.0)	0.76 ^a
30	N-H, n.o.	0.93, d (6.6)	N-H, n.o.	7.10-7.30 ^b	1.34 ^a	3.72, m	N-H, n.o.
31A	2.63, s	0.96, d (6.6)	-	7.10-7.30 ^b	0.82 ^a	O-H, n.o.	-
31B	-	-	-	-	1.09, m	-	-
32		N-H, n.o.	3.31 ^s	7.10-7.30 ^b	0.75, t (7.3)	0.91, d (6.2)	3.65, m
33A		-	2.94, dd (13.0, 4.8)	N-H, n.o.	0.64, d (6.9)	1.75, s	3.09, m
33B		-	3.05, dd (13.0, 9.8)	-	-	-	-
34		3.86 ^a	-	-	N-H, n.o.	1.75, s	-
35		1.49, d (5.0)	7.19, d (7.5)	3.25, m	1.72, s		7.23, dd (7.4, 2.3)
36A		N-H, n.o.	7.26, t (7.5)	2.90, dd (13.2, 5.1)			7.35 ^a
36B		-	-	2.98, dd (13.2, 5.1)			-
37		2.65, s	7.12, t (7.5)	-			7.34 ^a
38			7.26, t (7.5)	7.10-7.30 ^b			7.35 ^a

position	1	2	3	4	5	6	7
39			7.19, d (7.5)	7.10-7.30 ^b			7.23, dd (7.4, 2.3)
40			2.40, s	7.10-7.30 ^b			2.63, s
41			2.40, s	7.10-7.30 ^b			2.63, s
42				7.10-7.30 ^b			
43				2.25, s			
44				2.25, s			

n.o. = not observed. ^sOverlapping with solvent or water signal. ^aOverlapping signal. ^bSignals of aromatic protons could not be assigned to a specific position, due to overlapping of signals. All NMR spectra were recorded in methanol-*d*₄.

Table 6.2 ^{13}C NMR spectroscopic data (δ_{C} in ppm) for compounds **1-7**.

Position	1	2	3	4	5	6	7
1	130.4	129.6	110.9	110.3	128.2	128.6	129.8
2	126.3	126.4	121.5	121.2	125.5	125.4	126.6
4	171.6	171.0	170.6	170.2	n.o.	n.o.	171.9
5	59.3	56.1	61.3	61.1	51.4	51.4	59.7
7	172.4	172.1	173.1*	172.4	n.o.	169.6	172.8
8	66.6	66.7	66.2	66.5	56.8	56.7	66.5
9	83.2	83.4	79.0	78.6	80.9	81.2	84.2
11	158.4	158.4	151.8	151.5	n.o.	155.2	158.7
12	118.8	119.6	119.1	118.7	121.2	121.2	119.9
13	131.7	131.9	119.4	118.9	129.3	129.2	132.2
14	133.4	133.0	150.6	150.4	n.o.	131.7	133.6
15	130.6	130.5	123.2	122.9	130.2	130.1	130.9
16	121.7	122.1	112.0	111.8	118.4	118.6	122.3
17	38.5	38.9	36.6	36.7	41.0	41.0	38.5
18	25.2	137.9	26.1	26.1	24.2	24.2	25.3
19	11.0	130.1	11.2 or 10.8*	11.4	21.9	20.9	15.3
20	15.3	129.1	16.1	15.9	20.9	21.9	15.6
21	32.4	127.4	33.7	33.2	n.o.	138.1	32.7
22	47.0	129.1	47.6	47.0	128.1	130.0	47.2
23	-	130.1	-	-	128.0	129.7	-
24	167.8	32.4	171.8	170.9	128.1	129.7	170.7 or 171.5*
25	64.8	46.8	55.2	52.6	128.0	129.7	55.2
26	38.0	-	38.2	38.9	128.1	130.0	38.3
27	25.1	171.8	25.9	137.5	-	-	25.9
28	11.6	57.2	11.2 or 10.8*	127.1-130.1 ^a	n.o.	171.0	10.8
29	14.6	31.3	15.3	127.1-130.1 ^a	68.6	64.6	11.4
30	-	19.2	-	127.1-130.1 ^a	37.6	72.8	-
31	33.1	18.4	172.8*	127.1-130.1 ^a	24.3		170.7 or 171.5*
32		-	71.5	127.1-130.1 ^a	10.6	20.5	71.0
33		170.5	37.0	-	14.3	40.7	36.4
34		58.1	139.0	172.4	-	40.7	137.7
35		16.3	130.2	71.3	33.7		130.4
36		-	129.5	36.3			129.7
37		31.7	127.5	139.3			128.1
38			129.5	127.1-130.1 ^a			129.7
39			130.2	127.1-130.1 ^a			130.4

Position	1	2	3	4	5	6	7
40			42.6	127.1-130.1 ^a			42.6
41			42.6	127.1-130.1 ^a			42.6
42				127.1-130.1 ^a			
43				42.4			
44				42.4			

*Interchangeable. ^aSignals of aromatic carbon atoms could not be assigned to a specific position, due to overlapping of signals. All NMR spectra were recorded in methanol-*d*₄.

Thus, the phytochemical investigation of the stem bark of *Z. nummularia* and *Z. spina-christi* with advanced spectroscopic techniques led to the isolation of seven cyclopeptide alkaloids. Three compounds were reported for the first time, i.e. nummularine-U (**1**) in *Z. nummularia*, and spinanine-B (**3**) and spinanine-C (**4**) in *Z. spina-christi*. In addition, nummularine-D (**5**), nummularine-E (**6**) and amphibine-D (**7**) were reported for the first time in *Z. spina-christi*.

6.3 Experimental

6.3.1 General experimental procedures

See chapter 2, general experimental procedures, sections 2.1, chromatographic methods, and 2.2, spectroscopic methods.

6.3.2 Plant materials

Stem bark of *Ziziphus nummularia* (Burm.f.) Wight & Arn. (Rhamnaceae) and *Ziziphus spina-christi* (L.) Desf. (Rhamnaceae) was collected in July and August 2012 in Abdul Khail and in Giloti, Pakistan, respectively. The identification was done by Dr. Mushtaq Ahmad and voucher specimens (ABD/NZ & Khar khar / Khani and X3/X1 respectively) were deposited at the Herbarium of Pakistan, Quaid-i-Azam University, Islamabad, Pakistan.

6.3.3 Extraction and isolation

The plant material of both plants was dried and milled before extraction. 1.5 kg of stem bark of *Z. nummularia* (ZN) was percolated with 64 L of 80% methanol. After evaporation of the solvent under reduced pressure and freeze-drying, 162 g of crude extract was obtained. The crude extract was dissolved in 50% methanol/50% water and acidified to pH < 3 with 2 M HCl. Then, liquid-liquid partition was carried out with dichloromethane. Next, the pH of the acidified phase was increased to > 9 by adding NH₄OH (25%), followed by a second liquid-liquid partition with dichloromethane. In this way, three fractions were obtained: CH₂Cl₂ (I), CH₂Cl₂ (II) and CH₃OH/H₂O (pH > 9) (III). TLC analysis of these three fractions was performed with a mobile phase of CH₃OH/CHCl₃/formic acid (10:90:2). TLC indicated that alkaloids were present in the CH₂Cl₂ (II) phase (0.71 g), and further fractionation of 0.56 g of this fraction was performed by means of flash chromatography. A GraceResolv 40 g silica column was used with a mobile phase consisting of dichloromethane (A) and methanol (B) at a flow rate of 30 mL/min. During the run, the ratio of A:B changed stepwise from 100:0 to 0:75 in a time span of 104 min. ELSD and UV detection at 254 nm and 366 nm were used. Throughout the whole experiment the eluent was collected in test tubes, based on the ELSD and UV absorption intensity. Taking into account the obtained chromatograms and the results of a TLC analysis of the collected eluates, which was performed as described above, test tubes showing a

similar pattern were combined. This resulted in 15 fractions. On these fractions, a TLC analysis was performed, using the spraying reagents described in chapter 2, general experimental procedures, section 2.1.2, thin layer chromatography. In addition, an HPLC screening to assess the complexity of each fraction was carried out. Taking into account the results of both the TLC analysis and HPLC screening and also the amount of each fraction, fractions ZN7 (57.9 mg) and ZN8 (46.5 mg) were selected for further analysis. The isolation of single compounds was then performed by semi-preparative HPLC using a C₁₈ Luna column (250 mm × 10.0 mm, particle size 5 µm) from Phenomenex (Utrecht, the Netherlands) and a C₁₈ guard column (10 mm × 10 mm, particle size 5 µm) from Grace (Hesperia, CA, USA). As mobile phase, H₂O + 0.1% formic acid (A) and acetonitrile + 0.1% formic acid (B) were used at a flow rate of 3.0 mL/min. For fraction ZN7 the following gradient was applied: 0 to 5 min 85:15, 25 min 65:35, 30 to 35 min 0:100. An amount of 300 µL of the sample solution (3.5 mg/mL dissolved in DMSO / methanol (1:3)) was injected repetitively. For fraction ZN8 the gradient was: 0 to 5 min 85:15, 30 min 70:30, 35 to 40 min 85:15. The sample was dissolved in methanol in a concentration of 15 mg/mL, and the injection volume was 100 µL. The DAD spectrum was recorded from 200 nm to 400 nm and mass spectra were taken in ESI+ mode, with MS scan range: m/z 250 to 800. $V_{\text{capillary}}$ 3.00 kV, V_{cone} 50 V, $V_{\text{extractor}}$ 3 V, $V_{\text{RF-Lens}}$ 0.2 V, T_{source} 135 °C, $T_{\text{desolvation}}$ 400 °C, desolvation gas flow 750 L/h, cone gas flow 50 L/h. Interesting peaks were selected based on the UV spectrum and the m/z -value of each peak. The collection of the eluate was triggered as long as the intensity of selected m/z values exceeded the set threshold. For fraction ZN7 collection was triggered based on the intensity of the signal of the ion with m/z 471. For fraction ZN8 the collection triggers were m/z 471 and m/z 562.

With regard to *Z. spina-christi* (ZSP), 2.1 kg of stem bark was treated in a similar way as the stem bark of *Z. nummularia*, using 78.6 L of 80% methanol to prepare the crude extract (238 g). 225 g of this crude extract was then submitted to an acid-base liquid-liquid partition, as described above. TLC analysis of the three obtained fractions with CH₃OH/CHCl₃/NH₄OH (5:95:1) indicated that also in this case the CH₂Cl₂ (II) fraction (1.86 g) contained the highest amount of alkaloids and 1.5 g of this fraction was further separated into 9 subfractions by flash chromatography. A GraceResolv 80 g silica column was used with dichloromethane (A), ethyl acetate (B) and methanol (C) as the solvents and a flow rate of 30 mL/min. During the run, the ratio of A:B changed stepwise from 100:0 to 0:100 in a time span of 25 min, followed by a change from B:C from 0:100 to 50:50 in 40 min. The settings of the detector and handling of the samples were the same as for *Z. nummularia*. TLC analysis with the aforementioned spraying reagents, together with an HPLC screening to assess the complexity of each fraction and the amount of each fraction available, led to the selection of fractions ZSC6 (15.3 mg), ZSC7 (97.7 mg) and ZSC8 (105.1 mg) for further analysis.

Fraction ZSC6 was analyzed by HPLC-PDA-HRMS-SPE-NMR. Ten microliter of the sample, with a concentration of 15 mg/mL, was injected repetitively in the HPLC system. Separation was accomplished using a Phenomenex C₁₈(2) Luna column (150 mm × 4.6 mm, 3 μm particle size, 100 Å pore size), which was kept at 40 °C. The mobile phase consisted of 95% water/5% acetonitrile/0.1% formic acid (A) and 5% water/95% acetonitrile/0.1% formic acid (B) with the following gradient: 0 min 100:0 (A:B), 17 min 50:50, 20-25 min 0:100. The flow rate was 0.5 mL/min and the flow set for the K-120 pump was 1 mL/min. DAD spectra were recorded between 190 and 950 nm. ESI mass spectra were acquired in the positive ion mode in the range of *m/z* 50 to 1000, using a drying temperature of 200 °C, capillary voltage of 4100 V, nebulizer pressure of 2.0 bar and a dry gas flow of 7 L/min. The eluate was trapped as long as the UV absorption at 228 nm was higher than 600 mAu. Subsequently, the cartridge was eluted into 1.7 mm NMR tubes (Bruker Biospin, Rheinstetten, Germany) with methanol-*d*₄ (final volume in tube 35 μL).

Fraction ZSC7 was further separated by HPLC-DAD-SPE-NMR. The injection volume was 20 μL and the sample concentration 8.4 mg/mL. An XBridge column (C₁₈, 4.6 × 250 mm, 5μm, Waters (Milford, MA, USA)) was used with water + 0.1% ammonia (A) and acetonitrile (B) as the

mobile phase. The flow rate was 0.8 mL/min (2.4 mL/min for the K-120 pump) and the gradient was: 0 to 5 min 70:30 (A:B), 35 min 50:50, 40 to 45 min 0:100. DAD spectra were recorded between 190 and 450 nm. The threshold for trapping was set at 375 mAu for the UV signal at 210 nm. Trapped compounds were eluted with methanol-*d*₄ in 3 mm NMR tubes.

Semi-preparative HPLC-DAD-MS was used for isolation of two compounds from fraction ZSC8. A Luna C₁₈ column (250 mm × 10.0 mm, particle size 5 µm) from Phenomenex (Utrecht, the Netherlands) and a C₁₈ guard column (10 mm × 10 mm, particle size 5 µm) from Grace (Hesperia, CA, USA) were used. The mobile phase consisted of water + 0.1% formic acid (A) and acetonitrile (B) and the gradient was: 0 to 5 min 75:25 (A:B), 20 min 40:60, 25 to 30 min 0:100. The injection volume was 300 µL and the sample concentration 7.5 mg/mL. The flow rate was 3.0 mL/min. DAD spectra were recorded between 200 and 400 nm and mass spectra were recorded in ESI+ mode from *m/z* 250 to 800. Fraction collection was triggered when taking into account the signal intensity of the ions with *m/z* 523.3 or *m/z* 632.4.

1D (¹H, ¹³C) and 2D (COSY, HSQC, HMBC) NMR spectra were recorded for all compounds, and for compounds which were not described previously, accurate mass measurements were performed. Nummularine-U (**1**) was isolated by semi-preparative HPLC-DAD-MS from ZN7 and ZN8 and mauritine-F (**2**) only from fraction ZN8. Spinanine-B (**3**) and spinanine-C (**4**) were identified in fraction ZSC7 after HPLC-SPE-NMR. From fraction ZSC6 nummularine-D (**6**) was purified by HPLC-SPE-NMR, whereas nummularine-E (**7**) was obtained by semi-preparative HPLC-DAD-MS from fraction ZSC8, together with amphibine-D (**5**).

Nummularine-U (1): white powder (1 mg); UV λ_{\max} 207 nm; ^1H and ^{13}C NMR spectroscopic data: see Tables 6.1 and 6.2, respectively; HRESIMS m/z 471.2997 $[\text{M}+\text{H}]^+$, (calcd for $\text{C}_{26}\text{H}_{39}\text{N}_4\text{O}_4$, 471.2966).

Mauritine-F (2): white powder (6 mg); UV λ_{\max} 204 nm; $[\alpha]_{\text{D}} -173.3$ (c 0.6, CH_3OH); ^1H and ^{13}C NMR spectroscopic data: see Tables 6.1 and 6.2, respectively; ESIMS m/z 562.3 $[\text{M}+\text{H}]^+$.

Spinanine-B (3): white powder (4 mg); λ_{\max} 206, 267, 321 nm; $[\alpha]_{\text{D}} -218.3$ (c 0.4, CH_3OH); ^1H and ^{13}C NMR spectroscopic data: see Tables 6.1 and 6.2, respectively; HRESIMS m/z 648.3780 $[\text{M}+\text{H}]^+$, (calcd for $\text{C}_{36}\text{H}_{50}\text{N}_5\text{O}_6$, 648.3756).

Spinanine-C (4): (< 1 mg); UV λ_{\max} 202, 268, 322 nm; ^1H and ^{13}C NMR spectroscopic data: see Tables 6.1 and 6.2, respectively; HRESIMS m/z 682.3555 $[\text{M}+\text{H}]^+$, (calcd for $\text{C}_{39}\text{H}_{48}\text{N}_5\text{O}_6$, 682.3599).

Nummularine-D (5): (< 1 mg); UV λ_{\max} 225 nm; ^1H and ^{13}C NMR spectroscopic data: see Tables 6.1 and 6.2, respectively; ESIMS m/z 521.3 $[\text{M}+\text{H}]^+$.

Nummularine-E (6): white powder (27 mg); UV λ_{\max} 214 nm; $[\alpha]_{\text{D}} -184.0$ (c 0.5, $\text{CH}_3\text{OH}/\text{H}_2\text{O}/\text{formic acid}$ (50:50:0.1)); ^1H and ^{13}C NMR spectroscopic data: see Tables 6.1 and 6.2, respectively; ESIMS m/z 523.3 $[\text{M}+\text{H}]^+$.

Amphibine-D (7): white powder (2 mg); UV λ_{\max} 202 nm; $[\alpha]_{\text{D}} -136.7$ (c 0.2, CH_3OH); ^1H and ^{13}C NMR spectroscopic data: see Tables 6.1 and 6.2, respectively; ESIMS m/z 632.4 $[\text{M}+\text{H}]^+$.

References

- Abdel-galil, F. M. and El-Jissry, M. A., 1991. Cyclopeptide alkaloids from *Zizyphus spina-christi*. *Phytochemistry* 30(4), 1348-1349.
- Cristau, P., Temal-Laib, T., Bois-Choussy, M., Martin, M. T., Vors, J. P. and Zhu, J. P., 2005. Total synthesis of Mauritines A, B, C, and F: Cyclopeptide alkaloids with a 1-4-membered paracyclophane unit. *Chem. Eur. J.* 11(9), 2668-2679.
- Dwivedi, S. P. D., Pandey, V. B., Shah, A. H. and Eckhardt, G., 1987. Cyclopeptide Alkaloids from *Zizyphus nummularia*. *J. Nat. Prod.* 50(2), 235-237.
- El-Seedi, H., Zahra, M. H., Goransson, U. and Verpoorte, R., 2007. Cyclopeptide alkaloids. *Phytochem. Rev.* 6, 143-165.
- Farmani, F., Moein, M., Amanzadeh, A., Kandelous, H. M., Ehsanour, Z. and Salimi, M., 2016. Antiproliferative evaluation and apoptosis induction in MCF-7 cells by *Zizyphus spina christi* leaf extracts. *Asian Pac. J. Cancer P.* 17(1), 315-321.
- Gournelis, D. C., Laskaris, G. G. and Verpoorte, R., 1997. Cyclopeptide alkaloids. *Nat. Prod. Rep.* 14(1), 75-82.
- Goyal, M., Ghosh, M., Nagori, B. P. and Sasmal, D., 2013. Analgesic and anti-inflammatory studies of cyclopeptide alkaloid fraction of leaves of *Zizyphus nummularia*. *Saudi J. Biol. Sci.* 20(4), 365-371.
- Inayat-Ur-Rahman, Khan, M. A., Khan, G. A., Khan, L. and Ahmad, V. U., 2001. Cyclopeptide alkaloids of *Zizyphus* species. *J. Chem. Soc. Pakistan* 23(4), 268-277.
- Lin, H. Y., Chen, C. H., Liu, K. and Lee, S. S., 2003. 14-membered cyclopeptides from *Paliurus ramosissimus* and *P. hemsleyanus*. *Helv. Chim. Acta* 86(1), 127-138.
- Lin, H. Y., Chen, C. H., You, B. J., Liu, K. C. and Lee, S. S., 2000. Cyclopeptide alkaloids from *Paliurus ramossisimus*. *J. Nat. Prod.* 63(10), 1338-1343.
- Rauf, A., Ali, J., Khan, H., Mubarak, M. S. and Patel, S., 2016. Emerging CAM *Zizyphus nummularia* with in vivo sedative-hypnotic, antipyretic and analgesic attributes. *3 Biotech* 6.
- Ray, S. D. and Dewanjee, S., 2015. Isolation of a new triterpene derivative and *in vitro* and *in vivo* anticancer activity of ethanolic extract from root bark of *Zizyphus nummularia* *Aubrev. Nat. Prod. Res.* 29(16), 1529-1536.

- Shah, A. H., Ageel, A. M., Tariq, M., Mossa, J. S. and Al-Yahya, M. A., 1986. Chemical constituents of the stem bark of *Zizyphus spina-christi*. *Fitoterapia* 58(6), 452-454.
- Shahat, A. A., Pieters, L., Apers, S., Nazeif, N. M., Abdel-Azim, N. S., Vanden Berghe, D. and Vlietinck, A. J., 2001. Chemical and biological investigations on *Zizyphus spina-christi* L. *Phytother. Res.* 15(7), 593-597.
- Singh, B. and Pandey, V. B., 1995. An N-formyl cyclopeptide alkaloid from *Zizyphus nummularia* bark. *Phytochemistry* 38(1), 271-273.
- Tschesche, R., Elgamal, M., Miana, G. A. and Eckhardt, G., 1975. Alkaloids from rhamnaceae—XXVI. Nummularine-D, -E and -F, new cyclopeptide alkaloids from *Zizyphus nummularia*. *Tetrahedron* 31(23), 2944-2947.
- Tschesche, R., Fehlhaber, H. W. and Kaussmann, E. U., 1972. Alkaloids from Rhamnaceae. 13. Amphibine-B, amphibine-C, amphibine-D, amphibine-E, 4 peptide alkaloids from *Zizyphus amphibia* A. Cheval. *Chem. Ber.-Recl.* 105(9), 3094-3105.
- Tschesche, R., Khokhar, I., Spilles, C. and von Radloff, M., 1974. Peptide alkaloids from *Zizyphus spinachristi*. *Phytochemistry* 13(8), 1633.
- Tschesche, R., Khokhar, I., Wilhelm, H. and Eckhardt, G., 1976. Alkaloids from Rhamnaceae. 27. Jubanine-A and jubanine-B, new cyclopeptide alkaloids from *Zizyphus jujuba*. *Phytochemistry* 15(4), 541-542.
- Tuenter, E., Exarchou, V., Balde, A., Cos, P., Maes, L., Apers, S. and Pieters, L., 2016. Cyclopeptide Alkaloids from *Hymenocardia acida*. *J. Nat. Prod.* 79(7), 1746-1751.
- Wubshet, S. G., Moresco, H. H., Tahtah, Y., Brighente, I. M. G. and Staerk, D., 2015. High-resolution bioactivity profiling combined with HPLC-HRMS-SPE-NMR: alpha-glucosidase inhibitors and acetylated ellagic acid rhamnosides from *Myrcia palustris* DC. (Myrtaceae). *Phytochemistry* 116, 246-252.

CHAPTER 7

Gastrointestinal absorption and metabolic conversion of hymenocardine

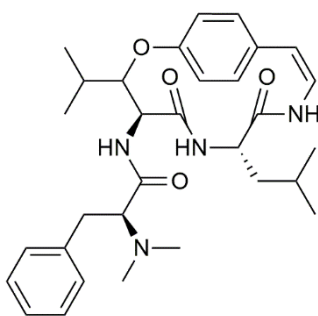
Adapted from:

Emmy Tuentler, Sebastiaan Bijttebier, Kenn Foubert, Annelies Breynaert, Sandra Apers, Nina Hermans, Luc Pieters

In vitro and *in vivo* study of the gastrointestinal absorption and metabolisation of hymenocardine, a cyclopeptide alkaloid

Planta Medica, **2017**, doi: 10.1055/s-0043-102494.

Hymenocardia acida Tul. (Phyllanthaceae) is a shrub or small tree that is indigenous to the African Savannah. In traditional African medicine, its leaves and roots are used to treat malaria and moderate *in vitro* antiplasmodial activity has previously been reported for extracts of the leaves of *H. acida*, as well as for hymenocardine, a cyclopeptide alkaloid isolated from the root bark of *H. acida* (Vontron-Senecheau *et al.*, 2003; Tuentner *et al.*, 2016a). Cyclopeptide alkaloids are polyamidic macrocyclic compounds, containing a 13-, 14- or 15-membered ring (Gournelis *et al.*, 1997; El-Seedi *et al.*, 2007). Apart from hymenocardine, *in vitro* antiplasmodial activity has been shown for several other cyclopeptide alkaloids, namely, ziziphines-N and -Q, mauritine-M, hemsine-A, hymenocardinol, hymenocardine N-oxide, nummularines-H and -R, O-desmethylnummularine-R and oxyphylline-F (Suksamrarn *et al.*, 2005; Panseeta *et al.*, 2011; Tuentner and co-workers, 2016a; 2016b). However, no *in vivo* studies concerning the antiplasmodial activity of this type of compounds have been performed yet, and in view of their peptide-like nature, the question can be raised whether cyclopeptide alkaloids are stable in the gastrointestinal tract, and whether they will be absorbed after oral administration; these are essential prerequisites to exhibit *in vivo* antiplasmodial activity.



Up till now only a few reports exist, which describe the pharmacological (sedative and anxiolytic) effects of cyclopeptide alkaloids *in vivo*, after oral administration (Han and co-workers, 1989; 2008; Ma *et al.*, 2008). As for the absorption and metabolic stability of this class of compounds, Suh and co-workers (1996, 1997), reported that franguloline (Figure 7.1)

is converted by enamide degradation, both *in vitro*, after incubation under acidic conditions, and *in vivo*, after IV (intravenous) injection to rats, leading to the formation of a substituted linear tripeptide. No other cyclopeptide alkaloids were investigated for their stability and/or gastrointestinal absorption. Since hymenocardine does not contain an enamide bond, a similar conversion as observed for franguloline is not possible. Therefore, the absorption and metabolic conversion of hymenocardine was investigated, *in vitro* as well as *in vivo* (Figure 7.2).

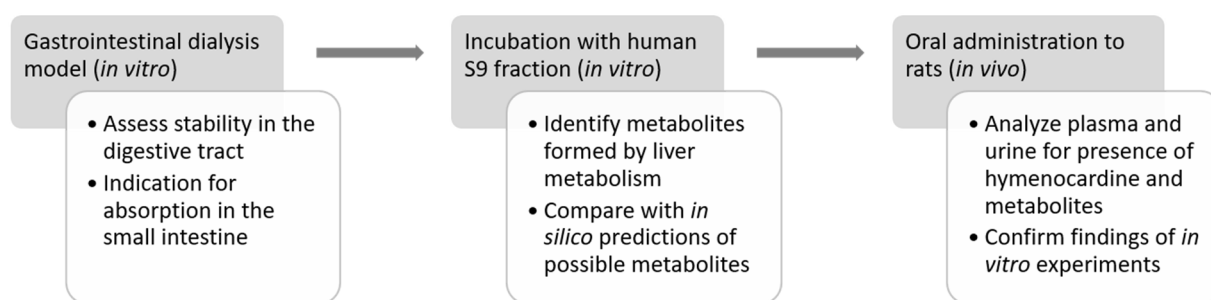


Fig. 7.2 Experimental overview.

In the first part of this study, hymenocardine was submitted to a gastrointestinal dialysis model (GIDM), to determine whether it can withstand the conditions of the digestive system and in order to assess possible absorption from the gastrointestinal tract. In addition, the liver metabolism of hymenocardine was investigated by incubation with a human S9 fraction, a liver homogenate containing both microsomes and cytosolic enzymes. In order to deduce which metabolites were formed, LC-HRMS profiles were recorded, data were treated by differential analysis to localize the metabolites and compared with a list of metabolites that was predicted *in silico*. The MS fragmentation pathway of hymenocardine was studied, which provided useful information for the interpretation of the product ions of the metabolites. Moreover, an *in vivo* study was performed, where hymenocardine was administered to rats *per os* and plasma and urine samples were analyzed for the presence of hymenocardine and its metabolites.

7.2 Results and Discussion

In the first part of our study, hymenocardine was submitted to an *in vitro* continuous flow GIDM. The compound was first incubated in a gastric phase, simulating the adult gastric environment, followed by a small intestinal phase. The continuous flow system that was applied in the small intestinal phase of the model, eliminates compounds diffusing through a semi-permeable membrane, thus simulating absorption by passive diffusion (Figure 7.3). This resulted in two fractions: a retentate (fraction remaining in the gastrointestinal tract) and a dialyzate (fraction absorbed in the small intestinal phase).

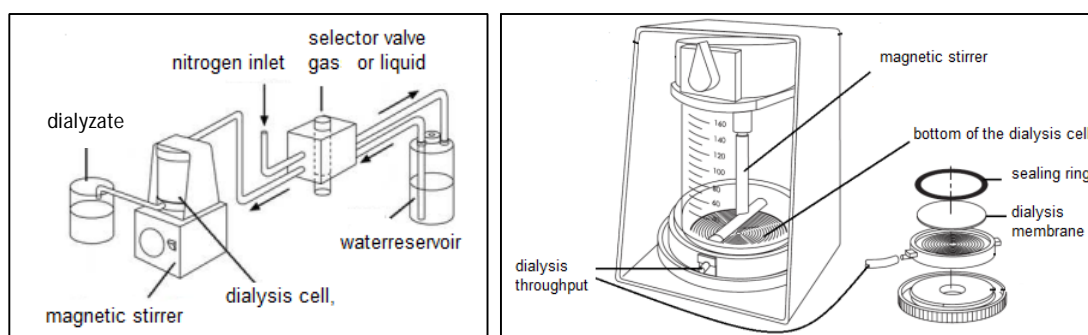


Fig. 7.3 Schematic representation of the experimental set-up for dialysis during the small intestinal phase (left), and magnification of a dialysis cell (right) of the GIDM.

Analysis of hymenocardine itself, and the retentate and dialyzate by UPLC-HRMS in positive ion mode, revealed the presence of hymenocardine in both fractions obtained with the dialysis model ($C_{37}H_{51}N_6O_6$, m/z 675.3992, $[M+H]^+$) (Figure 7.4). This indicated that hymenocardine was at least in part absorbed from the small intestine. In addition, no signals due to metabolites could be detected, neither in the dialyzate, nor in the retentate. This suggests that hymenocardine, in spite of its peptide-like character, is stable in gastric and small intestinal conditions and is not degraded.

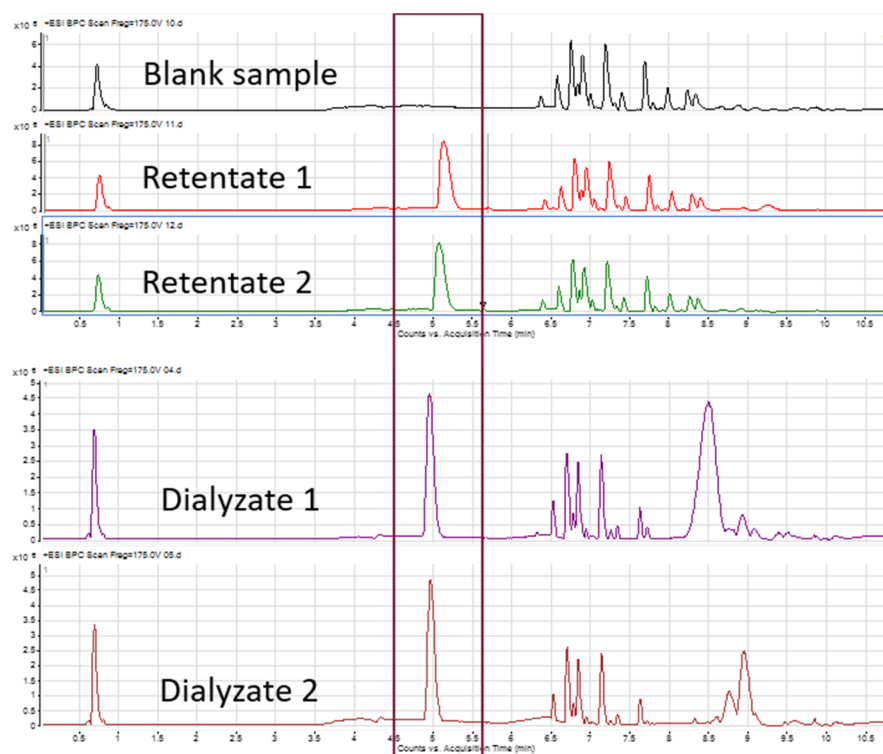


Fig. 7.4 LC-MS profiles of samples obtained with the GIDM. Both in the retentate and the dialyzate, hymenocardine could be detected (retention time \approx 5 min.), and this was confirmed by comparison with LC-HRMS data of hymenocardine itself. The retentate fraction that was obtained with the GIDM, without administration of hymenocardine, served as blank sample.

In vitro liver metabolism of hymenocardine was investigated by incubation with human S9 fraction and analysis of the samples by UPLC-HRMS in both positive and negative ESI mode. Moreover, hymenocardine was subjected to UPLC-HRMS fragmentation to determine the fragmentation pattern of this compound and to obtain insight in the expected fragmentation pattern of its metabolites. Two software programs for drug metabolism prediction, namely, Meteor Nexus and Metaprint2D-React Web Server, were used to generate phase-I metabolites from hymenocardine *in silico*. The list of *in silico* metabolites was matched with the list of metabolites retrieved from the S9 metabolism experiment and this resulted in 14 possible metabolites. The spectral and chromatographic data of the metabolites are listed in Table 7.1. For six of the metabolites, a tentative structure could be defined (Figure 7.5).

Table 7.1 Spectral and chromatographic data of hymenocardine and the metabolites formed during *in vitro* metabolism with human S9 fraction.

	compound	molecular formula	ESI pos full MS	ESI pos ddMS ²	ESI neg full MS	ESI neg ddMS ²	retention time (min)	peak intensity of [M+H] ⁺	biotransformation reaction	predicted by <i>in silico</i> tools ^a
1	Hymenocardine ^b	C ₃₇ H ₅₀ O ₆ N ₆	675.38605 [M+H] ⁺ ; 697.36774 [M+Na] ⁺	338.24; 241.19; 170.06; 114.13; 185.07; 159.09	673.37256 [M-H] ⁻ ; 719.37927 [M-H+FA] ⁻	336.14; 433.19; 544.32; 233.06; 207.08; 150.05; 93.03	13.47	1.70x10 ⁸	-	Not applicable
2	Hymenocardinol ^b	C ₃₇ H ₅₂ O ₆ N ₆	677.40166 [M+H] ⁺ ; 699.38310 [M+Na] ⁺ ; 339.20446 [M+2H] ⁺⁺	659.39; 437.22; 338.24; 185.07; 159.09; 114.13	675.38815 [M-H] ⁻ ; 721.39377 [M-H+FA] ⁻	657.38; 528.32; 444.18; 191.08; 134.06	12.67	6.60x10 ⁷	Reduction (ADH)	Meteor Nexus
3	<i>N</i> -monomethyl hymenocardine	C ₃₆ H ₄₈ O ₆ N ₆	661.37029 [M+H] ⁺ ; 683.35186 [M+Na] ⁺	643.36; 435.20; 227.18; 199.18; 185.07; 170.06; 159.09; 100.11	659.35680 [M-H] ⁻ ; 705.36243 [M-H+FA] ⁻	530.30; 433.19; 336.14; 233.06; 207.08; 150.05; 93.03	13.37	2.60x10 ⁷	Oxidative <i>N</i> -demethylation	Meteor Nexus, Metaprint2D-React Web Server
4	<i>N</i> -monomethyl hymenocardinol	C ₃₆ H ₅₀ O ₆ N ₆	663.38615 [M+H] ⁺ ; 685.36754 [M+Na] ⁺ ; 332.19654 [M+2H] ⁺⁺	645.38; 518.28; 437.22; 419.21; 227.18; 199.18; 185.1; 159.1; 130.1; 100.1	661.37289 [M-H] ⁻ ; 707.37839 [M-H+FA] ⁻	643.36; 514.30; 444.18; 217.06; 191.08; 134.06; 93.03	12.56	1.80x10 ⁷	Reduction (ADH) + oxidative <i>N</i> -demethylation	Meteor Nexus

	compound	molecular formula	ESI pos full MS	ESI pos ddMS ²	ESI neg full MS	ESI neg ddMS ²	retention time (min)	peak intensity of [M+H] ⁺	biotransformation reaction	predicted by <i>in silico</i> tools ^a
5	<i>N</i> -demethyl hymenocardine	C ₃₅ H ₄₆ O ₆ N ₆	647.35469 [M+H] ⁺ ; 669.33555 [M+Na] ⁺		645.34118 [M-H] ⁻	336.13; 150.05	13.14	4.10x10 ⁵	Oxidative <i>N</i> -demethylation	Meteor Nexus, Metaprint2D-React Web Server
6	Hymenocardine - terminal Ile-like moiety	C ₂₉ H ₃₅ O ₅ N ₅	534.27120 [M+H] ⁺ ; 556.25228 [M+Na] ⁺	516.26; 463.20; 321.12; 189.07; 170.06; 159.09; 132.12	532.25694 [M-H] ⁻ ; 578.26252 [M-H+FA] ⁻	403.20; 336.14; 207.08; 150.05	11.50	7.10x10 ⁵	Hydrolysis of amide	Meteor Nexus, Metaprint2D-React Web Server
7	Hymenocardinol - terminal Ile-like moiety	C ₂₉ H ₃₇ O ₅ N ₅	536.28640 [M+H] ⁺ ; 558.26794 [M+Na] ⁺	518.28; 447.20; 159.09; 130.07	534.27269 [M-H] ⁻	-	10.25	2.20x10 ⁵	Reduction (ADH) + hydrolysis of amide	Meteor Nexus
8	Dehydrogenation of hymenocardine	C ₃₇ H ₄₈ O ₆ N ₆	673.37002 [M+H] ⁺	241.19; 159.09; 114.13	671.35765 [M-H] ⁻ ; 717.36318 [M-H+FA] ⁻	-	13.14	1.80x10 ⁵	Dehydrogenation	-
9	Hymenocardine +H ₂ O ₂	C ₃₇ H ₅₂ O ₈ N ₆	709.39124 [M+H] ⁺	114.13; 241.19; 338.24; 469.21; 691.38	707.37840 [M-H] ⁻	-	11.47	1.40x10 ⁵	Reduction (ADH) + ring opening or hydroxylation	Meteor Nexus
10	Hymenocardine +H ₂ O (ring opened) or hymenocardinol +O	C ₃₇ H ₅₂ O ₇ N ₆	693.39640 [M+H] ⁺	114.13; 241.19; 338.24; 675.39	691.38324 [M-H] ⁻	-	11.03	8.80x10 ⁴	Multiple possibilities	Meteor Nexus,

	compound	molecular formula	ESI pos full MS	ESI pos ddMS ²	ESI neg full MS	ESI neg ddMS ²	retention time (min)	peak intensity of [M+H] ⁺	biotransformation reaction	predicted by <i>in silico</i> tools ^a
11, 12	<i>N</i> -monomethyl hymenocardinol +O or <i>N</i> -monomethyl hymenocardine +H ₂ O (ring opened)	C ₃₆ H ₅₀ O ₇ N ₆	679.38089 [M+H] ⁺	-	677.36731 [M-H] ⁻	-	10.80 and 12.09	1.50x10 ⁵	Multiple possibilities	Meteor Nexus
13, 14	Hymenocardine +O or hymenocardinol -2H+O	C ₃₇ H ₅₀ O ₇ N ₆	691.38054 [M+H] ⁺ ; 346.19411 [M+2H] ⁺⁺	-	689.36768 [M-H] ⁻	-	11.30 and 11.48	7.80x10 ⁴	Multiple possibilities	Meteor Nexus, Metaprint2D-React Web Server
15	Hymenocardine -C+2H+O or hymenocardinol -C+O	C ₃₆ H ₅₂ O ₇ N ₆	681.39566 [M+H] ⁺ ; 703.37631 [M+Na] ⁺ ; 341.20198 [M+2H] ⁺⁺	-	679.38313 [M-H] ⁻	-	11.83	1.10x10 ⁵	Multiple possibilities	-

^aMetabolites are only considered to be predicted by Meteor Nexus, in case the likelihood of their formation was classified as 'plausible' or 'probable'.

^bIdentification based on standard solution. ESI = electrospray ionization; pos: positive mode; neg: negative mode; ddMS²: data-dependent MS fragmentation; FA = Formic acid; ADH = alcohol dehydrogenase.

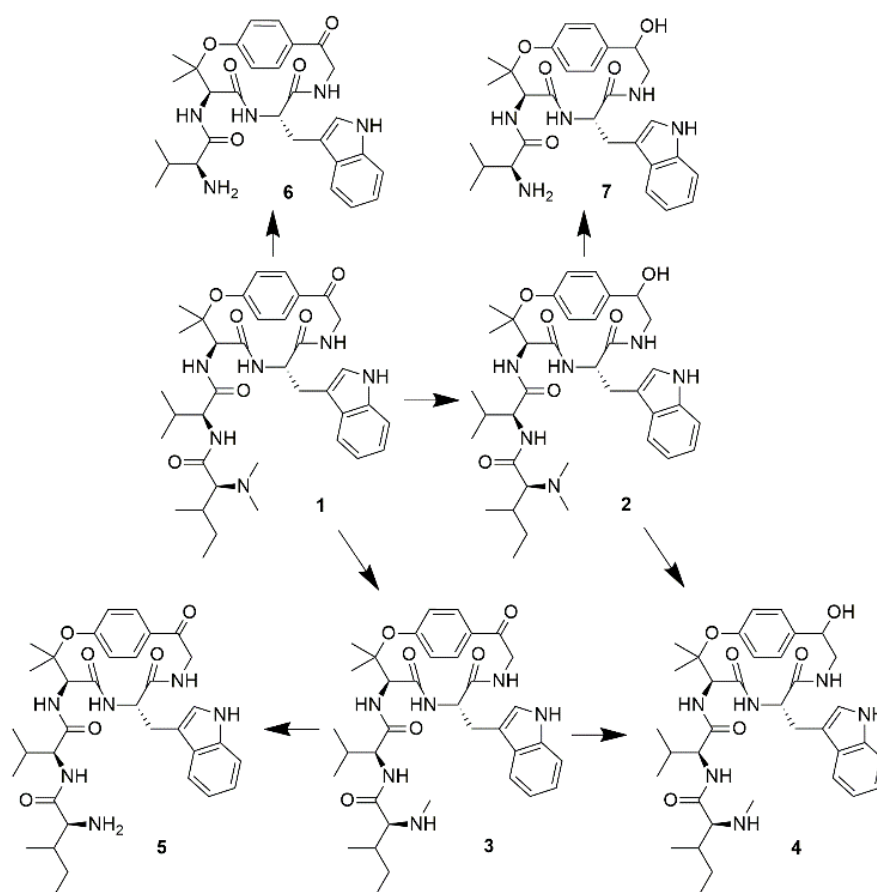


Fig. 7.5 Structures of six putative metabolites (**2-7**) of hymenocardine (**1**), detected with LC-HRMS, following S9 metabolism.

In positive ion mode, hymenocardine (**1**) follows the general peptide fragmentation rules, as described by Maleknia *et al.* (2011) (Figure 7.6). For example, the product ion at m/z 114.13, by far the most abundant product ion, corresponding to a most probable molecular formula $C_7H_{16}N$, originates from the breakage of the C-CO bond at the terminal isoleucine-like moiety, resulting in the formation of an *a* ion.

The product ion at m/z 241.19 ($C_{13}H_{25}O_2N_2$) results from a cleavage of the second amide bond of the side chain of hymenocardine. The product ion at m/z 338.24 ($C_{18}H_{32}O_3N_3$) seems to arise from a fission of the amide bond in the macrocyclic ring that is closest to the side chain, and an additional fission at the ether bond. The product ions at m/z 185.07 ($C_{11}H_9ON_2$), m/z 170.06 ($C_{11}H_8ON$) and m/z 159.09 ($C_{10}H_{11}N_2$) originate from a combination of cleavages of amide, C-CO, or C-NH bonds, resulting in the formation of product ions containing the indole moiety.

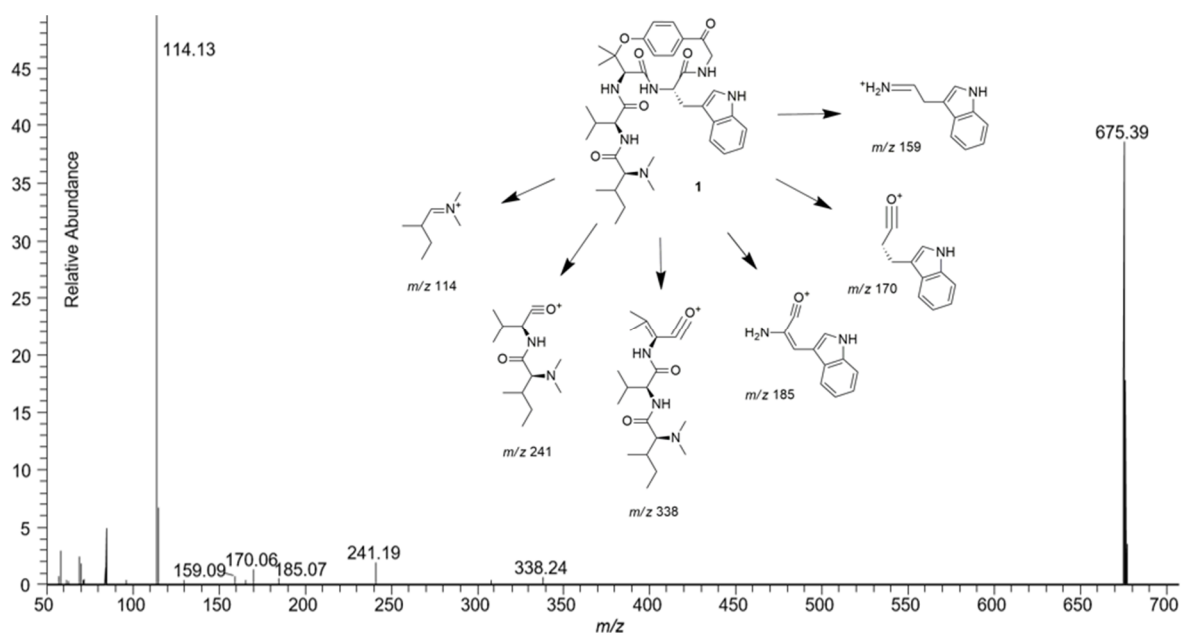


Fig. 7.6 Product ion spectrum and proposed fragmentation mechanism of hymenocardine (**1**) during HCD (higher-energy collisional dissociation) fragmentation in positive ion mode. The relative abundance of the product ion at m/z 114.13 is 100.

In negative ion mode, several abundant product ions were formed: m/z 336.14 ($C_{19}H_{18}O_3N_3$), m/z 433.19 ($C_{24}H_{25}O_4N_4$), m/z 544.32 ($C_{28}H_{42}O_6N_5$), m/z 207.08 ($C_{10}H_{11}O_3N_2$), m/z 150.05 ($C_8H_8O_2N$) and m/z 93.03 (C_6H_5O). The tentative structures of these product ions are depicted in Figure 7.7.

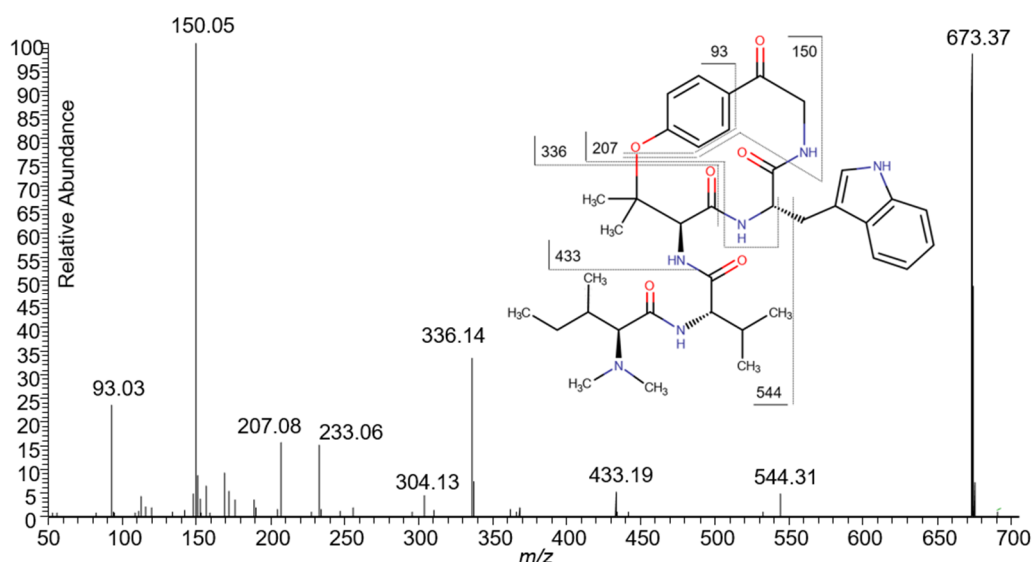


Fig. 7.7 Product ion spectrum of hymenocardine in negative ion mode.

Taking into account the fragmentation pathways of hymenocardine and the structural differences between hymenocardine and its metabolites, depicted in Figure 7.5, fragmentation of the metabolites should theoretically result in different, and therefore diagnostic product ions. Thus, the MS² spectra of the metabolites were investigated with the objective to confirm their tentative structures.

Metabolite **2** was identified as hymenocardinol (C₃₇H₅₂O₆N₆, *m/z* 677.40166, [M+H]⁺), formed by a reduction of the keto group of the *p*-hydroxy- ω -amino acetophenone moiety of hymenocardine. During fragmentation of this metabolite in positive ion mode, various product ions were observed that were also detected during fragmentation of hymenocardine (*m/z* 338.24, *m/z* 185.07, *m/z* 159.09 and *m/z* 114.13, Figure 7.6), indicating that the metabolic conversion did not occur at the side chain, the indole moiety, or the β -hydroxyvaline moiety. Other product ions were detected at *m/z* 659.39 (C₃₇H₅₀O₅N₆) and *m/z* 437.22 (C₂₄H₂₉O₄N₄). These ions confirmed the metabolic conversion of the carbonyl group next to the phenyl group into a hydroxyl group. The former ion is formed by a loss of water, the latter ion by a breakage of the amide bond between the β -hydroxyvaline moiety and the valine moiety. Fragmentation in negative ion mode also resulted in the occurrence of several diagnostic product ions, including the ions at *m/z* 191.08 (C₁₀H₁₁O₂N₂) and *m/z* 134.06 (C₈H₈ON). They correspond to product ions formed during fragmentation of hymenocardine in negative ion mode, but with a mass difference of 16.00 and 16.01 Da, respectively (*m/z* 207.08 and *m/z* 150.05). This additional loss originates from the metabolic conversion of the carbonyl group to a hydroxyl group. During fragmentation this hydroxyl group can easily be eliminated by loss of an H₂O-molecule, thus resulting in a net mass difference of 16 Da compared to the product ions detected for hymenocardine. Several other product ions in Table 7.1 provided additional structural confirmation. Comparison by LC-MS of a standard solution of hymenocardinol with compound **2** confirmed the identity of this metabolite. Hymenocardinol (**2**) is predicted as a possible metabolite of hymenocardine by the Meteor Nexus software; this conversion is catalyzed by the enzyme ADH (alcohol dehydrogenase).

The metabolite tentatively identified as *N*-monomethyl hymenocardine ($C_{36}H_{48}O_6N_6$, m/z 661.37029, $[M+H]^+$) (**3**) results from a loss of one of the *N*-methyl groups in the isoleucine-like moiety in the side chain. Fragmentation in positive ion mode rendered several diagnostic product ions. A very abundant product ion was observed at m/z 100.11 ($C_6H_{14}N$), resulting from a fragmentation pathway similar to that of the product ion of hymenocardine at m/z 114.13, described before. The difference in mass between the product ions arises from the change of the tertiary amine group to a secondary amine during metabolic conversion. Moreover, other product ions that were also diagnostic for the demethylation during biotransformation were observed, namely, an *a* ion at m/z 199.18 ($C_{11}H_{23}ON_2$) and a *b* ion at m/z 227.18 ($C_{12}H_{23}O_2N_2$). In addition, the presence of several other product ions that also occurred during fragmentation of hymenocardine (at m/z 159.09, m/z 170.06 and m/z 185.07) confirmed that the indole moiety in the 14-membered ring was not changed during metabolism.

During negative ion fragmentation of the metabolite tentatively identified as *N*-monomethyl hymenocardine, also a large amount of structurally informative product ions were formed. Most of the product ions were also found in the MS^2 spectrum of hymenocardine (m/z 93.03, m/z 150.05, m/z 207.08, m/z 336.14 and m/z 433.19) (Figure 7.7), thereby confirming that the metabolic conversion did not occur at the *para*-cyclophane part. Additionally, a product ion at m/z 530.30 ($C_{27}H_{40}O_6N_5$) was found, resulting from a fragmentation pathway similar to that of the product ion of hymenocardine at m/z 544.32. The mass difference between the product ion at m/z 544.32 and m/z 530.30 corresponds to the demethylation of the tertiary amino group in the side chain into a secondary amine, thereby confirming its structure depicted in Figure 7.5.

The tentative structure of the metabolite corresponding to $C_{36}H_{50}O_6N_6$ (*N*-monomethyl hymenocardinol, compound **4**) is the result of a combination of both reduction of the *p*-hydroxy- ω -amino acetophenone moiety (as in compound **2**) and *N*-demethylation (as in compound **3**). Fragmentation of this metabolite in positive ion mode resulted in a multitude of diagnostic product ions (Figure 7.8). For instance, the product ions at m/z 100.11, m/z 199.18 and m/z 227.18, which were encountered during fragmentation of the metabolite tentatively identified as *N*-monomethyl hymenocardine (**3**), were also detected for this

metabolite. These product ions are in agreement with the structure obtained by demethylation of the tertiary amine group in the side chain, resulting in a secondary amine group. Product ions confirming the metabolic conversion of the carbonyl group next to the phenyl group into a hydroxyl group were detected at m/z 437.22 ($C_{24}H_{29}O_4N_4$) and m/z 419.21 ($C_{24}H_{27}O_3N_4$). The first one was also detected in the product ion spectrum of compound **2**, while the second one is formed by an additional loss of water. Similar to the fragmentation of compound **2**, in negative ion mode product ions at m/z 191.08 ($C_{10}H_{11}O_2N_2$) and m/z 134.06 (C_8H_8ON) were detected, resulting from the loss of the hydroxyl group during fragmentation.

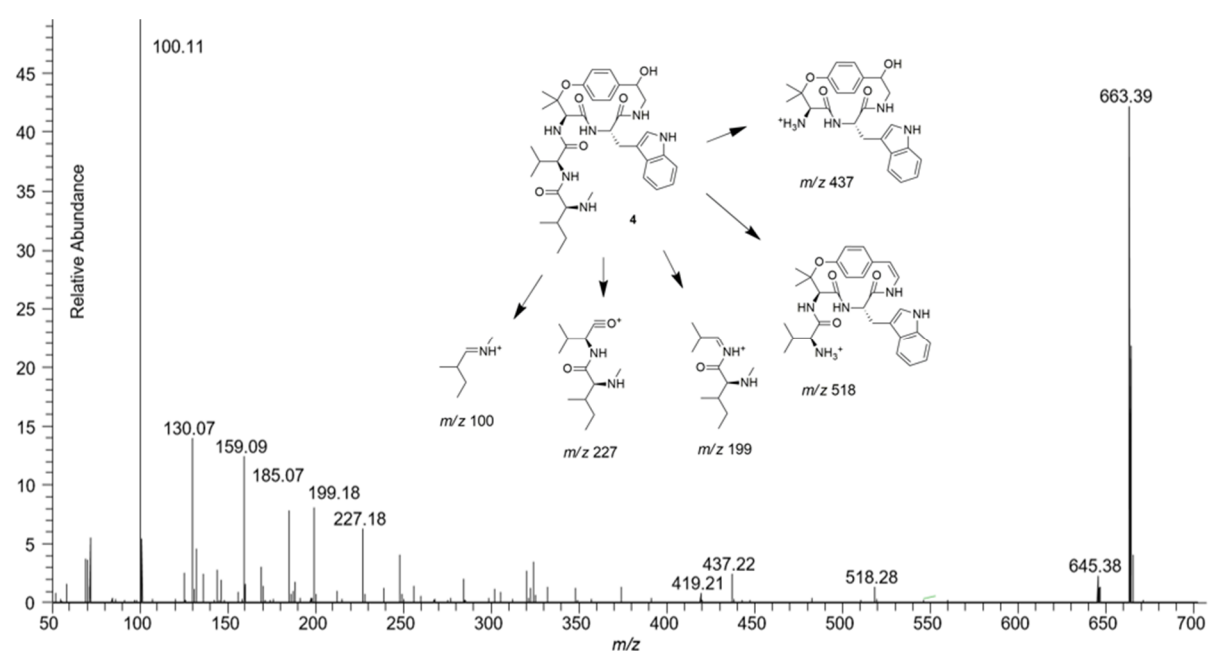


Fig. 7.8 Product ion spectrum and proposed fragmentation mechanism of the diagnostic product ions of the metabolite corresponding to $C_{36}H_{50}O_6N_6$ (**4**) during HCD fragmentation in positive ion mode. The relative abundance of the product ion at m/z 100.11 is 100.

Due to the low abundance of the metabolite tentatively identified as *N*-demethyl hymenocardine ($C_{35}H_{46}O_6N_6$, 647.35469, $[M+H]^+$) (**5**) (Figure 7.5), no product ions were detected in positive ion mode. Fragmentation in negative ion mode did, however, result in some product ions that were also detected during fragmentation of hymenocardine (m/z 336.13 and m/z 150.05, Figure 7.7). These product ions originate from the indole moiety and the *p*-hydroxy- ω -amino acetophenone moiety, indicating that the metabolic conversion most probably occurred at the side chain of hymenocardine, which is in agreement with the proposed structure. Single and double *N*-demethylation were predicted by Meteor Nexus and

Metaprint2D-React Web Server. According to the Meteor software, this type of metabolic conversion is catalyzed by enzymes belonging to the CYP450 (cytochrome P450) class.

Another metabolite that was predicted by both Meteor and Metaprint2D-React Web Server, and that could be identified in the metabolized hymenocardine samples, is the product of the hydrolysis of the amide bond linking the valine with the isoleucine-like moiety in the side chain. Fragmentation in positive ion mode of the metabolite tentatively labeled as 'hymenocardine – terminal isoleucine-like moiety' ($C_{29}H_{35}O_5N_5$, 534.27120, $[M+H]^+$) (**6**), resulted in several product ions that were also found during fragmentation of hymenocardine (Table 7.1). Others were different from hymenocardine fragmentation. These product ions confirmed that the substructure of hymenocardine containing the 14-membered ring and the indole moiety remained unmodified during metabolism into compound **6**. The most abundant product ion formed during hymenocardine fragmentation, m/z 114.13, originating from the cleavage of the amide bond at the terminal isoleucine-like moiety (Figure 7.6), is however absent during fragmentation of compound **6**. This confirms its tentative structure. Fragmentation in negative ion mode resulted mostly in the formation of product ions that were also observed during hymenocardine fragmentation, except for m/z 403.20 ($C_{20}H_{27}O_5N_4$), resulting from a fragmentation pathway similar to that of the product ion of hymenocardine at m/z 544.32. The mass difference between the product at m/z 544.32 and m/z 403.20 corresponds to the absence of the terminal isoleucine-like moiety in the metabolite $C_{29}H_{35}O_5N_5$, thereby confirming its structure depicted in Figure 7.5.

Compound **7** was tentatively labeled as 'hymenocardinol - terminal isoleucine-like moiety' ($C_{29}H_{37}O_5N_5$, m/z 536.28640, $[M+H]^+$). Likewise to the fragmentation observed in positive ion mode for compound **6**, fragmentation of **7** did not show a product ion at m/z 114.13. Furthermore, a diagnostic product ion was observed at m/z 447.20 corresponding to a fragment containing the three moieties taking part in the 14-membered ring, after the loss of the hydroxyl group ($C_{25}H_{27}O_4N_4$), thereby confirming the proposed structure in Figure 7.5.

Large differences in abundances were observed between the detected metabolites **2-7** (Table 7.1). Notwithstanding the fact that responses of similar structures often differ in LC-MS analysis, in our experience the observed differences are too large to be caused only by the differences in ionization efficiency. It can therefore be stated that three major metabolites are formed during metabolism of hymenocardine (**1**) with human S9 fraction, namely, those corresponding to $C_{37}H_{52}O_6N_6$ (**2**, hymenocardinol), $C_{36}H_{48}O_6N_6$ (**3**, *N*-monomethyl hymenocardine) and $C_{36}H_{50}O_6N_6$ (**4**, *N*-monomethyl hymenocardinol). Apart from compounds **2-7**, several other low-abundant metabolites were detected during UPLC-HRMS analysis, namely, the metabolites corresponding to $C_{37}H_{48}O_6N_6$ (**8**), $C_{37}H_{52}O_8N_6$ (**9**), $C_{37}H_{52}O_7N_6$ (**10**), $C_{36}H_{50}O_7N_6$ (**11** and **12**), $C_{37}H_{50}O_7N_6$ (**13** and **14**), and $C_{36}H_{52}O_7N_6$ (**15**). Protonated species of both $C_{36}H_{50}O_7N_6$ and $C_{37}H_{50}O_7N_6$ were detected at two different retention times, indicating that two structural isomers are formed, and thus, they correspond to two different metabolites.

A metabolite corresponding to the dehydrogenation of hymenocardine ($C_{37}H_{48}O_6N_6$, m/z 673.37002, $[M+H]^+$) (**8**) was detected (Table 7.1). Because of its relatively low abundance, only a small number of product ions were observed during fragmentation in positive ion mode. All product ions detected for this metabolite (m/z 241.19, m/z 159.09 and m/z 114.13) were also found during hymenocardine fragmentation (Figure 7.6). As these product ions originate from the side chain and the indole moiety, it can be concluded that the dehydrogenation reaction must have occurred at either the β -hydroxy valine moiety or the *p*-hydroxy- ω -amino acetophenone moiety. Nonetheless, no other product ions were detected, neither during negative ion fragmentation, so no further fine-tuning of the location of the dehydrogenation reaction could be done based on LC-HRMS fragmentation. Moreover, this metabolite was not predicted by the *in silico* tools.

Another low-abundant metabolite corresponding to $C_{37}H_{52}O_8N_6$ (**9**) was detected both in positive (m/z 709.39124, $[M+H]^+$) and negative ion mode (m/z 707.37840, $[M-H]^-$) (Table 7.1). Targeted fragmentation resulted in several product ions in positive ion mode at m/z 114.13, m/z 241.19, and m/z 338.24: these product ions originate from the side chain. The metabolite with m/z 693.39640 (**10**, $C_{37}H_{52}O_7N_6$, $[M+H]^+$) showed several product ions, resulting from the

side chain too (m/z 114.13, m/z 241.19, and m/z 338.24). These findings suggest that the metabolic conversions most probably occurred at the *p*-cyclophane part.

The *in silico* tools Meteor Nexus and Metaprint2D-React Web Server predicted several possible metabolic conversions, which, when combined, can lead to the formation of **11-15** (Figure 7.9). These reactions include the reduction of the carbonyl group of the *p*-hydroxy- ω -amino acetophenone moiety (as reported for compound **2**), opening of the 14-membered ring by oxidative *N*-demethylation, hydroxylation, epoxidation, and loss of an *N*-methyl group. However, given the low abundance of compounds **11-15**, it was not possible to obtain product ion spectra of these metabolites and no tentative structures could be provided for metabolites **8-15**.

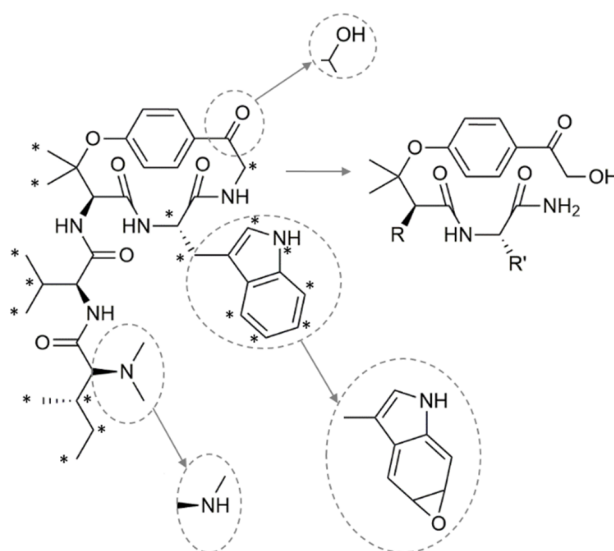


Fig. 7.9 Possible biotransformation reactions in hymenocardine, as predicted by the *in silico* tools Meteor and Metaprint2D-React Web Server. Asterisks indicate the positions where hydroxylation can occur.

In the third part of this study, hymenocardine was orally administered to rats and blood and urine samples were collected up to 48 and 24 h after administration, respectively, in order to obtain information about the *in vivo* absorption, metabolism and excretion of hymenocardine. The plasma and urine samples were analyzed by UPLC-QqQMS (triple quadrupole MS); purified hymenocardine and hymenocardinol, isolated before (Tuenter *et al.*, 2016a), were used as analytical standards for quantification.

Hymenocardine was detected in the plasma from 1 to 12 h after administration, with the highest concentration, 1.43 ng/mL plasma, measured 1 h after oral administration (Figure 7.10). Apart from hymenocardine, also hymenocardinol (**2**) could be detected from 1 to 24 h after administration of hymenocardine, and thus, it is present in plasma longer than hymenocardine itself. Based on the results of non-spiked vs. spiked samples, the average recovery of hymenocardine was found to be $106 \pm 8\%$ and $82 \pm 5\%$ for hymenocardinol.

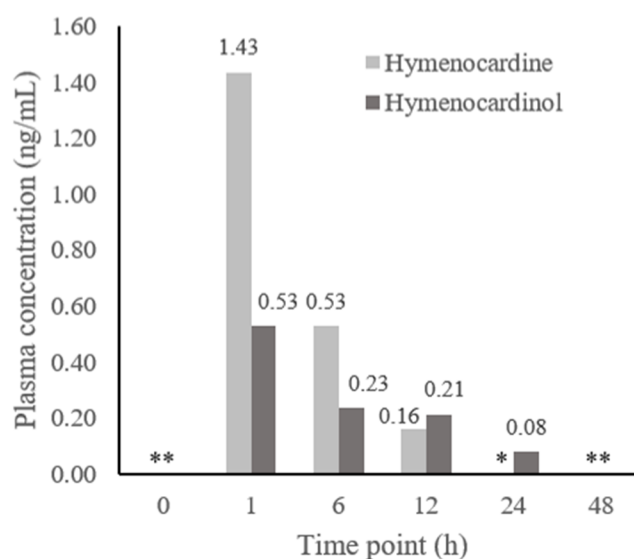


Fig. 7.10 Concentration of hymenocardine and hymenocardinol in rat plasma, determined by LC-QqQMS, before (time point 0 h) and at different time points after oral administration of hymenocardine. Each bar represents a single measurement of the pooled plasma samples.

*Plasma concentration < LOQ (0.07 ng/mL for hymenocardine and 0.03 ng/mL for hymenocardinol).

The maximum concentration of hymenocardinol (0.52 ng/mL), was detected in plasma after 1 h, which is less than half of the maximum concentration of hymenocardine (1.43 ng/mL), measured at the same time point. The concentration of hymenocardine decreased more quickly in time, and could be measured up to 12 h after administration, while the concentration of hymenocardinol decreased more slowly and can still be measured after 24 h. This slower decrease of the hymenocardinol level, compared to the level of hymenocardine, can be explained by the fact that, although both compounds are excreted in urine, causing a decrease in the plasma levels of both compounds, the metabolism of hymenocardine into hymenocardinol will proceed as long as hymenocardine is present. This metabolism will have an additive effect on the decrease of the plasma levels of hymenocardine, while at the same time the formation of more hymenocardinol will partly outweigh its urinary excretion.

Gastrointestinal absorption and metabolic conversion of hymenocardine | 210

Therefore, hymenocardinol can persist in plasma for a longer period of time than hymenocardine.

Urine of the rats was collected between 2 and 24 h after administration of hymenocardine. Analysis of these samples also resulted in the identification of both hymenocardine and hymenocardinol, with a concentration of 11.8 ± 0.3 ng/mL and 16.0 ± 0.6 ng/mL, respectively. Based on the results of non-spiked vs. spiked samples, the average recovery was found to be $87.2 \pm 2.0\%$ for hymenocardine and $85.8 \pm 0.3\%$ for hymenocardinol.

These data suggest that hymenocardine is partly excreted unchanged, and at least in part as hymenocardinol. No additional metabolites were detected in plasma and urine, and also a specific search for the molecular species corresponding to the metabolites identified in the S9 experiment and their glucuronide and sulphate adducts was negative. In the S9 experiment, *N*-monomethyl hymenocardine and *N*-monomethylhymenocardinol were identified as major metabolites, together with hymenocardinol. However, the former two were not detected in the plasma and urine samples. Likely, the specific CYP450 enzyme, which catalyzes the oxidative *N*-demethylation, is absent in rats, and thus, this reaction cannot take place. Other metabolites that were identified in the S9 experiment, were only minor metabolites, and taking into account the fact that the levels of hymenocardine and hymenocardinol in plasma and urine are relatively close to the limit of detection, it seems likely that the analysis of the *in vivo* samples is not sufficiently sensitive to detect any minor metabolites.

The results indicate that, as observed in an *in vitro* gastrointestinal dialysis model, a biotransformation study with human microsomal S9 fraction, and an *in vivo* study in rats, reduction of hymenocardine to hymenocardinol is by far the most important metabolic pathway. Interestingly, hymenocardinol showed a comparable IC₅₀ value against *Plasmodium falciparum* as hymenocardine (Tuenter *et al.*, 2016a), and the reduction of hymenocardine will not interfere with its potential *in vivo* antimalarial activity.

7.3 Materials and Methods

7.3.1 Chemicals and reagents

Pepsin (from porcine stomach mucosa, 800-2500 U/mg protein), bile salts (porcine) and pancreatin (from porcine pancreas, 149 U/mg amylase) were purchased from Sigma-Aldrich (Steinheim, Germany). Human liver S9 fraction and NADPH RS (Reduced nicotinamide adenine dinucleotide phosphate regenerating system) were purchased from XenoTech (Pfungstadt, Germany). For information about other chemicals and reagents, see Chapter 2, general experimental procedures, section 2.1.1, solvents and reagents.

Hymenocardine (94%) and hymenocardinol (82%) were isolated from root bark of *Hymenocardia acida*. The purity of these two compounds was determined by HPLC analysis. The analysis was performed using a XBridge C₁₈ column (4.6 × 250 mm, 5µm, Waters) and water + 0.1% formic acid (A) and acetonitrile (B) as mobile phase. The flow rate was 1.0 mL/min and the following gradient was applied: 0 to 5 min 80% A and 20% B, 40 to 45 min 100% B. UV detection was done at 201 nm.

7.3.2 *In vitro* gastrointestinal dialysis model (GIDM)

Hymenocardine (25 mg) was submitted to a GIDM (stomach and small intestinal phase), as reported by Breynaert *et al.* (2015). Dialysis tubing with a molecular mass cutoff of 12 to 14 kDa (Visking size 6 Inf Dia 27/32–21.5 mm, length 30 m) was obtained from Medicell Ltd. (Liverpool, UK). Stirred ultrafiltration cells (model 8200, 200 mL, 63.5 mm diameter), the related controller (controller MF2 and a reservoir RC800) and the ultrafiltration discs (Ultracel molecular mass cutoff 1,000 Da; 63.5 mm diameter) were purchased from Millipore.

The obtained dialyzate and retentate fractions were freeze-dried and 1/20 of each fraction was dissolved in 500 µL water. To this solution, 500 µL acetonitrile was added and the samples were subsequently vortexed and centrifuged for 10 min at 12,000 g and 4 °C. The supernatant of these samples was analyzed by UPLC-HRMS, as was hymenocardine itself (sample concentration 0.1 µg/mL). The analyses were performed on an Agilent 1290 series HPLC system with a sample manager, binary pump, temperature-controlled column compartment and QTOF 6530 mass spectrometer (Santa Clara, CA, USA), equipped with an Agilent Jetstream source. MassHunter version B.06 software was used for data processing. The samples were

analyzed on an Acquity BEH C₁₈ column (2.1 mm x 100 mm; 1.7 µm) from Waters (Milford, MA, USA) with water + 0.1 % formic acid (A) and acetonitrile + 0.1% formic acid as (B) as the mobile phase. The flow rate was 0.4 mL/min and the gradient applied was as follows: from 0.00 min to 0.90 min 80% A and 20% B, from 0.90 min to 4.86 min a linear change to 70% A and 30% B, from 4.86 min to 7.84 min a linear change to 0% A and 100% B. The injection volume was 4 µL.

The mass spectrometer was operated in ESI+ mode at a resolution of 20,000. Calibration was done externally and the following settings were applied: gas temperature 325 °C, gas flow 7 L/min, nebulizer pressure 40 psi, sheath gas temperature 325 °C, sheath gas flow 11 L/min. Capillary, fragmentor, and skimmer voltages were set to 3500 V, 175 V, and 65 V, respectively, and the OCT 1 RF Vpp was set at 750 V. An MS scan was performed in the range of *m/z* 100 to 1000.

7.3.4 Incubation with liver S9 fraction

To investigate the formation of phase-I metabolites of hymenocardine, reaction mixtures containing 420 µL 65 mM TRIS buffer (pH adjusted to 7.4 at 37 °C), 25 µL human liver S9 fraction and 5 µL hymenocardine (5 mM) were preincubated in triplicate in a shaking water bath at 37 °C for 3 min. The reaction was initiated by the addition of 50 µL NADPH RS and samples were incubated for 1 h at 37 °C in a shaking water bath (30 RPM). The reaction was quenched after 1 h by adding 450 µL of ice-cold acetonitrile and storing the tubes on ice. In addition, blank samples (with acetonitrile instead of test compound solution) were prepared in duplicate and negative control samples (with 450 µL of acetonitrile added before, instead of after the incubation) were prepared in triplicate. The samples were vortexed and centrifuged for 5 min at 9,500 g and 4 °C and the supernatant was analyzed by UPLC-HRMS. Briefly, 5 µL of each sample was injected with a CTC PALTM autosampler (CTC Analytics, Zwingen, Swiss) on a Waters Acquity BEH SHIELD RP18 column (3.0 mm x 150 mm; 1.7 µm; Waters) and thermostatically (40 °C) eluted with an AccelaTM quaternary solvent manager and a 'Hot Pocket' column oven (Thermo Fisher Scientific, Waltham, MA, USA). The mobile phase solvents consisted of water + 0.1% formic acid (A) and acetonitrile + 0.1% formic acid (B), and the gradient was set as follows: 0.00 min 99% A and 1% B, 9.91 min 74% A and 26% B, 18.51 min 35% A and 65% B, 18.76 min until 20.76 min 0% A and 100% B, 20.88 min until 23.00 min

99% A and 1% B. For detection, an high-resolution mass spectrometer (Q Exactive™; Thermo Fisher Scientific) was used with HESI (heated electrospray ionization). During a first analysis, full scan data were acquired using polarity switching with an m/z range of 70-1050 and resolving power set at 70,000 at full width at half maximum (FWHM). Spray voltage was set at ± 2.5 kV, sheath gas and auxiliary gas at 47 and 15 (arbitrary units), respectively, and capillary temperature at 350 °C. Fragmentation data were also recorded using higher-energy collisional dissociation (HCD) and data-dependent fragmentation (ddMS²) in positive and negative ionization mode (one analysis per mode) to obtain additional structural information (resolving power set at 17,500 FWHM, stepped collision energy 10, 30, 50 eV, isolation window: 4 m/z , top 10 of most abundant ions selected for fragmentation). If fragmentation was not triggered due to low abundance of metabolites, targeted MS² was carried out in an effort to obtain diagnostic product ion spectra.

SIEVE software for differential analysis and Xcalibur software (both from Thermo Fisher Scientific) were used for processing of raw data. The full scan data were processed in SIEVE to locate the metabolites that were formed: the software compares the metabolized hymenocardine data with the negative control data and method blanks and filters out the differences. Subsequently, more structural information was obtained for the detected metabolites by examining the product ion spectra in both positive and negative ion mode (if available) (Table 7.1). Software for drug metabolism prediction (Meteor Nexus version 2.1.0, Lhasa Limited, Leeds, UK and Metaprint2D-React Web Server (University of Cambridge, Cambridge, UK) were used to predict phase-I metabolites from hymenocardine *in silico*. In Meteor, human metabolites (S9) were predicted to a maximum depth of three levels. Redox and non-redox reactions were included and metabolites with a plausible or probable likelihood were taken into account. In Metaprint2D-React Web Server, default settings were used and also here, the human model was selected. The resulting list of *in silico* metabolites was matched with the list of metabolites retrieved from the S9 metabolism experiments by linking the *in silico* metabolites with the most probable molecular formulae obtained with LC-HRMS. This resulted in fourteen tentative metabolites.

7.3.5 Animal study

Five male Wistar rats, 9 weeks old, weighing approximately 300 g to 325 g, were purchased from Janvier (Le Genest-Saint-Isle, France). The study was approved by the institutional ethical committee for animal experiments (ECD file number: 2016-034, date of approval: May 9th 2016) and throughout the whole experiment, the guidelines for the accommodation and care of animals used for experimental and other scientific purposes, as described by the European Commission, were followed. Rats were housed for 1.5 week in a climate- and light-controlled environment with free access to water and food in order to acclimatize before the start of the experiment. By this time, their weight had increased to 369 g, on average. Four of the rats were given a dose of 20 mg/kg hymenocardine, administered by oral gavage in the form of a suspension (5 mg/mL in water), while one rat was treated with only vehiculum. About 500 µL of blood was taken from the tail vein at time-points 0 (before administration), 1, 6, 12, 24 and 48 hours after administration. Between time-point 2 and 24 h, rats were kept in a metabolic cage and urine was collected. All blood samples were centrifuged at 2,000 g for 10 min at 4 °C and plasma samples were collected. The four plasma samples of the rats which were administered hymenocardine and which were obtained at the same time point were pooled. Also, urine samples of the rats which were administered hymenocardine were pooled and both plasma and urine samples were stored at -80 °C until analysis.

Sample preparation of plasma: To 100 µL of plasma, 300 µL of methanol was added and samples were vortexed for 15 s and centrifuged at 13,680 g for 10 min at 4 °C. The supernatant was dried under a flow of nitrogen gas and was redissolved in 100 µL of 80% water/20% methanol. Samples were vortexed shortly again and centrifuged at 18,625 g for 10 min at 4 °C. The supernatant was diluted five times and was transferred to HPLC vials for UPLC-HRMS analysis. In order to estimate the recovery of the sample preparation and possible effects of matrix suppression during the MS analysis, also four samples (plasma samples taken at time points 0, 12, 24 and 48 hours, of the rats that were administered hymenocardine) were spiked at the start of the sample preparation procedure with hymenocardine (82.5 ng/mL plasma) and hymenocardinol (70.0 ng/mL plasma).

Analysis of plasma samples: The plasma samples were analyzed on a UPLC-QqQMS instrument (Acquity UPLC with XEVO TQ-S mass spectrometry system, Waters). The injection volume was 10 μ L. Separation was achieved on an Acquity BEH SHIELD RP18 column (2.1 mm x 100 mm; 1.7 μ m, Waters) and water + 0.1% formic acid (A) and acetonitrile + 0.1% formic acid (B) as mobile phase with the following gradient: 0.00 min to 0.50 min 95% A and 5% B, 3.40 min until 4.50 min 0% A and 100% B, 4.60 min until 6.60 min 95% A and 5% B. The flow rate was set at 0.5 mL/min and the target column temperature was 40.0 °C. Mass spectra were recorded in ESI+ mode, using MRM. For hymenocardine, the transitions of the protonated molecule with m/z 675.48, $[M+H]^+$, into m/z 114.12 and m/z 241.16 were monitored, with the collision energy set at 44 and 26 V, respectively, and a cone voltage of 60 V. For hymenocardinol, the transitions of the protonated molecule with m/z 677.48, $[M+H]^+$, into m/z 114.22 and m/z 241.22 were monitored, with the collision energy set at 45 and 28 V, respectively, and a cone voltage of 50 V. Other settings of the mass spectrometer were as follows: $V_{\text{capillary}}$ 3.00 kV, T_{source} 150 °C, $T_{\text{Desolvation}}$ 450 °C, desolvation gas flow 800 L/h, and cone gas flow 150 L/h. Calibration curves were constructed in a concentration range from 0.015 ng/mL to 33.00 ng/mL for hymenocardine and from 0.004 to 27.98 ng/mL for hymenocardinol with 8 and 9 calibration points, respectively, and were used to calculate the levels of the respective compounds in the plasma samples.

Sample preparation of urine: 500 μ L of 4% formic acid was added to 500 μ L urine. Sample clean-up was performed in triplo with Oasis MCX 3cc (60 mg) extraction cartridges (Waters). The cartridges were conditioned with 10 mL methanol, 10 mL water and 10 mL water with 4% formic acid. Next, the samples were loaded and the cartridges were washed with 2 mL water and 5 mL methanol. Finally, elution was done with twice 1 mL of 60:40 acetonitrile: methanol + 5% NH_4OH . In order to estimate the recovery of the sample preparation and possible effects of matrix suppression during the MS analysis, also spiked samples were prepared in triplicate at the start of the sample preparation procedure. Spiking was done with both hymenocardine (50.0 ng/mL urine) and hymenocardinol (57.6 ng/mL urine).

Analysis of urine samples: Urine samples were analyzed with an Acquity UPLC-DAD-QqQMS instrument, comprised of a binary solvent manager, sample manager, temperature-controlled column compartment, diode array detector and TQD (Waters). Data processing was done with MassLynx 4.1. The injection volume was 4 μ L. An Acquity BEH C₁₈ column (2.1 mm x 50 mm; 1.7 μ m, Waters) was used, with water + 0.05% formic acid (A) and acetonitrile + 0.05% formic acid (B) as mobile phase and with the following gradient: 0.00 min to 0.50 min 95% A and 5% B, 5.00 min 40% A and 60% B, 6.00 to 7.00 min 0% A and 100% B, 7.10 to 8.00 min 95% A and 5% B. The flow rate was 0.5 mL/min. Mass spectra were recorded in ESI+ mode, using MRM, between 0.00 min and 2.70 min for hymenocardinol (m/z 677.4, [M+H]⁺, fragmentation into m/z 659.3, 114.2 and 85.1 with $V_{\text{collision}}$ set at 23, 39 and 80 eV, respectively, and a cone voltage of 54 V) and between 2.70 min and 8.00 min for hymenocardine (m/z 675.3, [M+H]⁺, fragmentation into m/z 241.3, 114.1 and 85.1 with $V_{\text{collision}}$ set at 27, 39 and 79 eV, respectively, and a cone voltage of 59 V). Other settings of the mass spectrometer were as follows: $V_{\text{capillary}}$ 2.30 kV, $V_{\text{extractor}}$ 1 V, $V_{\text{RF-Lens}}$ 0.5 V, T_{source} 120 °C, $T_{\text{Desolvation}}$ 450 °C, desolvation gas flow 850 L/h, and cone gas flow 50 L/h.

A calibration curve was constructed in a concentration range from 1.23 ng/mL to 100.0 ng/mL for hymenocardine and from 3.05 ng/mL to 82.3 ng/mL for hymenocardinol with 7 and 6 calibration points, respectively, and used to calculate the levels of the respective compounds in the urine samples.

References

- Breynaert, A., Bosscher, D., Kahnt, A., Claeys, M., Cos, P., Pieters, L. and Hermans, N., 2015. Development and validation of an *in vitro* experimental gastrointestinal dialysis model with colon phase to study the availability and colonic metabolism of polyphenolic compounds. *Planta Med* **81**(12-13): 1075-1083.
- El-Seedi, H. R., Zahra, M. H., Goransson, U. and Verpoorte, R., 2007. Cyclopeptide alkaloids. *Phytochem Rev* **6**(1): 143-165.
- Gournelis, D. C., Laskaris, G. G. and Verpoorte, R., 1997. Cyclopeptide alkaloids. *Nat Prod Rep* **14**(1): 75-82.
- Han, B. H., Park, M. H. and Park, J. H., 1989. Chemical and pharmacological studies on sedative cyclopeptide alkaloids in some Rhamnaceae plants. *Pure Appl Chem* **61**(3): 443-448.
- Han, H., Ma, Y., Eun, J. S., Yun, S. R., Kim, C. S., Hong, J. T. and Oh, K. W., 2008. Anxiolytic-like effects of sanjoinine A isolated from *Zizyphi spinosi* semen: involvement of GABA receptors. *Planta Med* **74**(9): 963-963.
- Ma, Y., Han, H., Nam, S. Y., Kim, Y. B., Hong, J. T., Yun, Y. P. and Oh, K. W., 2008. Cyclopeptide alkaloid fraction from *Zizyphi spinosi* semen enhances pentobarbital-induced sleeping behaviors. *J Ethnopharmacol* **117**(2): 318-324.
- Maleknia, S. D. and Johnson, R., 2011. Mass Spectrometry of Amino Acids and Proteins. In: Amino Acids, Peptides and Proteins in Organic Chemistry. ed. Wiley-VCH Verlag GmbH & Co. KGaA, Weinheim, pp. 1-50.
- Panseeta, P., Lomchoey, K., Prabpai, S., Kongsaree, P., Suksamrarn, A., Ruchirawat, S. and Suksamrarn, S., 2011. Antiplasmodial and antimycobacterial cyclopeptide alkaloids from the root of *Ziziphus mauritiana*. *Phytochemistry* **72**(9): 909-915.
- Suh, D. Y., Kim, Y. C., Han, Y. N. and Han, B. H., 1996. Unusual enamide cleavage of franguloline under mild acidic condition. *Heterocycles* **43**(11): 2347-2351.
- Suh, D. Y., Kim, Y. C., Kang, Y. H., Han, Y. N. and Han, B. H., 1997. Metabolic cleavage of franguloline in rodents: *in vitro* and *in vivo* study. *J Nat Prod* **60**(3): 265-269.
- Suksamrarn, S., Suwannapoch, N., Aunchai, N., Kuno, M., Ratananukul, P., Haritakun, R., Jansakul, C. and Ruchirawat, S., 2005. Ziziphine N, O, P and Q, new antiplasmodial

- cyclopeptide alkaloids from *Ziziphus oenoplia* var. *brunoniana*. *Tetrahedron* **61**(5): 1175-1180.
- Tuenter, E., Exarchou, V., Balde, A., Cos, P., Maes, L., Apers, S. and Pieters, L., 2016a. Cyclopeptide alkaloids from *Hymenocardia acida*. *J Nat Prod* **79**(7): 1746-1751.
- Tuenter, E., Ahmad, R., Foubert, K., Amin, A., Cos, P., Maes, L., Apers, S., Pieters, L. and Exarchou, V., 2016b. Isolation and structure elucidation by LC-DAD-MS and LC-DAD-SPE-NMR of cyclopeptide alkaloids from the roots of *Ziziphus oxyphylla* and evaluation of their antiplasmodial activity. *J Nat Prod* **79**: 2865-2872.
- Vonthron-Senecheau, C., Weniger, B., Ouattara, M., Bi, F. T., Kamenan, A., Lobstein, A., Brun, R. and Anton, R., 2003. *In vitro* antiplasmodial activity and cytotoxicity of ethnobotanically selected Ivorian plants. *J Ethnopharmacol* **87**(2-3): 221-225.

CHAPTER 8

SAR study

Published:

Emmy Tuenter, Karen Segers, Kyo Bin Kang, Johan Viaene, San Hyun Sung, Paul Cos, Louis Maes, Yvan Vander Heyden and Luc Pieters

Antiplasmodial activity, cytotoxicity and structure-activity relationship study of cyclopeptide alkaloids

Molecules, **2017**, 22(2), 224.

8.1 Introduction

With an estimated amount of 214 million new cases in 2015, malaria is still one of the most important infectious parasitic diseases worldwide (WHO, 2015). It is caused by the *Plasmodium* parasite, and it is transferred via the bite of an *Anopheles* mosquito. Because of increasing resistance against the currently available antimalarial drugs, there is a compelling need for new therapeutic agents. It is well recognized that plants are interesting sources for identifying new lead compounds (Harvey, 2008), which is well exemplified by the alkaloid quinine or the terpene artemisinin.

This manuscript focuses on a particular subclass of alkaloids, namely, the cyclopeptide alkaloids. These are macrocyclic compounds, containing a 13- 14- or 15-membered ring. The ring consists of a hydroxystyrylamine moiety, a typical amino acid and a β -hydroxy amino acid; attached to the ring is a side chain, usually comprised of one or two more amino acid moieties. Their basic character is related to the *N*-atom of the terminal amino acid moiety in the side chain; however, in some cases a cinnamoyl instead of an amino acid moiety is present, and this type of cyclopeptide alkaloids is referred to as 'neutral cyclopeptide alkaloids'.

Certain plants containing cyclopeptide alkaloids are used in traditional medicine for the treatment of malaria, for example, leaves and roots of *Hymenocardia acida* (Vonthron-Senecheau *et al.*, 2003). The *in vitro* antiplasmodial activity of 19 cyclopeptide alkaloids has been published so far. Suksamrarn *et al.* (2005) found antiplasmodial activity for ziziphines-N and -Q (IC₅₀ 3.92 and 3.5 μ g/mL, corresponding to 6.4 and 5.9 μ M, respectively), while ziziphines-O and -P were not active. Panseeta *et al.* (2011) identified mauritine-M, nummularine-H and hemsine-A as antiplasmodial compounds, with IC₅₀-values ranging between 3.7 and 7.3 μ M. Nummularine-B was found to be moderately active (IC₅₀ 10.3 μ M) against *Plasmodium falciparum*, but not mauritine-L and nummularine-B methiodide. Our research group has previously reported the antiplasmodial activity of cyclopeptide alkaloids from *Hymenocardia acida* and *Ziziphus oxyphylla* (Tuenter and co-workers, 2016a; 2016b). Based on these results, some preliminary conclusions concerning their SAR (structure-activity relationship) were drawn, but given the fact that the number of compounds tested in each of

these studies was relatively small, it was not possible to arrive at solid conclusions. In the present paper, the antiplasmodial and cytotoxic activities of ten cyclopeptide alkaloids are reported, of which only the antiplasmodial activity of nummularine-B was reported before (Panseeta *et al.*, 2011). These results were then combined with previous data obtained by our group in the same test conditions for 9 other cyclopeptide alkaloids from *H. acida* and *Z. oxyphylla* (Tuenter and co-workers, 2016a; 2016b), in order to perform a SAR study, and to identify the molecular characteristics that can account for a high antiplasmodial activity.

8.2 Results and Discussion

8.2.1 Antiplasmodial and cytotoxic activities

The *in vitro* antiplasmodial activity against *P. falciparum* strain K1 and cytotoxicity against MRC-5 cells was determined for ten cyclopeptide alkaloids, isolated from the stem bark of *Ziziphus nummularia*, *Ziziphus spina-christi*, *Ziziphus jujuba* and the root of *Hovenia dulcis*, all belonging to the family of the Rhamnaceae, and the results are shown in Table 8.1. The results that were previously reported for cyclopeptide alkaloids isolated from the root bark of *Hymenocardia acida* (Phyllanthaceae) and the roots of *Z. oxyphylla* (Rhamnaceae) are also included in this table. The highest antiplasmodial activity was found for spinanine-B (**3**), with an IC_{50} value of 2.1 μ M and without cytotoxic effects in concentrations of 64.0 μ M or less. Nummularine-B (**8**) showed a promising antiplasmodial activity too (IC_{50} value 3.6 μ M), and did not have any cytotoxic effects up to a concentration of 64.0 μ M. However, Panseeta *et al.* (2011), previously considered this compound to be only moderately active (IC_{50} value 10.3 μ M).

Table 8.1 Antiplasmodial activity against *P. falciparum* and cytotoxicity against MRC-5 cells (IC₅₀ µM) for cyclopeptide alkaloids isolated from *Hymenocardia acida*, *Hovenia dulcis*, and different *Ziziphus* spp.

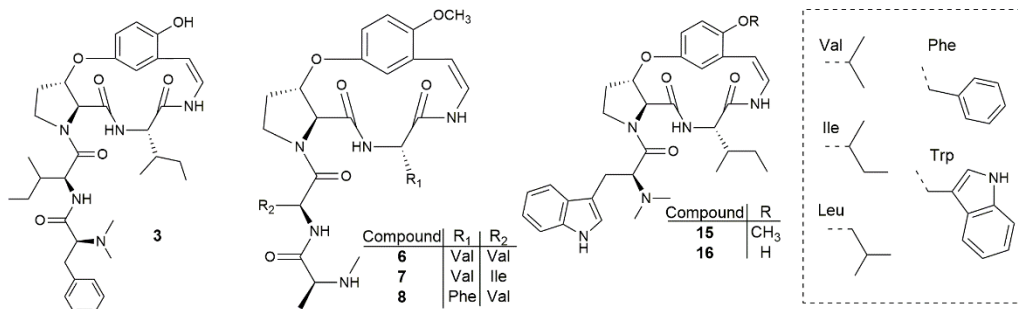
	compound	plant source	<i>P. falciparum</i> K1	MRC-5
1	nummularine-U	<i>Ziziphus nummularia</i>	23.0 ± 8.5	> 64.0
2	mauristine-F		34.2 ± 9.14	> 64.0
3	spinanine-B	<i>Ziziphus spina-christi</i>	2.1 ± 0.3	> 64.0
4	nummularine-E		> 64.0	> 64.0
5	amphibine-D		8.9 ± 1.5	> 64.0
6	jubanine-F	<i>Ziziphus jujuba</i>	12.8 ± 2.9	> 64.0
7	jubanine-G		4.7 ± 2.4	> 64.0
8	nummularine-B		3.6 ± 1.3	> 64.0
9	adouetine-X		7.5 ± 1.8	19.1 ± 11.9
10	frangulanine	<i>Hovenia dulcis</i>	14.9 ± 5.2	30.6 ± 6.5
11	hymenocardine	<i>Hymenocardia acida</i>	16.4 ± 6.8	51.1 ± 17.2
12	hymenocardinol		17.5 ± 8.7	> 64.0
13	hymenocardine N-oxide		12.2 ± 6.6	> 64.0
14	hymenocardine-H		27.9 ± 16.5	> 64.0
15	nummularine-R	<i>Ziziphus oxyphylla</i>	3.2 ± 2.6	30.6 ± 4.0
16	O-desmethylnummularine-R		7.1 ± 1.6	> 64.0
17	hemsine-A		13.6 ± 9.3	> 64.0
18	ramosine-A		> 32.0	> 64.0
19	oxyphylline-F		7.4 ± 3.0	31.2 ± 1.4
Control 1	Chloroquine		0.15 ± 0.05	nt
Control 2	Tamoxifen		nt	10.0 ± 0.3

nt: not tested

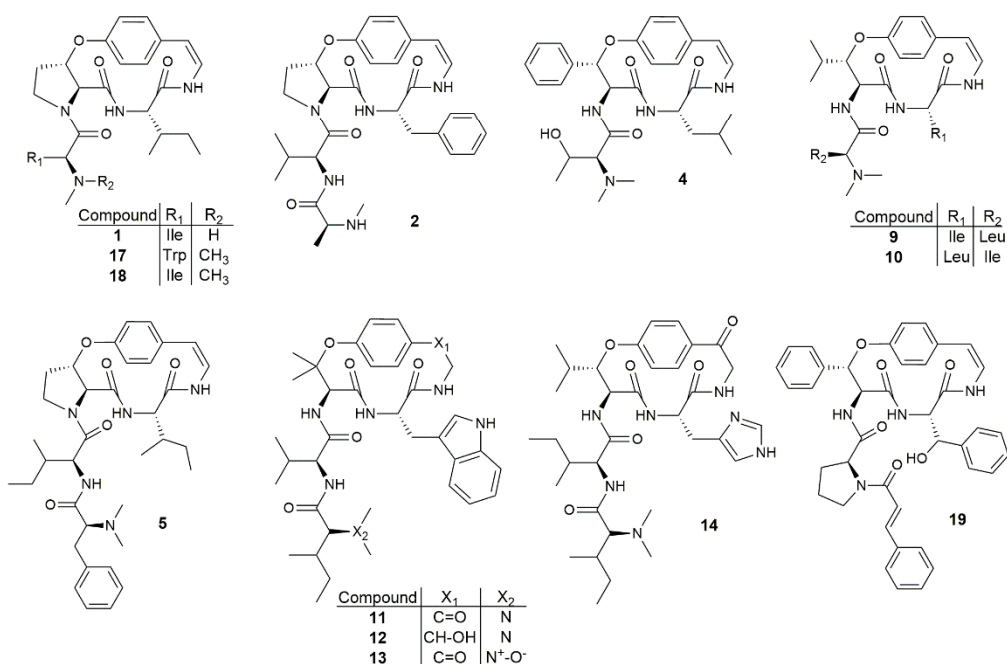
8.2.2 Qualitative structure-activity relationship study

The chemical structures of all 19 cyclopeptide alkaloids are shown in Figure 8.1. Based on these structures and the results obtained for the antiplasmodial activity, a preliminary structure-activity relationship study was performed. From the 19 cyclopeptide alkaloids tested, eight had an IC_{50} -value below 10 μM . Out of these eight, five belong to the 13-membered and three to the 14-membered cyclopeptide alkaloids. Interestingly, the five most promising results were found for cyclopeptides bearing a 13-membered ring, with IC_{50} -values ranging between 2.1 and 7.1 μM . From these results, it could be concluded that a *meta*-cyclophane structure (13-membered ring) is more likely to be associated with a high antiplasmodial activity compared to a *para*-cyclophane structure (14-membered ring). Moreover, out of the six tested 13-membered cyclopeptide alkaloids, only one showed an IC_{50} -value above 10 μM , namely, jubanine-F (**6**) (IC_{50} 12.8 μM), but this result still indicates moderate activity. Thus, all tested *meta*-cyclophane compounds are found to be antiplasmodially active. As for the 14-membered cyclopeptide alkaloids on the other hand, only three of the 13 tested compounds were found to have an IC_{50} -value below 10 μM , while nummularine-E (**4**), for example, could not inhibit *P. falciparum* in concentrations up to 64.0 μM . These findings support our hypothesis that a 13-membered ring is favorable in view of high antiplasmodial activity.

13-membered cyclopeptide alkaloids



14-membered cyclopeptide alkaloids



Val: valine; Phe: phenylalanine; Ile: isoleucine; Trp: tryptophan; Leu: leucine.

Fig. 8.1 Chemical structures of cyclopeptide alkaloids **1-19**.

When looking further into the compounds containing a 13-membered macrocyclic ring, two contain a styrylamine moiety, hydroxylated in position 2 of the aromatic ring, while the other four possess a 2-methoxy styrylamine moiety. With respect to this structural feature, Suksamrarn *et al.* (2005) who assessed the antiparasmodial activity of four 13-membered cyclopeptide alkaloids, proposed that the methoxy group is crucial to display antiparasmodial activity. Our results do not support this, since the tested hydroxylated *meta*-cyclophane compounds were found to be active too, but interestingly, compound **15** (nummularine-R, IC₅₀ 3.2 μM) seemed to be more active than compound **16** (*O*-desmethylnummularine-R, IC₅₀ 7.1 μM), with their only difference being the presence of a hydroxy or a methoxy group, respectively. Based on this result, it can be concluded that cyclopeptide alkaloids containing

either a methoxy group or a hydroxy group can display antiplasmodial activity, but that methoxylated compounds might be associated with higher activity. In view of this, it would be interesting to determine the antiplasmodial activity of paliurine-C, for example, which is the methoxylated analog of spinanine-B. Moreover, it would be interesting to test 13-membered cyclopeptide alkaloids without a methoxy or hydroxy group, to establish how this will affect their antiplasmodial activity. However, to the best of our knowledge, such cyclopeptide alkaloids have not been reported up till now (Tuenter *et al.*, 2016c), but possibly, they could be obtained by semi-synthesis.

One common feature of all tested *meta*-cyclophane compounds is the presence of a β -hydroxy proline amino acid moiety. Panseeta *et al.* (2011) suggested that this feature could be linked to a relatively high antiplasmodial activity. They found promising results for the 13-membered cyclopeptide alkaloids mauritine-M and nummularine-H, and for hemsine-A (**17**), the latter one belonging to the *para*-cyclophane compounds. In our case, all *para*-cyclophane compounds bearing a β -hydroxylated proline showed only moderate or weak activity against *P. falciparum*, except amphibine-D (**5**) (IC₅₀ 8.9 μ M). Moreover, 14-membered cyclopeptide alkaloids comprised of a β -hydroxy phenylalanine (oxyphylline-F) (**19**) or a β -hydroxy leucine (adouetine-X) (**9**) showed promising antiplasmodial activities. These results indicate that a β -hydroxy proline moiety is not crucial for displaying antiplasmodial activity. In order to confirm whether this finding is applicable to the 13-membered cyclopeptide alkaloids as well, it would be worthwhile to know to which extent *meta*-cyclophane cyclopeptide alkaloids with different β -hydroxy amino acid moieties are capable of inhibiting the growth of the *Plasmodium* parasite. However, to the best of our knowledge, all reported 13-membered cyclopeptide alkaloids contain such a β -hydroxy proline moiety, thus, for the moment, it is not possible to determine the activity of other types of *meta*-cyclophane cyclopeptide alkaloids.

Another interesting finding is the difference in activity of adouetine-X (**9**) (IC₅₀ 7.5 μ M) and frangulanine (**10**) (IC₅₀ 14.9 μ M). These two compounds show many structural similarities, and differ only in two aspects: adouetine-X contains an isoleucine moiety as ring-bound amino acid, while frangulanine contains a leucine moiety in this position. The opposite is applicable for the side chain, with a leucine unit found in adouetine-X and an isoleucine moiety found in frangulanine. Leucine and isoleucine are constitutional isomers, hence, a small difference in

chemical structure can affect the antiplasmodial activity. Suksamrarn *et al.* (2005) concluded that substitution of a leucine unit with a valine unit, both aliphatic amino acid units too, resulted in similar biological activities. In their case, the substitution took place in the side chain (ziziphine-N vs. ziziphine-Q). The cyclopeptide alkaloids jubanine-F (**6**) and -G (**7**) differ only in one amino acid unit in the side chain too, with jubanine-F containing a valine moiety and jubanine-G an isoleucine moiety. However, the antiplasmodial activity found for jubanine-G (IC_{50} 4.7 μ M) was significantly higher than the activity for jubanine-F (IC_{50} 12.8 μ M). Thus, the statement made by Suksamrarn *et al.* (2005) is not supported by our results, and it must be concluded that substitution of one aliphatic amino acid with another does affect the resulting antiplasmodial activity.

8.2.3 Quantitative structure-activity relationship study

In order to have a quantitative understanding of the structure-activity relationships underlying some of the compounds' selectivity with respect to antiplasmodial activity, a QSAR (quantitative structure-activity relationship) study was carried out. PLS (partial least squares regression) and MLR (multiple linear regression) models were built, linking a set of molecular descriptors with the antiplasmodial activity. Different data pretreatments, i.e. autoscaling, direct orthogonal signal correction (DOSC) (Westerhuis *et al.*, 2001) and their combinations were first applied to the descriptor data. DOSC was found to result in the best PLS model. The MLR models were built selecting the descriptors based on their importance in the best DOSC-PLS model. Three models, with three, six or eight descriptors were built, and revealed which molecular descriptors were of main importance for the antiplasmodial activity. The model with eight descriptors performed similarly well as the best PLS model.

The RMSECV (root mean squared error of cross validation) and RMSEC (root mean squared error of calibration) values of each model were calculated, in order to select the best model. For the best DOSC-PLS model, RMSECV was 0.0134 (and RMSEC 0.0051). The more descriptors included in the MLR models, the lower the RMSECV value found. For the model built with three descriptors, the RMSECV was 0.4306 (RMSEC 0.2150); for that with six descriptors 0.0725 (0.0505) and when eight descriptors were included 0.0257 (0.0095). However, the four models predicted the activity of the calibration samples well, even when they were considered as unknown compounds in the cross validation. The following MLR equation (eight-descriptor

model) can, for instance, be applied in order to have an estimation of the IC₅₀ value obtained in the antiparasmodial activity assay:

$$\begin{aligned} \text{IC}_{50} \text{ value } (\mu\text{M}) = & 0.0002 + 0.0436 * \text{Platt index} + 0.0345 * \text{MMFF94 energy} + \\ & 0.0203 * \text{Dreiding energy} + 0.0188 * \text{Maximal projection area} + \\ & 0.0104 * \text{Minimal projection area} + 0.0105 * \text{Wiener polarity} + \\ & 0.0088 * \text{C}(\%) + 0.0089 * \text{Aliphatic bond count} \end{aligned}$$

The eight molecular descriptors that were identified as most influential (in sequence added in the three models) were: the Platt index, a path-based topological descriptor which is defined as the sum of the edge degrees of a molecular graph, and two geometrical descriptors, MMFF94 energy and the Dreiding energy (both given in kcal/mol), which are measures for the internal energy of a given conformer. In addition to these three descriptors, two other geometrical descriptors, i.e. the maximal and minimal projection area (given in Å²); the Wiener polarity, which represents the number of three bond length distances in the molecule (topological descriptor); the percentage of C-atoms in the molecule and the aliphatic bond count. For all descriptors in the model, a higher value is associated with a higher IC₅₀-value and thus lower antiparasmodial activity. Unfortunately, theoretical descriptors cannot always easily be linked to the physicochemical properties of the molecule.

Additionally, the models were used to predict the activity of a number of potentially interesting structures, as indicated by the qualitative SAR study. Earlier we already stated that it would be interesting to determine the antiparasmodial activity of paliurine-C, the methoxylated analog of spinanine-B, as well as of 13-membered cyclopeptide alkaloids without a methoxy or hydroxy group. The models built predict that both paliurine-C and 13-membered cyclopeptide alkaloids without methoxy group, would have a rather high activity. Moreover, the importance of the β -hydroxy proline moiety in 13-membered cyclopeptide alkaloids was questioned, and it would be worthwhile to find out to which extent *meta*-cyclophane cyclopeptide alkaloids with different β -hydroxy amino acid moieties are capable of inhibiting *P. falciparum*. Thus, a prediction of the activity of 13-membered cyclopeptide alkaloids, bearing either a β -hydroxy leucine, β -hydroxy valine or β -hydroxy phenylalanine moiety was made, although such compounds have not been identified from natural sources

yet. The theoretical descriptors derived from their structures allowed predicting a high activity for these compounds. In addition, the models seem to confirm high activity for the 13-membered-ring compounds.

One has to take into account when interpreting the predictions that the calibration set was small (19 compounds), and that the structure for which the activity is predicted may be suboptimally represented in it. Moreover, the data set mainly consisted of active and intermediately active compounds, while inactive compounds are underrepresented. Therefore, to our opinion, the interpretation of the activity should or could, at this moment, not go further than the indication whether or not a given compound is expected to be rather active or inactive. Better predictive models for this type of compounds will require a larger, more representative calibration set.

The chemical structures of promising cyclopeptide alkaloids defined in the qualitative discussion of this paper allowed predicting high activity using any of the QSAR models. The QSAR approach thus did not contradict the expectations gained from the qualitative study. In a future step promising compounds could be isolated from natural sources or constructed (semi-)synthetically, after which testing of their antiplasmodial activity can be performed.

8.3 Materials and Methods

8.3.1 General experimental procedures

Marvinsketch version 16.10.31.0 (ChemAxon, Budapest, Hungary) was used for obtaining the set of 73 molecular descriptors, and the QSAR models were developed in Matlab™ version 7.1 (The Mathworks, Natick, MA, USA).

8.3.2 Plant material, extraction and isolation

The extraction, isolation and structure elucidation of 17 of the 19 cyclopeptide alkaloids included in this manuscript was reported before (Kang *et al.*, 2015; Tuenter and co-workers,

2016a; 2016b; 2017). The isolation procedure of adouetine-X and fragulanine is described here briefly:

Adouetine-X (25.1 mg) was isolated from the roots of *Ziziphus jujuba*. The roots were collected in JinJu, Korea, in 2012. The plant was identified by Prof. Eun Ju Jeong (Gyeongnam National University of Science and Technology, JinJu, Republic of Korea). A voucher specimen (SUPH-1204-01) is deposited in the Herbarium in the Medicinal Plant Garden, College of Pharmacy, Seoul National University, Korea. The dried and powdered plant material (14.5 kg) was macerated with methanol and the obtained crude extract was fractionated by liquid-liquid partitioning. Further fractionation of the alkaloid fraction was accomplished by means of column chromatography on a silica column (Kieselgel 60 silica gel (40–60 μm , 230–400 mesh, Merck, Darmstadt, Germany) and a Sephadex column (Sephadex LH-20 (25–100 μm , Pharmacia, Piscataway, NJ, USA) consecutively, as described by Kang *et al.* (2015). By means of preparative HPLC, adouetine-X was isolated from fraction A2c. The preparative HPLC system consisted of a G-321 pump (Gilson, Middleton, WI, USA), a G-151 UV detector (Gilson). An XBridge C₁₈ column (250 mm x 10 mm i.d.; 5 μm , Waters, Milford, MA, USA) was used to obtain separation (0.1% NH₄Ac in H₂O-acetonitrile, 5:5, 4 mL/min). Structure elucidation was done on the basis of NMR and HRESIMS experiments and comparison of the spectroscopic data to the literature (Trevisan *et al.*, 2009).

Fragulanine was isolated from the methanolic extract of *Hovenia dulcis* roots. The plant material was cultivated at the Medicinal Plant Garden, College of Pharmacy, Seoul National University, Koyang, Korea, and was collected in September 2015. A voucher specimen (SUPH-1509-03) is deposited in the Herbarium of the Medicinal Plant Garden. Powdered, dried roots of *H. dulcis* (2.7 kg) were extracted with methanol by ultrasonication at room temperature (2 \times 12 L, for 3 h each). The crude extract (87.1 g) was suspended in water and partitioned successively with dichloromethane (17.7 g), ethyl acetate (22.0 g), and butanol (33.5 g). The CH₂Cl₂ fraction was subjected to silica gel column chromatography and eluted with mixtures of CHCl₃–CH₃OH (100:1, 50:1, 20:1, 15:1, 10:1, 5:1, and 3:1) to yield ten fractions (MC1–MC10). Subfraction MC5 was further divided into six subfractions (MC5a–MC5f) by passage over Sephadex LH-20, eluted with a mixture of CH₂Cl₂–CH₃OH (3:1). The CH₃OH-insoluble precipitate of subfraction MC5d was collected and purified by washing with CH₃OH, and was

identified as frangulanine (28.3 mg) by comparison of its spectroscopic data (NMR, HRESIMS) to data reported in the literature (Medina *et al.*, 2016).

8.3.3 Antiplasmodial and cytotoxic activities

The antiplasmodial and cytotoxic activity determinations of all cyclopeptide alkaloids were performed as described in chapter 2, general experimental procedures, section 2.3, biological activity testing. Each experiment was performed at least in triplicate and average IC₅₀-values were calculated.

8.3.4 QSAR

Molecular models of all cyclopeptide alkaloids were generated using the software program MarvinSketch. For the generation of the lowest energy conformer, the conformer plugin was used and the following settings were applied: Force field: Dreiding; optimization limit: very strict; prehydrogenize. Then, for each compound, 73 molecular descriptors were calculated, related to the elemental analysis, protonation, partitioning, solubility, topological analysis, geometrical properties, polar and molecular surface area, *H* bond donor/acceptor characteristics and refractivity. Two more descriptors were added, i.e. the number of subunits and *N*-methyl groups, since they were considered possibly important in relation to the bioactivity of the cyclopeptide alkaloids.

Prior to the actual molecular modelling, the descriptors which showed >95% correlation or which were constant were identified. The latter were deleted and of the former, the one best correlated to the activity was kept. This resulted in 41 remaining descriptors. Based on the set of molecular descriptors and the average IC₅₀-values obtained in the antiplasmodial activity assay, partial least squares (PLS) and multiple linear regression (MLR) modelling were carried out. Models were selected on the basis of leave one out cross validation. The RMSECV and RMSEC were calculated for each model, in order to be able to compare the predictive value, and the fit of the different models, respectively. All steps involved in the activity modelling were conducted in Matlab.

8.4 Conclusions

The antiplasmodial and cytotoxic activities of ten cyclopeptide alkaloids were assessed, with the most promising result found for spinanine-B, with an IC_{50} -value of 2.1 μ M and without cytotoxic effects in concentrations up to 64.0 μ M. Combining these results with those previously reported by our group for nine other cyclopeptide alkaloids, a qualitative structure-activity relationship study concerning the antiplasmodial activity was performed. The obtained results indicated that a 13-membered ring is preferred over a 14-membered, and that methoxylation in position 2 of the styrylamine moiety, which takes part in this ring, is beneficial, although also hydroxylated compounds displayed antiplasmodial activity. However, in order to confirm the importance of the methoxy group and the β -hydroxy proline moiety, and in order to determine the exact role of different aliphatic amino acids (leucine, isoleucine, valine) in either the macrocyclic ring or the side chain, further research is required.

For each of the tested cyclopeptide alkaloids, 75 molecular descriptors were calculated for their lowest energy conformer. In this way, a library with data of 19 cyclopeptide alkaloids was created, which was used to develop QSAR models, based on PLS and MLR modelling. These QSAR models define quantitative correlations between molecular descriptors and the antiplasmodial activity and indicated which molecular descriptors can explain the most variance regarding the antiplasmodial activity. These descriptors were, in order of decreasing importance: the Platt index, the MMFF94 energy, the Dreiding energy, the maximal and minimal projection area, the yield polarity, the percentage of C-atoms and the aliphatic bond count. The obtained models can be applied for the prediction of the antiplasmodial activity of other cyclopeptide alkaloids. These predictions were often extrapolations relative to our small calibration set, but seem to confirm our qualitative SAR study (were at least not contradicting the expectations).

References

- Harvey, A. L., 2008. Natural products in drug discovery. *Drug Discov Today* **13**(19-20): 894-901.
- Kang, K. B., Ming, G., Kim, G. J., Ha, T. K. Q., Choi, H., Oh, W. K. and Sung, S. H., 2015. Jubanines F-J, cyclopeptide alkaloids from the roots of *Ziziphus jujuba*. *Phytochemistry* **119**: 90-95.
- Medina, R. P., Schuquel, I. T. A., Pomini, A. M., Silva, C. C., Oliveira, C. M. A., Kato, L., Nakamura, C. V. and Santin, S. M. O., 2016. Ixorine, a new cyclopeptide alkaloid from the branches of *Ixora brevifolia*. *J Brazil Chem Soc* **27**(4): 753-758.
- Panseeta, P., Lomchoey, K., Prabpai, S., Kongsaree, P., Suksamrarn, A., Ruchirawat, S. and Suksamrarn, S., 2011. Antiplasmodial and antimycobacterial cyclopeptide alkaloids from the root of *Ziziphus mauritiana*. *Phytochemistry* **72**(9): 909-915.
- Suksamrarn, S., Suwannapoch, N., Aunchai, N., Kuno, M., Ratananukul, P., Haritakun, R., Jansakul, C. and Ruchirawat, S., 2005. Ziziphine N, O, P and Q, new antiplasmodial cyclopeptide alkaloids from *Ziziphus oenoplia* var. *brunoniana*. *Tetrahedron* **61**(5): 1175-1180.
- Trevisan, G., Maldaner, G., Velloso, N. A., Sant'Anna, G. D., Ilha, V., Gewehr, C. D. V., Rubin, M. A., Morel, A. F. and Ferreira, J., 2009. Antinociceptive effects of 14-membered cyclopeptide alkaloids. *J Nat Prod* **72**(4): 608-612.
- Tuenter, E., Exarchou, V., Balde, A., Cos, P., Maes, L., Apers, S. and Pieters, L., 2016a. Cyclopeptide Alkaloids from *Hymenocardia acida*. *J Nat Prod* **79**(7): 1746-1751.
- Tuenter, E., Ahmad, R., Foubert, K., Amin, A., Cos, P., Maes, L., Apers, S., Pieters, L. and Exarchou, V., 2016b. Isolation and structure elucidation by LC-DAD-MS and LC-DAD-SPE-NMR of cyclopeptide alkaloids from the roots of *Ziziphus oxyphylla* and evaluation of their antiplasmodial activity. *J Nat Prod* **79**: 2865-2872.
- Tuenter, E., Exarchou, V., Apers, S. and Pieters, L., 2016c. Cyclopeptide alkaloids. *Phytochem Rev*: 1-15. DOI: 10.1007/s11101-016-9484-y.
- Tuenter, E., Foubert, K., Staerk, D., Apers, S. and Pieters, L., 2017. Isolation and structure elucidation of cyclopeptide alkaloids from *Ziziphus nummularia* and *Ziziphus spina-christi* by HPLC-DAD-MS and HPLC-PDA-(HRMS)-SPE-NMR. *Phytochemistry* **138**: 163-169.

- Vonthron-Senecheau, C., Weniger, B., Ouattara, M., Bi, F. T., Kamenan, A., Lobstein, A., Brun, R. and Anton, R., 2003. *In vitro* antiplasmodial activity and cytotoxicity of ethnobotanically selected Ivorian plants. *J Ethnopharmacol* **87**(2-3): 221-225.
- Westerhuis, J. A., de Jong, S. and Smilde, A. K., 2001. Direct orthogonal signal correction. *Chemom Intell Lab Syst* **56**(1): 13-25.
- WHO, 2015. World Malaria Report 2015. ed. WHO Press, Geneva, Switzerland.
<http://www.who.int/malaria/publications/world-malaria-report-2015/report/en/>
(accessed on 6 January 2017).

CHAPTER 9

Advanced glycation end products (AGEs)

9.1 Introduction

In Chapter 1, the formation of advanced glycation end products (AGEs) was proposed as a possible target for cyclopeptide alkaloids. Choudhary *et al.* (2011) has reported *in vitro* AGEs inhibiting activities for nummularine-R and hemsine-A, with IC₅₀-values of $720.2 \pm 10.9 \mu\text{M}$ and $277.7 \pm 7.6 \mu\text{M}$ respectively, while rutin was used as a positive control and showed an IC₅₀-value of $294.5 \pm 1.5 \mu\text{M}$. These results were obtained with the 'BSA-MGO assay' (bovine serum albumin – methylglyoxal assay). Apart from this publication, no other cyclopeptide alkaloids have been tested for their AGEs inhibiting activity, and nothing was known about their possible mechanism of action. Thus, it seemed interesting to test the obtained library of cyclopeptide alkaloids for their potential to inhibit AGEs formation in general, and, if relevant, to perform further experiments in order to determine in which steps of the AGEs formation process they interfere.

In this chapter, an overview is given of the different experiments that were performed. The methodology is described, the obtained results are shown and an extensive discussion is included, where both the advantages and the downsides of each experiment are considered.

9.2 Experimental Procedures

9.2.1 BSA-Glc assay

The BSA-Glc assay was performed according to Sero *et al.* (2013) and Upadhyay and co-workers (2014a, 2014b) with minor modifications. In the BSA-Glc assay, samples are prepared with BSA (bovine serum albumin) (135 μL , final concentration 10 mg/mL), D-glucose (135 μL , final concentration 500 mM) and test compound (30 μL , final concentrations ranging from 0.5 mM to 10 mM), with a final volume of 300 μL . BSA and D-glucose solutions were prepared in sodium phosphate buffer (50 mM, pH 7.4), containing 0.02% sodium azide (NaN_3). Solutions of test compounds were made in DMSO. Aminoguanidine (final concentrations between 0.05 mM and 5.0 mM) was used as reference compound. Control samples were prepared with 30 μL of DMSO (without test compound). One set of the samples was incubated at 37 °C, another set was incubated at 4 °C (blank samples). After 7 days, 150 μL of each sample was transferred

to a black, flat bottom 96-well plate (Greiner Bio-One, Kremsmünster, Austria) and fluorescence intensities were measured on a Tecan™ Infinite M200 (Giessen, The Netherlands). Two different sets of excitation/emission wavelengths were selected: λ_{exc} 335 nm and λ_{em} 385 nm, and λ_{exc} 370 nm and λ_{em} 440 nm. The AGEs inhibition was calculated as follows:

$$\% \text{ AGEs inhibition} = \left(1 - \frac{RFU_{test} - RFU_{test,bl}}{RFU_{ctr} - RFU_{ctr,bl}} \right) \times 100$$

Where RFU is the amount of relative fluorescence units.

9.2.2 BSA-Glc assay, with protein precipitation

In order to remove any remaining free glucose and test compound from the samples obtained with the regular BSA-Glc experiment (section 9.2.1), an extended sample preparation procedure was followed, involving protein precipitation. The applied procedure is based on the methodology reported by Matsuura *et al.* (2002), with minor modifications. The samples were prepared as described in paragraph 9.2.1. After 7 days incubation at 37 °C or 4 °C (for test or blank samples, respectively), 100 μ L of each sample was transferred to an Eppendorf tube and 10 μ L of 100% (w/v) trichloroacetic acid (4 °C), was added to allow precipitation of proteins and any protein-bound AGEs. The samples were then kept at 4 °C for 10 min, followed by centrifugation at 15,000 RPM and 4 °C for 4 min. The supernatant was discarded and the precipitate was redissolved with 500 μ L PBS (phosphate-buffered saline, containing 137 mM NaCl, 8.1 mM Na₂HPO₄, 2.68 mM KCl, 1.47 mM KH₂PO₄, pH 10.0) and fluorescence measurements were performed as described in section 9.2.1.

9.2.3 BSA-MGO assay

The BSA-MGO assay (Choudhary *et al.*, 2011, with slight modifications) was performed in a similar way to the BSA-Glc assay, but samples were prepared with methylglyoxal (MGO, 135 μ M, final concentration 5.75 mM) instead of glucose and the samples were incubated for 24 hours.

9.2.4 Fructosamine determination

The amount of fructosamine that was formed, was determined according to the method of Chompoo *et al.* (2011). 40 μ L of the samples prepared in the BSA-Glc assay were transferred

to a transparent flat-bottom 96-well plate (Thermo Fisher Scientific, Roskilde, Denmark) and 160 μL of freshly prepared NBT (nitro blue tetrazolium chloride, 300 μM , dissolved in sodium bicarbonate buffer, 100 mM, pH 10.35) was added. After 15 min incubation at 37 °C, the UV absorbance at 530 nm was measured. Blank samples were prepared using 160 μL of sodium bicarbonate buffer instead of NBT. The inhibition of the fructosamine formation was calculated as:

$$\% \text{ fructosamine inhibition} = \left(1 - \frac{A_{\text{test}} - A_{\text{test,bl}}}{A_{\text{ctr}} - A_{\text{ctr,bl}}} \right) \times 100$$

Where A is the measured absorbance.

9.2.5 Dicarbonyl entrapment

The entrapment of glyoxal (GO) was assessed by a two-step procedure (Upadhyay *et al.*, 2014a, with modifications): In the first part of the experiment, 1.0 mL GO (1.1 mM in sodium phosphate buffer, see 9.2.1), 0.2 mL of the test compound (5.0 mM in DMSO) and 0.8 mL sodium phosphate buffer were combined. Control samples were prepared with 0.2 mL of DMSO (without test compound). Aminoguanidine was used as reference compound. Blank samples were prepared without GO (using 1.8 mL instead of 0.8 mL sodium phosphate buffer). The samples were prepared in triplicate and were incubated at 37 °C and at time points 0, 5, 10, 15, 30, 45, 60, 75, 90, 105, and 120 min, 100 μL of the samples was taken and was frozen at -80 °C until further processing.

In the second part of the experiment, 850 μL of sodium formate buffer (500 mM, pH 2.90) and 50 μL of a 500 mM solution of Girard's reagent T ((carboxymethyl)trimethylammonium chloride hydrazide) in sodium formate buffer were added to each sample (final volume 1.0 mL). Samples were incubated for 1 h at room temperature. Then, the UV absorbance at 290 nm was measured, using a Genesys-10 UV spectrophotometer (Thermo Fisher Scientific). One sample was prepared by adding 2 μL DMSO to 1800 μL phosphate buffer. The sample was kept at room temperature and was used to set the spectrophotometer to zero. The % GO entrapment was calculated as follows:

$$\% \text{ GO entrapment} = \left(1 - \frac{A_{\text{test}} - A_{\text{test,bl}}}{A_{\text{ctr}}} \right) \times 100$$

Where A is the measured absorbance.

9.2.6 ELISA (enzyme linked immunosorbent assay)

Assessment of general AGEs formation by means of ELISA was reported before (Kiho *et al.*, 2004; Jang *et al.*, 2007; Sadowska-Bartosch *et al.*, 2014) and an attempt was made to determine the amount of AGEs formed in the BSA-glucose assay by means of a bovine AGEs ELISA kit (NeoScientific, Cambridge, MA, USA). The assay is a quantitative competitive immunoassay and a schematic overview is shown in Figure 9.1. The assay procedure was as follows: 100 μL of samples obtained in the BSA-Glucose assay, or standard solutions (6 concentrations of AGEs, ranging from 0 pg/mL to 1000 pg/mL , included in the ELISA kit) were transferred in duplicate to a 96-well plate, coated with AGEs specific antibody. To each well, 50 μL of enzyme-conjugated AGEs antigen solution was added. The 96-well plate was covered and incubated for 1 h at 37 °C in a humid chamber. Then, each well was washed five times with 300-400 μL wash solution. (The wash solution was prepared by diluting the concentrated wash solution, which is included in the ELISA kit, 25 times with deionized water.) After the last wash, the plate was inverted and dried by tapping on absorbent paper. Next, 50 μL of substrate A was added to each well, followed by 50 μL of substrate B. The 96-well plate was covered and incubated for 10 to 15 minutes at room temperature, protected from light. In order to stop the reaction, 50 μL of stop solution was added to each well. Then the absorbance was measured at 450 nm, on a BioTek EON instrument (Winooski, VT, USA), using the software program Gen5, version 2.06. Data processing was performed with Graphpad Prism 6 (La Jolla, CA, USA).

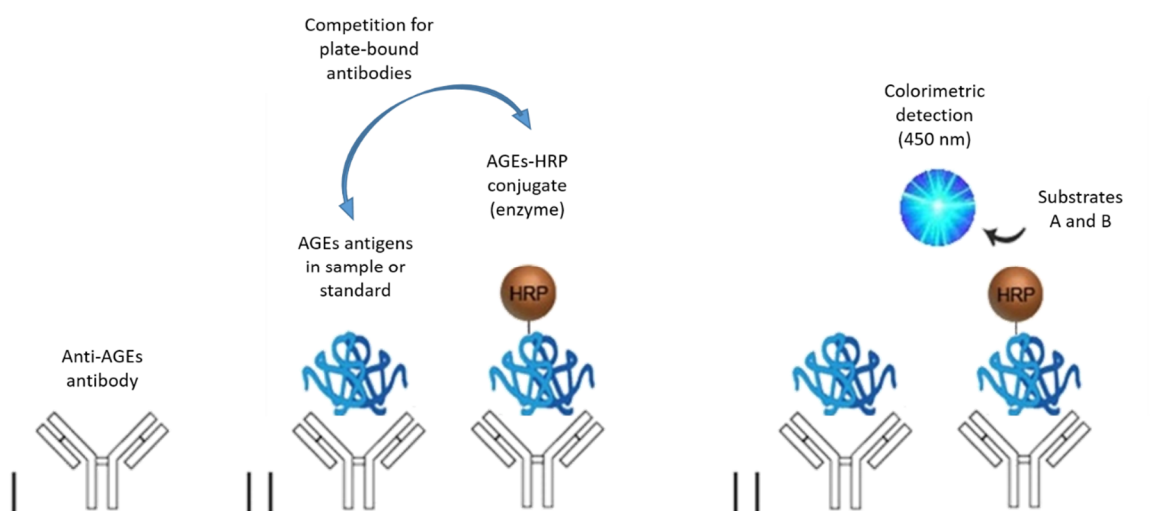


Fig. 9.1 Schematic overview of competitive bovine AGEs ELISA assay.
AGEs: advanced glycation end products; HRP: horseradish peroxidase.

9.3 Results and Discussion

9.3.1 BSA-Glc assay

The BSA-Glc assay is a general assay in which AGEs are formed through both oxidative and non-oxidative reactions. Thus, results obtained with this assay indicate whether the tested compounds possess AGEs inhibiting properties, but no conclusions can be drawn concerning their mode of action. Fluorescence detection is done at two different sets of wavelengths: the intensity of the fluorescence signal at λ_{exc} 335 nm / λ_{em} 385 nm is indicative for the amount of pentosidine-like AGEs (pentosidine, argpyrimidine), while fluorescence intensity at λ_{exc} 370 nm / λ_{em} 440 nm is indicative for vesperlysine-like AGEs (vesperlysines-A, -B and -C and crossline). Tested compounds can show AGEs inhibition in these two sets of wavelengths to a different extent, since their mode of action might cause a reduction in the formation of only a certain type of AGEs.

Initially, the test was performed with hymenocardine in a concentration range of 0.01 to 1 mM; however, the results were not as expected and instead of a concentration-dependent decrease, an increase in the fluorescence was observed with higher concentrations of hymenocardine (data not shown). This could be an indication of AGEs induction instead of AGEs inhibition, however, since the same trend was seen in the blank samples (with minimal AGEs formation), it seemed possible that the measurement could be susceptible to autofluorescence of hymenocardine itself. In order to confirm this, three different types of samples with varying concentrations of hymenocardine were analyzed: hymenocardine; hymenocardine + BSA; hymenocardine + Glc. The samples were treated as in the BSA-Glc assay and the results are shown in Figure 9.2.

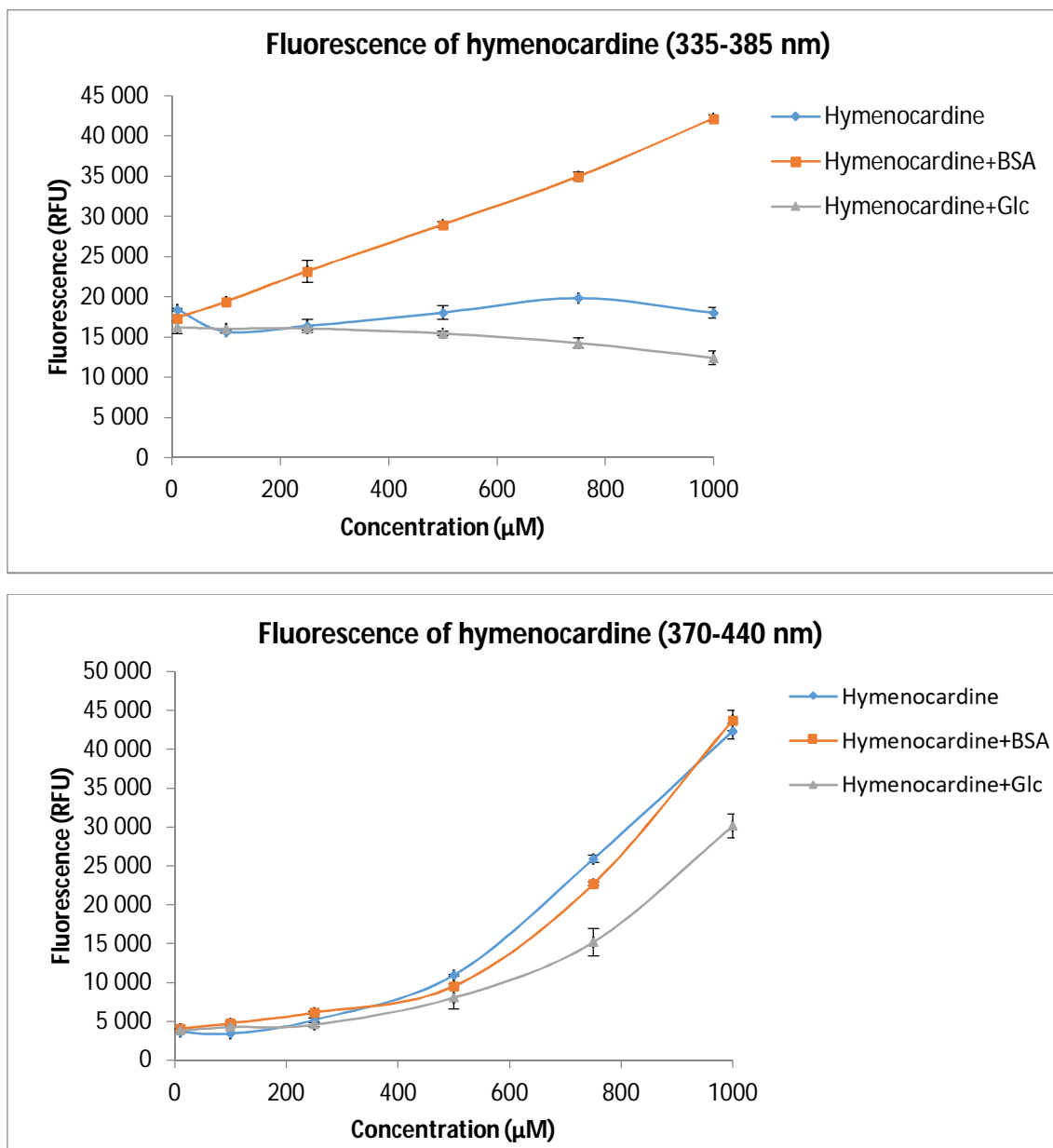


Fig. 9.2 Fluorescence of hymenocardine (final concentration 0 to 1000 μM) with and without BSA or Glc. Upper graph: detection at λ_{exc} 335 - λ_{em} 385 nm. Lower graph: detection at λ_{exc} 370 - λ_{em} 440 nm.

At λ_{exc} 335 - λ_{em} 385 nm, samples with hymenocardine alone, and hymenocardine with Glc did not show an increase in fluorescence with increasing concentrations of hymenocardine. However, this was not the case for the samples containing hymenocardine and BSA (as is the case for test samples in the BSA-Glc assay). In these samples, the detected fluorescence signal increased as the concentration of hymenocardine increases. Possibly, hymenocardine forms a fluorescent complex with BSA, thus causing interference in the detection of AGEs in the BSA-Glc assay.

At λ_{exc} 370 - λ_{em} 440 nm, for all three types of samples the fluorescence signal showed a positive correlation to the concentration of hymenocardine. Therefore, it must be concluded that in both sets of wavelengths interference will occur due to the presence of hymenocardine and the results obtained with a standard BSA-Glc assay will not lead to reliable results for this cyclopeptide alkaloid. Apart from hymenocardine, a concentration-dependent increase in fluorescence was also found for oxyphylline-F, with or without BSA (Figure 9.3) and interference in the BSA-Glc assay also led to aberrant results for this cyclopeptide alkaloid.

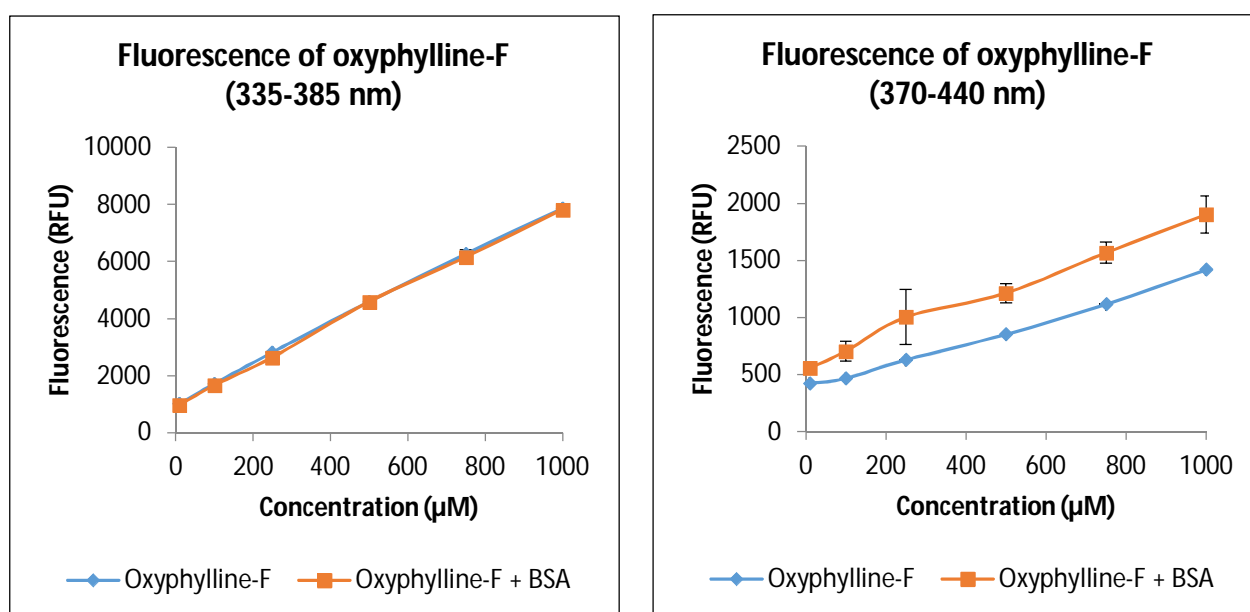


Fig. 9.3 Fluorescence of oxyphylline-F (final concentration 0 to 1000 μM) with and without BSA. Left: detection at λ_{exc} 335 - λ_{em} 385 nm. Right: detection at λ_{exc} 370 - λ_{em} 440 nm.

Theoretically, subtraction of the signal of the blank samples would correct for the interference of the tested compounds; however, since the autofluorescence affected the measured fluorescence signal in the BSA-Glc samples to a great extent, this was not considered appropriate. In order to limit the interference, the BSA-Glc assay was eventually performed with lower concentrations of the test compounds (0.05mM, 0.25 mM and 0.5 mM of hymenocardine, hemsine-A, nummularine-R and oxyphylline-F) and the results are shown in Figure 9.4.

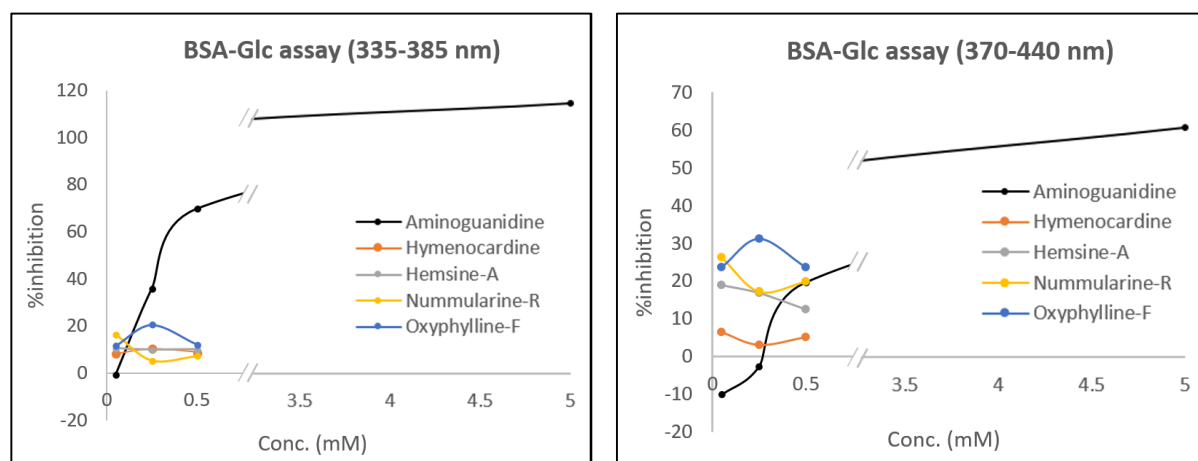


Fig. 9.4 AGEs inhibition of hymenocardine, hemsine-A, nummularine-R and oxyphylline-F (final concentration between 0.05 and 0.5 mM) and aminoguanidine (final concentration between 0.05 and 5 mM), according to the BSA-Glc assay. Left: detection at λ_{exc} 335 - λ_{em} 385 nm. Right: detection at λ_{exc} 370 - λ_{em} 440 nm.

Lowering the concentration of the test compounds will obviously lead to lowered interference due to autofluorescence, but no clear AGEs inhibition could be seen for any of the cyclopeptide alkaloids in this concentration range.

Aminoguanidine, the positive control, was used in a concentration range of 0.05 mM up to 5 mM and displayed an IC_{50} value of approximately 3 mM in relation to inhibition of vesperlysine-like AGEs formation (370-440 nm); six times higher than the highest tested concentration of the cyclopeptide alkaloids. Thus, the fact that no clear inhibition by hymenocardine, hemsine-A, nummularine-R or oxyphylline-F could be observed in this experiment, does not infer the total lack of AGEs inhibiting properties. Perhaps the test compounds would show activity in higher concentrations. However, as mentioned before, it is not possible to obtain reliable readings for those more highly concentrated samples.

At λ_{exc} 335 - λ_{em} 385 nm, the IC_{50} value found for aminoguanidine is significantly lower, and does fall within the concentration range used for the cyclopeptide alkaloids, but no clear AGEs inhibition was found for any of the cyclopeptide alkaloids at this set of wavelengths either.

In conclusion, no AGEs inhibiting potential could be proven for the four tested cyclopeptide alkaloids based on the results of the BSA-Glc test. Since the followed methodology did not lead to satisfactory results, attempts were made to develop alternative, more reliable methods.

9.3.2 BSA-Glc assay, with protein precipitation

In order to eliminate any possible interference of the test compounds in the fluorescence measurement, the extended BSA-Glc assay with protein precipitation was performed. Samples were prepared and incubated in the same way as in the regular BSA-Glc assay, but after AGEs formation has taken place, proteins are precipitated with trichloroacetic acid. Next, the supernatant, containing remaining free glucose and test compound is removed and the precipitate is redissolved. The fluorescence intensity of these samples is measured, and thus, only fluorescence of protein-bound AGEs is taken into account.

The results that were obtained for hymenocardine, hemsine-A and nummularine-R are shown in Figure 9.5 and Table 9.1.

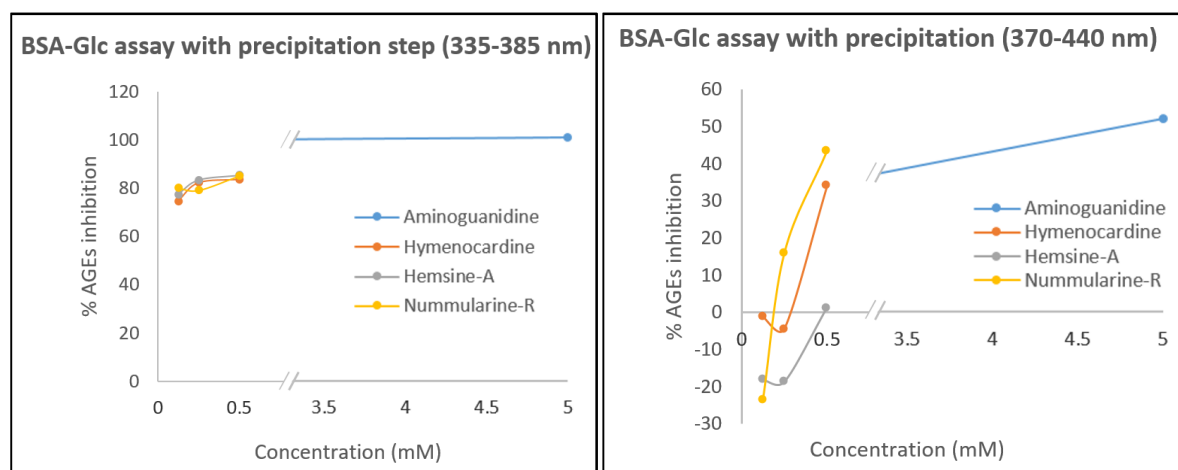


Fig. 9.5 AGEs inhibition by hymenocardine, hemsine-A, nummularine-R (final concentration between 0.125 and 0.5 mM) and aminoguanidine (final concentration between 1.25 and 5 mM), according to the BSA-Glc assay, with protein precipitation. Left: detection at λ_{exc} 335 - λ_{em} 385 nm. Right: detection at λ_{exc} 370 - λ_{em} 440 nm.

Table 9.1 Fluorescence values and calculated data for the BSA-Glc assay with protein precipitation.

AGEs inhibition at 370 nm / 440 nm.									
compound	Conc. (mM)	RFU (1) (x10 ⁴)	RFU (2) (x10 ⁴)	Avg. RFU (x10 ⁴)	RFU bl (1) (x10 ⁴)	RFU bl (2) (x10 ⁴)	Avg. RFU bl (x10 ⁴)	RFU - RFU bl (x10 ⁴)	%inh
aminoguanidine	5	2.0	2.1	2.1	1.1	1.1	1.1	1.0	52
	2.5	2.5	2.5	2.5	1.0	1.1	1.1	1.4	30
	1.25	2.7	2.9	2.8	1.1	1.1	1.1	1.6	19
hymenocardine	0.5	3.8	3.6	3.7	2.2	2.5	2.4	1.3	34
	0.25	3.2	3.8	3.5	1.3	1.4	1.4	2.1	-5
	0.125	3.5	3.2	3.4	1.3	1.3	1.3	2.1	-1
hemsine-A	0.5	3.2	3.4	3.3	1.3	1.2	1.3	2.0	1
	0.25	4.5	3.1	3.8	1.4	1.4	1.4	2.4	-19
	0.125	3.7	4.00	3.9	1.7	1.2	1.5	2.4	-18
ramosine-A	0.5	3.3	3.2	3.3	2.8	1.4	2.1	1.2	43
	0.25	3.5	3.3	3.4	2.1	1.3	1.7	1.7	16
	0.125	3.4	4.5	3.9	1.5	1.3	1.4	2.5	-24
control		3.3	3.5	3.4	1.2	1.4	1.3	2.0	

AGEs inhibition at 335 nm / 385 nm.									
compound	Conc. (mM)	RFU (1) (x10 ⁴)	RFU (2) (x10 ⁴)	Avg. RFU (x10 ⁴)	RFU bl (1) (x10 ⁴)	RFU bl (2) (x10 ⁴)	Avg. RFU bl (x10 ⁴)	RFU - RFU bl (x10 ⁴)	%inh
aminoguanidine	5	3.8	3.8	3.8	3.7	3.9	3.8	-0.02	101
	2.5	3.8	3.9	3.8	3.7	3.9	3.8	0.01	99
	1.25	3.9	4.0	4.0	3.8	3.9	3.9	0.1	95
hymenocardine	0.5	4.1	4.3	4.2	3.8	3.9	3.9	0.3	84
	0.25	4.1	4.3	4.2	3.8	3.9	3.8	0.4	82
	0.125	4.2	4.3	4.2	3.7	3.8	3.7	0.5	75
hemsine-A	0.5	4.0	4.2	4.1	3.9	3.8	3.8	0.3	85
	0.25	4.3	4.1	4.2	3.9	3.8	3.8	0.3	83
	0.125	4.2	4.2	4.2	3.9	3.7	3.8	0.5	78
ramosine-A	0.5	4.1	4.1	4.1	3.8	3.8	3.8	0.3	85
	0.25	4.2	4.1	4.2	3.8	3.8	3.8	0.4	79
	0.125	4.2	4.3	4.2	3.9	3.8	3.8	0.4	80
control		4.2	4.0	4.1	3.8	3.7	3.7	0.4	

RFU: relative fluorescence units; Avg.: average; bl: blank; %inh: % of inhibition.

When comparing the results obtained at λ_{exc} 370 nm and λ_{em} 440 nm, in most test samples which initially contained cyclopeptide alkaloids, the fluorescence signal is still higher than the fluorescence in the control sample, indicating that not all interfering products are removed after precipitation. A possible explanation is that the tested compounds may have bound to BSA, as mentioned previously for hymenocardine, and in that case, they will not be removed by following the precipitation procedure. Thus, the %AGEs inhibition still can not be determined accurately. The results obtained for aminoguanidine are in correspondence to the results of the standard BSA-Glc assay.

As for the AGEs detected at λ_{exc} 335 nm and λ_{em} 385 nm, the values of the test samples and the blank samples lie approximately in the same range, while this was not the case prior to precipitation. This could indicate that a significant amount of the pentosidine-like AGEs was not precipitated, but remained in the supernatant, and thus, could not be detected. Possibly the pentosidine-like AGEs occur in free, non-protein bound form more than vesperlysine-like AGEs.

Interestingly, the test samples prepared with hemsine-A in a concentration of 0.5 mM show fluorescence values of around 32,800 RFU, while the samples with a concentration of 0.125 mM hemsine-A had fluorescence values of approximately 38,600 RFU (at 370 nm / 440 nm). The latter result indicates that auto-fluorescence is still present, since the control samples (with maximum AGEs formation) only showed a fluorescence signal of 33,750 RFU. However, if it is hypothesized that the increase to 38,600 RFU is due to auto-fluorescence, then even higher RFU values would be expected for the samples with higher concentrations of hemsine-A. The fact that lower values are found, might indicate that hemsine-A does have AGEs inhibiting activity, even though the values do not differ much from the values obtained for the control samples. This can be explained as follows: the measured RFU value is defined by the fluorescence signal originating from the AGEs plus the auto-fluorescence signal of the tested cyclopeptide alkaloid. The samples with higher concentrations of hemsine-A will show more profound autofluorescence, but if the detected fluorescence intensity is similar to the control sample, less AGEs must be present in the sample with hemsine-A, and thus, the hemsine-A must have prohibited AGEs formation to a certain extent. However, since the auto-fluorescence signal and the fluorescence signal due to AGEs can not be distinguished, the %AGEs inhibition can not be calculated.

9.3.3 BSA-MGO assay

In the BSA-MGO assay, AGEs formation occurs solely through non-oxidative reactions. Since dicarbonyl compounds, like MGO, are much more reactive compared to glucose, 24 h of incubation of the samples is sufficient, vs. 7 days in the BSA-Glc assay. Based on the results of this experiment, it can be distinguished whether the AGEs inhibiting activity of a test compound is due to antioxidant or metal chelating properties, or if the activity must be attributed to another mechanism of action.

The assay was performed with hymenocardine, hemsine-A, nummularine-R, oxyphylline-F and aminoguanidine (reference compound) in the same concentrations as used in the BSA-Glc assay and the results are shown in Figure 9.6.

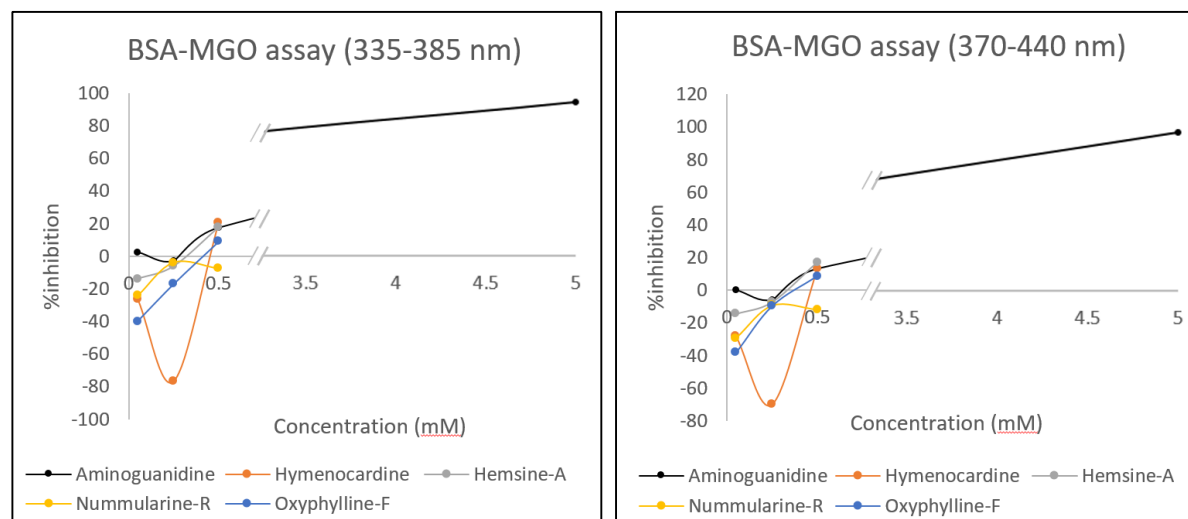


Fig. 9.6 AGEs inhibition by hymenocardine, hemsine-A, nummularine-R, oxyphylline-F (final concentration between 0.05 and 0.5 mM) and aminoguanidine (final concentration between 0.05 and 5 mM), according to the BSA-MGO assay. Left: detection at λ_{exc} 335 - λ_{em} 385 nm. Right: detection at λ_{exc} 370 - λ_{em} 440 nm.

As in the BSA-Glc assay, no AGEs inhibiting activity was found for any of the cyclopeptide alkaloids in the concentration range in which they were tested. Also here, it must be noted that these compounds might express AGEs inhibiting properties in a higher concentration range, as is the case for the reference compound aminoguanidine. However, due to the autofluorescence of the test compounds, no reliable readings can be performed at higher concentrations.

Choudhary *et al.* (2012) reported an IC_{50} value of $277.7 \pm 7.6 \mu\text{M}$ for hemsine-A and an IC_{50} value of $720.2 \pm 10.9 \mu\text{M}$ for nummularine-R in the BSA-MGO assay. These results could not be reproduced by us. It has to be taken in mind though, that their experimental procedure involved incubation for 9 days as opposed to only a 1-day incubation period in our case. Moreover, they did not include extra steps to correct for the auto-fluorescence of the test compounds.

9.3.4 Fructosamine determination

Fructosamine is an Amadori product and is thus formed in the early stages of the glycation process. In this specific assay, fructosamine will react with NBT, resulting in oxidation of fructosamine into fructosimine and reduction of NBT into formazan, the latter being detected by measuring the visible light intensity of the sample at 530 nm. In case the tested compounds are able to cause a significant reduction in the amount of fructosamine, it can be deduced that their mode of action relies either on inhibition of the Schiff base formation or inhibition of the Amadori rearrangement. The assay was performed with the samples that were prepared conform the BSA-Glc assay and the results are shown in Figure 9.7.

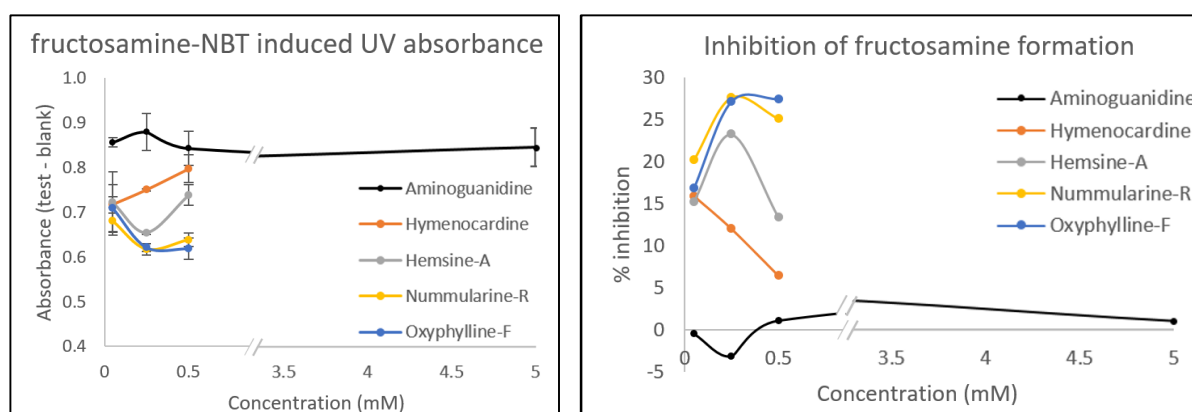


Fig. 9.7 Inhibition of fructosamine formation by hymenocardine, hemsine-A, nummularine-R, oxyphylline-F (final concentration between 0.05 and 0.5 mM) and aminoguanidine (final concentration between 0.05 and 5 mM). Left: UV absorbance at 530 nm after reaction of BSA-Glc samples with NBT. Right: % fructosamine inhibition.

As for the determination of the amount of fructosamine, in most articles aminoguanidine is used as a positive control, despite it is only a weak inhibitor of fructosamine formation. The same result was found by us; however, in order to check the performance of the applied method, it would be useful to include a positive control which displays a more profound activity. A literature search was conducted to identify such a positive control compound, but no alternative to aminoguanidine was found. Thus, the performance of our method could not be proven. Moreover, the results obtained for the cyclopeptide alkaloids are not very consistent, and again do not allow to draw solid conclusions.

9.3.5 Dicarbonyl entrapment

In the dicarbonyl entrapment assay, the entrapment of GO is monitored for a period of 120 min following addition of the test compound to a GO solution. The relative amount of GO is determined after reaction with the Girard-T reagent, forming a hydrazone, which is detected at 290 nm. The experiment was conducted with four of the isolated cyclopeptide alkaloids, namely, hymenocardine, hemsine-A, nummularine-R and oxyphylline-F. Aminoguanidine was used as a reference compound. The results are shown in Figure 9.8.

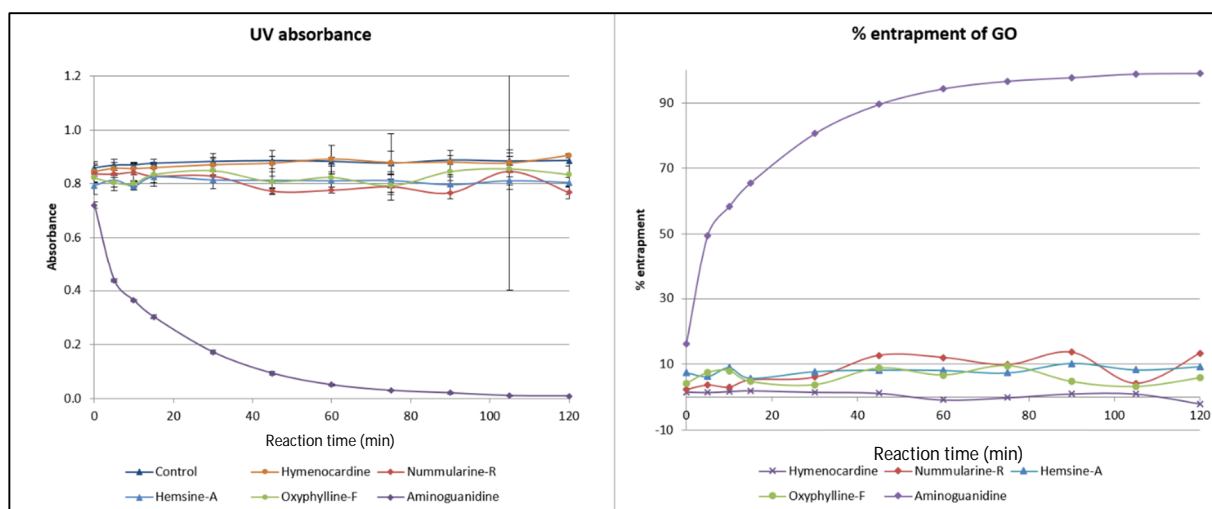


Fig. 9.8 Results of the dicarbonyl entrapment assay. Test compounds (final concentration: 0.50 mM) were incubated with GO (final concentration 0.55 mM) and the UV absorbance was measured at 290 nm after reaction of GO with Girard-T reagent.

Left: Change of UV absorbance in time. Right: % of GO entrapment.

Aminoguanidine clearly showed GO entrapment. After 5 min, already a 49.5 ± 0.7 % reduction in GO is measured. After 60 min, 94.3 ± 1.7 % of the GO is trapped. After 120 min only 1.1 % of the initial amount of GO is remaining. As for the tested cyclopeptide alkaloids, the highest GO entrapment, 13.6 ± 0.4 % and 13.4 ± 0.4 , measured after 90 min and 120 min, respectively, was found for nummularine-R. However, it has to be noted that the results obtained at different time points are not consistent and at 105 min only 4% GO entrapment was found. Nonetheless, a trend can be seen, indicating that nummularine-R acts as a weak AGEs inhibitor by dicarbonyl entrapment. Hemsine-A showed up to 9% GO entrapment, which was rather consistent within the 2-hour period, while for oxyphylline-F the results fluctuated over time and it has to be concluded that this compound does not display any clear activity in this assay. Hymenocardine did not show GO entrapment.

All four tested cyclopeptide alkaloids show UV absorbance at 290 nm to a certain extent themselves. This caused interference in the obtained results, which is corrected for by subtracting the values obtained for the respective blank samples. The strongest interference was seen for oxyphylline-F and absorbance values outside the linear range of the spectrophotometer were measured for these samples. Possibly, this is an explanation for the fluctuating results that were found for this compound.

9.3.6 ELISA experiment

The ELISA assay that was performed is a quantitative competitive immunoassay. A schematic overview of the assay is shown in Figure 9.1. The 96-well plate is coated with an AGEs specific antibody. Samples or standards are incubated in each well, along with an AGEs-HRP (horseradish peroxidase) conjugate. The AGEs in the samples or standards will compete with the AGEs-HRP conjugate for binding to the plate-bound antibody, and higher levels of AGEs from samples or standards will lead to decreased binding of AGEs-HRP conjugate binding. The captured AGEs-HRP conjugate will convert substrates A and B into colorimetric reaction products, which can be quantitatively measured by the absorbance signal at 450 nm.

Since this assay is highly specific, and since any possible interfering test compounds are removed during the wash step, the problems that were faced in the above mentioned assays were expected to be overcome by using this assay.

Six standard solutions, included in the ELISA kit, and with an AGEs concentration ranging from 0 to 1000 pg/mL, were analyzed in duplo. The measured absolute absorbance values were converted to relative values (%A, compared to the standard with the highest measured absorbance, containing 0 pg/mL AGEs) and a sigmoidal, 4 parameter logistic calibration curve was made, using the 12 values obtained for the standard solutions (Figure 9.9).

	conc. AGEs (pg/mL)	Log conc. AGEs	A (1)	A (2)	A% (1)	A% (2)
Std. A	0	0	1.601	1.724	92.87	100.00
Std. B	50	1.699	1.464	1.515	84.92	87.88
Std. C	100	2.000	1.241	1.206	71.98	69.95
Std. D	250	2.398	0.738	0.797	42.81	46.23
Std. E	500	2.699	0.436	0.473	25.29	27.44
Std. F	1000	3.000	0.209	0.221	12.12	12.82

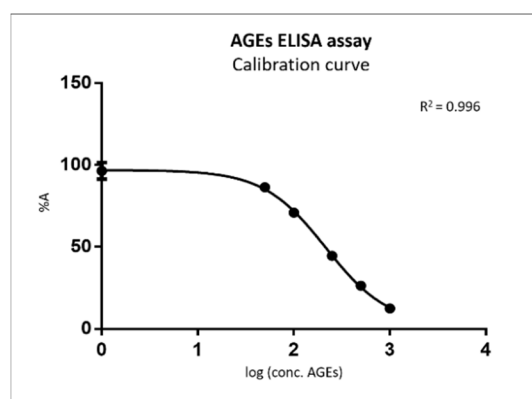


Fig. 9.9 Results obtained with the AGEs ELISA assay for 6 standard solutions of AGEs, analyzed in duplo.

The concentration of AGEs present in the test samples can now be deduced by interpolation. In order to establish the applicability of this ELISA assay, the experiment was first performed with two known AGEs inhibitors. The following samples were prepared, according to the BSA-Glc assay: two control samples, three test samples with aminoguanidine (25 mM, 10 mM, 5 mM final conc.), three test samples with quercetin (25 mM, 10 mM, 5 mM), one blank sample with aminoguanidine (25 mM) and one blank sample with quercetin (25 mM). (The concentrations of the test compounds are relatively high; in the range of, or higher than the expected IC_{50} -value, to be able to see a clear inhibitory effect in the results of the ELISA assay.) After 7 days of incubation, the ELISA assay was performed and the results are shown in Table 9.2.

Table 9.2 Data obtained with AGEs ELISA assay, performed on samples resulting from the BSA-Glc assay.

sample	conc. test compound (mM)	A (1)	A (2)	A% (1)	A% (2)	log conc. test compound	% Abs	conc. AGEs (pg/mL)
control 1		0.657	0.703	39.44	40.78	2.46	40.11	291
control 2		0.645	0.609	36.37	35.32	2.53	35.85	336
control, bl		0.794	0.774					245
aminoguanidine	25	0.591	0.546	32.98	31.67	2.58	32.32	381
aminoguanidine	10	0.714	0.716	41.47	41.53	2.44	41.50	278
aminoguanidine	5	0.700	0.737	41.68	42.75	2.43	42.21	272
aminoguanidine (blank)	25	0.501						431
quercetin	25	0.121	0.130	7.28	7.54	3.26	7.41	1810
quercetin	10	0.105	0.107	6.15	6.21	3.35	6.18	2239
quercetin	5	0.127	0.126	7.34	7.31	3.26	7.32	1834
quercetin (blank)	25	0.340						653

bl: blank sample; AG: aminoguanidine; QUE: quercetin.

In the control samples, without inhibition of AGEs formation, an average concentration of 314 pg/mL AGEs was found (38.0 A%). In the samples incubated with aminoguanidine and quercetin, higher absorbance values would be expected, since less AGEs are supposed to be formed. However, the measured absorbance values do not reflect this. Moreover, the blank samples, which are supposed to contain the lowest amount of AGEs, should give the highest absorbance values and this is not the case for aminoguanidine, nor for quercetin.

With quercetin, solubility issues were observed, which might have caused the aberrant results. Thus, the experiment was repeated with lower concentrations of the test compound (0.50 mM, 0.25 mM and 0.05 mM). This resulted in relative absorbance values of 2.2 %, 3.6 % and 9.5%, respectively, while for the control samples, values in the same range as during the previous experiment were found (37.8% and 39.1%). Again, this would lead to the conclusion that more AGEs are present in the samples with quercetin, compared to the control samples. Overall, it must be concluded that this ELISA-assay is not a good method for determining *in vitro* AGEs inhibition for samples prepared according to the BSA-glucose method.

9.4 Conclusions

In order to investigate the AGEs inhibiting properties of cyclopeptide alkaloids, several assays were performed, either to determine general AGEs inhibition or to investigate the inhibition of a specific step in the AGEs pathway.

The BSA-Glc assay is suitable for the assessment of general AGEs inhibition, in case there is no strong interference of the test compound. The BSA-Glc method followed by an additional precipitation step to remove remaining free Glc and test compound is not sufficient to fully eliminate any interference problems. The BSA-MGO can indicate inhibition of non-oxidative AGEs formation, but can also only be applied when the test compounds do not cause interference in the measured fluorescence signal.

As for the determination of the amount of fructosamine, in most articles, aminoguanidine is used as a positive control, despite it is only a very weak inhibitor of fructosamine formation. Thus, it is not clear how reliable the experimental method is. Moreover, also in this assay some cyclopeptide alkaloids showed interference in the detected absorbance signal, and the results are not conclusive.

Furthermore, the ELISA did not give satisfactory results, not even for aminoguanidine or quercetine as positive control compounds, and also this assay was not considered as reliable.

Aminoguanidine is a potent, well-known dicarbonyl entrapping compound, and indeed, this was also found in our GO entrapment assay. However, no clear activity was found in this experiment for any of the tested cyclopeptide alkaloids.

In conclusion, further research is needed in order to develop a reliable method for the determination of AGEs inhibition, which can be used for a wide range of compounds, including the cyclopeptide alkaloids (See 'General conclusions and future perspectives').

References

- Chompoo, J., Upadhyay, A., Kishimoto, W., Makise, T. and Tawata, S., 2011. Advanced glycation end products inhibitors from *Alpinia zerumbet* rhizomes. *Food Chem* **129**(3): 709-715.
- Choudhary, M. I., Adhikari, A., Rasheed, S., Marasini, B. P., Hussain, N., Kaleem, W. A. and Attur-Rahman, 2011. Cyclopeptide alkaloids of *Ziziphus oxyphylla* Edgw as novel inhibitors of alpha-glucosidase enzyme and protein glycation. *Phytochem Lett* **4**(4): 404-406.
- Jang, D. S., Lee, G. Y., Kim, Y. S., Lee, Y. M., Kim, C. S., Yoo, J. L. and Kim, J. S., 2007. Anthraquinones from the seeds of *Cassia tora* with inhibitory activity on protein glycation and aldose reductase. *Biol Pharm Bull* **30**(11): 2207-2210.
- Kiho, T., Usui, S., Hirano, K., Aizawa, K. and Inakuma, T., 2004. Tomato paste fraction inhibiting the formation of advanced glycation end-products. *Biosci Biotech Bioch* **68**(1): 200-205.
- Matsuura, N., Aradate, T., Sasaki, C., Kojima, H., Ohara, M., Hasegawa, J. and Ubukata, M., 2002. Screening system for the Maillard reaction inhibitor from natural product extracts. *J Health Sci* **48**(6): 520-526.
- Sadowska-Bartosz, I., Galiniak, S. and Bartosz, G., 2014. Kinetics of glycoxidation of bovine serum albumin by glucose, fructose and ribose and its prevention by food components. *Molecules* **19**(11): 18828-18849.
- Sero, L., Sanguinet, L., Blanchard, P., Dang, B. T., Morel, S., Richomme, P., Seraphin, D. and Derbre, S., 2013. Tuning a 96-well microtiter plate fluorescence-based assay to identify AGE inhibitors in crude plant extracts. *Molecules* **18**(11): 14320-14339.
- Upadhyay, A., Tuenter, E., Ahmad, R., Amin, A., Exarchou, V., Apers, S., Hermans, N. and Pieters, L., 2014a. Kavalactones, a novel class of protein glycation and lipid peroxidation inhibitors. *Planta Med* **80**(12): 1001-1008.
- Upadhyay, A., Tuenter, E., Amin, A., Exarchou, V., Hermans, N., Apers, S. and Pieters, L., 2014b. 5-O-demethylnobiletin, a polymethoxylated flavonoid, from *Citrus depressa* Hayata peel prevents protein glycation. *J Funct Foods* **11**: 243-249.

GENERAL CONCLUSIONS AND FUTURE PERSPECTIVES

The aim of this project was to perform a targeted isolation and structure elucidation of cyclopeptide alkaloids, to assess their antiplasmodial activity, cytotoxicity and AGEs inhibiting properties, and to establish structure-activity relationships. For this purpose, four plants were selected: *Hymenocardia acida*, *Ziziphus oxyphylla*, *Ziziphus nummularia* and *Ziziphus spina-christi*. Moreover, the gastrointestinal absorption and metabolism of cyclopeptide alkaloids should be taken into account when considering *in vivo* experiments, and thus, hymenocardine was investigated for its gastrointestinal stability after oral ingestion, and for its hepatic metabolism.

Twenty cyclopeptide alkaloids in total were isolated from *Hymenocardia acida*, *Ziziphus oxyphylla*, *Ziziphus nummularia* and *Ziziphus spina-christi*, of which 11 were reported for the first time: hymenocardinol, hymenocardine *N*-oxide and hymenocardine-H from *H. acida*; *O*-desmethylnummularine-R, *O*-desmethylnummularine-R *N*-oxide, hemsine-A *N*-oxide, oxyphyllines-E and -F from *Z. oxyphylla*; nummularine-U from *Z. nummularia* and spinanines-B and -C from *Z. spina-christi*. (Although it is not uncommon that cyclopeptide alkaloids are isolated as *N*-oxides, together with tertiary amines, the possibility that the *N*-oxides are artefacts formed during drying, extraction, or isolation cannot completely be excluded.)

For 14 of these cyclopeptide alkaloids, antiplasmodial and cytotoxic activities were determined. Moreover, the antiplasmodial activity and cytotoxicity of five cyclopeptide alkaloids, previously isolated during another project, were assessed. From the 19 tested compounds, an IC_{50} -value below 10 μM against *Plasmodium falciparum* K1 was found for 8 compounds. Spinanine-B showed the most promising results with an IC_{50} value of $2.1 \pm 0.3 \mu M$ against *P. falciparum*, and no cytotoxic effects against MRC-5 cells in concentrations up to 64.0 μM . However, since over 200 cyclopeptide alkaloids are known, and a vast majority has not been tested for their antiplasmodial and cytotoxic activities, it would be interesting to expand the research, to isolate more compounds and to assess also their activity. Moreover, it is expected that this will lead to the discovery of new cyclopeptide alkaloids, given the fact that 39 new cyclopeptide alkaloids were reported in the last decade, and that the existence of other cyclopeptide alkaloids, in particular neutral ones, seems plausible.

Both a qualitative and a quantitative structure-activity relationship (SAR) study were performed, based on the obtained set of 19 cyclopeptide alkaloids and their corresponding IC₅₀ values against *P. falciparum*.

The qualitative SAR study indicated that a 13-membered ring is preferred over a 14-membered ring, and that methoxylation in position 2 of the styrylamine moiety, which takes part in this ring, is beneficial, although also hydroxylated compounds displayed antiplasmodial activity. Moreover, the presence of a β -hydroxy proline moiety could correlate with a higher antiplasmodial activity. However, in order to confirm the importance of the methoxy group and the β -hydroxy proline moiety, and in order to determine the exact role of different aliphatic amino acids (leucine, isoleucine, valine) in either the macrocyclic ring or the side chain, further research is required.

In the quantitative SAR study, QSAR models were developed, based on PLS and MLR modelling. These QSAR models define quantitative correlations between molecular descriptors and the antiplasmodial activity and indicated which molecular descriptors can explain most of the variance regarding the antiplasmodial activity. The obtained models can be applied for the prediction of the antiplasmodial activity of other cyclopeptide alkaloids. However, although the predictions that were made seemed to confirm the findings of our qualitative study, they were often extrapolations relative to our small calibration set. Therefore, it would be valuable to obtain more alkaloids and to expand the dataset with additional molecular descriptors and bioactivity results. This will allow a more profound qualitative SAR study and will lead to the creation of QSAR models with a higher predictive value. Furthermore, the results of the cytotoxicity tests could be integrated in the models, and in this way predictions can be made, not only for compounds with high antiplasmodial activity, but also for compounds with a high selectivity index.

In the current work, predictions were made for certain cyclopeptide alkaloids, of which the existence in Nature has not yet been reported, but for which a high antiplasmodial activity could be expected based on the SAR study. It would be interesting to obtain these compounds, possibly by (semi)-synthesis, and to establish their activity as well, which could result in the identification of a new lead compound. Moreover, in this way the predictive value of the developed QSAR models could be checked.

The research concerning the gastrointestinal absorption and metabolism of hymenocardine led to the conclusion that this cyclopeptide alkaloid is absorbed from the gastrointestinal tract after oral ingestion at least in part unchanged, and resulted in the identification of hymenocardinol as its major metabolite *in vivo*. Moreover, several metabolites were found *in vitro*, after incubation with a S9 fraction, the major ones being hymenocardinol, *N*-monomethylhymenocardine and *N*-monomethylhymenocardinol. However, these results also raise many more questions which could be investigated in future projects. First of all, it would be interesting to perform a pharmacokinetic study with hymenocardine. The study reported in Chapter 7 was mainly intended for obtaining qualitative information, and was not performed for quantitative purposes, and another *in vivo* experiment with both IV and PO (per os) administration could be performed, in order to determine, for example, the t_{\max} and bioavailability of hymenocardine. Apart from this, it would be valuable to carry out the same type of research on other cyclopeptide alkaloids. Most cyclopeptide alkaloids contain a *p*-hydroxystyrylamine moiety and not a *p*-hydroxy- ω -amino acetophenone moiety, as in hymenocardine. The reduction of this acetophenone moiety was found to result in the formation of hymenocardinol, as a major metabolite. Thus, for other cyclopeptide alkaloids a different metabolism pathway is expected and it would be interesting to obtain more insight in these pathways. In addition, it would be valuable to determine the antiplasmodial and cytotoxic activities of the metabolites, since this can be of great importance to the therapeutic effect of the administered alkaloid. To obtain sufficient amounts of the respective metabolites for performing these bioactivity assays, the metabolites either should be formed in higher quantities by carrying out the S9 experiment on a larger scale, followed by their purification, or they could be obtained by (semi-) synthesis.

Apart from that, additional studies in rats could be performed for the most promising cyclopeptide alkaloids, in order to determine their *in vivo* antiplasmodial activity.

As for the experiments performed in relation to the AGEs, we faced several drawbacks when applying the most commonly used methods, and efforts still have to be made to develop a reliable method, which can be used for a wide range of compounds. Currently, the development of an LC-MS method is ongoing in our lab. With this method, it will be possible to quantify specific AGEs, like CML and CEL, which will serve as markers for the general AGEs inhibition. Mass spectrometry is both a sensitive and a specific technique, thus eliminating the

problem of interference of the tested compounds. Furthermore, additional experiments, like the assessment of the dicarbonyl entrapment, can still be carried out for compounds that possess activity, in order to obtain knowledge about their mechanism of action.

SUMMARY

Cyclopeptide alkaloids are polyamidic, macrocyclic compounds, containing a 13- 14- or 15-membered ring. The ring system consists of a hydroxystyrylamine moiety, an amino acid and a β -hydroxy amino acid; attached to the ring is a side chain, which is usually comprised of one or two more amino acid moieties. This relatively small class consists of approximately 230 known compounds, with 39 new cyclopeptide alkaloids reported in the past decade. Although they occur in various plant families, they are most widely distributed in the Rhamnaceae family, notably the genus *Ziziphus*.

In traditional medicine, several cyclopeptide alkaloid-containing plants are used for the treatment of malaria, for example, *Hymenocardia acida*, and *in vitro* antiplasmodial activity was reported for a limited number of compounds belonging to this class. Thus, one specific aim of this research was to isolate cyclopeptide alkaloids from selected plant species and to assess their antiplasmodial activity, together with their cytotoxicity.

Moreover, plants containing cyclopeptide alkaloids, like *Ziziphus oxyphylla*, are traditionally used in the treatment of diabetes. The increased formation of AGEs is thought to play a role in the development of diabetic complications and *in vitro* AGEs inhibiting activity was reported for nummularine-R and hemsine-A. Thus, investigation of the AGEs inhibiting properties of the isolated cyclopeptide alkaloids was selected as the second target of this PhD research.

Based on the obtained results, a structure-activity relationship study could then be performed to reveal which structural features of this class of compounds are of importance in order to express biological activity.

From the root bark of *Hymenocardia acida*, four cyclopeptide alkaloids were isolated. In addition to the known compound hymenocardine, three other alkaloids were isolated for the first time from a natural source. These included a hymenocardine derivative with a hydroxy group instead of a carbonyl group, which was named hymenocardinol, as well as hymenocardine *N*-oxide, and a new cyclopeptide alkaloid containing an unusual histidine moiety named hymenocardine-H. The isolated cyclopeptide alkaloids were tested for their antiplasmodial activity and cytotoxicity. All four compounds showed moderate antiplasmodial activity, with IC₅₀ values ranging from 12.2 to 27.9 μ M, the most active one being hymenocardine *N*-oxide, with an IC₅₀ value of $12.2 \pm 6.6 \mu$ M.

Nine cyclopeptide alkaloids, of which five were described herein for the first time, were isolated from roots of *Ziziphus oxyphylla*. Nummularine-R, a previously known constituent from this species, was isolated along with its new derivatives *O*-desmethylnummularine-R and *O*-desmethylnummularine-R *N*-oxide. In addition, the known compounds hemsine-A and ramosine-A, as well as hemsine-A *N*-oxide were isolated. Moreover, oxyphylline-C, a known constituent of *Z. oxyphylla* stems, was obtained, and two new compounds were identified, oxyphyllines-E and -F. Just like oxyphylline-C, oxyphyllines-E and -F belong to the relatively rare class of neutral cyclopeptide alkaloids. The antiplasmodial activity and cytotoxicity of five out of nine alkaloids was evaluated and the most promising activity was found for *O*-desmethylnummularine-R, which exhibited an IC₅₀ value of $3.2 \pm 2.6 \mu\text{M}$ against *Plasmodium falciparum* K1, whereas an IC₅₀ value of $> 64.0 \mu\text{M}$ was evident for its cytotoxicity against MRC-5 cells.

Seven cyclopeptide alkaloids were isolated from the stem bark of *Ziziphus nummularia* and *Ziziphus spina-christi*. Three new compounds were identified: nummularine-U from *Z. nummularia*, and spinanines-B and -C from *Z. spina-christi*, together with the known compounds mauritine-F, nummularines-D and -E, and amphibine-D. The antiplasmodial activity was determined for five of them and spinanine-B displayed the highest activity with an IC₅₀ value of $2.1 \pm 0.3 \mu\text{M}$ against *Plasmodium falciparum* K1, whereas no cytotoxic effects were observed against MRC-5 cells in concentrations up to $64.0 \mu\text{M}$.

Thus, a total of 20 cyclopeptide alkaloids were isolated from *Hymenocardia acida*, *Ziziphus oxyphylla*, *Ziziphus nummularia* and *Ziziphus spina-christi*, by means of conventional separation methods as well as semi-preparative HPLC with DAD and ESIMS detection and LC-DAD-(HRMS)-SPE-NMR. Structure elucidation was done by spectroscopic means. Eleven out of 20 cyclopeptide alkaloids were reported for the first time and for 14 of the obtained compounds, **antiplasmodial** and **cytotoxic activities** were determined. Moreover, the antiplasmodial activity and cytotoxicity of five cyclopeptide alkaloids, previously isolated during another project, were assessed. Overall, the result of spinanine-B was the most promising.

Based on the obtained set of 19 cyclopeptide alkaloids and their corresponding IC₅₀ values against *P. falciparum*, both a **qualitative** and a **quantitative structure-activity relationship study** were performed. The qualitative SAR study indicated that a 13-membered macrocyclic ring is preferable over a 14-membered one. Furthermore, the presence of a β -hydroxy proline moiety could correlate with higher antiplasmodial activity, and also methoxylation (or, to a lesser extent, hydroxylation) of the styrylamine moiety could be important for displaying antiplasmodial activity. In addition, QSAR models were developed, using PLS and MLR. These models allow indicating the most important descriptors (molecular properties) responsible for the antiplasmodial activity and can be used to make predictions for the antiplasmodial activity of other cyclopeptide alkaloids. Predictions made for interesting structures, as deduced from the qualitative SAR study, were not in contradiction with the expectations raised in that study.

When considering *in vivo* experiments with cyclopeptide alkaloids, a factor that has to be taken into account is, in view of their peptide-like nature, the potential **metabolism** after oral ingestion. Thus, a study was performed with hymenocardine, in order to assess its stability, small intestinal absorption and hepatic metabolism. Analysis of the dialyzate and retentate obtained from the GIDM, indicated that hymenocardine is absorbed unchanged from the gastrointestinal tract, at least in part. After S9 metabolism, several metabolites of hymenocardine could be identified, the major ones being formed by reduction, and/or the loss of an *N*-methyl group. The *in vivo* study confirmed that hymenocardine is absorbed from the gastrointestinal tract unchanged, since it could be identified in both rat plasma and urine, together with hymenocardinol, its reduction product.

As for the **AGEs inhibiting properties** of cyclopeptide alkaloids, unfortunately no solid conclusions could be drawn. Several drawbacks were encountered when applying the most commonly used methods, and hindered any progress in relation to this specific target. However, the development of a new method for determining AGEs inhibition is ongoing, and once this method is validated, it will be possible to assess the inhibition of AGEs formation by the acquired set of cyclopeptide alkaloids.

SAMENVATTING

Cyclopeptide alkaloiden zijn polyamidische, macrocyclische producten, die een 13-, 14- ofwel 15-ledige ring bevatten. Deze ring is opgebouwd uit een hydroxystyrylamine eenheid, een aminozuur en een β -hydroxy aminozuur. Aan deze ring is een zijketen gekoppeld, welke doorgaans bestaat uit één of twee aminozuren. De cyclopeptide alkaloiden vormen een relatief kleine klasse van ongeveer 230 gekende producten en in het laatste decennium zijn 39 nieuwe cyclopeptide alkaloiden gerapporteerd. Hoewel ze in verscheidene plantenfamilies voorkomen, zijn ze het meest wijdverspreid in the Rhamnaceae familie, meer bepaald in het genus *Ziziphus*.

In de traditionele geneeskunde worden diverse planten die cyclopeptide alkaloiden bevatten gebruikt voor de behandeling van malaria, bijvoorbeeld *Hymenocardia acida*, en *in vitro* antiplasmodiale activiteit is reeds gerapporteerd voor een beperkt aantal producten uit deze klasse. Daarom werd het isoleren van cyclopeptide alkaloiden uit een aantal geselecteerde plantensoorten, en bepaling van hun antiplasmodiale activiteit en cytotoxiciteit als eerste target van dit onderzoek gekozen.

Daarnaast worden planten met cyclopeptide alkaloiden traditioneel ook gebruikt voor de behandeling van diabetes. De toename in de vorming van AGEs (gevorderde glycatie eindproducten) wordt beschouwd als stimulerende factor in het ontstaan van diabetes-gerelateerde complicaties en *in vitro* AGEs inhibitie is reeds gerapporteerd voor nummularine-R en hemsine-A. Op basis van deze gegevens werd het onderzoeken van de AGEs inhiberende eigenschappen van de geïsoleerde cyclopeptide alkaloiden gekozen als tweede target van dit doctoraatsonderzoek.

Aan de hand van deze data kan een structuur-activiteits relatie onderzoek uitgevoerd worden, om te achterhalen welke structurele kenmerken van deze klasse van producten van belang zijn voor het vertonen van biologische activiteit.

Uit de wortelschors van ***Hymenocardia acida*** werden vier cyclopeptide alkaloiden opgezuiverd. Naast het reeds gekende hymenocardine werden drie andere alkaloiden voor de eerste maal geïsoleerd vanuit natuurlijke bronnen. Het betrof een hymenocardine-afgeleide met een hydroxy groep in plaats van een carbonyl groep, die hymenocardinol genoemd werd, hymenocardine *N*-oxide en een nieuw cyclopeptide alkaloïde met een ongebruikelijke histidine eenheid, genaamd hymenocardine-H. De antiplasmodiale activiteit en cytotoxiciteit

van deze cyclopeptide alkaloiden werden bepaald en alle vier de producten vertoonden een matige antiplasmodiale werking, met IC_{50} waarden variërend van 12.2 tot 27.9 μM . Hymenocardine *N*-oxide was het meest actief, met een IC_{50} waarde van $12.2 \pm 6.6 \mu M$.

Negen cyclopeptide alkaloiden werden opgezuiverd uit de wortels van ***Ziziphus oxyphylla***. Vijf van de negen werden hier voor de eerste maal beschreven. Nummularine-R, voorheen reeds beschreven als inhoudsstof van deze plantensoort, werd geïdentificeerd, samen met de nieuwe afgeleiden *O*-desmethylnummularine-R en *O*-desmethylnummularine-R *N*-oxide. Ook werden de gekende producten hemsine-A en ramosine-A opgezuiverd, en daarnaast ook hemsine-A *N*-oxide. Verder werd oxyphylline-C gevonden, voorheen gerapporteerd als inhoudsstof in de stam van *Z. oxyphylla*. Ook werden twee nieuwe producten geïdentificeerd: oxyphylline-E en oxyphylline-F. Zowel oxyphylline-C, als oxyphyllines-E en -F behoren tot de relatief zeldzame klasse van neutrale cyclopeptide alkaloiden.

De antiplasmodiale activiteit en cytotoxiciteit van vijf van de negen alkaloiden werd nagegaan. Het meest beloftevolle resultaat werd gevonden voor *O*-desmethylnummularine-R, met een IC_{50} waarde van $3.2 \pm 2.6 \mu M$ tegen *Plasmodium falciparum* K1 en een IC_{50} waarde hoger dan 64.0 μM voor cytotoxiciteit tegen MRC-5 cellen.

Zeven cyclopeptide alkaloiden werden geïsoleerd uit de schors van de stam van ***Ziziphus nummularia*** en ***Ziziphus spina-christi***. Drie nieuwe producten werden geïdentificeerd: nummularine-U uit *Z. nummularia*, en spinanines-B en -C uit *Z. spina-christi*. Ook werden de gekende alkaloiden mauritine-F, nummularines-D, en -E en amphibine-D geïdentificeerd. Voor vijf van deze inhoudsstoffen werd de antiplasmodiale activiteit en cytotoxiciteit bepaald. De hoogste activiteit werd gevonden voor spinanine-B met een IC_{50} waarde van $2.1 \pm 0.3 \mu M$ tegen *P. falciparum*, terwijl geen cytotoxisch effect tegen MRC-5 cellen waargenomen werd in concentraties tot en met 64.0 μM .

In totaal werden 20 cyclopeptide alkaloiden geïsoleerd uit *Hymenocardia acida*, *Ziziphus oxyphylla*, *Ziziphus nummularia* en *Ziziphus spina-christi*, door middel van conventionele opscheidingstechnieken, alsook semi-preparatieve HPLC met DAD en ESIMS detectie en LC-DAD-(HRMS)-SPE-NMR. Structuuropheldering werd gedaan door middel van spectroscopische technieken. Elf van de 20 cyclopeptide alkaloiden werden voor de eerste maal gerapporteerd

en voor 14 van deze producten werden de **antiplasmodiale** en **cytotoxische activiteit** bepaald. Bovendien werden deze testen uitgevoerd op vijf andere cyclopeptide alkaloiden die in een eerder project opgezuiverd waren. Van alle geteste producten was het resultaat verkregen voor spinanine-B het meest beloftevol.

Gebaseerd op de verkregen set van 19 cyclopeptide alkaloiden en de corresponderende IC₅₀ waarden tegen *P. falciparum*, werden zowel een **kwalitatief**, als een **kwantitatief structuur-activiteits relatie (SAR) onderzoek** uitgevoerd. De kwalitatieve SAR studie toonde aan dat een 13-ledige ring de voorkeur heeft boven een 14-ledige ring. Ook zou de aanwezigheid van een β -hydroxy proline eenheid kunnen correleren met een hogere antiplasmodiale activiteit. Verder zou methoxylering (of, in mindere mate, hydroxylering) van de styrylamine eenheid belangrijk kunnen zijn voor het vertonen van antiplasmodiale activiteit. Naast de kwalitatieve SAR studie werden ook kwantitatieve structuur-activiteits relatie modellen ontwikkeld, gebruik makende van PLS (partiële kleinste kwadraten regressie) en MLR (meervoudige lineaire regressie). Deze modellen laten enerzijds toe om de belangrijkste descriptoren (moleculaire eigenschappen), verantwoordelijk voor de antiplasmodiale activiteit te identificeren en kunnen anderzijds gebruikt worden om voorspellingen te maken van de mate van activiteit tegen *P. falciparum* voor andere cyclopeptide alkaloiden. Voorspellingen die gedaan werden voor mogelijk beloftevolle structuren, afgeleid uit de kwalitatieve SAR studie, waren niet in tegenspraak met de verwachtingen gewekt door die studie.

Een aspect waar rekening mee gehouden dient te worden bij het overwegen van *in vivo* experimenten met cyclopeptide alkaloiden is, gezien hun peptide-achtige karakter, de mogelijke **metabolisatie** na orale inname. Daarom werd een studie uitgevoerd op hymenocardine, om zijn stabiliteit, absorptie vanuit de dunne darm en metabolisatie in de lever na te gaan. Analyse van het dialysaat en retentaat, verkregen na passage van het gastrointestinaal dialyse model, leidde tot de constatering dat hymenocardine, in ieder geval deels onveranderd, wordt geabsorbeerd vanuit de gastrointestinale tractus. Na S9 metabolisatie konden verschillende metabolieten van hymenocardine geïdentificeerd worden. De voornaamste werden gevormd door reductie en/of afsplitsing van een *N*-methyl groep. De *in vivo* studie bevestigde dat hymenocardine onveranderd wordt opgenomen vanuit

het gastrointestinale stelsel, aangezien dit product teruggevonden werd in zowel plasma als urine van ratten, samen met hymenocardinol, het product gevormd na reductie.

Wat betreft de **AGEs inhiberende eigenschappen** van de cyclopeptide alkaloiden kunnen helaas geen concrete conclusies getrokken worden. Verschillende problemen kwamen aan het licht bij het uitvoeren van de meest gebruikte analyse methoden, en dit maakte het boeken van vooruitgang in relatie tot dit specifieke target lastiger dan verwacht. Echter, de ontwikkeling van een nieuwe methode voor de bepaling van AGEs inhibitie is momenteel gaande, en zodra deze methode gevalideerd is, zal het mogelijk zijn om te bepalen of, en zo ja, in welke mate, de verkregen set van cyclopeptide alkaloiden de vorming van AGEs kan remmen.

ACKNOWLEDGEMENT – DANKWOORD

Allereerst gaat mijn dank uit naar mijn promotor, Prof. Luc Pieters, die mij de kans heeft gegeven om mijn doctoraatsonderzoek onder zijn supervisie uit te voeren. Wanneer ik een vraag had kon ik letterlijk altijd bij u aankloppen en wanneer ik mijn verslagen, presentaties, manuscripten en uiteindelijk mijn thesis naar u doorstuurde voor feedback, dan hoefde ik nooit lang op een antwoord wachten. Ook wil ik graag mijn co-promotor, Prof. Nina Hermans bedanken voor haar bijdrage aan dit project en in het bijzonder, de *in vivo* studie. Mijn speciale dank gaat ook uit naar Prof. Sandra Apers; weliswaar kan een doctoraatsstudent officieel slechts twee promotoren hebben, maar voor mijn gevoel was zij mijn derde promotor. Zij toonde altijd interesse in de progressie van mijn onderzoek en ze was altijd bereid om te helpen indien mogelijk. Ik ben deze drie professoren hier erg dankbaar voor.

Daarnaast gaat mijn dank uit naar alle (ex-)collega's van de onderzoeksgroep NatuRA: Tania, Mart, Tess, Laura, Sebastiaan, Anastasia, Andrés, Deborah, Yunita, en Atul. De sfeer was altijd gemoedelijk en aangenaam en het is/was fijn om met jullie samen te werken!

Bedankt voor alles!

Natuurlijk zijn er ook nog enkele personen die hier in het bijzonder een plaatsje verdienen:

Allereerst wil ik Kenn bedanken, die mij de beginselen van het phytochemisch onderzoek heeft bijgebracht. Ruim 5 jaar geleden begon ik onder jouw hoede als masterstudent en zag ik jou onder andere de NMR bedienen (en dacht ik bij mezelf: "wauw, hoe kan zij al die code's en commando's van buiten kennen?!") Na die masterproef begon ik aan mijn eigen doctoraatsonderzoek, (zoals je wel weet, met véél scheitrechters, gevuld met o.a. ZOX en ZOR materiaal), en ook in deze jaren heb je me ontzettend vaak en goed geholpen. Ik vind het nog altijd zeer waardevol om jouw kijk op bepaalde zaken te horen, dus m.a.w.: je bent (helaas) nog niet van me af en ik zal nog regelmatig aan je bureau staan met vragen...!

Also I would like to thank Vasiliki. Your enthusiasm and working mentality were very inspiring and I am grateful for the many, many things that I've learnt from you. It was a shame that you left our lab, but luckily you still come by every now and then, to enlighten us with some more NMR tips and tricks, and I hope we will have the opportunity to collaborate more in the future. Apart from being a nice colleague, you've also become a close friend and I want to thank you

for the times when you were there to pick me up when I was feeling down, and for all the nice moments we've spent. I hope many more will follow. ☺

Stefy and Maxime, it was and is a pleasure to have you as my colleagues and to share an office with you. I hope you still think the same about me, inspite of my recurring frustrations about page numbering, image editing, and other computer-related issues during the past few months... :P By the time you'll be writing your PhD thesis, I guess you might feel the same sometimes, and hopefully I'll be able to cheer you up then, like you did with me.

Apart from seeing each other in the lab, we also tend to go for 'teambuilding activities' outside the lab, with a bunch of other colleagues (visits to the cinema, ballet performances, football matches, escape rooms,...). This is always fun and we still have plenty ideas for new activities, so I'm already looking forward to the next night out!

Stefy, I will also definetely remember the (crazy) times that we spent together with Yancho and I want to thank him for these nice moments too. I don't think many Dutch people can say they've watched a Eurocup match, cheering for the Belgian Red Devils, together with two Bulgarians. (And it didn't even matter that they lost, we had a party afterwards anyway.) ☺

Adnan (or in fact, Dr. Amin is more appropriate!) our PhD adventures started off at approximately the same time, and throughout the years I've come to know you as a very sincere and kind person. We may have had some heated discussions concerning the AGEs experiments, but I hope you know that those had nothing to do with you personally. I was grateful to be invited to your PhD celebration dinner, where I also had the chance to meet Hina, your lovely wife. You and the kids returned to Pakistan last year and you won't be able attend my PhD defense and celebration dinner, but I will make sure that you receive this message. I hope we will stay in touch and I wish you and your family all the best for the future.

Roger, drie jaar lang heb ik samen met u in A1.06 vertoefd en ik wil u graag bedanken voor alle keren dat u mij geholpen heeft met ICT-gerelateerde problemen en ook met mobiliteits-gerelateerde problemen (sleutelen aan mijn fiets, als die weer eens stuk was!). Het was fijn om een bureau met u te delen en om u wat beter te leren kennen.

Annelies en Annelies, beter bekend als Annelies V. en Annelies B., bedankt om er altijd te zijn als ik (op weg van mijn bureau naar de toiletten of omgekeerd) nood had aan een praatje. Annelies B., ook bedankt voor je hulp met het GIDM en de ratjes en Annelies V., nog heel veel succes met jouw doctoraat!

Rica, Hans en Ines, 'de oude garde'. Jullie gaven het goede voorbeeld; bij jullie kon ik 'afkijken' hoe het moest. ☺ Een voor een hebben jullie je PhD afgerond en inmiddels hebben jullie alle drie ons labo verlaten... Bedankt voor de leuke momenten samen, zowel in het labo als op verschillende congressen, en ik hoop dat we elkaar af en toe nog eens zullen spreken.

Labo medische biochemie (Lesley en Gwendolyn) en labo toxicologie (Matthias en Neele), bedankt voor jullie gastvrijheid en jullie hulp met de Tecan, met Meteor en met het S9 experiment. Ook bedankt aan het labo medicinale chemie (Sofie en Dries) voor het willen delen van jullie NMR toestel.

Dan zijn er natuurlijk nog mijn Farma-vriendinnen, Natalie en Sanne. Na vijf jaar studie was ik de enige die zo zot was om nog een paar jaar langer op de unief te willen blijven en soms leverde dit mij wel de nodige stress op, maar dan waren er altijd de ontspannende etentjes, feestjes en citytripkes samen met jullie. Vooral dat laatste is wat mij betreft een traditie die in stand gehouden moet worden en ik kijk uit al uit naar ons volgende reisje. (Porto, here we come! ☺)

Tenslotte nog een woordje gericht aan mijn ouders en aan Annelies, mijn zusje.

Papa, bedankt voor de vele goede gesprekken. Als ik weer eens aan mezelf twijfelde dan was jij er altijd om me te vertellen dat dat absoluut niet nodig was en dat het allemaal wel goed zou komen. Mama, lieve mama. Ook jij bedankt voor alle steun. Je hebt altijd het beste met me voor en ik ben trots dat ik in zoveel aspecten op je lijk.

Annelies, ook jij verdient hier een plaatsje natuurlijk! Bedankt voor het feit dat je altijd eerlijk je mening geeft, voor je nuchtere kijk op de zaken en voor je goede gevoel voor humor. Zonder jou zou het leven een stuk saaier zijn. :)

SCIENTIFIC CURRICULUM VITAE

Scientific curriculum vitae

Personalia

Name: Emmy Tuenter
Date of birth: 10 September 1989
Place of birth: Roosendaal, the Netherlands
E-mail: Emmy.Tuenter@uantwerpen.be

Education

2000-2007 Secondary school, subjects of choice: mathematics, physics, chemistry, biology and Latin
Gertrudiscollege
Roosendaal, the Netherlands

2007-2010 Bachelor in Pharmaceutical Sciences, great distinction
University of Antwerp
Wilrijk, Belgium

2010-2012 Master in Drug Development; Pharmacist, greatest distinction
University of Antwerp
Wilrijk, Belgium

2012–2017 PhD student in Pharmaceutical Sciences
PhD fellowship granted by the Agency for Innovation by Science and Technology in Flanders (IWT)
Natural Products & Food Research and Analysis (NatuRA)
University of Antwerp
Wilrijk, Belgium

Scientific experience

- Feb – June 2012: Masterthesis
“Research on antiplasmodially active metabolites after oral intake of a *Nauclea pobeguinii* extract”
Natural Products & Food Research and Analysis (NatuRA)
University of Antwerp
Wilrijk, Belgium
- Sept 2012 – Present PhD thesis
“Cyclopeptide Alkaloids: Isolation, Structure Elucidation, Antiplasmodial Activity and AGEs Inhibiting Properties”
Natural Products & Food Research and Analysis (NatuRA)
University of Antwerp
Wilrijk, Belgium
- April – May 2016 Research stay at the Department of Drug Design and Pharmacology,
University of Copenhagen, Copenhagen, Denmark

Scientific publications

Papers in peer-reviewed journals

- 2017 Emmy Tuenter, Karen Segers, Kyo Bin Kang, Johan Viaene, San Hyun Sung, Paul Cos, Louis Maes, Yvan Vander Heyden, Luc Pieters - Antiplasmodial activity, cytotoxicity and structure-activity relationship study of cyclopeptide alkaloids. *Molecules*, 2017, 22(2), 224
DOI: 10.3390/molecules22020224
- Emmy Tuenter, Kenn Foubert, Dan Staerk, Sandra Apers, Luc Pieters - Isolation and structure elucidation of cyclopeptide alkaloids from *Ziziphus nummularia* and *Ziziphus spina-christi* by HPLC-DAD-MS and HPLC-PDA-(HRMS)-SPE-NMR. *Phytochemistry*, 2017, 138: 163-169
DOI: 10.1016/j.phytochem.2017.02.029

Emmy Tuenter, Sebastiaan Bijttebier, Kenn Foubert, Annelies Breynaert, Sandra Apers, Nina Hermans, Luc Pieters - *In vitro* and *in vivo* study of the gastrointestinal absorption and metabolism of hymenocardine, a cyclopeptide alkaloid. *Planta Med.*, 2017

DOI: 10.1055/s-0043-102494

Adnan Amin, Emmy Tuenter, Kenn Foubert, Jamshed Iqbal, Paul Cos, Louis Maes, Vassiliki Exarchou, Sandra Apers, Luc Pieters - *In vitro* and *in silico* antidiabetic and antimicrobial evaluation of constituents from *Kickxia ramosissima* (*Nanorrhinum ramosissimum*). *Front. Pharmacol.*, 2017

DOI: 10.3389/fphar.2017.00232

2016 Emmy Tuenter, Vassiliki Exarchou, Aliou Baldé, Paul Cos, Louis Maes, Sandra Apers, Luc Pieters - Cyclopeptide alkaloids from *Hymenocardia acida*. *J. Nat. Prod.*, 2016, 79(7): 1746-1751

DOI: 10.1021/acs.jnatprod.6b00131

Emmy Tuenter, Rizwan Ahmad, Kenn Foubert, Adnan Amin, Maria Orfanoudaki, Paul Cos, Louis Maes, Sandra Apers, Luc Pieters, Vassiliki Exarchou - Isolation and structure elucidation by LC-DAD-MS and LC-DAD-SPE-NMR of cyclopeptide alkaloids from the roots of *Ziziphus oxyphylla* and evaluation of their antiplasmodial activity. *J. Nat. Prod.*, 2016, 78(11): 2865-2872

DOI: 10.1021/acs.jnatprod.6b00633

Emmy Tuenter, Vassiliki Exarchou, Sandra Apers, Luc Pieters - Cyclopeptide alkaloids. *Phytochem. Rev.*, 2016

DOI: 10.1007/s11101-016-9484-y

Adnan Amin, Emmy Tuenter, Vassiliki Exarchou, Atul Upadhyay, Paul Cos, Louis Maes, Sandra Apers, Luc Pieters – Phytochemical and pharmacological investigations on *Nympoides indica* leaf extracts. *Phytother. Res.*, 2016, 10: 1624-1633

DOI: 10.1002/ptr.5663

Adnan Amin, Emmy Tuenter, Paul Cos, Louis Maes, Vassiliki Exarchou, Sandra Apers, Luc Pieters – Antiprotozoal and antiglycation activities of sesquiterpene coumarins from *Ferula narthex* exudate. *Molecules*, 2016 21, 1287

DOI: 10.3390/molecules21101287

Rizwan Ahmad, Niyaz Ahmad, Atta Abbas Naqvi, Vassiliki Exarchou, Atul Upadhyay, Emmy Tuenter, Kenn Foubert, Sandra Apers, Nina Hermans and Luc Pieters - Antioxidant and antiglycating constituents from leaves of *Ziziphus oxyphylla* and *Cedrela serrata*. *Antioxidants*, 2016, 5(1), 9

DOI: 10.3390/antiox5010009

Luiz Carlos Klein-Júnior, Johan Viaene, Emmy Tuenter, Juliana Salton, André L. Gasper, Sandra Apers, Jan P.M. Andries, Luc Pieters, Amélia T. Henriques, Yvan Vander Heyden - The use of chemometrics to study multifunctional indole alkaloids from *Psychotria nemorosa* (Palicourea comb. nov.). Part II: Indication of peaks related to the inhibition of butyrylcholinesterase and monoamine oxidase-A. *J. Chromatog. A*, 2016, 1463: 71-80

DOI: 10.1016/j.chroma.2016.08.005

Desiré Musuyu Muganza, Barbara Fruth, José Lami Nzunzu, Emmy Tuenter, Kenn Foubert, Paul Cos, Louis Maes, Richard Cimanga Kanyanga, Vassiliki Exarchou, Sandra Apers, Luc Pieters – *In vitro* antiprotozoal activity and cytotoxicity of extracts and isolated constituents from *Greenwayodendron suaveolens*. *J. Ethnopharmacol.*, 2016, 193, 510-516

DOI: 10.1016/j.jep.2016.09.051

2014 Atul Upadhyay, Emmy Tuenter, Adnan Amin, Vasiliki Exarchou, Nina Hermans, Sandra Apers, Luc Pieters - 5-O-Demethylnobiletin, a polymethoxylated flavonoid from *Citrus depressa* Hayata peel prevents protein glycation. *J. Funct. Foods*, 2014, 11, 243-249
DOI: 10.1016/j.jff.2014.10.012

Atul Upadhyay, Emmy Tuenter, Rizwan Ahmad, Adnan Amin, Vasiliki Exarchou, Sandra Apers, Nina Hermans, Luc Pieters - Kavalactones, a novel class of protein glycation and lipid peroxidation inhibitors. *Planta Med.*, 2014, 80, 1001-1008
DOI: 10.1055/s-0034-1382949

- 2013 Ying-Shu Zou, Kenn Foubert, Emmy Tuenter, Filip Lemièrre, Paul Cos, Louis Maes, Jan M.M. Smits, René de Gelder, Sandra Apers, Luc Pieters - Antiplasmodial and cytotoxic activities of *Striga asiatica* and *Sauropus spatulifolius* extracts, and their isolated constituents. *Phytochem. Lett.*, 2013, 6(1), 53-58
DOI: 10.1016/j.phytol.2012.10.018

Oral presentations

- 2016 Gastrointestinal absorption and liver metabolization of hymenocardine, a cyclopeptide alkaloid from *Hymenocardia acida*. Tuenter E., Bijttebier S., Foubert K., Breynaert A., Hermans N., Pieters L.; 19th forum of Pharmaceutical Sciences (Belgian Society of Pharmaceutical Sciences) – 17th October 2016, Brussels, Belgium
(Rewarded with 'Best presentation' award.)

Antiplasmodial activity of cyclopeptide alkaloids from *Hymenocardia acida* and *Ziziphus oxyphylla*. Tuenter E., Exarchou V., Ahmad R., Baldé A., Cos P, Maes L, Apers S, Pieters L.; 9th Joint Natural Products Conference 2016 – 24th July 2016, Copenhagen, Denmark; *Planta Med.* 81(S 01): S1-S381
DOI: 10.1055/s-0036-1596169

Antiplasmodial activity of cyclopeptide alkaloids from *Hymenocardia acida* and *Ziziphus oxyphylla*. Tuenter E., Exarchou V., Ahmad R., Baldé A., Cos P, Maes L, Apers S, Pieters L.; Departmental Research Day of Pharmaceutical Sciences, University of Antwerp – 11th May 2016, Antwerp, Belgium

- 2015 Cyclopeptide alkaloids of *Ziziphus oxyphylla*. Tuenter E., Exarchou V., Ahmad R., Apers S., Hermans N., Pieters L. 4th International Congress on Pharmacology of Natural Products (Fapronatura 2015) - 22th September 2015, Topes de Collantes, Cuba

Isolation and structural elucidation of cyclopeptide alkaloids from *Hymenocardia acida*. Tuenter E., Exarchou V., Balde A., Cos P., Maes L., Apers S., Pieters L.; 18th forum of Pharmaceutical Sciences (Belgian Society of Pharmaceutical Sciences) - 29th May 2015, Blankenberge, Belgium

- 2014 A new cyclopeptide from *Hymenocardia acida*. Emmy Tuenter, Vassiliki Exarchou, Aliou Baldé, Sandra Apers, Luc Pieters; 62nd International Congress and Annual Meeting of the Society for Medicinal Plant and Natural Product Research (GA) - 31st August 2014, Guimarães, Portugal; *Planta Med.*, 2014; 80(16) - WS6.

- 2013 Kavalactones inhibit the formation of advanced glycation endproducts. Emmy Tuenter, Atul Upadhyay, Nina Hermans, Sandra Apers, Luc Pieters; 17th forum of Pharmaceutical Sciences (Belgian Society of Pharmaceutical Sciences) - 18th October 2013, Spa, Belgium

Poster presentations

- 2016 Antiplasmodial activity of cyclopeptide alkaloids from *Hymenocardia acida* and *Ziziphus oxyphylla*. Tuenter E., Exarchou V., Ahmad R., Baldé A., Cos P, Maes L, Apers S, Pieters L.
9th Joint Natural Products Conference 2016 – 24th July 2016, Copenhagen, Denmark

- 2014 A new cyclopeptide from *Hymenocardia acida*. Emmy Tuenter, Vassiliki Exarchou, Aliou Baldé, Sandra Apers, Luc Pieters; 62nd International Congress and Annual Meeting of the Society for Medicinal Plant and Natural Product Research (GA) - 31st August 2014, Guimarães, Portugal;

- 2013 Atul Upadhyay, Emmy Tuenter, Rizwan Ahmad, Nina Hermans, Sandra Apers, Luc Pieters - Kavalactones as inhibitors of advanced glycation endproducts (AGEs) formation. 61st International Congress and Annual Meeting of the Society for Medicinal Plant and Natural Product Research (GA) – 3rd September 2013, Münster, Germany; *Planta Med.*, 2013, 79 – PN114
DOI: 10.1055/s-0033-1352456